UNIVERSITAT POLITÈCNICA DE CATALUNYA BARCELONATECH

Departament d'**Enginyeria de Sistemes, Automàtica i Informàtica Industrial**

Contribution to the development of methods and systems for the automatization during the early stages of Bioprocess development.

Thesis presented for the qualification of Ph.D.

Program: **Biomedical Engineering**

Author: ***Andreu Francesc Fontova i Sosa***

Director: ***Ramon Bragós i Bardia.***

Barcelona 2015

Electronic and Biomedical Instrumentation Group. **IEB**

Departament d'Enginyeria Electrònica

Agraïments.

El conjunt dels reptes i les dificultat afrontades durant el desenvolupament d'aquest treball no es restringeixen només al context de la tesi doctoral, sinó que han format part del dia a dia d'una aventura empresarial anomenada HEXASCREEN CULTURE TECHNOLOGIES s. l. amb l'ambiciós objectiu de desenvolupar i portar al mercat un producte tecnològicament avançat i capaç de donar solucions a un dels sectors industrials més exigents del món, la Biotecnologia mèdica i farmacèutica.

Malgrat que el projecte empresarial no ha tingut l'èxit esperat, cal posar en valor tant la feina com l'actitud amb la que els treballadors i alguns socis de la companyia van recolzar el projecte i que va permetre no només fer realitat el producte sinó també aconseguir èxits remarcables com ara la col·laboració amb el *Biotechnology Process Engineering Center* del *Massachusets Institute of Technology* i la reconversió del producte pel cultiu de cèl·lules mare embrionàries humanes per a la *University of Calgary*.

Agrair també l'ajuda sempre incondicional per part dels grups de recerca *d'Enginyeria Cel·lular i Tissular* de la *Universitat Autònoma de Barcelona* i de *Instrumentació i Enginyeria Biomèdica* de la *Universitat Politècnica de Catalunya*. Així com en especial al meu director de tesi, el Dr. Ramon Bragós qui a més de proporcionar un assessorament crític i didàctic ha estat sempre un exemple a seguir per la seva talla professional i humana.

Finalment adreço el meu agraïment més profund a la meva germana Laura i el meus pares Núria i Andreu, els quals sempre m'han recolzat, tant en els moments d'èxit com els més difícils.

Contents:

Abstract.

The present dissertation deals about some of the tools and methods used in Biomedicine and Biotechnology to discover new innovative therapeutic agents. Whose development and production still involve an important amount of manual labour. Currently, such fields are considered as a zone of frontier in science [1]. Therefore, it exists an urgent need for more efficient and reproducible manners to carry out experiments and get results. In this direction bioreactors and fermenters are being used not just for production but for testing the potentiality of some cell species to produce such therapeutic agents. The most widespread concept of a bioreactor is made of a vessel connected to a control unit by means of an ensemble of probes and actuators with the aim of monitoring the growth of some cell specie (the biocatalyst), its metabolic activity, and controlling some important physical and chemical conditions, for instance: temperature, pH, pO_2…

In order to make such systems useful for the early bioprocess development stages (Cell screening, Clone optimisation, and Process optimisation) engineers and biotechnologists have the challenge of designing the processes keeping in mind the following requirements:

- Capability to perform an statistically significant number of experiments (*High Throughput Screening*),
- Capability to produce results being representative of the future production stages (*Scalability*).
- Capability to produce reliable results at low cost.

That's why during the last decade an important scientific and commercial interest on miniaturised disposable cell culture systems has risen. Different approaches have been developed [2] [3] [4]. Some of them focused on increasing the experimental throughput by reducing the culture volume and others on offering bigger volumes but including stunning automation and monitorization features. Probably it doesn't still exist an optimum compromise between the experimental throughput and how bio-process significant the results are for every application. Therefore, the right measurement and control methods shall be chosen depending on the type of cells cultured and the type and size of the bioreactor used.

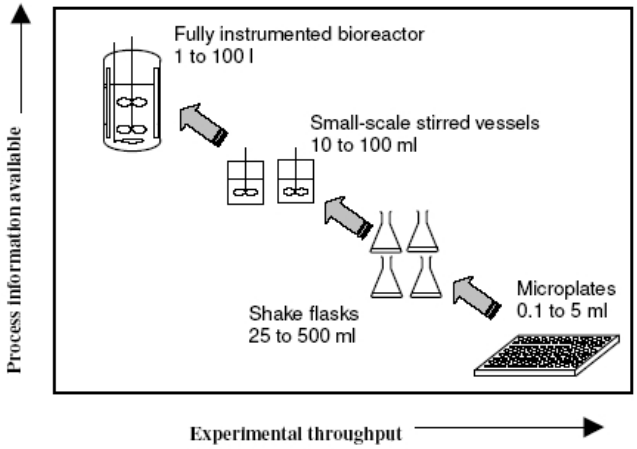

Figure 1
Trade-off between the data throughput and how bio-process significant the data are.
From D. Doig S., I. Betts J. et al. [5] [6]

The work here presented aims to be a contribution to the state of the art on cell culture monitoring and control techniques applied to the bioprocess development taking into account the requirements mentioned above. Specifically about the design and construction of instrumentation for the estimation of the *Oxygen Uptake Rate* (OUR) on miniaturized disposable bioreactors. OUR has been described as a key variable for tracking and monitoring the metabolic activity in animal cell culture [7][8]. This work proposal fits within this framework and tries to demonstrate the feasibility of a new method for the continuous estimation of the OUR. The proposed method is based on the accurate control of the oxygen concentration by means of *Pulse Width Modulated* (PWM) valves and the use of internal control loop variables to estimate the OUR. The method claims for a cheaper, continuous and accurate estimation, as well as being free of cell stress due to strong changes in the medium's oxygen concentration, as happens with the *Dynamic Method*, being this the most common technique.

To that end, after the study of the background and the system modelling and simulation three different testing platforms were built and every technical mean required to carry out the experimentation was developed. The first and the second testing platforms are experimental prototypes named as HexaScreen® Hexa-Batch and MonoScreen® Fed-Batch; they are disposable Minibioreactors (MBR's) manufactured by HEXASCREEN CULTURE TECHNOLOGIES S.L., the third platform is based on a Biostat® Bplus Bench-Scale bioreactor by SARTORIOUS AG. Such developments required some additional effort to design instruments and algorithms not just for measuring and control the Dissolved Oxygen (DO), but the pH, Temperature, Cell Concentration, and a wide set of means to allow the cell growth (such design will be specifically introduced in chapter 4. Therefore, although the main topics under focus are the OUR estimation and the Dissolved Oxygen (DO) measurement, due to the fact that the cultivation of cell species requires a number of considerations besides the oxygen consumption, the general scope of the present dissertation ranges from the state of the art in Minibioreactor design to different techniques applied for measure and control, as well as for monitoring the metabolic activity of the cell species.

A number of original hardware and instrumental contributions will be introduced. Below some of the main achievements:

- Development and construction of two state-of-the-art Minibioreactor platforms useful to essay the OUR estimation and DO measurement methods under study.
- Development and construction of a low cost, state-of-art. DO measurement instrument to perform a highly accurate control of the medium's DO concentration.
- Demonstration of the feasibility of a new method for the continuous estimation of the OUR, based on the accurate control of the DO concentration and especially suited for animal cell culture.

Therefore, the following chapters introduce a theoretical approach to a new method for the estimation of the OUR, which has been demonstrated by means of the experiments carried out with three different types of bioreactors, being two of them, as will be shown, an innovative embodiment within the field of disposable bioreactors.

References:

[1] M. S. F. M. S. G. Audrey R. Chapman, "Stem Cell Research and Applications Monitoring the Frontiers of Biomedical Research," American Association for the Advancement of Science & Institute for Civil Society, 1999.

[2] V. Glasser, "Disposable Bioreactors gaining favor," *Genetic Engineering and Biotechnology News,* vol. 26, no. 12, 2006.

[3] V. Glasser, "Bioreactor and Fermentor market trends," *Genetic Engineering and*

Biotechnology News, vol. 29, no. 14, 2004.

[4] V. Glaser, “Bioreactor and Fermentor Market trends,” *Genetic Engineering & Biotechnology News,* vol. 29, no. 19, 2009.

[5] B. F. J. L. G. D. Doig S, “High-Throughput screening and process optimization,” in *Basic Biotechnology*, Cambridge, 2006, pp. 289-305.

[6] B. F. I Betts J., «Miniature Bioreactors: Current practices and future opportunities,» *Microbial Cell Factories,* p. 5:21, 2006.

[7] E. G. V. E. S. J. C. M. Felix Garcia-Ochoa, “Oxygen uptake rate in microbial processes: An overview,” *Biochemical Engineering Journal,* vol. 49, pp. 289-307, 2010.

[8] U. v. S. I. W. M. Pierre-Alain Ruffieux, “Measurement of volumetric (OUR) and determination of specific (qO2) oxygen uptake rates in animal cell cultures,” *Journal of biotechnology,* vol. 63, no. 2, pp. 85-95, 1998.

Introduction.

The fundamentals of the in vitro tissue and animal cell culture techniques were developed in the late nineteenth and early twentieth centuries and their basis are still valid (W. Roux 1885, Arnold 1887, Ljunggren and L. Loeb 1897, R. Harrison 1907, Carrel A. Burrows 1911 and 1912) [1].These essentially consist in placing the cells inside some type of container (Petri dishes , test tubes, Carrel bottles, T-flasks ...) along with an appropriate culture medium, typically a buffered solution of amino acids, vitamins, and other nutrients, all incubated in sterile conditions in an atmosphere of 5 % CO_2 and warmed at 37 °C. This ensures that the cell line will grow continuously, even being able to express its phenotype. In some cases the surface of the container allows the cells to attach forming a monolayer growth. Using this procedure, Alexis Carrel was able to keep a strain of fibroblasts obtained from the heart of chicken embryos in active multiplication over twenty-five years [2]. The evolution of these techniques led to the concept of Bioreactor, where the most widespread embodiment is the stirred tank, which is made of a sterile vessel featuring some sort of turbine for mixing, a gas supply and the culture medium. Once the Bioreactor is seeded with a certain initial concentration of cells, they will keep growing attached to the vessel walls or in suspension

until some limiting factor is reached. Additionally, said vessel is usually connected to a control unit by means of an ensemble of probes and actuators used for monitoring the cells growth and their metabolic activity as well as controlling some important physical and chemical conditions. Typically: Temperature, Stirring Rate, pH and pO_2. The key concepts related to the performance of a Bioreactor will be introduced in the following sections.

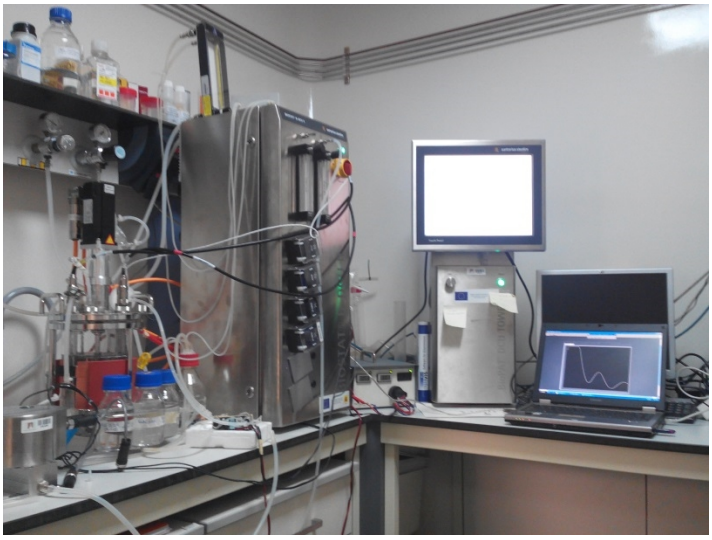

Figure 1
Typical 2-3 litres bench scale bioreactor at the facilities of the Universitat Autònoma de Barcelona.

At present, the applications of animal cell culture or other species are of enormous social interest and represent a high added-value economic activity. Can be counted among the applications for example, the production of biological compounds assets, ranging from small molecules, organic acids, vitamins or antibiotics to therapeutic proteins or plasmid vectors for gene therapy [3]. This allows qualifying as strategic any effort aimed to improve, systematize, or automatize any of the parties involved in the Bioprocess development. Four stages have been stated: a) Cellular screening, b) Cell enhancement, c) Process optimization and d) Scale-Up.

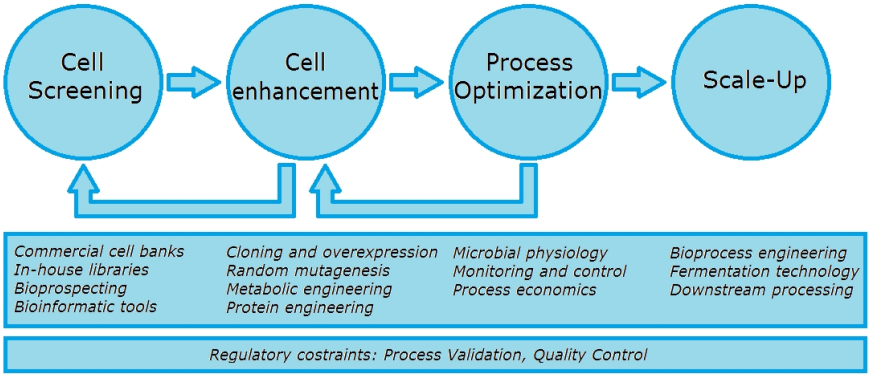

Figure 2
Schematic representation of the Bioprocess development. The key inputs of each phase are appointed. A number of iterations can be usually required during the first stages.
Adapted from D.Doig D. et al. [3]

At present most of the work done during Cell screening and Cell enhancement stages are performed either through expensive robots capable of handling thousands of samples per day, or either through manual operation using incubators and a variety of Petri dishes, multiwell plates and T-flasks, which are specially usual in basic science. Both systems have two common disadvantages as the inability to control and monitor in real-time the culture evolution and conditions, and the inability to provide significant data representative of the later stages of cultivation with higher volumes. According to information provided directly by some laboratories and biotech companies, it is not possible to establish a direct scalability between the cell culture protocols during the screening stages and the production conditions. This is especially critical when coming to high added-value cell lines such as stem cells. To explain the scale-up issue, often a loss of homogeneity of the culture medium for higher volumes is pointed, which does not happen for the experimentation volumes (0.1 to 2 mL). There are a number of parameters involved affecting the kinetics of the cell culture behaviour and bringing the appearance of limiting factors (Flow topology, Cell stress, as well as the existence of physical and chemical gradients). Usually it becomes quite difficult to guess how each one of these parameters is contributing to the lack of scalability. This problem becomes a matter of research which is faced through numerical simulations that provide the guidelines to take into account during the later geometrical design of the bioreactor. However, there's one parameter that has been pointed as the main key factor in Bioreactor design. The ability to transfer oxygen to the culture medium, which is related to the maximum biomass concentration the Bioreactor can hold [4] [5]. This becomes specially important as we grow in scale and extremely delicate cell lines are involved [6], [7]. This is related to the great interest that has risen on developing instruments and techniques to overcome the trade-off between the experimental through-put versus the data significance [Abstract - Figure 1]. Multi parallel Miniaturized Bioreactor systems are meant to simplify the Cell enhancement and Process optimization stages by establishing a great number of physical, chemical and biological conditions, and analyzing a huge amount of data obtained under controlled conditions. This task is known as High Throughput Screening (HTS) or High Throughput Experimentation (HTE) and is currently performed by applying Design of experiments (DoE) and Quality by design (QbD) rules [8] [9] [10].

The following pages will introduce some of the key concepts in bioreactor design to let a better understanding of the following chapters.

2.1 Metabolism and kinetics of microbial growth

The growth of an organism is linked to its metabolism, which consists of an account of biochemical reactions for the degradation of the existing diluted nutrients within the surrounding medium to obtain simple molecules (catabolism) and the use of such simple molecules to produce all major cell constituents and their intermediate precursors to finally divide into another cell (anabolism). In some cases, the sought product may happen to be the cells themselves. In other cases the product is obtained by means of some catabolic pathways which are usually emphasized using genetic engineering techniques that modify the balance

between the catabolic and biosynthetic reactions. This leads to the concepts of primary and secondary metabolism [11]. Primary metabolism occurs during the exponential growing phase of the organism, also known as Tropophase, in which all nutrients are available in excess and cells are constantly reproducing themselves until depletion of some nutrient happens and the biosynthesis rate slows down. Secondary metabolism occurs once the lack of some nutrient has been detected by the cell, this is known as stationary stage or Idiophase. Then, more energy demanding catabolic pathways are activated and the cells start consuming other nutrients that could even be previously produced during the Tropophase. During this stage some interesting secondary products may be obtained. Nevertheless, as the environment is turning hostile due to the increasing concentration of inhibiting molecules produced throughout the culture, the growth rate tends to get flattened until the cells finally die. Figure 2 shows the different microbial growth stages. The lag phase involves adaptation to the new environment, this is followed by the exponential and stationary phases, and later after a period of death a long-term stationary phase is reached in which a small number of individuals can survive for long periods of time in a non-growing state.

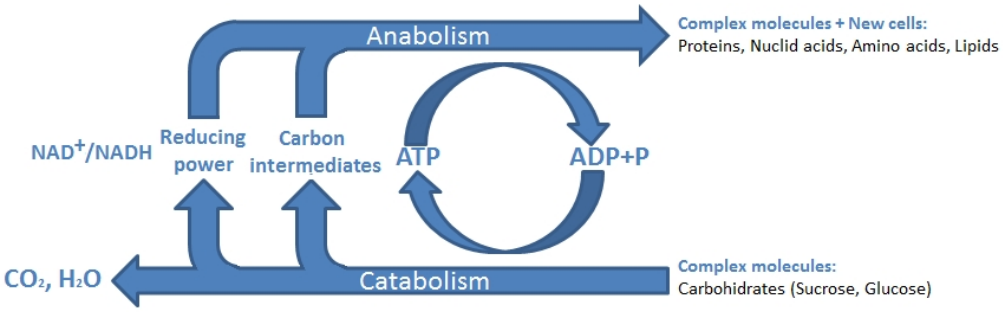

Figure 3
Basic metabolic pathway of degradation and biosynthesis

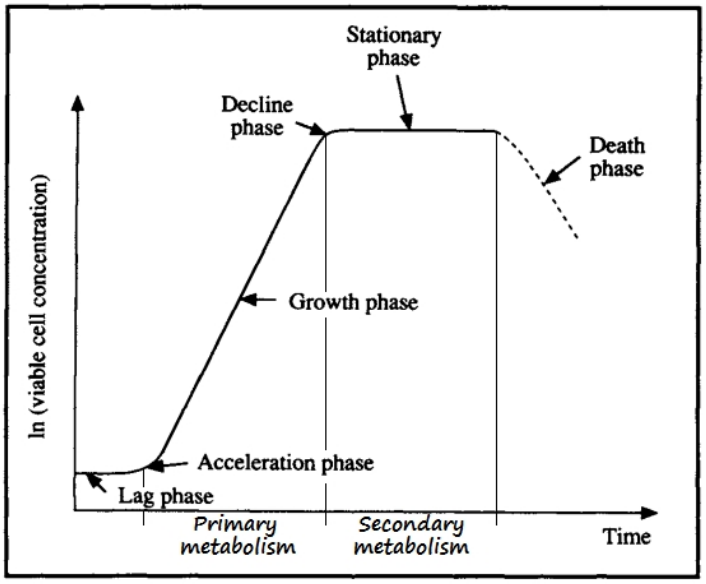

Figure 2
Microbial growth stages. Adapted from P. M. Doran [12]

Obviously there is an interest to estimate the overall fermentation production and how long the whole process will take. To that end, mathematical kinetic models are developed to fit the experimental data during the exponential growth phase. Unfortunately the pace of events during the Idiophase is quite unknown and highly dependent on the cell species and the media composition making difficult the use of mathematical models beyond the end of the Tropophase. Despite that the aim of this dissertation is not the development of cell growth models, it will be necessary to count on a growth model leading a variable and realistic oxygen consumption profile.

In general, during the Tropophase the growth rate for any cell species matches the so said exponential profile, being proportional to the number of individuals. This can be written as a first order differential equation.

$$\frac{dx}{dt} = \mu \cdot x$$

Where:

- x [mg/l or cell/ml]: Cell concentration.
- μ [h^{-1}]: Specific growth rate is related to the doubling time t_d[h] of the cell concentration through the following expression.

$$t_d = \frac{\ln 2}{\mu}$$

If the differential equation is solved the time dependent expression is obtained:

$$x(t) = x_0 \cdot e^{\mu \cdot t} = x_0 \cdot e^{\frac{ln2}{t_d} \cdot t}$$

The model for the oxygen uptake rate is obtained just by multiplying it by the cell specie's specific oxygen consumption qO_2 [mg·$cell^{-1}$·h^{-1}]:

$$\text{OUR} = qO_2 \cdot x_0 \cdot e^{\frac{ln2}{t_d} \cdot t}$$

2.2 Stirred Tank bioreactors.

Different types of bioreactors are available depending on the application, Bubble column, Airlift, Fluidised and Packed bed bioreactors, however the most widely used type for biopharmaceutical applications is the Stirred Tank, which consists of a cylindrical vessel with a motor-driven central shaft supporting a turbine where the aeration is performed by means of a pipe ring sparger or sintered diffusor placed below the turbine. In microbial culture the name Fermenter is typically used instead Bioreactor and some differences intended for increasing the mass transfer capability (gas to liquid exchange) may be found. That's because of the higher oxygen demand of bacteria and yeast compared with animal cells; typically more than one impeller may be used, as well as baffles attached to the walls. Animal cell culture

bioreactors are usually not so demanding in terms of mass transfer but a lot of care must be taken with the possible Shear Stress produced by the fluid dynamics. Next picture shows a typical pilot plant stirred tank bioreactor. Additionally to the elements mentioned above, there are some other common parts of bioreactors like ports for sampling and addition of feed, antifoam or other chemicals for instance for pH control, a minimum set of probes (Temperature, pH & DO), windows for inspection, means for thermoregulation, sealing rings for the moving parts, and specifically for industrial bioreactors steam connections for sterilization.

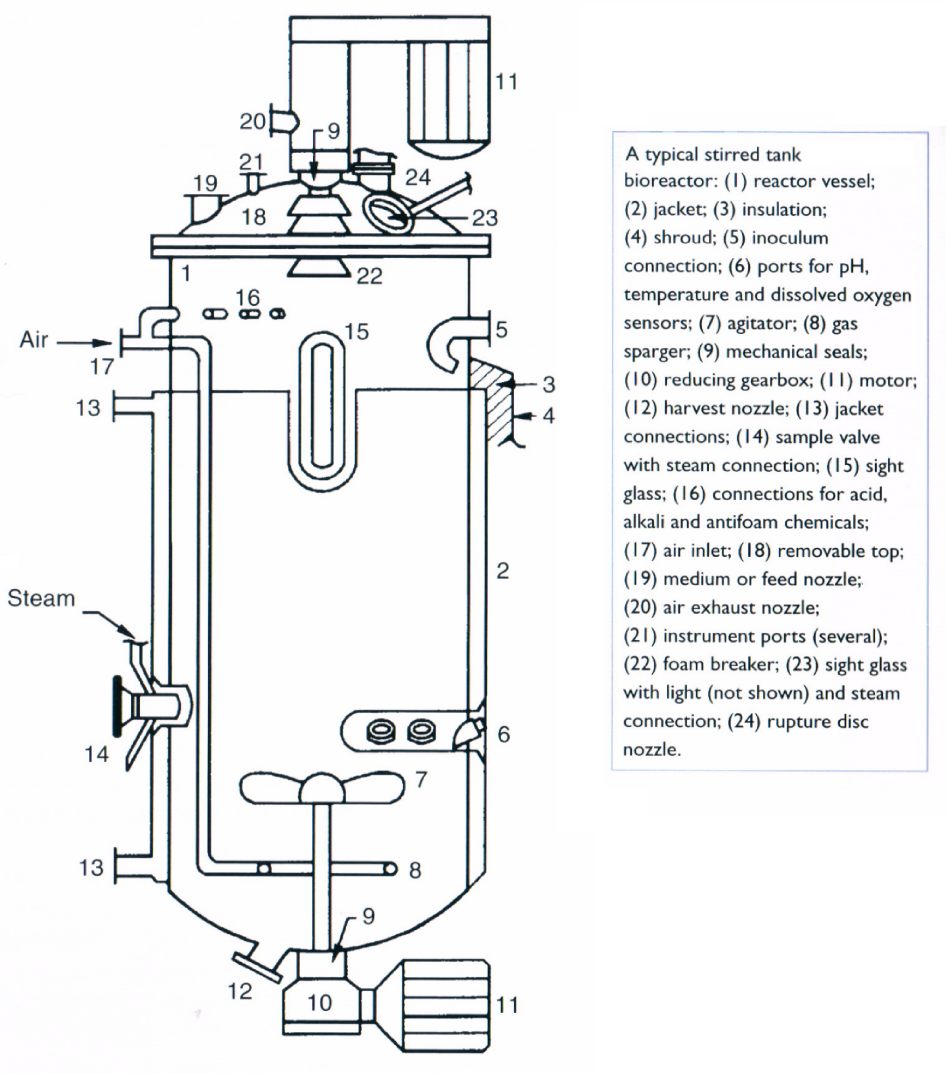

Figure 2
Pilot plant-scale stirred tank bioreactor. From Chisti, Yusuf [6]

As suggested above, the bioreactor's fluid-dynamics implies a certain trade-off between Mass transfer capability and the Shear Stress. In one hand, the Mass transfer is related to the bioreactors capability to homogeneously dilute a gas within the medium's volume; normally the higher possible cell concentration will be desired. To achieve it a maximum oxygen transfer rate (OTR) will be a must and that's only possible for turbulent flow conditions, which are obtained for high rotating speeds and using aggressive turbines and baffles. On the other

hand, Shear Stress summarizes all the forces in a bioreactor that can damage certain cell types like mammalian cells. This is due to the lack of a thick cell wall which makes them especially sensitive to a number of physical situations; the micro-eddies produced under turbulent conditions; the different types of collisions among cells, against the walls and the impeller, and other phenomena related to the bubbles formation, coalescence and rupture may have a great impact on Shear Stress. It becomes obvious that the design of a bioreactor intended to provide a high oxygen mass transfer will go in the opposite direction than another to obtain low level of Shear Stress conditions. However, a proper stirring is the key factor to obtain a homogeneous mixing to avoid gradients of concentration, sedimentation of solids and other physical conditions. To accomplish such requirements it is important to keep in mind that the bioreactor will have to respect some dimensional ratios regarding the vessel, turbine and baffles. Figure 3 shows the most common ratios for three different types of turbines.

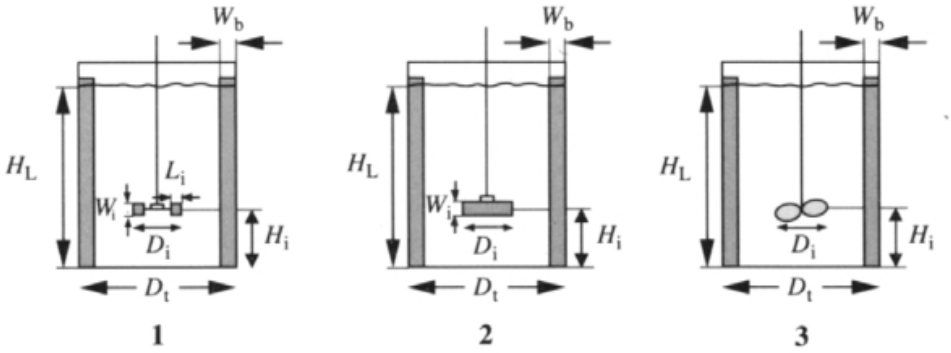

Impeller	D_t/D_i	H_L/D_i	H_i/D_i	Baffles	
				W_b/D_t	Number
1. Rushton turbine $W_i/D_i = 0.2$, $L_i/D_i = 0.25$	3	3	1	0.1	4
2. Paddle $W_i/D_i = 0.25$	3	3	1	0.1	4
3. Marine propeller Pitch = D_i	3	3	1	0.1	4

Figure 3
Standard dimensional ratios for different types of turbines. From P. M. Doran [13]

The selected turbine depends on said compromise between the turbulence and the shear stress produced. Typically, robust and prolific cells like bacteria and yeast require the use of Rusthon turbines with vigorous aeration by means of sparging; this generates a radial flow pattern featuring maximum turbulence even for moderate rotating speeds. However, for more delicate species like embryonic stem cells, unbaffled vessels with headspace aeration and paddle stirring may be preferred due to the harmless rotational laminar flow produced. Productive animal cell lines are usually the ones that may require bigger effort to find the best configuration to adapt them to the suspended growth conditions. Figure 4 shows the three basic flow patterns depending on the stirring method. Nevertheless, geometry is not the only

parameter affecting the flow topology. Rotating speed, Density and viscosity of the medium, and bubbles coalescence are additional variables affecting the flow's behavior. This is usually represented through the Power number N_p and the Reynolds number Re_i for a given geometry, medium's rheology and stirring conditions.

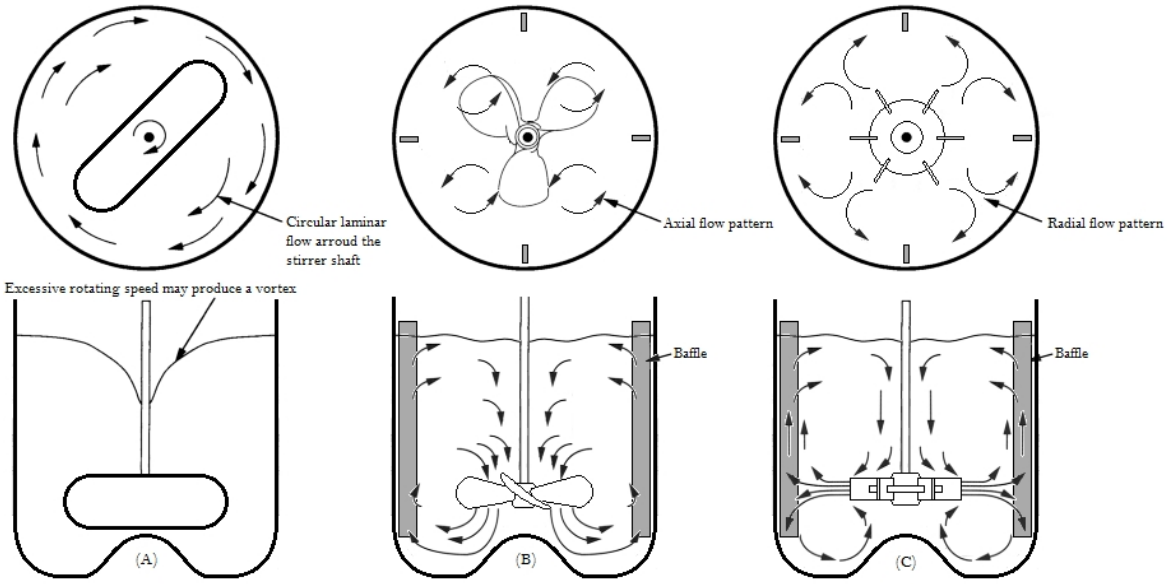

Figure 4

A) Unbaffled vessel with paddle/bar for Embryonic Stem Cell, B) Baffled vessel with marine propeller or pitch blade turbine for productive animal cells like CHO, C) Baffled vessel with Rushton turbine for microbial culture. Adapted from [13] [14] [15]

The Reynolds number Re_i is used to predict the Laminar or Turbulent behaviour within some fluid. For instance, a non aereated Newtonian medium being stirred within some of the bioreactor configurations represented above will typically show a Laminar flow for Re_i < 10, and a Turbulent flow for Re_i > 10,000. Anything in between is considered as a Transition regime and both types of flow can be found within the volume.

$$Re_i = \frac{\rho \cdot N_i \cdot D_i^2}{\mu}$$

Where:

- ρ [kq/m^3] : Fluid's density
- μ [kg/m·s]: Fluid's viscosity
- D_i [m]: Impeller diameter
- N_i [rps]: Stirrer speed

The power number N_p regards only to the mechanical energy applied to the medium within the bioreactor; A difference must be made between the actual energy applied to the fluid and the total electrical power consumed by the stirrer motor, since the bioreactor's

power input P is not taking into account the motor efficiency nor the loss of energy due the mechanical parts (gearbox, seal rings, etc…).

$$N_p = \frac{P}{\rho \cdot N_i^3 \cdot D_i^5} = \frac{2 \cdot \pi \cdot N_i \cdot M}{\rho \cdot N_i^3 \cdot D_i^5}$$

Where:

- P [W/m^3]: Power input
- M [N·m]: Induced torque due to the impeller's friction and the drag of the fluid.
- ρ [kq/m^3] : Fluid's density
- D_i [m]: Impeller diameter
- N_i [rps]: Stirrer speed

The N_p - Re_i ratio it has been determined experimentally for different types of impellers and bioreactor configurations. The figure below displays such relationship for the bioreactor configurations shown in figure 3 and non-aereated Newtonian fluids. It can be observed how the power number N_p tends to become constant within the turbulent regime and lower than under laminar flow conditions. Next section will explain how this is related to the shear stress.

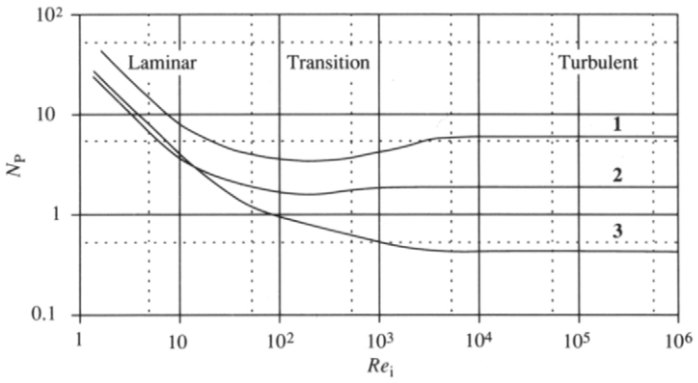

Figure 5

N_p - Re_i experimental correlations for: Rushton turbines (1); downward pumping Pitch-blade turbines (2); and Marine propellers (3) in baffled bioreactors and non-aereated Newtonian fluids. From [13]

Despite that the previous expressions have been defined just for non-aerated Newtonian fluids, they can be used for a rough design of the bioreactor mixing system. However, aeration is usually a key point for most of purposes in biotechnology since the use of non-aereated systems is commonly restricted to research applications with very shear sensitive cell species. Therefore, the calculation of the power input P needs to take into account the reduction of the fluid's density due to the presence of small bubbles; this is made through empiric correlations obtained for every bioreactor configuration depending on the gas volume flowing through the bioreactor, the following equation is defined for Rushton turbines in baffled vessels [6] [16]:

$$P = 0.783 \cdot \left(\frac{P_0^2 \cdot N_i \cdot D_i^3}{Q^{0.56}} \right)^{0.459}$$

Where:

- P_0 [W/m^3]: Power input under unaerated conditions
- Q [m^3/s]: Volumetric aeration rate
- D_i [m]: Impeller diameter
- N_i [rps]: Stirrer speed

For a more accurate assessment on the physical phenomena affecting the mixing capability in aereated systems, as well for non-Newtonian fluids, a further detailed and deeper explanation is provided by references [6] [7] [13] [16].

2.3 Shear Stress

After the previous introduction on the basis of stirred tank bioreactors design, in this section the most common methodology for estimating the shear stress in stirred tank bioreactors will be presented. The shear stress term is used as an ambiguous concept regarding any hydrodynamic conditions leading to the cell death or a slowing down of the cell growth or product synthesis. This may happens due to different reasons when cells are brought under a gradient of forces produced by spatial differences in the fluid's velocity; such situation is not significantly harmful when all forces are applied in the same direction (laminar flow). In this case, cells are trapped within the flow in a rotational movement induced by the differences in the fluid's velocity. However, when forces are distributed in different directions (shear forces) the possibility of cell damaging is dramatically increased, this happens for high stirring and gas sparging rates (Turbulent flow). In stirred tank bioreactors, the Turbulent regime is featured by the chaotic formation of eddies around the impeller and baffles, the length of the fluid eddies depends on the impeller's geometry, its size and the rotational speed. The faster the stirring is the shorter eddies are.

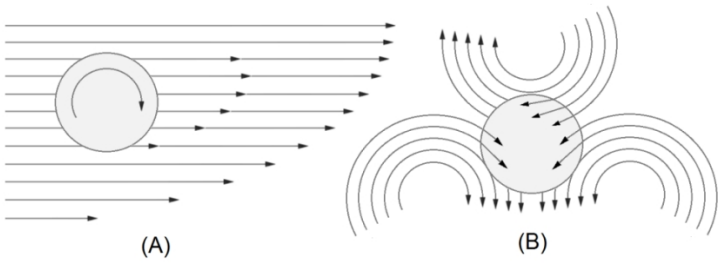

Figure 6
Freely suspended particles: (A) Under laminar flow conditions; (B) Under turbulent flow conditions

A straightforward method for estimating the shear stress is by comparison of the mean length λ of the fluid eddies and the diameter of the biocatalyst [6] [13]. The bigger the biocatalyst is the more harmful eddies are, that's why small organism like bacteria and yeast, besides of their protective cell wall, are so insensitive to the high turbulences produced by fermenters, since they become easily trapped by the eddies without experiencing a significant

shear stress. On the other hand, bigger cell species like animal, plant and fungi cells are definitely more sensitive to the distribution of the shear forces within the fluid. Those lines which are not adapted to grow in suspension demand special care since they will grow forming relatively big cell flocks attached on microcarrier beads or embryonic bodies which can be easily damaged by bead to bead collisions and small eddies.

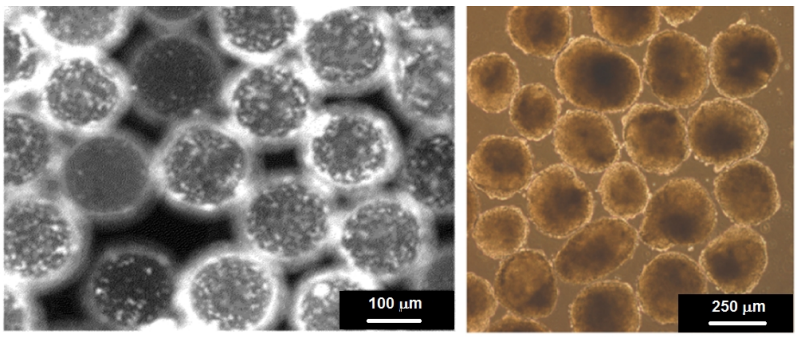

Figure 7
(A) Cell flocks on microcarriers [17]; (B) Embryonic stem cells [18].

The mean length λ of the fluid eddies can be calculated through the Kolmogorov scale if the type of flow can be considered as isotropically turbulent:

$$\lambda = \left(\frac{\nu^3}{E}\right)^{1/4}$$

Where:

- ν [m^2/s]: Kinematic viscosity of the fluid.
- E [m^2/s^3]: Turbulent energy dissipated. In order to avoid an underestimation of the dissipated energy it's important to decide whether the turbulent regime is isotropically distributed along the whole volume or just around the impeller, according to the size of the bioreactor:

Turbulence is dissipated isotropically along the whole volume: $E = \frac{P}{\rho \cdot V_l}$

Turbulence is concentred around the impeller: $E = \frac{P}{\rho \cdot D_i^3}$

Where:

- P [W/m^3]: Aereated or unaerated power input calculated as explained in the previous section.
- ρ [kq/m^3] : Fluid's density.
- D_i [m]: Impeller diameter.
- V_l [m^3]: Total volume of the fluid.

In Stirred tank bioreactors the shear rate can be calculated through the following equation [6]:

$$\gamma = k_i \cdot \left(\frac{4 \cdot n}{3 \cdot n + 1}\right)^{n/n-1} \cdot N_i$$

Where:

- n []: Flow index of the fluid, equals 1.0 for all Newtonian liquids which are any sort of aqueous solutions and most of culture media.
- N_i [rps]: Stirrer speed
- k_i [m]: Parameter depending on the impeller type, Typical values are:
  - 11-13 for six-bladed disk turbines
  - 10-13 for paddle impellers
  - ~ 10 for propellers
  - ~ 30 for helical ribbon impellers

The shear rate can be converted to a parameter known as the shear stress through the following expression:

$$\tau = \gamma \cdot \mu$$

Where:

- μ [kg/m·s]: Fluid's viscosity

Other cell damaging phenomena different than turbulence are related to the dynamics of the aeration through gas sparging, bubbles formation, coalescence and rupture can dissipate energies producing high shear forces around the event, this is particularly important for the bursting bubbles reaching the bioreactor headspace. As the bubble rises some cells attach to its surface, when the bubble approaches the surface the liquid is pushed into a thin film hemispherical shape until tension forces become too weak to stand the bubbles buoyancy, the rupture of the film is produced and high acceleration forces are released so the cells attached around the bubble's surface are brought under high pressure conditions, afterwards upwards and downwards jets are produced. The shear forces produced during this sequence use to be higher enough to destroy the wall of most animal cells.

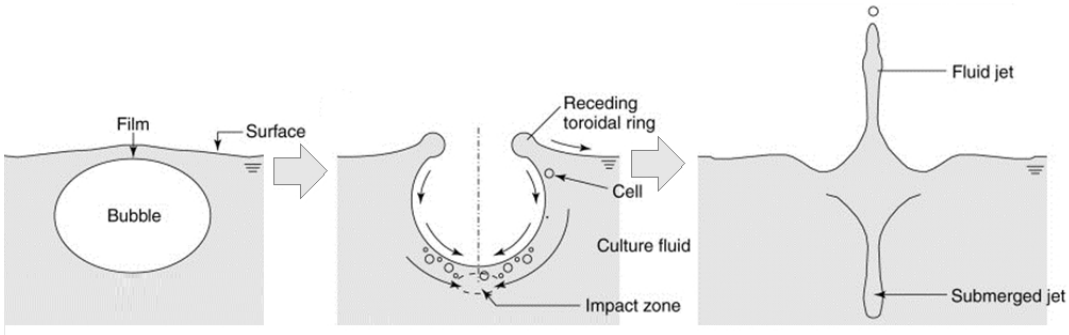

Figure 8
Bubble burst at the liquid-gas interface [19].

For both cases, turbulent eddies and bursting bubbles, some protective products may be added to the medium. On one hand, the use of thickening additives to increase the viscosity gives as a result longer and less dangerous eddies. On the other hand, surfactants minimize the magnitude of the bubble bursting as well as avoid the cell attachment to the bubbles surface.

2.4 Mass transfer

Oxygen is usually considered as the most important nutrient in aerobic processes due to the fact that its depletion implies an immediate slowdown of the cell growth or metabolite production. That's why it is imperative to ensure a proper oxygen supply to the cells. However, its reduced solubility in water makes it a pretty difficult task, which is strongly influenced by an important number of variables related to the bioreactor's geometry, the aeration system, the stirring system and the medium's rheology. In most types of bioreactors, the aeration is performed by means of some sort of submerged gas sparger or microdiffusor used to produce bubbles that will transfer the oxygen and other gasses from the gas phase to the liquid phase through its surface. Flick's law states that the gas flux J through the walls of a steady bubble is proportional to the oxygen concentration gradient in the direction of the transport (between both phases):

$$J = -D \cdot {}^{dC}/_{dx}$$

Where D is the diffusivity, dC/dx is the transfer coefficient and dC is the increment of oxygen concentration or driving force. Such definition was used by Whitman (1923) for the development of the first and simplest theory on gas-liquid mass transfer, known as the two-film model.

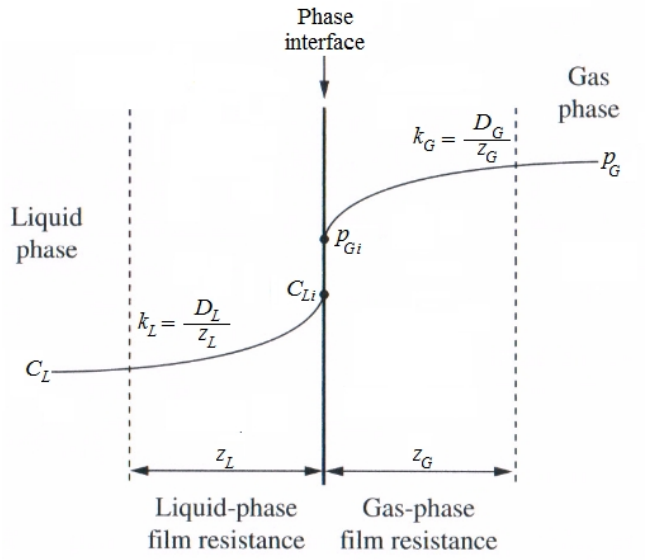

Figure 9
Whitman's two-film model. Adapted from [7] [16] [20]

Two attached films are described to explain the properties of the medium between both phases. Within the gas film, oxygen is diffused towards the interface driven by an increment of the partial pressure and then is decreasingly transferred into the liquid film. The overall oxygen flux J^O known as oxygen transfer rate (OTR) is hence limited by the film resistances at both sides of the phase boundary. This can be written as follows:

$$J^O = k_L \cdot (C_{Li} - C_L) = k_G \cdot (p_G - p_{Gi})$$

Nevertheless, the interfacial values C_{Li} and p_{Gi} are not directly measurable. That's why mass transfer rate is normally written in function of the oxygen saturation concentration in the bulk liquid C_L^* and the global transfer coefficient K:

$$J^O = K \cdot (C_L^* - C_L)$$

It can be demonstrated that the global transfer coefficient K_L may be written as the combination of the gas and liquid mass transfer coefficients k_G, k_L:

$$\frac{1}{K_L} = \frac{1}{H \cdot k_G} + \frac{1}{k_L}$$

Where:

- H [l·atm/mol]: Is the Henry's constant under certain medium and temperature conditions.

The reduced solubility of oxygen in water makes commonly accepted that the global mass transfer coefficient approximately equals the liquid mass transfer coefficient. That means that the main resistance happens within the liquid film. The volumetric OTR is then obtained multiplying the overall oxygen flux J^O by the gas-liquid interfacial area per unit of volume of the bioreactor a.

$$\text{OTR} = k_L \cdot a \cdot (C_L^* - C_L)$$

The $k_L{\cdot}a$ product is an essential parameter used to express how fast oxygen is transported from the gas phase to the liquid where is consumed by the cells. As well as to estimate the potential of a bioreactor to support a certain cell concentration. The $k_L{\cdot}a$ is usually referred as the most important criterion for bioprocess scale up. However, the complexity to separately measure both parameters k_L and a, makes necessary its use as a single parameter.

Due to said importance, different methods and numerous empirical correlations have been developed to measure or estimate its value. The measurement methods of the $k_L{\cdot}a$ are classified depending on whether they are performed with or without oxygen consumption. A number of chemical methods have been described, however they are not currently very well accepted due to their influence in the properties of the culture broth that could lead to overestimated values of the $k_L{\cdot}a$. Physical methods are by far more accurate and reliable, they are usually based on the global mass balance equations like:

$$\frac{dC_L}{dt} = \text{OTR} - \text{OUR} = k_L \cdot a \cdot (C_L^* - C_L) - \text{OUR}$$

Where:

- dC_L/dt [mol/s]: Oxygen accumulation rate.
- OUR[mol/l·s]: Oxygen uptake rate or cell's volumetric oxygen consumption.

A difference can be made between the available measurement methods depending on whether oxygen consumption exists or not. The most widely used procedures are the Dynamic method and the Gas phase global balance method.

The simplest version of the Dynamic method is performed without cells (OUR = 0) and is based on the measurement of the rise and decay times of the dissolved oxygen concentration during the absorption and desorption of oxygen. The first step consists on the aeration of the bioreactor with air or pure oxygen until the dissolved concentration in equilibrium with the gas phase is reached, that's the saturation concentration. The whole process needs to be realized using some medium, stirring rate and bioreactor configuration relevant of the culture conditions. The second step consists on replacing the air flow with nitrogen to force a total desorption of oxygen (C_L = 0). Thus, the mass balance equation within the liquid state is modified as follows:

$$\frac{dC_L}{dt} = -k_L \cdot a \cdot C_L$$

The general solution is:

$$C_L = C_L^* \cdot e^{-k_L \cdot a \cdot t} \mid t = 0 \rightarrow C_L = C_L^*$$

Thus, if logarithms are taken on both sides of the general solution, $k_L{\cdot}a$ may be found as the slope of the linear regression of the logarithm of the oxygen extinction profile divided by the saturation concentration:

$$ln\left(\frac{C_L}{C_L^*}\right) = -k_L \cdot a \cdot t$$

This formula may be found in several books and reviews on bioprocess engineering and assumes that the k_L factor is the same for oxygen and nitrogen. Nevertheless, this is not an accurate approach since the nitrogen's solubility in water is approximately half of oxygen's solubility [21]. Such difference lead to a slower desorption of oxygen than absorption. Thus, it makes sense to distinguish between two different mass transfer coefficients depending on desorption or absorption:

$$ln\left(\frac{C_L}{C_L^*}\right) = -k_{Des} \cdot t$$

During the third step, reoxygenation of the bioreactor is produced by aeration with air or pure oxygen at the culture conditions flow rate. This time, just the consumption term is removed of the mass balance equation:

$$\frac{dC_L}{dt} = k_L \cdot a \cdot (C_L^* - C_L)$$

The general solution is:

$$C_L = C_L^* \cdot \left(1 - e^{-k_L \cdot a \cdot t}\right) \mid t = 0 \rightarrow C_L = 0$$

Therefore, the $k_L{\cdot}a$ can be solved the same after taking logarithms on both sides of the equation:

$$ln\left(1 - \frac{C_L}{C_L^*}\right) = -k_L \cdot a \cdot t$$

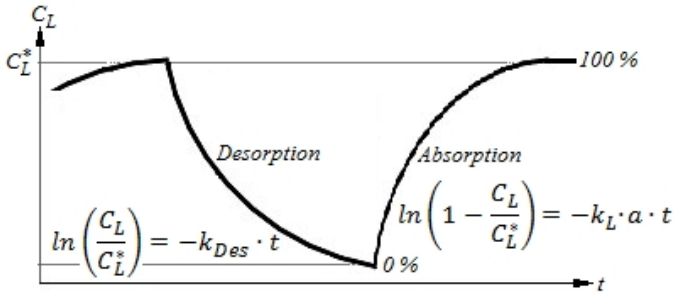

Figure 10
Profile of the dissolved oxygen after application of the Dynamic method

The Dynamic method is widely accepted to be used for well mixed bench scale bioreactors due to its accuracy and simplicity. Limited only by the transient response of the oxygen probe. Fortunately, nowadays this is not a common situation, since the transient response of the currently available optical dissolved oxygen sensors uses to be fast enough for almost any application (a few seconds).

The Gas phase global balance method can be applied under cell growth conditions (OUR ≠ 0). It takes into account the global balance at steady state, which implies the existence of some sort of control loop to keep the dissolved oxygen concentration constant.

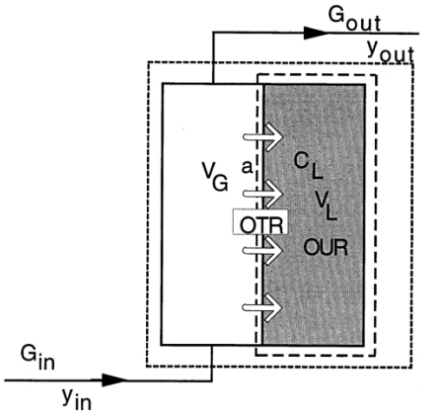

Figure 11
Schematic representation of a generalized aeration system showing phase boundaries. From I. Betts J. & Baganz F. [22].

Figure 11 represents a generalized model of the phase boundaries within a bioreactor. An inlet gas flow G_{in} with a certain molar fraction of oxygen y_{in} enters the gas phase of the bioreactor V_G where some of the oxygen diffuses towards the liquid phase V_L through the interfacial area a driven by the concentration gradient. No matters if diffusion happens just across the headspace surface or the bubble surface, the mentioned control loop modifies the $G_{in} \cdot y_{in}$ product to keep the dissolved oxygen concentration C_L constant so the transfer rate equals the consumption rate ($\mathrm{OTR} = \mathrm{OUR}$) and the concentration y_{out} of the outlet flow $G_{out} = G_{in}$ is decreased. This is written as:

$$G_{in} \cdot (y_{in} - y_{out}) = \mathrm{OUR} \cdot V_L$$

Where from the global mass balance equation:

$$\mathrm{OUR} = \mathrm{OTR} = k_L \cdot a \cdot (C_L^* - C_L)$$

Then the $k_L \cdot a$ product can be solved:

$$k_L \cdot a = \frac{G_{in} \cdot (y_{in} - y_{out})}{V_L \cdot (C_L^* - C_L)}$$

The Gas phase global balance method shows two major advantages. It is well suited for large scale bioreactors and OUR estimation is implicit. However, the need for a well modelled gas mixing system and highly sensitive mass spectrometers makes the procedure a complex and expensive option strongly dependent on the accuracy of the inlet and outlet gas composition measurements, since tiny calibration errors can lead to significant errors for low level consumption rates.

Additionally to the methods available for the measurement of the $k_L \cdot a$ product, numerous empirical correlations have been defined for different bioreactor topologies, mediums and stirring systems. However, such correlations cannot be directly extrapolated unless no significant changes are made in comparison with the reference conditions. For instance, the addition of surfactants or other chemicals produces considerable discrepancies between the theoretical and actual $k_L \cdot a$ values. Nevertheless, depending on the combination of the correlated variables, stirring rate N, superficial gas velocity V_s, effective viscosity μ_0 or several dimensionless parameters like the Reynolds number, certain empirical correlations can still be useful to help on the design of bioreactors and their scale up.

A very popular correlation for non-viscous Newtonian fluids in stirred tank bioreactors is the one proposed by Van't Riet (1979), stating that no influence exists of stirrer geometry on mass transfer, this is a controversial issue that has been investigated by numerous authors and a number of correlations have been proposed under different experimentation conditions. The equation below shows the applicable form to such correlations, changing the value of the coefficients:

$$k_L \cdot a = C \cdot V_s^{\alpha} \cdot \left(\frac{P}{V_L}\right)^{\beta} \cdot \mu_0^{\gamma}$$

Where:

- C []: Is the constant parameter depending on the vessel's geometry and the stirrer type used.
- P/V_L [W/l]: Total power input per volume.
- V_s [m/s]: Superficial gas velocity.
- μ_0 [Pa·s]: Effective viscosity

The following table shows the exponent values in the previous equation for some common correlations and working conditions. A more extensive explanation on other correlations in different working conditions and mass transfer parameters prediction can be found in the review by Garcia-Ochoa (2009) [16].

Autors	System	N [rpm]	β	α	γ	Volume (L)	Stirrer Type
Yagi and Yoshida (1975)	Water + glycerol	132	0.8	0.3	−0.4	12	6FBT
	CMC / PANa		0.8	0.3			
Figueiredo and Calderbank (1979)	Water	–	0.6	0.8	–	600	FBT
Van't Riet (1979)	Water	–	0.4	0.5	–	2–2600	Any
Nishikawa et al. (1981)	Water Millet /CMC	144	0.8	0.33	−0.5	2.7–170	FBT & FBP
		144					
Chandrasekharan and Calderbank (1981)	Water	–	0.55	$0.55 \cdot D^{-1/2}$		50–1430	FBT
Davies et al. (1985)			0.8	0.45		20–180	6FBT
Kawase and Moo-Young (1988)			1.0	0.5			
Ogut and Hatch (1988)		54		0.7		100	6FBP
		30		0.5	−0.4		
Linek et al. (1991)	Water		0.65	0.4		20	6FBT
			1.1				
Pedersen et al. (1994)	Water+xanthan	162	–	0.5–0.7	–	15	Two-6FBT
Gagnon et al. (1998)			0.6–0.8	0.5		22	6FBT
Arjunwadkar et al. (1998)	Water + electrolytes / CMC		0.68	0.4–0.58		5	FBT & PBT
Vasconcelos et al. (2000)	Water		0.62	0.49		5	Two-6FBT
Garcia-Ochoa and Gomez (1998, 2001)	Water/Water+xanthan	120	0.6	0.5–0.67	−0.67	2–25	1,2-FBT, CBT, FBP,
					−1*		CBP, PBP
Puthli et al. (2005)	Water+electrolytes./CMC		0.57–0.98	0.53	−0.84	2	1,2-FBT, FBP, PBP

* Casson viscosity model.
Acronyms for Stirrers on Table 2: CBT: Curved Blade Turbine. CBP: Curved Blade Paddle. FBP: Flat Blade Paddle. FBT: Flat Blade Turbine. PBP: Pitched Blade Paddle. PBT: Pitched Blade Turbine. Two-6FBT: Two stirrers of the type indicated (6FBT, in the example).

Table 1
Correlation parameters for non-viscous Newtonian mediums in stirred tank bioreactors.
Adapted from G. Ochoa F. & Gomez E. [16]

2.5 Objectives

Once identified the key concepts involved in bioreactor design, the goals of the thesis can be stated:

1st. Development and construction of a state-of-the-art single-use Minibioreactor system, intended for a vast range of species including cells with therapeutic interest. The system must meet the following general features:

- To enable Multi-parallel experimentation and being suitable for High Throughput Screening applications in Biotechnology.
- To take long term experiments. No less than two weeks of continuous operation.
- Control of the most common culture conditions (Thermoregulation, Mixing and aeration)
- Control and/or monitorization of the most common physical parameters (Dissolved Oxygen, pH, Cell density)

2nd. Feasibility study on the development of a state-of-the-art DO measurement system based on fluorescence, appropriate for testing the proposed new OUR estimation method.

3rd. Feasibility study on a continuous Oxygen Uptake Rate estimation method (OUR), based on the accurate control of the dissolved oxygen concentration (DO) that avoids the cell stress that happens with the dynamic method, as well as its development and implementation.

References:

[1] Langdom S., «Basic principles of Cancer cell culture methods in Molecular Medicine,» *Cancer Cell Culture: Methods and Protocols,* vol. 88, pp. 3-15, 2004.

[2] Martín Casanovas, "Cultivo de tejidos," in *Enciclopedia de la ciencia y la tecnología*, vol. II, Barcelona, Ediciones Danae, 1974, pp. 874-876.

[3] B. F. J. L. G. D. Doig S, «High-Throughput screening and process optimization,» de *Basic Biotechnology*, Cambridge, 2006, pp. 289-305.

[4] B. F. J. L. G. D. Doig S, "High-Throughput screening and process optimization," in *Basic Biotechnology*, Cambridge, 2006, pp. 289-305.

[5] B. F. I Betts J., «Miniature Bioreactors: Current practices and future opportunities,» *Microvial Cell Factories,* p. 5:21, 2006.

[6] C. Y., «Bioreactor design,» de *Basic Biotechnology*, 2006, pp. 181-200.

[7] N. H., «Mass transfer,» de *Basic Biotecnology*, 2006, pp. 201-217.

[8] S. Peppers, "DoE Helps Optimize a Cell Culture Bioproduction System," *BioProcess International,* pp. 24-27, 2009.

[9] S. M. David Zhang, "Creation of a well Characterized Small Scale Model for High-Through Process Development," *Bioprocess International,* vol. 7, no. 9, pp. 28-31, 2009.

[10] A. A. Z. D. B. K. K. J. R. M. C. J.Gifford, «An Efficient Approach to Cell Culture Medium Optimization - a statistical method to medium minxing,» de *Animal Cell Technology Meets, Proceedings of the 18th ESACT Meeting* , Granada, 2003.

[11] C. Ratledge, "Biochemistry and physiology of Growth and Metabolism," in *Basic Biotechnology*, Cambridge, Cambridge University Press, 2006, pp. 26-54.

[12] P. M. Doran, "Homogeneous Reactions," in *Bioprocess Engineering Principles*, Kidlington, Oxford, Academic Press, 2013, p. 636.

[13] P. M. Doran, “Fluid Flow and Mixing,” in *Bioprocess Engineering Principles*, Sydney, Elsevier Science & Technology Books, 1995, pp. 141-153.

[14] R. Mirro and K. Voll, “Which impeller is Right for your Cell Line? A guide to Impeller Selection for Stirred-Tank Bioreactors,” *BioProcess International,* pp. 52-57, 2009.

[15] I. D. G. &. M. S. K. Allison Van Winkle, “Small-Scale Bioreactors forthe Culture of Embryonic Stem Cells,” in *Embryonic Stem Cells - Basic Biology to Bioengineering*, Rijeka, Croatia, InTech, 2011, pp. 73-88.

[16] E. G. F. Garcia-Ochoa, “Bioreactor scale-up and oxygen transfer rate in microbial processes: An overview,” *Biotechnology Advances,* no. 27, pp. 153-176, 2009.

[17] S. K. S. F. V. Kevin Robert McCarthy, “Synthetic microcarriers for culturing cells”. USA Patent US20120288912 A1, 29 6 2009.

[18] J. A. Hunt, “Regenerative medicine: Materials in a cellular world,” *Nature Materials,* no. 7, pp. 617 - 618, 2008.

[19] Y. Chisti, “Animal-cell damage in sparged bioreactors,” *Trends in Biotechnology,* vol. 18, no. 10, p. 420–432, 2000.

[20] P. M. Doran, “Mass Tranfer,” in *Bioprocess Engineering Principles*, Kidlington, Oxford, Academic Press, 2013, pp. 379-433.

[21] L. Gevantman, «Solubility of selected gases in water,» de *CRC Handbook of Chemistry and Physics*, Elsevier Science B.V., 2003, pp. 82-83.

[22] U. v. S. I. W. M. Pierre-Alain Ruffieux, “Measurement of volumetric (OUR) and determination of specific (qO2) oxygen uptake rates in animal cell cultures,” *Journal of Biotechnology 63 (1998) 85–95,* no. 63, pp. 85-95, 1998.

State of the art.

To provide a full coverage on the basis of the work here presented, the state of the art cannot be explained pointing out only the OUR estimation techniques, but also by referring the means used to measure the dissolved oxygen (DO) and the features of the bioreactors where the cell cultures are carried out, that's why this chapter is divided into three sections. The first section will provide a complete review about the most relevant developments on Minibioreactor systems with special attention on those intended for animal cell culture; basically they are miniaturised versions of the well-known bench-scale bioreactors or fermenters. The second section will be focused on the explanation of the most straightforward technique for DO measurement (Fluorescence quenching) and its different possible implementations. Finally, the mass balance equations and the three previously reported OUR estimation methods will be introduced.

3.1 Minibioreactor systems.

During the last decade a significant number of systems and several reviews have been developed and published exposing the advances and motivations on the design of Minibioreactor systems for screening and bioprocess development [1] [2] [3]. Among the features of the reported systems; the reduced culture volume, usually no bigger than 500 ml; innovations regarding the measurement technologies, in special for the pH and dissolved oxygen (DO) and capability for multiple experimentation on high throughput screening (HTS) were stablished as major cornerstones. Additionally, some of the products linked to such developments were approached from a disposable product concept point of view, which currently has become a well stablished business within the biopharmaceutical sector [4] [5] [6]. The most successful products are appointed in table 1. Their suitability to be used for animal cell culture cannot be judged just on the features herein shown. Obviously, the concepts presented across the introductory chapter (mass transfer, shear stress, mixing power, etc…), should also be carefully taken into account to evaluate the appropriateness of any of the systems for a specific cell line or strain.

Name	Type	Volume [ml]	Stirring/Aeration	Instrumentation	Number of Channels	Disposable
BioLector™ m2p Labs [7] [8] [9]	Multi-well plate	0.1-1	Shaker / Headspace	Non-invasive DO, pH and Scattering probes	6-96	Yes
SimCell™ Seahorse Biosciences [10] [11] [12]	Microfluidic cartridge	0.3-0.8	Gas permeable membranes	Non-invasive DO, pH, CO_2 and OD probes	6x200	Yes
m-24™ Pall [13]	Multi-well plate	3-5	Shaker / Permeable membranes	Non-invasive DO, And pH	24	Yes
AMBR15™ TAP / SSB [14] [www.tapbiosystems.com]	Stirred tank	10-15	Turbine / Sparger	Non-invasive DO, And pH	24-48	Yes
AMBR250™ TAP / SSB [15] [www.tapbiosystems.com]	Stirred tank	100-250	Turbine / Sparger	Non-invasive DO, And pH	12-24	Yes
DASbox™/BioBLU© DASGip / Eppendorf [www.dasgip.com]	Stirred tank	100-250	Turbine / Sparger	Invasive pH and DO electrochemical probes	4-32	Yes
Mini Bio™ Applikon [www.aplikon.com]	Stirred tank	250-1000	Turbine / Sparger	Invasive pH and DO, as well other conventional probes	1xN	No

Table 1

Currently most successful Minibioreactors products appropriate for animal cell culture.

- BioLector™ [7] [8] [9] was introduced in 2009, intended for monitoring the most critical process parameters i.e., pH, DO, biomass concentration as well as some fluorescent indicators via non-invasive optical probes (Price > 60,000 €). The product consists of an incubation chamber featuring measurement instrumentation and a shaking tray where a disposable multi-well plate needs to be placed. The glass made bottom of each individual well is used to hold the pH and DO fluorescent sensors, as well as to perform the cell concentration measurement by means of light back-scattering. Additionally, the flower shaped vessel walls mimics the behaviour of baffles in stirred tanks, this and its reduced culture volume allows to obtain high mass transfer rates ($k_L{\cdot}a$ = 100 to 350 h^{-1}) which makes the system useful not just for animal cell culture but for microbial applications. m2p-Labs has recently introduced the RoboLector™ which provides

robotized liquid handling, adding new capabilities to the BioLector™ like automatic sampling and seeding, media preparation and fed-batch operation. This makes it an especially well suited instrument for specific screening tasks (e.g., transfection processes). However, in spite of such interesting features, the fact that shaking is not a widely used method during the production stages, as well as the lack of pH and DO controls, limits the use of BioLector™ for scale-up or screening studies under controlled conditions.

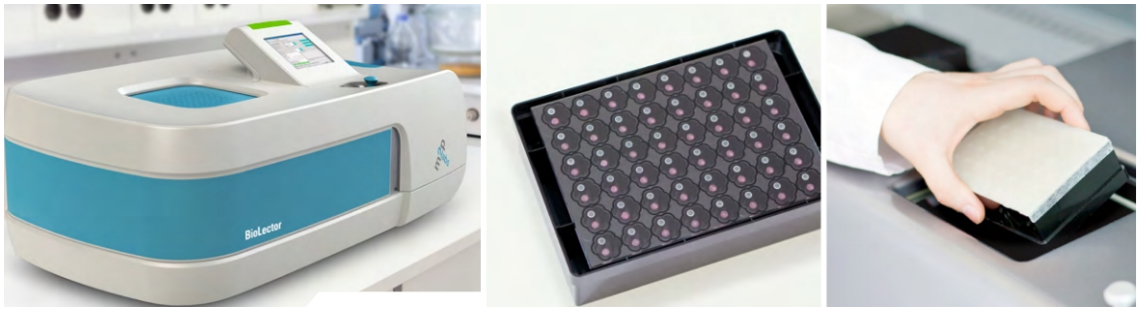

Figure 1
BioLector™ parallel micro-bioreactor by m2p-Labs.

- SimCell™ [10] [11] [12] is by far the most complex and expensive product intended for screening, media and process optimization. Introduced in 2009, the system is animal cell oriented, fully robotized and its experimentation throughput is unmatched i.e., up to 1200 simultaneous experiments (Price > 830,000 €). The cultivation unit consist of a 6 chambers cartridge where mass transfer is performed through gas permeable membranes ($k_L{\cdot}a$ = 1 to 10 h^{-1}), liquids handling (pH control, feeding, seeding and sampling) is done via septum, pH, DO and DCO_2 are measured by means of fluorescent sensors just like the BioLector™ does, and cell concentration is measured by means of forward light scattering OD. In order to keep cells in suspension, the cartridges are held by a sort of spinning carrousel inside the incubation modules, periodically the cartridges are moved one after the other from the incubators through the sensing, sampling and dispensing modules and back to the incubators.

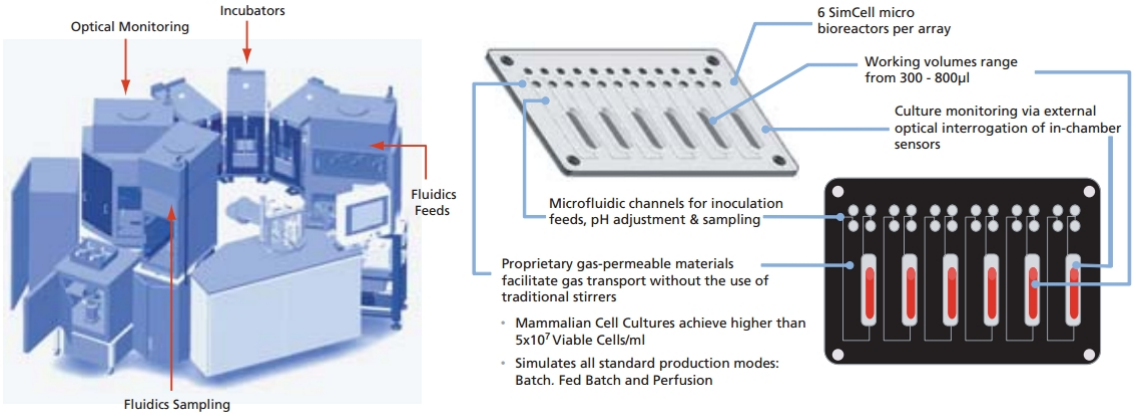

Figure 2
SimCell™ micro-bioreactor system by Seahorse Biosciences.

The greatest obvious advantage of the SimCell™ system is a stunning number of concurrent possible experiments; this makes it currently the most powerful tool for DoE and hence for process development. However, despite that a good reproducibility with bench-top bioreactors has been reported, a proper scale-up assessment cannot be done due to the difficulty to compare other scale-up criteria different than the $k_L{\cdot}a$ such as the power number N_p or the stirring rate. Besides, its complexity of use and an unaffordable price makes the SimCell™ system a non-realistic solution for most companies.

- μ-24™ [13] was initially developed and introduced by MicroReactor Technologies in 2007 and is currently distributed by the companies Pall and Applikon (Price ≈ 80,000 €). It shows some similarities with the BioLector™, on one hand the cultivation unit also consists of a disposable micro-well plate with embedded pH and DO fluorescence sensors that must be attached to a shaking tray inside an incubation chamber. However, on the other hand the vessels of the μ-24's plate may hold a slightly bigger volume, the temperature of each vessel can be individually controlled and the aeration is performed through a gas permeable membrane placed on the bottom of the vessel, which is capable to supply oxygen enough even for some microbial applications ($k_L{\cdot}a$ = 33 to 57 h^{-1}). The BioLector was designed just for monitoring, on the contrary the μ-24 is meant for the pH and DO control through the individual mixing of different gas supplies.

  Again, a system that shows some interesting features for screening applications but lacks of some other essential requirements useful for development of bioprocesses, e.g., an on-line, non-invasive cell density related measurement instrument, and some mechanism for the liquids handling, at least for culture sampling and media addition.

Figure 3
μ-24™ micro-bioreactor system by MicroReactor Technologies.

- The AMBR15™ & AMBR250™ systems were developed by The Automation Partnership, and nowadays they may be considered as the ones that better fulfil the market requirements within the Minibioreactor niche. The success of the AMBR15™ introduced in 2011 is due to the combination of a pseudo stirred tank topology (tic-tac box), the use of non-invasive pH and DO sensing technologies, and a robotized approach that makes possible to take care of the liquid handling for a significant number of vessels during the experiment, as well as the previous medium preparation.

(Price ranging from 166,000 € to 319,000 €). Additionally, since the disposable Minibioreactors feature a miniaturized sparger (microdiffusor is optional for the AMBR250™) both cell culture and microbial applications are possible ($k_L \cdot a$ = 8,5 to 40 h^{-1}). The AMBR15™ [14] consists of a table holding a number of vessels for mediums and chemicals, pipetting supplies and up to four cultivation units in charged to provide thermoregulation, gas supply, stirring and pH and DO measurements, each cultivation unit has capacity to hold up to 12 individual Minibioreactors. During the experiment the robot sequentially handles every Minibioreactor taking samples, adding feed medium, or acid and alkali solutions for pH control. Despite that the AMBR15™ system still lacks of some on-line non-invasive cell density measurement, its features make it a good of option for a lot of tasks where DoE and QbD are must.

Figure 4
Tic-Tac box Minibioreactor & AMBR15™ system by The Automation Partnership.

Up to now no appreciation has been made regarding sterility, that's because most of the previously presented systems are supposed to be operated within a sterile area like a cabinet hood or laminar flow. This becomes an important restriction as the culture volume gets bigger. To evaluate the increase in size and complexity observe the following figure showing the AMBR250™ [15] in a four Minibioreactors set-up. The system is built as a cabinet hood big enough to contain a sophisticated robotic arm, a number of vessels for the different mediums and chemicals, pipetting supplies, and of course all the individual instrumentation and hardware per each Minibireactor. Taking into account that the system can be expanded to conduct up to 24 simultaneous experiments the total size of the system becomes significantly big. From the operation point of view the system works mostly the same as the AMBR15™. A remarkable difference is the increase of the pH measurement range in comparison with the optical fluorescence technology thanks to the use of an embedded pH electrode within the disposable vessel.

The AMBR250™ introduced in 2014 is the newest in the list (price ≈ 639,000 €), and an important number of good attributes can be pointed; a standardized stirred tank design (scalability); robotized liquid handling; fully individual control per Minibioreactor; disposable sensing technologies; and all the benefits of the single use philosophy. However, the size, price and complexity of the system make it an inappropriate solution for most biotechnologists and just a few big bio-pharma companies are currently taking advantage of its features.

Figure 5
AMBR250™ multiple bioreactor system by The Automation Partnership.

- DASbox™ presented in 2012 can be explained as a multiple miniaturized conventional stirred tank bioreactor system that uses either disposable MiniBLU© vessels from Epperdorf or reusable glass vessels. The whole system supports up to 24 simultaneous experiments, four per each cultivation unit. The product is appropriate for most cell lines and any type of cultivation strategies (batch, fed-batch, perfusion and continuous) and useful for DoE and QbD. Nevertheless, despite that the size and price could be relatively affordable for many users, the need for numerous manual operations during the set-up process, and the fact that the instrumentation for pH and DO measurement relies on conventional electrochemical probes, strongly limits the final potential uses of the system, just because of the need for probes sterilization and labour required.

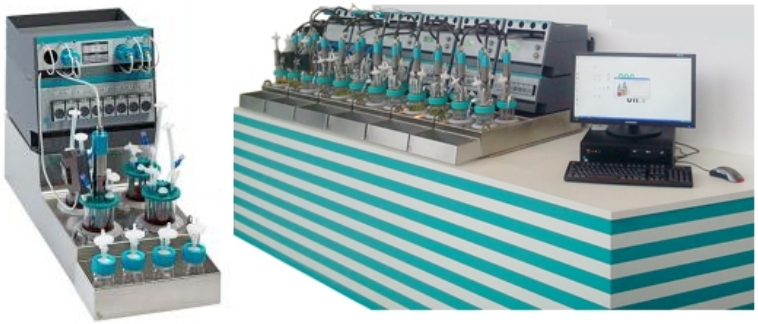

Figure 6
DASbox multiple bioreactor system by The DASGip

- Despite that Mini Bio™ is no more than a single miniaturized conventional stirred tank, with little innovation in comparison with bigger bench-top bioreactors (Price ≈ 25,000 €/unit). The product is becoming quite popular due to comprehensive control software based on an embedded web server and its compact design which lets the user to add as many units as wanted whenever is needed. The commercial success of this product since 2010 demonstrates that as far the required functionalities are properly met; a cheap and small enough product supported by appropriate software can be as

powerful and useful as some of the more expensive previously introduced systems. The obvious disadvantages are the lack of some sort of on-line cell density measurement; the labour required to set-up every new experiment and the need for a relatively high volume of culture medium, leading to increased economic cost per experiment.

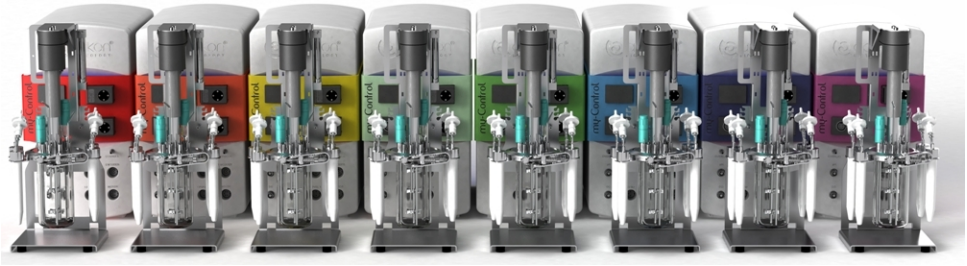

Figure 7
MiniBio bioreactor by Applikon

Despite that many other products could be found in the market, the ones mentioned above make a good picture of the state of the art in the development of Minibioreactor systems during the last five years. The author of this thesis has also developed several Minibioreactor systems, where some of them will be described in chapter 4.

Besides the achievements of the industry, remarkable academic contributions to the state of the art have also been made; the following table appoints some relevant contributions.

Authors	Type	Volume [ml]	Stirring/Aeration	Instrumentation	Number of Channels
Peter Harms, Yordan Kostov, Joseph A. French, Mohammed Soliman, M. Anjanappa, Arun Ram, Govig Rao [16] **Yordan Kostov, Peter Harms, Lisa Randers-Eichhorn, Govind Rao** [17]	Stirred tank	1	Turbine / Sparger	Non-invasive DO, pH OD, GFP probes.	24
Doig SD, Ortiz-Ochoa K., Ward JM, Baganz F. [18]	Bubble column	2	Shaker / Sparger	Non-invasive DO and pH probes	12
Doig SD, Diep A. Baganz F. [19]					
S. R. Lamping, H. Zhang, B. Allen, P. Ayazi Shamlou [20]	Stirred tank	6	Turbine / Sparger	Non-invasive DO, pH and OD probe.	1
Robert Puskeiler, Kaufmamm K., Dirk Weuster-Botz [21] **Robert Puskeiler, Andreas Kusterer, Gernot T. John, Dirk Weuster-Botz** [22]	Stirred tank	8-12	Customized Turbine / Sparger	Non-invasive DO, pH and OD probes.	8-48
Emmanuel Franchon, Vincent Bondet, Hélène Munier Lehmann, Jacques Bellalou [23]	Bubble column	80	Sparger only	Electrochemical DO and pH electrodes plus a non-invasive OD probe.	8
Antonio de León, Héctor Mayani & Octavio T. Ramirez [24]	Stirred tank	75 to 250	Magnetic stir bar / Headspace	Electrochemical DO, pH and Redox electrodes.	1

Table 2
Remarkable academic contributions in Minibioreactors design.

- One of the first integrations of a Minibioreactor system was reported by A. de León et al. in 1998 [24]. Such development consisted of a glass vessel placed on a magnetic stirrer-heater plate and connected to a number of commercial devices for control and monitorization of the culture conditions. A set of temperature and electrochemical

conventional probes (pH, DO and Redox potential) were placed on the cap of the vessel and connected to a computer through an A/D - D/A interface module. Aeration was supplied through headspace and three independent mass flow controllers for O_2, N_2 and CO_2 were used to obtain a proper pH and DO control. This set-up allowed on-line determination of the OUR from the mass balance in the liquid phase (This method will be further explained in the third section of this chapter). The system was validated for the expansion of human hematopoietic cells from umbilical cord blood. The stirring method, a hanging stir bar, demonstrated its feasibility in terms of shear stress for such very specific application. Nevertheless, the low mass transfer coefficient achieved ($k_L{\cdot}a$ = 1 to 3,6 h^{-1}), would make it insufficient for high cell density applications with microbes or some productive animal cell lines.

- In spite of the fact that the use of OD, pH, and DO non-invasive sensors in bioreactors had already been discussed by R. P. Cox [25] and B. H. Weigl et al. [26] in 1984 and 1994 respectively, the department of Chemical and Biochemical Engineering of the University of Maryland deserves recognition due to the appliance of such non-invasive measurement techniques for the monitorization of a Minibioreactor system with multi-parallelization potentiality. The first version of the system was described by Y. Kostov et al. in 2000 [16] and G. Rao in 2001 [27]. The system was based on a 4 ml cuvette, featuring pH and DO fluorescence sensors, as well as an optical path to measure the cell culture's optical density. Despite that the set-up was validated for microbial applications using an Escherichia Coli strain, the initially obtained mass transfer coefficient was not very high ($k_L{\cdot}a$ = 20 h^{-1}). This happened due to the insufficient mixing power of stirring/aeration method consisting of a tiny magnetic stir bar lying on the bottom of the cuvette and a small sparger. Two new improved approaches were reported by P. Harms in 2005 [16], both consisting of 24, 1 ml stirred tanks. The first prototype, consisted of a standard 24-well plate with pH and DO fluorescence sensors attached on the well's bottom surface. The micro-well plate was held by a measurement board including all the signal conditioning and acquisition stages for pH, DO, OD and GFP, and a sterilizable lid featuring miniaturized spargers and stirrers. The system shown a significant high volumetric mass transfer coefficient ($k_L{\cdot}a$ > 75 h^{-1}) for stirring rates > 500 rpm what it makes it suitable for most microbial applications. However, the large number of tubes and wiring harnesses made it impractical for its use with a pipetting robot (pH control, fed-batch and sampling). Hence, a second prototype was developed; made of an array of 24 independent 5 ml flat bottom glass vials, each of them featuring pH, DO fluorescence sensors and a sterilizable cap with individual sparger and stirrer. Such embodiment became to be more appropriate for a future implementation of a robotized liquid handling system. Fluorometrix, a spin-off company of the University of Maryland claimed for the development of such system named as CellStation™ consisting of a carrousel of 12 independent 35 ml disposable glass Minibioreactors, featuring aeration by means of a sparger and a stirring turbine. The parameters (pH, DO and OD) were sequentially monitored and controlled by a robot but no liquid handling abilities were included. Nevertheless, either its detailed features or validation of such system has never been properly reported.

- In 2003 S.R. Lamping et al. [20] reported a nice embodiment of a miniature bioreactor, with a footprint equivalent to a standard 24 micro-well plate. The system included miniaturized baffles, sparger and turbines, as well as fiber optic based probes for the measurement of the pH, DO and OD. Regardless of the high mass transfer rate obtained ($k_L{\cdot}a$ = 100 to 400 h^{-1}) the aim of the study was not to obtain a high biomass density within a miniaturized bioreactor but to provide comprehensive data of its performance in comparison with a 20 l conventional fermenter. The most important conclusion of the study was that in spite of the lower $k_L{\cdot}a$ of the Minibioreactor than the one obtained for the 20 l fermenter under the same power input conditions, it was found that the linear fit for both cases could easily be predicted within a 40 % deviation from the Van Riet's equation, showing the same slope. That, makes possible to stablish the volumetric power input scale-up ratio to keep the $k_L{\cdot}a$ constant in microbial bioprocess development.

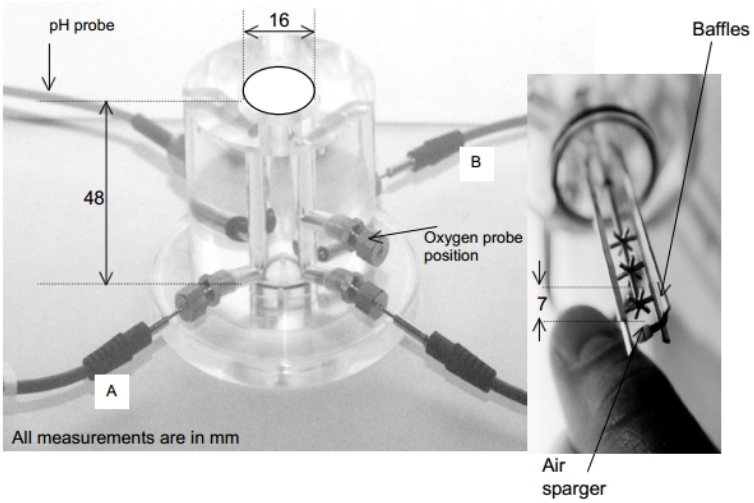

Figure 8
Main components of the miniature bioreactor. Adapted from [20]

The minibioractor was also operated under shaken like and bubble column conditions, that is without aeration and stirring respectively, giving the following conclusions: since in shaken micro-well systems oxygen transfer is achieved by headspace surface aeration only, the potential risk of oxygen depletion is highly related to the culture volume and shaking speed; However, bubble column bioreactors have the potentiality to provide a mass transfer comparable to typical values obtained at low stirring rates but still bigger than shaken systems.

- Doig et al. [18] [19] described in 2005 the construction and characterization of a glass made bubble column Minibioreactor in the scales from 2 to 100 ml, equipped with sintered gas diffusors for aeration, fluorescent patches for pH and DO monitoring, and temperature-control by means of heat-exchange liquid circuits. It was demonstrated that the mass transfer ($k_L{\cdot}a \approx 220\ h^{-1}$) was comparable with values usually obtained for stirred tanks. Regardless of the fact that such development was intended for microbial applications only (tested for E. Coli and Bacillus Subtilis). Doig et al. made a remarkable contribution regarding the correlations of the $k_L{\cdot}a$ with the diameter of the bubble, the superficial gas velocity and the volumetric power consumption.

- The chair for Bioprocess Engineering of the Faculty of Mechanical Engineering in the Technische Universität München, made a great contribution to the aeration techniques in stirred tanks for microbial fermentation by introducing a new gas induction turbine for maximizing the mass transfer. R. Puskeiler et al. [21] [22] used such turbine to describe in 2005 a system for Batch and Fed-Batch culture in the scale of 8 to 12 ml, with capability up to 48 simultaneous experiments. A stunning value of the $k_L{\cdot}a$ ($k_L{\cdot}a$ > 1440 h^{-1}) ranks the system as the most efficient in terms of mass transfer ever reported, becoming ideal for the production of ultra-high biomass densities. On the other hand, the high level of turbulence produced makes it absolutely inappropriate for any sort of shear sensitive species such as mycellial fungi or animal and insect cell lines.

  Additionally, the system was complemented with an automated liquid handling robot (Tecan, RSP 150) that once or twice per hour sequentially sampled each Minibioreactor and delivered the sample on a standard multi-well plate enabled for pH and DO fluorescence measurements as well as for OD (Fluostar Galaxy).

  The Fed-Batch operations as well the addition of NaOH for the pH regulation were also performed by means of the liquid handling robot. In spite of the great achievement related to the design of the mentioned above novel gas inducing turbine capable of providing an unmatched mass transfer rate. A number of drawbacks are obvious, the consumption of culture media for the monitorization, lack of DO control, as well as a very slow pH control action for microbial species (just once or twice per hour) for sure will require a further development.
- In 2006 E. Franchon et al. [23] introduced a multiple mini-fermenter battery based on a bubble column topology analogous to the one propose by Doig et al. nevertheless a bigger $k_L{\cdot}a$ value was reported, probably due to the different volume and dimensions ($k_L{\cdot}a$ = 750 h^{-1}). The most relevant contribution of this work regards to the subsystem for the measurement of an expanded range of OD (0.05 to 100) which consists of a near infrared LED and a photodetector placed at both sides of the vessel and a control loop that modulates the power applied to the LED in order to keep the photodetected signal constant regardless of the biomass density. The measurement dynamic range is maximized by the fact that a minimum amount of light is always measured by the photodetector and by the use of a single near infrared wavelength to diminish the effect of scattering. Finally, the OD is related to the modulating signal through an empirically obtained calibration curve.

HexaScreen Culture Technologies introduced the HexaScreen system in 2012 [28]. Nevertheless, given that such device was developed by the author of this thesis, its description and features will be deeply introduced in chapter 4. The references provided above demonstrate the existence of a well stablished niche of Minibioreactor systems for bioprocess development, as well as a significant dispersion of results especially from the academic point of view. That's why there's still need for products with well-defined correlations easy to scale-up and affordable enough to be used for extensive screening studies.

3.2 Dissolved oxygen measurement by means of fluorescent quenching.

It has been demonstrated that the DO control or even just monitorization is a key point in most cell culture and fermentation processes and a good indicator of the metabolical activity [28] [29]. A number of well-known techniques for the detection of oxygen are available: gas chromatography, mass spectroscopy, paramagnetic resonance, and the methods based on electrochemical electrodes and fluorescence. Nevertheless, just the last two options are appropriate to be used within the liquid phase. Regarding the first technique, polarographic probes or Clark electrodes which were developed since 1940, are made of a pair of electrodes Pt / AgCl submerged in an electrolytic solution and isolated from the medium by means of a porous membrane permeable to the O_2 molecules. Electrodes are connected to a potentiostat circuit in order to produce the oxidation-reduction reaction that generates the electrical current which is proportional to the oxygen partial pressure. Then, such electrical current can be measured by means of an electrometric amplifier. Despite that this technique is widely used and still valid, it shows some inconveniences: Slow response time (depends on the analyte's diffusion through the membrane), reduced signal to noise ratio, electrolyte consumption, analyte consumption (inappropriate for monitoring low volumes), drift due to aging and temperature, and finally the need for sterilization since the electrode must be in touch with the culture medium. On the other hand, the measurement techniques based on the fluorescence emitted by certain chemical compounds or elements depending on the dissolved oxygen concentration, show some advantages: Fast response, good signal to noise ratio, as well as no need for maintenance. In addition, the possibility to build patch like sensors that can be glued on the inner wall of any transparent vessel and measured from outside makes this technology an ideal choice for the development of sterile disposable products. That's why the use of DO fluorescence probes as well as for other parameters (pH and CO_2) is currently becoming a golden standard in Bioprocess engineering.

Instruments based on fluorescence usually consist of three stages; a porous polymeric matrix permeable to the analyte that is wanted to be measured, such matrix is used to immobilize the fluorescent element or compound; an optical front-end made of lenses and/or fiber optics for irradiating the matrix and collecting the emitted light; and finally a photodetector and conditioning circuit to transduce the electrical signals into the optical domain and vice versa [30] [31] [32] [33] [34].

When the immobilized fluorophore is irradiated by a beam of light at a given wavelength the absorbed photons push electrons to a higher quantum level for a short period of time (lifetime). After that, when electrons fall down to their original fundamental quantum level, a new wave of light at a longer wavelength is produced. Hence the emitted wavelength depends on the energy difference between such fundamental and excitation quantum levels:

$$\lambda_e = \frac{c \cdot h}{S_1 - S_0}$$

Where:

- λ_e [m]: Emitted wavelength.
- c[m·s^{-1}]: Speed of light in vacuum (299 792 458 m·s^{-1}).
- h[m^2·kg·s^{-1}]: Planc constant (6.626 069 57 × 10^{-34} m^2·kg·s^{-1}).
- S_0[kg·m^2·s^{-2}]: Energy of the fundamental level.
- S_1[kg·m^2·s^{-2}]: Energy of the excitation level.

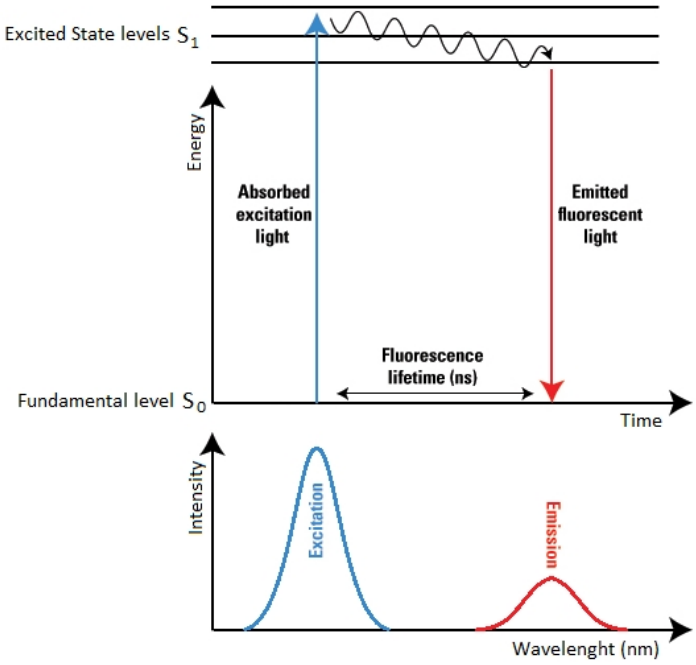

Figure 9
Jablonsky energy diagram of fluorescence

The mean time before a single photon is emitted due to fluorescence uses to be quite short (10 ns) and may be modulated by the existence of certain analytes. That's known as fluorescence quenching and is expressed through the Stern-Volmer equation which relates the intensity and duration of the response depending on the analyte's or quencher concentration:

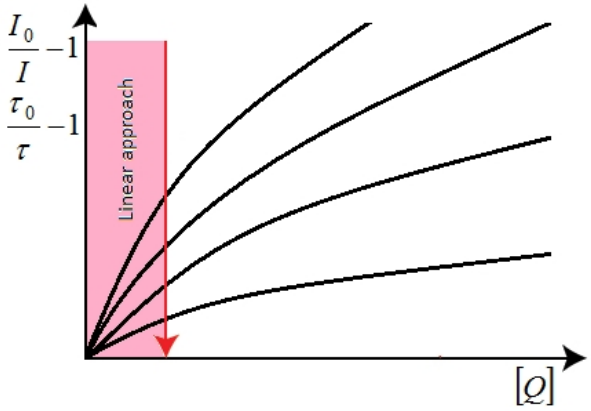

Figure 10
The Stern-Volmer diagram suggests how for low quencher concentrations
Linear fitting may be applied for calibration

$$\frac{I_0}{I} - 1 = \frac{\tau_0}{\tau} - 1 = k_{SV} \cdot [Q] = k_q \cdot \tau_0 \cdot [Q]$$

Where:

- I: Luminescent intensity in presence of the analyte.
- I_0: Luminescent intensity in absence of the analyte.
- τ[s]: Lifetime in presence of the analyte.
- τ_0[s]: Lifetime in absence of the analyte.
- [Q][mol·m^{-3}]: Analyte's or quencher concentration.
- k_{SV}[m^3·mol^{-1}]: Stern-Volmer constant.
- k_q[m^3·mol^{-1}·s^{-1}]: Quenching rate coefficient. It may be referred also as the bimolecular extinction constant and calculated from the Stokes-Einstein relation:

$$k_g = \frac{8 \cdot R \cdot T}{3 \cdot \eta}$$

Where:

- R[J·K^{-1}·mol^{-1}]: Universal constant of ideal gases (8.314 472 J·K^{-1}mol^{-1}).
- T[K]: Temperature.
- η[kg·m^{-1}·s^{-1}]: Lifetime in presence of the analyte.

The immediate consequence of the Stern-Volmer equation is the measurement method itself. Analyte concentration can be determined either from the intensity ratio I_0/I or the fluorescence delay ratio τ_0/τ.

$$[Q] = \frac{1}{k_{SV}}\left(\frac{I_0}{I} - 1\right) = \frac{1}{k_{SV}}\left(\frac{\tau_0}{\tau} - 1\right)$$

Nevertheless, a number of several physical issues have been demonstrated to have a great impact on the fluorescence response; the method for the fluorophore immobilization within the matrix; the aging of the fluorophore compound known as photobleaching; Temperature; as well as the front-end's optical topology [35] [36] [37]. It also has been found that the determination of [Q] through the fluorescence delay ratio becomes more robust than through the intensity ratio, since the lifetime cannot be affected by the attenuation or other mechanical artefacts. Additionally, the τ_0/τ ratio offers two measurement options either in the time or frequency domains.

3.2.1 Time domain method (Lifetime)

The time domain absolute method consists on the excitation of a fluorescent sensor patch by a burst of pulsed light where the pulse width is significantly shorter than the fluorescence lifetime. Based on the previous description and the given electrical engineering

background of the author of this thesis, it has been considered appropriate to approach the phenomena through a model based on linear system theory. The behaviour of the fluorescence sensor plus the associated photodetector can be modelled as a low-pass first-order linear time-invariant system matching an impulse response function *h(t)* featured by a certain lifetime and luminescent responsivity. The impulse response function can be found by means of the following convolution product:

$$y(t) = x(t) \otimes h(t)\big|_{t\geq 0}$$

$$I \cdot e^{-t/\tau} \cdot u(t) + b = I_u \cdot (1 - u(t)) \otimes h(t)\Big|_{t\geq 0}$$

Where:

- $y(t)$: Is the response signal.
- $x(t)$: Is the excitation signal. A Dirac-Delta function $\delta(t)$ with magnitude I_u.
- I: Is the fluorescent luminescence responsivity.
- I_u: Magnitude of the excitation pulse.
- b: Is the off-set value introduced by the photodetector.

A quick path to the solution is to solve the equation in the frequency domain.

$$h(t) = \mathcal{F}^{-1}\{H(f)\}$$

$$H(f) = \frac{\mathcal{F}\{y(t)\}}{\mathcal{F}\{x(t)\}} = \frac{\dfrac{I \cdot \tau + b \cdot \delta(f)}{1 + j \cdot 2 \cdot \pi \cdot f}}{-\dfrac{I_u}{j \cdot 2 \cdot \pi \cdot f}} = -\frac{I}{I_u} \cdot j \cdot 2 \cdot \pi \cdot f \cdot \left(\frac{1}{\dfrac{1}{\tau} + j \cdot 2 \cdot \pi \cdot f} \right)$$

$$h(t) = \mathcal{F}^{-1}\left\{ -\frac{I}{I_u} \cdot j \cdot 2 \cdot \pi \cdot f \cdot \left(\frac{1}{\dfrac{1}{\tau} + j \cdot 2 \cdot \pi \cdot f} \right) \right\} = -\frac{I}{I_u} \cdot \left[e^{-\frac{t}{\tau}} \cdot \delta(t) - \frac{e^{-\frac{t}{\tau}}}{\tau} \cdot u(t) \right]$$

$$h(t) = \begin{cases} 0 & ;t = 0 \\ \dfrac{I}{I_u \tau} \cdot e^{-t/\tau} & ;\forall t > 0 \end{cases}$$

Hence, since the decay of the fluorescence is related to the lifetime through the impulse response function, it could be estimated just by measuring the time period between the falling edge of the excitation pulse and the moment the emitted light reaches a pre-established minimum value. However, such method lacks of accuracy due to extremely high noise sensitivity. The most straightforward structure for lifetime measurement is the gated detector [34], which is basically made of a fast switch and an integration amplifier controlled by means of a timer or a microcontroller. Figure 12 describes the operation of the gated detector, showing the timing signals as well as the decay of the fluorescence response.

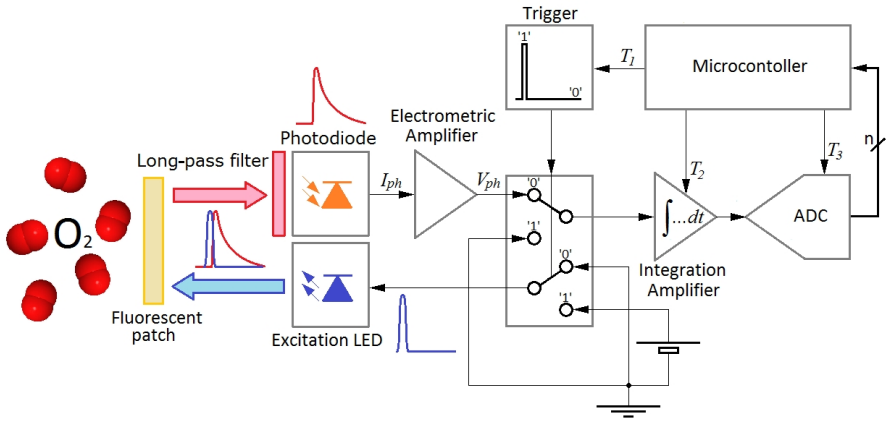

Figure 11
Schematic block diagram of a gated detector for lifetime measurement

During the excitation period, T_1 is logic high so the light source is switched on and the input of the integration amplifier is connected to ground. After a short period, when T_1 goes logic low the light source is switched off and the input of the integration amplifier is connected to the photodetector. Then, the extinction profile is sampled by the integration amplifier and the A/D converter in three sections F_1, F_2 and F_3. The first two sections F_1, F_2 are immediately acquired after the excitation pulse since they are related to the fluorescence's magnitude and lifetime. The third section F_3 is used for determination of the off-set value so it must be acquired once the fluorescence response is totally extinct.

$$F_1 = I_0 \cdot \int_{t_1}^{t_1+x} e^{\frac{t}{\tau}} \cdot dt + B$$

$$F_2 = I_0 \cdot \int_{t_2}^{t_2+x} e^{\frac{t}{\tau}} \cdot dt + B$$

$$B = b \cdot \int_{t_3}^{t_3+x} dt$$

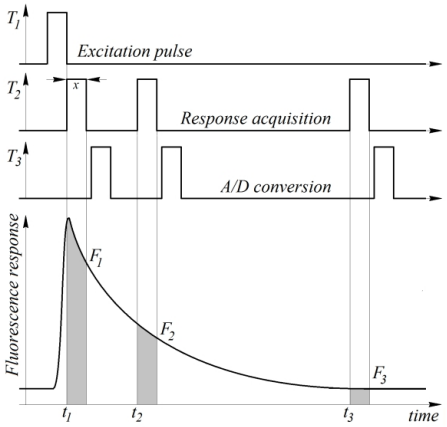

Figure 12
Gated detector operation

In fact, the use of an integration amplifier is not compulsory. It could be easily replaced by a sample and hold stage. Nevertheless, since the output signal provided by the photodetector is usually very weak and noisy, integration offers additional noise rejection and an increased dynamic range (As far noise shows a Gaussian distribution). Finally the lifetime τ is solved by computing the following equation:

$$\tau = \frac{t_2}{\ln\left(\frac{F_2 - B}{F_1 - B}\right)}$$

3.2.2 Frequency domain methods (Phase shift)

Frequency domain methods are based on the phase shift experienced by the emitted fluorescence by the sensor patch when excited by a sinusoid modulated light source at a certain frequency. Such phase shift is related to the lifetime and hence to the analyte concentration [33] [34]. This is shown by the figure below where the Stern-Volmer law is exemplified. The phase delay and magnitude of the fluorescent response increases as the analyte concentration decreases and vice versa because of the quenching phenomena.

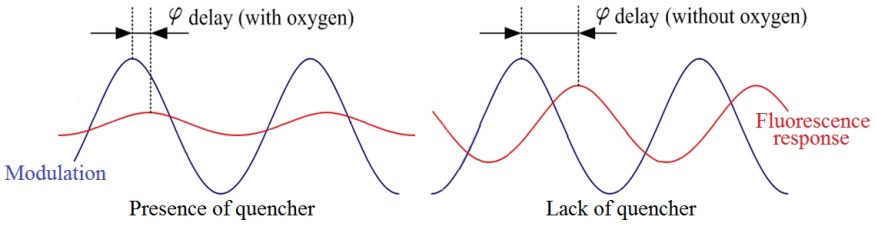

Figure 13
Phase shift due to the fluorescence quenching phenomena

As previously introduced, the determination of the oxygen concentration through the lifetime ratio offers a robust solution against possible changes of the attenuation on the optical path, which makes it more convenient than the intensity ratio. The relationship between the lifetime τ and the phase shift $\Delta\text{£}$ may be found by solving the convolution product between the excitation signal *x(t)* and the impulse response function *h(t)*

$$x(t) = I_u \cdot \sin(2 \cdot \pi \cdot f_o \cdot t) \Rightarrow \mathcal{F}\{x(t)\} = j \cdot \frac{I_u}{2} \cdot [\delta(f + f_o) - \delta(f - f_o)]$$

$$h(t) = \frac{I}{I_u \tau} \cdot e^{-t/\tau}\Big|_{\forall t>0} \Rightarrow \mathcal{F}\{h(t)\} = -\frac{I}{I_u} \cdot j \cdot 2 \cdot \pi \cdot f \cdot \left(\frac{1}{\frac{1}{\tau} + j \cdot 2 \cdot \pi \cdot f}\right)$$

$$y(t) = I_u \cdot \sin(2 \cdot \pi \cdot f_o \cdot t) \otimes \frac{I}{I_u \tau} \cdot e^{-t/\tau}\Big|_{\forall t>0}$$

$$Y(f) = -I \cdot \pi \cdot f_o \cdot \left[\frac{\delta(f + f_o)}{1/\tau - 2 \cdot j \cdot \pi \cdot f_o} + \frac{\delta(f - f_o)}{1/\tau + 2 \cdot j \cdot \pi \cdot f_o} \right]$$

Notice that the denominators of the terms between brackets can be expressed exponentially to find an easier solution of the inverse Fourier transform, and get the temporal expression of the fluorescence response. This is therefore, a sine wave with a fluorophore lifetime modulated phase.

$$Y(f) = -\frac{I \cdot \pi \cdot f_o}{\sqrt{1/\tau^2 + 4 \cdot (\pi \cdot f_o)^2}} \left[e^{j \cdot \left[tg^{-1}(2 \cdot \pi \cdot f_o \cdot \tau) \right]} \cdot \delta(f + f_o) + e^{-j \cdot \left[tg^{-1}(2 \cdot \pi \cdot f_o \cdot \tau) \right]} \cdot \delta(f - f_o) \right]$$

$$y(t) = \mathcal{F}^{-1}\{Y(F)\} = -\frac{2 \cdot I \cdot \pi \cdot f_o}{\sqrt{1/\tau^2 + 4 \cdot (\pi \cdot f_o)^2}} \cdot \cos(2 \cdot \pi \cdot f_o \cdot t - tg^{-1}(2 \cdot \pi \cdot f_o \cdot \tau))$$

Where the phase shift between the excitation and the fluorescence response is:

$$|\Delta\theta| = tg^{-1}(2 \cdot \pi \cdot f_o \cdot \tau) + \pi/2$$

The equation above, points to the coherent demodulation method as the most appropriate technique to acquire both the magnitude and phase information. Its main advantages are the potentiality to obtain an increased signal to noise ratio and the capability to reject the low frequency interfering sources, as for instance the daylight. Coherent detectors have been widely used for very diverse applications such as analog communication systems and sensor conditioning. Numerous detection architectures may be found throughout the specialized bibliography. Figure 14, shows one of the most commonly used structures known as the balanced or quadrature demodulator. The structure's operation is based on the isolation of the P-Q components of the fluorescence response by multiplying the signal response by a sinusoid of the same frequency. To analyse its operation, the measured signal needs to be expressed as the addition of both components:

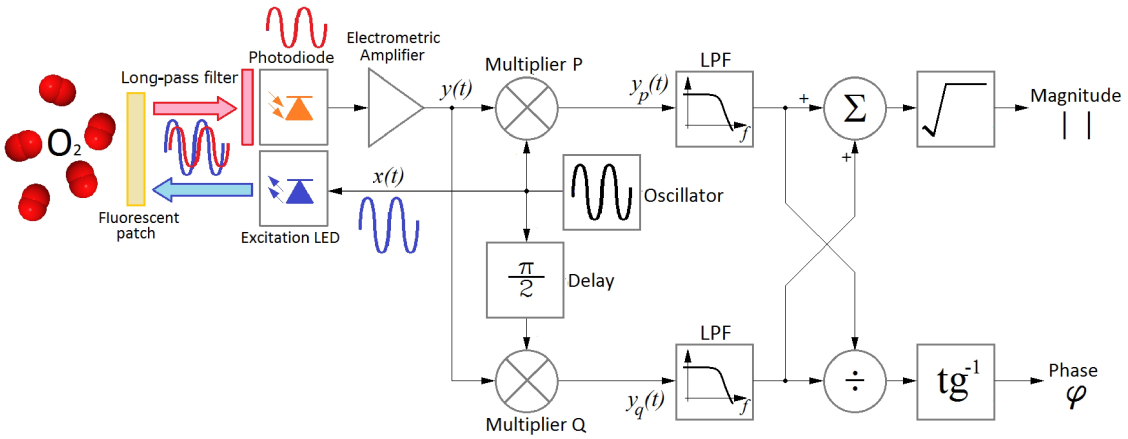

Figure 15

Quadrature demodulator applied for DO fluorescence phase shift detection.

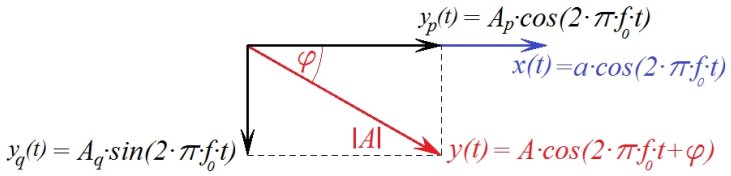

Figure 16
Polar decomposition of the fluorescence response signal

$$y(t) = A \cdot \cos(2 \cdot \pi \cdot f_o \cdot t + \varphi) = A \cdot \cos(2 \cdot \pi \cdot f_o \cdot t) \cdot \cos(\varphi) - A \cdot \sin(2 \cdot \pi \cdot f_o \cdot t)$$

$$y(t) = A_p \cdot \cos(2 \cdot \pi \cdot f_o \cdot t) - A_q \cdot \sin(2 \cdot \pi \cdot f_o \cdot t)$$

Resolution of the P component after low-pass filtering:

$$y_p(t) = \frac{A_p}{2}(1 + \cos(4 \cdot \pi \cdot f_o \cdot t)) - \frac{A_q}{2}\sin(4 \cdot \pi \cdot f_o \cdot t)$$

$$y_p(t) \otimes h_{LPF}(t) = \frac{A_f}{2} = \frac{A \cdot \cos(\phi)}{2}$$

Resolution of the Q component:

$$y_q(t) = \frac{A_p}{2}\sin(4 \cdot \pi \cdot f_o \cdot t) - \frac{A_q}{2}(1 - \cos(4 \cdot \pi \cdot f_o \cdot t))$$

$$y_q(t) \otimes h_{LPF}(t) = -\frac{A_q}{2} = -\frac{A \cdot \sin(\varphi)}{2}$$

Magnitude and phase delay can now be solved as:

$$|y(t)| = \sqrt{A_p^2 + A_q^2}$$
$$\angle\{y(t)\} = tg^{-1}\left(\frac{A_q}{A_p}\right)$$

Sensitivity will greatly depend on the modulation frequency, which it can be experimentally found by performing a frequency sweep in the spectra, from a few hundreds of Hertz up to a hundred of kilo-Hertz and then choosing the frequency that maximizes the phase delay for a given increment of the DO concentration. An example of such experimental evaluation is shown in the following figure. The evolutions of the magnitude and phase shift along the spectra are represented for a DO gradient ranging from 0 % to 100 %. It can be noticed how the maximum increment of magnitude is produced for lower frequencies <10 kHz, on the contrary a maximum phase shift of 12 degrees is found around 50 kHz. Therefore, a compromise exists between the optimum modulation frequency and the band-width of the photodetector.

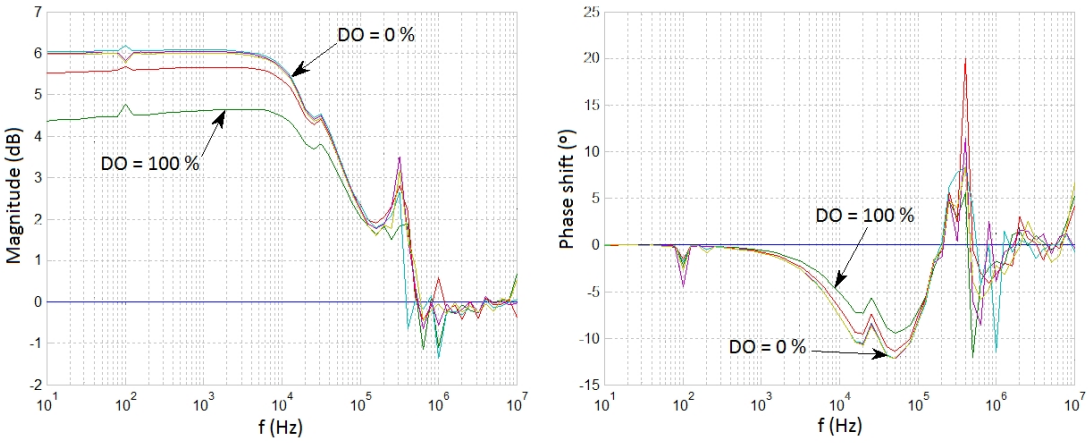

Figure 17

Relative spectral fluorescence response for a DO gradient ranging from 0 % to 100 %.

Another very wide spread coherent structure is the well-known XOR phase detector, which is used in many IC's. The quadrature structure is an optimum but expensive solution, the XOR phase detector is not that robust in terms of noise rejection but a cheaper option capable to perform reliable and accurate enough phase detection useful for most of the applications. Its operation consists on the comparison of the excitation and emission signals by means of a non-linear device, a XOR logic gate. The comparison generates a pulsed signal featured by a certain duty cycle. After proper low-pass filtering, the DC signal obtained in the output is proportional to the phase shift (figure 19).

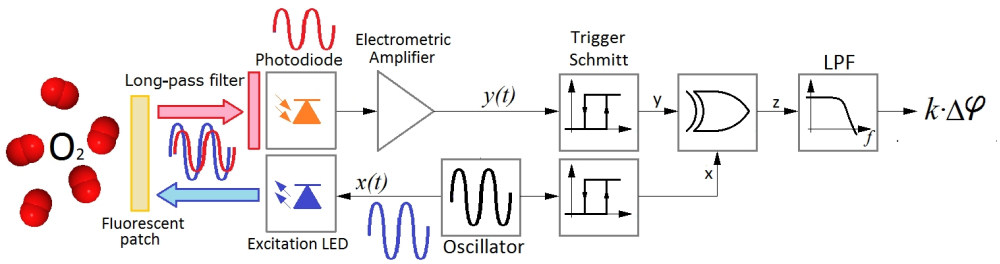

Figure 18

XOR phase demodulator applied for DO fluorescence phase shift detection.

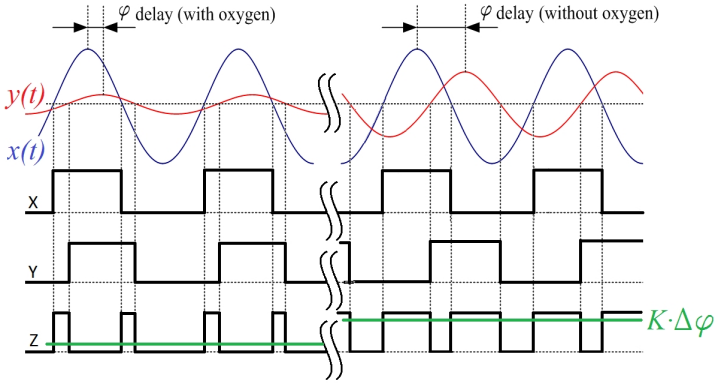

Figure 19

Operation of the XOR phase demodulator.

It is important to mention that despite the frequency domain methods are virtually insensitive to the magnitude uncertainty; this is only true if the optical cross-talk is kept below the sensitivity threshold of the system. Otherwise, the phase variation range as well the signal to noise ratio will be reduced and the uncertainty will be increased proportionally to the magnitude of the excitation light reaching the photodiode. Therefore, the feasibility of such fluorescence detection systems is not only a matter of electronic design but optical and mechanical issues must be also carefully taken into account.

3.2.3 Ratiometric methods

Some variations of the previously explained methods include ratiometric techniques [33] [38], developed to overcome the limitations imposed by the lack of stability of the fluorescence intensity due to not only mechanical reasons, i.e. temperature or photodecomposition may have a great impact on the calibration's accuracy as well as on the general feasibility of the sensor. Ratiometric techniques are based on the combination of two individual fluorophores within the same matrix. One of them is meant to be used a reference and the other to produce a signal dependent on the analyte concentration. Fluorescence ratiometric techniques can also be referred as Dual Lifetime Referenced (DLR) or Dual Emission Ratiometric (DER) techniques. They are already very well stablished for the measurement of some relevant analytes (pH, Ca^{2+}, Mg^{2+} and Zn^{2+}). The fact that the reference fluorophore is insensitive to the analyte concentration and features a longer lifetime than the signal fluorophore, leads to several possible measurement strategies, where the lifetime and phase delay techniques can still be used.

a) Dual Excitation-Single Detection: The sensor is alternatively irradiated by two different wavelengths and the fluorescence response of both fluorophores is measured at once by a single photodiode within a wavelength region where the individual responses are partially overlapped or as a whole by means of a long-pass filter. Since each fluorophore shows different absorption maxima and analyte sensitivity, the ratio of both measured intensities can be related to the analyte concentration [34].
b) Single Excitation-Dual Detection: The sensor is irradiated at a single wavelength and each fluorophore individual response (signal and reference) is measured individually by means of a separate filter and photodiode. The analyte concentration is then related to the ratio of both measured intensities [39].
c) Single Excitation-Single Detection: In this case, since only one light source and photodetector are used, some imaginative method is needed to produce a differentiated fluorescence response dependent on the analyte concentration. This is achieved by operating the system in the frequency domain. The excitation light source is modulated by a sinusoid at two different frequencies. When the modulation frequency approaches the inverse lifetime of the signal fluorophore the measured response equals the total emission of both fluorophores. However, when the frequency gets closer to inverse lifetime of the reference fluorophore

the response can be approached just to the reference fluorophore response. Then the ratio can be solved [40]

3.3 OUR estimation methods.

Given the importance of oxygen as a substrate for the cell's metabolism, the Oxygen Uptake Rate (OUR) has been pointed as a key indicator of the metabolical activity. Nevertheless, the OUR estimation cannot be directly measured. Hence, its determination may show some difficulties especially for animal cell lines [41]. Their low specific consumption rates make the minimum measurement threshold to become an important merit factor; the cell's sensitivity to the sudden changes of the oxygen concentration; and finally the difficulty to satisfy an appropriate oxygen transfer rate without damaging the cells because of the shear stress produced by the aeration and stirring methods.

$qO_2 x10^{-12}$ mol $O_2 \cdot cell^{-1} \cdot h^{-1}$	Cell line
0.15 – 0.36	KS1/4 (Hybridoma)
0.21 – 0.25	NB1 (Hybridoma)
0.223 – 0.248	Cla (Hybridoma)
0.05	FS-4 (Human diploid cell)
0.19 – 0.4	AB2 – 143.2 (Hybridoma)
0.023 – 0.087	167.4G5.3 (Hybridoma)
$qO_2 x10^{-12}$ mol $O_2 \cdot kg\ X^{-1} \cdot h^{-1}$	Cell line
2 – 15	Xanthomomas Campestris NRRL 1775 (Bacteria)
0.9 – 23	Escherichia Coli K 12a (Bacteria)
31 – 31.2	Bacillus Acidocaldarius NRRC-207 F (Bacteria)
2 – 3	Trigonopsis Variabilis CBS 4095 (Yiest)
0.3 – 1	Candida Bombicola NRRL Y-17069 (Yiest)
0.8	Hansenula or Pichia Anomala CBS6759 (Yiest)

Table 3

Specific consumption rates qO_2 for some cell species commonly used in productive biotechnology. Adapted from Ruffieux P-A. et al. [41] and Felix Ochoa et. Al. [43]

Most of the available methods for OUR estimation are based on the mass balance equation [42]; some cases are considering the whole bioreactor or just the liquid phase where the oxygen concentration can be kept constant or not. For a proper understanding of the different methods the generalized model of the phase boundaries within a bioreactor must be considered [Figure 11, Introduction].

3.3.1 Global mass balance method

This method is based on the comparison of the gas compositions measured on the gas Inlet and outlet taking into account the whole bioreactor. Hence, the mass balance equation is expressed as follows:

$$\frac{dC_L}{dt}\cdot V_L + \frac{dC_G}{dt}\cdot V_G = G_{in}\cdot y_{in} - G_{out}\cdot y_{out} - \mathrm{OUR}\cdot V_L$$

Where:

- V_L[l]: Liquid phase volume.
- V_G[l]: Gas phase volume.
- G_{in}[lpm]: Inlet gas flow.
- G_{out}[lpm]: Outlet gas flow.
- y_{in}[mol/l]: Oxygen inlet molar fraction.
- y_{out}[mol/l]: Oxygen outlet molar fraction.

If no oxygen accumulation happens within the bioreactor (the medium's DO concentration is kept constant) then the equation can be rewritten as:

$$\mathrm{OUR} = \frac{G_{in}\cdot y_{in} - G_{out}\cdot y_{out}}{V_L}$$

This is in fact equivalent to the Gas phase global balance method for the $k_L{\cdot}a$ determination explained in section 2.4. As mentioned, this method has not historically been very widespread due to the need for very sophisticated and expensive instrumentation like mass spectrometers and very accurate DO control systems (A very tight DO drift below ±0.05 % is required [41] [43]). Nevertheless, the current capabilities of the latest DO probes and mass flow controllers, as well as the improvements on the accuracy of the gas phase oxygen sensor technologies (fluorescence quenching and ZrO_2 [44] [45]) will probably make in the near future a more common usage of the Global mass balance method. Aehle et al. [46] compared the OUR data of a CHO cell line fermentation, when inlet and outlet gas compositions were measured by means of a mass spectrometer and an oxygen/CO_2 combined sensor (ZrO_2/IR, BCpreFerm, Bluesens [47]). Results showed a much lower transient response for the combined sensor than the mass spectrometer but still fast enough for the application since an almost perfect correlation of the data provided by both instruments was demonstrated.

3.3.2 Stationary liquid phase mass balance method

This method consists on determining the required oxygen concentration on the gas phase to set a constant DO value in the liquid phase. Therefore, no accumulation happens and the mass transfer equals the consumption. On the contrary to the Global mass balance, only the gas to liquid mass exchange is considered:

$$\frac{dC_L}{dt} = k_l\cdot a\cdot\left(C_L^* - C_L\right) - \mathrm{OUR}$$

$$k_l\cdot a\cdot\left(C_L^* - C_L\right) = \mathrm{OUR} = \mathrm{OTR}$$

Where:

- C_L[mol/l]: DO concentration in the liquid.
- C_L^*[mol/l]: DO concentration in the liquid in equilibrium with the gas phase.

Therefore to solve the OUR, previous knowledge of the mass transfer coefficient and the dissolved oxygen concentration in equilibrium with the gas phase are necessary. On one hand, the $k_L{\cdot}a$ value can be obtained through the application of any of the procedures introduced in section 2.4 while reproducing some physical and chemical conditions representative of the experiment. On the other hand C_L^*can be related to the gas phase oxygen's partial pressure and molar fraction through the Henry's law.

$$C_L^* = \frac{P_{tot} \cdot y_G}{H} = y_L^* \cdot H$$

Where:

- P_{tot} [atm]: Total gas supply pressure.
- y_G [ ]: Oxygen's molar fraction in the gas phase.
- y_L^* [ ]: Oxygen's molar fraction in the liquid phase.
- H [l·atm·mol^{-1}]: Henry's constant. Which it can be approximated for a certain temperature in a aqueous solution through the Van't Hoff equation:

$$H(T) = H(T_0) \cdot e^{-k\cdot\left(\frac{1}{T}-\frac{1}{T_0}\right)}$$

Where:

- T_0 [K]: Reference temperature (298 K)
- $H(T_0)$ [l·atm·mol^{-1}]: Oxygen's dilution constant in water at the reference temperature (769.23 l·atm·mol^{-1}).
- K [K]: Scale factor (1700 K)

As for the previous method, the fact that the DO concentration is kept constant throughout the culture is an important advantage from the biological point of view, since the cells are not subjected to stressful changes of the oxygen tension. Despite that the Stationary liquid mass balance method offers minimum cell stress and great estimation accuracy. It has not become of extended usage due to the need of expensive mass flow controllers and means for the determination of the inlet gas composition. Ducommun et al. [48] integrated a set-up consisting of 2l stirred tank aereated by means of a PTFE made porous pipe connected to three mass flow controllers for DO an pH control (O_2, N_2, CO_2). The DO was measured by means of a standard polarographic probe and its signal acquired by a computer running custom control software used to operate the mass flow controllers. The inlet oxygen's molar fraction was calculated as a function of the set points of each mass flow controller. The set-up was tested under cell culture conditions for a CHO cell line showing that it was possible to obtain an on-line accurate OUR estimation within ±5 %.

Other realisations chasing a higher accuracy, may also include additional instrumentation for a more precise determination of the gas phase composition (infra-red, paramagnetic analysers or mass spectrometers) [41].

3.3.3 Dynamic method.

The Dynamic method is currently the most widely used for the OUR determination. The method consists on replacing the oxygen in the gas phase with some inert gas to force the dissolved oxygen desorption, producing an extinction profile that fits to a negative exponential curve featured by a slope proportional to the oxygen consumption and a time constant inversely proportional to the mass transfer coefficient. This task is commonly done by means of a 3-way electrovalve that periodically switches the gas supply from air to nitrogen always maintaining the oxygen concentration between two predefined levels (typically 50 to 30 %) where the duration of both states are named t_{On} and t_{Off} respectively. That's why, on the contrary to the previously explained methods the mass balance equation needs to be written in two parts:

$$\frac{dC_L(t)}{dt} = \begin{cases} k_l \cdot a \cdot \left(C_L^* - C_L(t)\right) - \mathrm{OUR} & \forall t \in t_{On} \\ -k_{des} \cdot C_L(t) - \mathrm{OUR} & \forall t \in t_{Off} \end{cases}$$

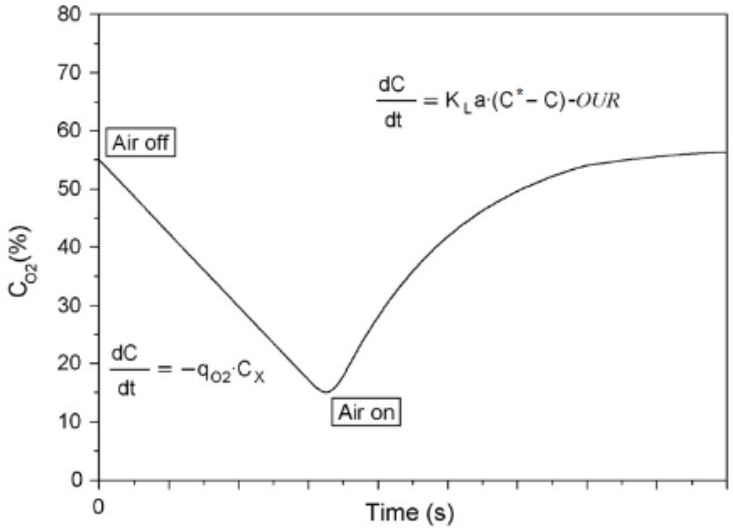

Figure 20

DO response for the dynamic estimation of the OUR. Adapted from F García-Ochoa et al. [42]

To solve the mass balance equations, two assumptions need to be made. The first is that the removal of the oxygen in the gas phase of the bioreactor happens fast enough to consider it as an instantaneous event, the second assumption is that the consumption variation is really slow when compared to the t_{On} and t_{Off} periods, so it can be considered as a constant. Obviously, such assumption implies inconsistency when $t \to \infty$. However, the solution will be valid if the aeration period t_{On} and the oxygen removal period t_{Off} are kept small when compared to the growth rate of the cell species but still bigger than the absorption and desorption constants.

$$k_l \cdot a, k_{des} \ll {t_{On}}^{-1}, {t_{Off}}^{-1} \ll \mu$$

Hence, the solution of the mass balance equation can be written as:

$$C_L(t) = \begin{cases} C_L^* - \dfrac{\mathrm{OUR}}{k_{des}} + \alpha \cdot e^{-k_{des} \cdot t} & \forall t \in t_{On} \\ -\dfrac{\mathrm{OUR}}{k_{des}} + \beta \cdot e^{-k_{des} \cdot t} & \forall t \in t_{Off} \end{cases}$$

The OUR instantaneous value can be found through the integration of $C_L(t)$ along the t_{Off} period:

$$\int_0^{t_{Off}} \frac{dC_L(t)}{dt} = -k_{des} \cdot \int_0^{t_{Off}} C_L(t) \cdot dt - \mathrm{OUR} \cdot \int_0^{t_{Off}} dt$$

$$\mathrm{OUR} = -\frac{\left[C_l(t)\right]_0^{t_{Off}} + k_{des} \cdot \int_0^{t_{Off}} C_L(t) \cdot dt}{t_{Off}}$$

Iterated repetition of this process allows reliable on-line monitoring of the oxygen consumption. However, this technique shows some drawbacks. Previous knowledge of $k_l{\cdot}a$ is required; Accuracy is dependent on the oxygen consumption; Need for an initial minimum inoculum to set the lower estimation threshold; and finally an obvious compromise between the "measurement" period and the potential damage suffered by the growing cells because of the necessary variations of the DO concentration. In animal cell culture, such compromise comes out with a very poor temporal resolution of 5 to 10 samples a day making difficult a proper on-line interpretation to define new cultivation strategies. Nevertheless, such compromise is not that dramatic for the monitorization of microbial processes due to their robustness and higher oxygen demand. This has been reported by numerous authors specially for monitoring activated sludge systems [49] [50] [51]. A simplified version of the Dynamic method was used by Anderlei T. et.al. to develop the RAMOS system (Respiration Activity Monitoring System) [52] [53] [54]. It consists of several shake flasks using a customized cap featured by two inlet and outlet aeration ports. The system operates in two stages, during the rising stage the vessels are put down a constant air flow to force DO equilibrate with the gas phase, during the measurement stage two electrovalves close both aeration ports producing and certain increment of the oxygen partial pressure in the headspace due to respiration of the microorganisms. Then OUR can be calculated from such increment:

$$\mathrm{OUR} = -\frac{\Delta pO_2 \cdot V_G}{\Delta t \cdot R \cdot T \cdot V_L}$$

Where:

- T [K]: Temperature
- R [atm·l·K^{-1}·mol^{-1}]: Universal constant of ideal gases (0.08205746 atm·l·K^{-1}·mol^{-1}).
- V_L[l]: Liquid phase volume.
- V_G[l]: Gas phase volume.

Between all the explained methods only the dynamic method can still be considered as a standard. This is because a good trade-off between accuracy and the economical investment

for its implementation. Some other methods have also been reported but they are just suitable for very specific applications like the Yield coefficient method [55] or may have physical implementation concerns especially for low-volume bioreactors like the OUR probe developed by K. Konstantinov et.al. [56] [57].

References:

[1] A. d. Palma, «Microbioreactors Carve Out Growing Niche,» *Genetic Engineering & Biotechnology News,* vol. 30, nº 3, 2010.

[2] F. B. Jonathan I Betts, "Miniature bioreactors: Current practices and future opportunities," *Microbial Cell Factories,* vol. 5, no. 21, 2006.

[3] C. W. E. H. Sathish Kumar, "Minibioreactors," *Biotechnology letters,* no. 26, pp. 1-10, 2004.

[4] V. Glasser, «Finding a Bioreactor that's right for you,» *Genetic Engineering and Biotechnology News,* vol. 31, nº 14, 2011.

[5] V. Glasser, "Bioreactor and Fermentor market trends," *Genetic Engineering and Biotechnology News,* vol. 29, no. 14, 2004.

[6] V. Glasser, "Disposable Bioreactors gaining favor," *Genetic Engineering and Biotechnology News,* vol. 26, no. 12, 2006.

[7] M.-N. G. B. J. Samorski M, «Quasi-continous combined scattered light and fluorescence measurements: a novel measurement technique for shake microtiter plates.,» *Biotechnology and Bioengineering,* vol. 92, nº 1, pp. 61-68, 2005.

[8] E. Z. C. F. R.-K. T. J. B. Frank Kensy, "Validation of a high-throughput fermentation system based on online monitoring of biomass and fluorescence in continuously shaken microtiter plates," *Microbial Cell factories,* vol. 8, no. 31, 2009.

[9] C. E. J. B. Frank Kensy, "Scale-up from microtiter plate to laboratory fermenter: evaluation by online monitoring techniques of growth and protein expression in Escherichia coli and Hansenula polymorpha fermentations," *Microbial Cell Factories,* vol. 8, no. 68, 2009.

[10] J. M. O. M. H. Z. A. B. S. A. H. P. R. Ashraf Amanullah, "Novel Microbioreactor High Throughput Technology for cell culture development: Reproducibility, and Scalability assessment in Fed-Batch CHO Cultures," *Biotechnology and Bioengineering,* vol. 106, no. 1, pp. 57-67, 2010 .

[11] G. S. Z. R. L. S. Ache Stokelman, «High Throughput Cell Culture Experimentation with BioProcessors SimCell™ Platform,» de *CPAC Sattellite Meeting*, Rome, 2006.

[12] G. Wilson, “Evaluation of a Novel Micro-Bioreactor System For Cell Culture Optimisation,” in *9th ESACT Meeting*, Harrogate, UK, June 5-8, 2005.

[13] R. C. D. C. A. A. Aaron Chen, “Twenty-four well plate Miniature Bioreactor System as a Scale-Down Model fer Cell Culture Process Development,” *Biotechnology and Bioengineering,* vol. 102, no. 1, pp. 148-160, 2008.

[14] N. B. R. O. K. W. D. P. Rachel Bareither, “Automated disposable small scale reactor for high throughput bioprocess development: A proof of concept study,” *Biotechnology and Bioengineering,* vol. 110, no. 12, p. 3126–3138, 2013.

[15] T. D. C. Z. U. H. G. T. A. C. F. Davy De Wilde, «Superior Scalability of Single-Use Bioreactors,» *BioProcess international,* vol. 12, nº 8s, 2014.

[16] Y. K. J. A. F. M. S. M. A. A. R. G. R. Peter Harms, “Design and performace of a 24-Station High Throughput Microbioreactor,” *Biotechnology and Bioengineering,* vol. 93, no. 1, pp. 6-13, 2006.

[17] P. H. L. R.-E. G. R. Yordan Kostov, “Low-Cost Microbioreactors for High-Throughput Bioprocess,” *Biotechnology and Bioengineering,* vol. 72, no. 3, pp. 346-352, 2001.

[18] O.-O. K. W. J. B. F. Doig SD, “Characterization of Oxygen Transfer in Miniature and Lab-Scale bubble column bioreactors and comparison of microbial growth performance based on constant kla,” *Biotechnology progress,* no. 21, pp. 1175-1182, 2005.

[19] D. A. B. F. Doig SD, “Characterization of a novel miniaturized bubble column bioreactor for high throughput cell cultivation bioreactor system for mammalian cell culture,” *Biochemical Engineering,* no. 23, pp. 97-105, 2005.

[20] H. Z. B. A. P. A. S. S. R. Lamping, “Design of a prototype miniature bioreactor for high throughput automated bioprocessing,” *Chemical Engineering Science,* no. 58, pp. 747-758, 2003.

[21] K. K. D. W.-B. Robert Puskeiler, “Development parallelization and automation of a gas-inducing millilitre-scale bioreactor for high-throughput bioprocess design,” *Biotechnology and Bioengineering,* no. 89, pp. 512-523, 2005.

[22] A. K. G. T. J. D. W.-B. Robert Puskeiler, “Miniature bioreactors for automated high-throughput bioprocess design (HTBD): reproducibility of parallel fed-batchcultibations with Escherichia coli,” *Biotechnology and Applied Biochemistry,* no. 42, pp. 227-235, 2005.

[23] V. B. H. M. L. J. B. Emmanuel Franchon, “Multiple Microfermentor Battery: a Versatile Tool for Use with Automated Parallel Cultures of Microorganisms Producing Recombinat Proteins and for Optimization of Cultivation Protocols,” *Applied and Environmental Microbiology,* vol. 72, no. 8, pp. 5225-5231, 2006.

[24] H. M. O. T. R. Antonio de León, “Design, characterization and application of a minibioreactor for the culture of human hematopoietic stem cells.,” *Cytotechnology,* no. 28, pp. 127-138, 1998.

[25] M. M. J. B. N. M. N. J. K. T. Raimond P. Cox, “Continous turbidometric measurements of microbial cell density in bioreactors using a light emitting diode and a photodiode,” *Journal of Microbiological Methods,* no. 10, pp. 25-31, 1989.

[26] A. H. W. T. I. K. H. K. P. O. O. S. W. B. H. Weigl, «Optical Triple Sensor for Measuring pH, Oxygen and Carbon Dioxide,» *Journal of Biotechnology,* nº 32, pp. 127-138, 1994.

[27] G. Rao, “Bioreactor and Bioprocessing Technique”. USA Patent US 6,673,532 B2, 4 January 2004.

[28] N. H., “Mass transfer,” in *Basic Biotechnology*, Cambridge University Press, 2006, pp. 201-217.

[29] M. H. H. S. Y. K. K. A. B. D. D. F. A. R. M. G. R. Xudong Ge, “Validation of an optical sensor-based high-throughput bioreactor system for mammalian cell culture,” *Journal of Biotechnology,* vol. 122, no. 3, pp. 293-306, 2006.

[30] I. Bergman, “Rapid-response Atmospheric Oxygen Monitor based on Fluorescence Quenching,” *Nature , 396 (27 April 1968); doi:10.1038/218396a0,* vol. 218, no. 396, 1968.

[31] R. C. M. J. Palatine and S. M. L. Hoffman, “Optical sensor for monitoring the partial pressure of oxygen”. USA Patent 4,725,115, 21 June 1988.

[32] T. E. P. J. A. M. R. B. G. C. B. B. Arthur E. Colvin Jr, “A novel Soli-State Oxygen Sensor,” *Johns Hopkins apl Technical Digest,* vol. 17, no. 4, pp. 377-384, 1996.

[33] O. Wolfbeis, “Fiber-Optic Chemical Sensors and Biosensors,” *Analytical Chemistry,* vol. 80, p. 4269–4283, 2008.

[34] Y. K. H. Lam, “Optical Instrumentation for Bioprocess Monitoring,” in *Optical Sensor Sytems in Biotechnology*, Springer, 2009, pp. 14-23.

[35] N. W. P. J. Q. F. H. K. M. C. R. R. A. B. G. C. L. R. J. L. M. Thanassis Papaioannou, “Performance evaluation of fiber optic probes for tissue lifetime fluorescence spectroscopy,” in *Proceedings of SPIE Vol. 4958*, San Jose CA, 2003.

[36] M. A. M. J. R. D. B. L. I. V. A. G. M. V. P. G. L. C. D. Patrick O'Neal, “Oxygen sensor based on the fluorescence quenching of a Ruthenium complex immobilized in biocompatible Poly(Ethylene Glycol) hydrogel,” *IEEE Sensors Journal,* vol. 4, no. 6, pp. 728-734, 2004.

[37] L. C. K. C. C. Samantha M. Grist, “Optical Oxygen sensors for applications in microfluidic cell culture,” *Sensors,* vol. 10, pp. 9286-9316, 2010.

[38] S.-B. I. C.-F. J. S.-M. A. Hochreiner H., “Dual emission probe for luminescence oxygen sensing: a critical comparison between intensity, lifetime and ratiometric measurements,” *Talanta,* vol. 66, no. 3, pp. 611-618, 2005.

[39] R. L. M. W. S. K. P. J. S. John F. McCarthy, “A Fiber-optic System for Measuring Single Excitation-Dual Emission Fluorescence Ratios in Real Time,” *Biotechnology progress,* vol. 8, no. 4, pp. 360-368, 2008.

[40] P. H. R. S. P. G. R. Yordan kostov, “Ratiometric oxygen sensing: detection of dual-emission ratio through a single emissio filter.,” *The Analyst,* vol. 125, pp. 1175-1178, 2000.

[41] U. v. S. I. W. M. Pierre-Alain Ruffieux, “Measurement of volumetric (OUR) and determination of specific (qO2) oxygen uptake rates in animal cell cultures,” *Journal of biotechnology,* vol. 63, no. 2, pp. 85-95, 1998.

[42] E. G. V. E. S. J. C. M. Felix Garcia-Ochoa, “Oxygen uptake rate in microbial processes: An overview,” *Biochemical Engineering Journal,* vol. 49, pp. 289-307, 2010.

[43] D. C. D. T. J. E. C. Dorresteijn R. C., “A method for simultaneous determination of solubility and mass transfer coefficient of oxygen in aqueous media using off-gas mass spectrometry,” *Biotechnology and Bioengineering,* vol. 43, pp. 149-154, 1994.

[44] SensorTechnics, “Oxygen sensors XYO Series,” [Online]. Available:

http://www.sensortechnics.com/cms/upload/datasheets/DS_Standard-XYO_E_11818.pdf. [Accessed 4 12 2014].

[45] SensorTechnics, “Oxygen sensors XYA Series,” [Online]. Available:

http://www.sensortechnics.com/cms/upload/datasheets/DS_Standard-XYA_E_11637.pdf. [Accessed 4 12 2014].

[46] A. K. S. S. R. S. A. L. Mathias Aehle, “Simplified off-gas analyses in animal cell cultures for process monitoring and control purposes,” *Biotechnology Letters,* vol. 33, no. 11, pp. 2103-2110, 2011.

[47] BlueSens, “Brochure BCpreFerm,” [Online]. Available:

http://www.bluesens.com/fileadmin/user_upload/grafik/pdf/Brochure_BCpreFerm.pdf. [Accessed 4 12 2014].

[48] P.-A. R. M.-P. F. I. M. U. v. S. Paul Ducommun, “A new method for on-line measurement of the volumetric oxygen uptake rate in membrane aerated animal cell cultures,” *Journal of Biotechnoloy,* vol. 78, pp. 139-147, 2000.

[49] P. R. B. J. S. d. R. N. A. C. v. H. Valnyr V. Lira, “Estimation of Dissolced Oxygen Dynamics for Sequencing Batch Aerobic Reactors,” in *IMTC 2004 - Instrumentation and Measurement*

Technology Conference, Como, 2004.

[50] G. S. D. A. C. v. H. R. C. S. F. Sebastian Yuri Cavalcanti Catunfa, "Feedback Control Method for Estimating the Oxygen Uptake Rate in Activated Sludge Systems," *IEEE Transactions in instrumentation and measurement,* vol. 48, no. 4, pp. 864-869, 1999.

[51] J. S. d. R. P. R. B. A. C. v. H. Valnyr V. Lira, "Autamation of an Anaerobic-Aerobic Wastewater Treatment Process," *IEEE Transactions on Instrumentation and Measurement,* vol. 52, no. 3, pp. 909-915, 2003.

[52] W. Z. M. P. J. B. Tibor Anderlei, "Online respiration activity measurement (OTR, CTR, RQ) in shake flasks," *Biochemical Engineering Journal,* vol. 17, p. 187–194, 2004.

[53] J. J. B. Marco Scheidle, "Combination of On-line pH and Oxygen Transfer Rate Measurement in Shaken Flasks by Fiber Optical Technique and Respiration Activity Monitoring System (RAMOS)," *Sensors,* vol. 7, pp. 3472-3480, 2007.

[54] I. H. B. L. J. B. Sven Hansen, "Development of a modified Respiration Activity Monitoring System for accurate and highly resolved measurement of respiration activity in shake flasks fermentors," *Journal of Biological Engineering,* vol. 6, no. 11, pp. 1754-1611, 2012.

[55] E. G. F. Garcia-Ochoa, "Bioreactor scale-up and oxygen transfer rate in microbial processes: An overview," *Biotechnology Advances,* no. 27, pp. 153-176, 2009.

[56] K. B. K. Sung-jin Yonn, "Continuous, real-time monitoring of the oxygen uptake rate (OUR) in animal cell bioreactors," *Biotechnology and Bioengineering,* vol. 44, no. 8, pp. 983-990, 2004.

[57] L. M. T. S. K. K. K. Joeris, "Development of a new probe for in-situ oxygen uptake rate (OUR) measurement in mammalian cell culture processes.," in *10th International IFAC Symposium on Computer Applications in Biotechnology*, Cancún, 2007.

[58] P. M. Doran, "Homogeneous Reactions," in *Bioprocess Engineering Principles*, Kidlington, Oxford, Academic Press, 2013, p. 636.

[59] Langdom S., «Basic principles of Cancer cell culture methods in Molecular Medicine,» *Cancer Cell Culture: Methods and Protocols,* vol. 88, pp. 3-15, 2004.

[60] B. F. J. L. G. D. Doig S, «High-Throughput screening and process optimization,» de *Basic Biotechnology*, Cambridge, 2006, pp. 289-305.

[61] B. F. I Betts J., «Miniature Bioreactors: Current practices and future opportunities,» *Microvial Cell Factories,* p. 5:21, 2006.

[62] C. Y., «Bioreactor design,» de *Basic Biotechnology*, 2006, pp. 181-200.

[63] N. H., «Mass transfer,» de *Basic Biotecnology*, 2006, pp. 201-217.

[64] R. Mirro and K. Voll, "Which impeller is Right for your Cell Line? A guide to Impeller Selection for Stirred-Tank Bioreactors," *BioProcess International,* pp. 52-57, 2009.

[65] I. D. G. &. M. S. K. Allison Van Winkle, "Small-Scale Bioreactors forthe Culture of Embryonic Stem Cells," in *Embryonic Stem Cells - Basic Biology to Bioengineering*, Rijeka, Croatia, InTech, 2011, pp. 73-88.

[66] Y. Chisti, "Animal-cell damage in sparged bioreactors," *Trends in Biotechnology,* vol. 18, no. 10, p. 420–432, 2000.

[67] P. M. Doran, "Fluid Flow and Mixing," in *Bioprocess Engineering Principles*, Sydney, Elsevier Science & Technology Books, 1995, pp. 141-153.

[68] J. A. Hunt, "Regenerative medicine: Materials in a cellular world," *Nature Materials,* no. 7, pp. 617 - 618, 2008.

[69] S. K. S. F. V. Kevin Robert McCarthy, "Synthetic microcarriers for culturing cells". USA Patent US20120288912 A1, 29 6 2009.

[70] C. Ratledge, "Biochemistry and physiology of Growth and Metabolism," in *Basic Biotechnology*, Cambridge, Cambridge University Press, 2006, pp. 26-54.

[71] P. M. Doran, "Mass Tranfer," in *Bioprocess Engineering Principles*, Kidlington, Oxford, Academic Press, 2013, pp. 379-433.

[72] L. Gevantman, «Solubility of selected gases in water,» de *CRC Handbook of Chemistry and Physics*, Elsevier Science B.V., 2003, pp. 82-83.

[73] U. v. S. I. W. M. Pierre-Alain Ruffieux, "Measurement of volumetric (OUR) and determination of specific (qO2) oxygen uptake rates in animal cell cultures," *Journal of Biotechnology 63 (1998) 85–95,* no. 63, pp. 85-95, 1998.

Development of single use Bioreactors

Three different systems were used to carry out the experimentation. The first two are disposable Minibioreactors systems (MBR's) named as HexaScreen® and MonoScreen® *Fed-Batch. B*oth were designed within the context of the here presented research works but also from a commercial perspective linked to the position of the author of this thesis as CTO in the spin-off company HEXASCREEN CULTURE TECHNOLOGIES S.L. The third system was made of a commercial Bench-Scale Bioreactor known as Biostat® B-plus by SARTORIOUS AG and a custom external oxygen controller. Despite that the last set-up does not totally match the chapter's title since the Biostat® B-plus system is not a disposable one, its description has been included since it was used to test (within the bench-scale volume) the oxygen control algorithm as well as the simplified implementation of the OUR stationary liquid phase balance estimation method.

Therefore, this chapter offers a rough description of the instrumentation, algorithms and means involved in the development of such systems.

4.1 The HexaScreen® Bioreactor.

HexaScreen is an expandable and automated multiple Minibioreactor to be used with HexaScreen Minibioreactor plates, the system provides constant culture conditions in terms of temperature, stirring and aeration, on-line data on pH, dissolved oxygen (DO) and cell density from up to six simultaneous cell cultures. HexaScreen is intended for screening tasks in biotechnology when the labour and materials costs of the experimentation with animal cells (compared to costs of manual operation and reusable Bench-Scale Bioreactors) are required to be reduced. Some of the claimed applications are: clone selection, cell characterization, cell adaptation, formulation and optimization of culture medium, cell toxicity tests and bioprocess optimization. Concept was described in the granted patent [1] next table shows an overview of the system's technical features.

Typical Culture volume:	6 x 10 … 15 ml
Stirring method:	Magnetic pendulum, 6 actuators, 0 ... 400 rpm ± 10 rpm
Aeration method:	Headspace
Gas supplies:	2 channels (Air/O_2 and N_2) with water traps + 75 ml humidifiers.
MBR's Temperature measurement method:	Pt100
Dissolved oxygen measurement method:	Phase delay measurement on the frequency domain.
OUR estimation method:	Dynamic (Discontinuous action – 6 multiplexed channels).
pH & optical density measurement method:	Estimation by means optical absorbance spectroscopy
Accuracy of measurements & control ranges:	
-Temperature control range:	+25 ... +40 °C
-Temperature accuracy:	± 0,3 °C
-Dissolved oxygen:	0 … 100 % / ± 10 %
-Absorbance spectra (aprox):	300 ... 1000 nm (depending on each individual)
-Optical Density:	0 ... 1 AU / ± 0,05 AU
-pH estimation:	6,5 ... 8,5 / ± 0,03 at 15 mg/l phenol red (via abs. Spectroscopy)
Communications:	Ethernet (10Base-T)
Dimensions (aprox):	
-Height (closed/opened)	640/800 mm
-Width	340 mm
-Depth	300 mm
-Weight:	30 kg

Table 1
HexaScreen Technical features

Through the following sections a description of the system starting with its architecture will be provided. Given the importance of the non-invasive optical measurements a specific point has been devoted to the optical layout.

4.1.1System overview.

The system is made of three parts, the Minibioreactors plate, the workstation, and a software package which runs on a host PC connected to the workstation. The plate is made of transparent biocompatible plastic (polystyrene) equipped with six Minibioreactors, including gas filters, inoculation septum, miniaturized ports for probe's allocation and a magnetic

pendulum made of silicone for stirring. The Minibioreactors plate is single use and has previously been sterilized by means of gamma radiation inside a plastic bag which should only be opened for Minibioreactors filling within a sterile area. Once the water-bath and the Minibioreactors have been filled and inoculated, the plate can be placed inside the workstation which is in charge of providing the right physical conditions to carry out the experiment (Temperatures, Stirring, Aeration) and taking measurements to follow the cultures behaviour (OD, pH, DO)

Next figures show the plate's parts and assembly as well as the workstation.

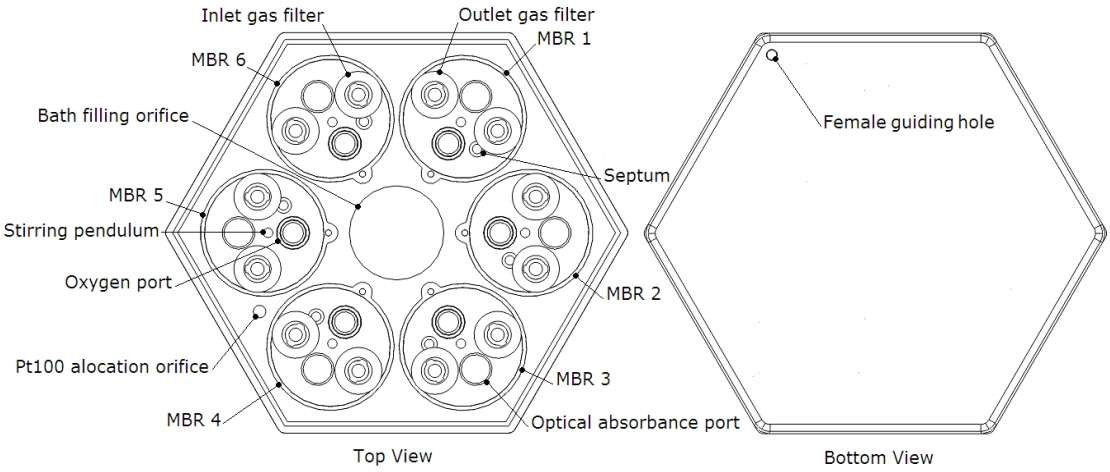

Figure 1
Minibioreactors plate

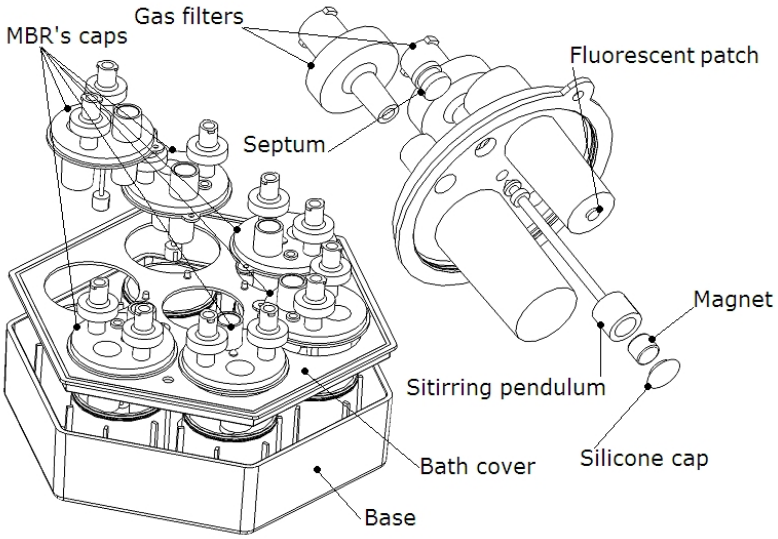

Figure 2
HexaScreen's Minibioreactors plate assembly

The workstation is shaped as a hexagonal column divided in two boxes, upper and lower, the Minibioreactors plate is placed inside the thermally insulation chamber located between the two boxes. Once the system is closed, all the gas fittings are connected and probes located in such a manner that becomes impossible to break the sterile barrier. Closing

is guided by means of three columns like shafts that slip through linear ball bearings in order to favour reproducibility on gas fittings and probes allocation. Once closed, the user may inspect the culture, opening the first stage of the upper box to look through the transparent wall of the insulation chamber.

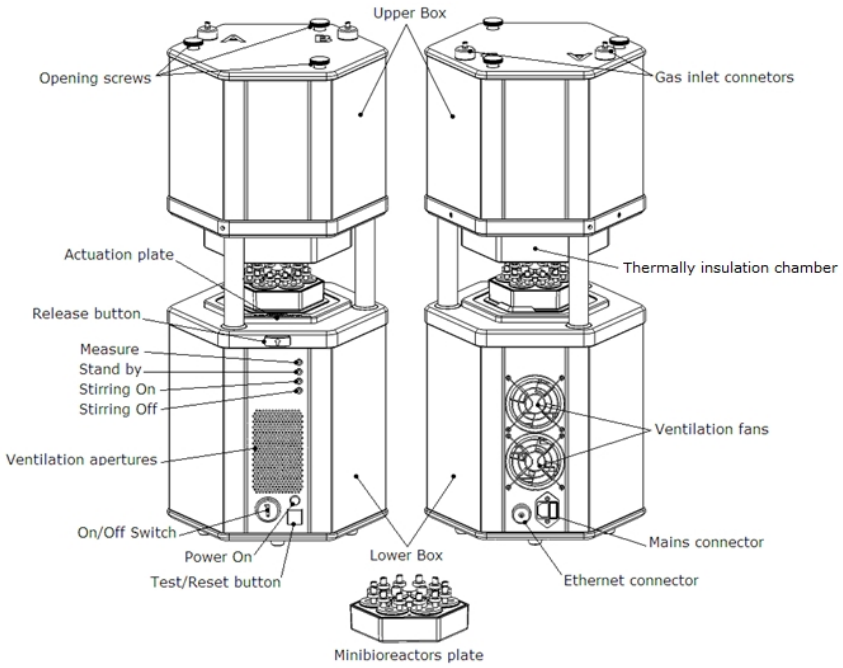

Figure 3
HexaScreen's workstation front and rear panels

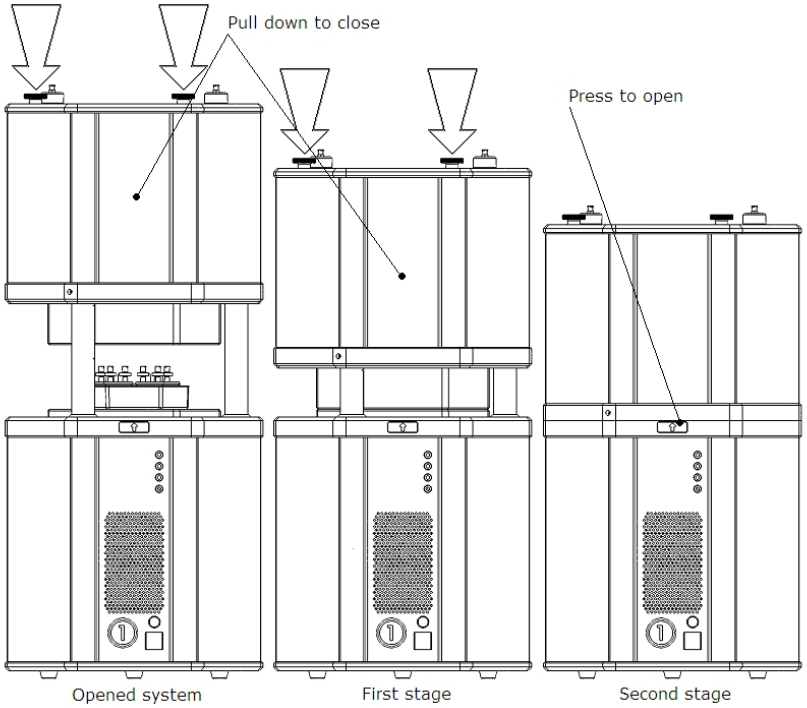

Figure 4
Workstation closing and opening

Communication is point to point, between the host PC and the workstation, and just requires a RJ45 crossover cable. TCP/IP protocol is used to support the data exchange, such a capability allows setting up a 6-device array in order to increase the screening capability or even to provide remote access to the on-line data .That requires the use of a simple Ethernet hub or switch as for any Local Area Network.

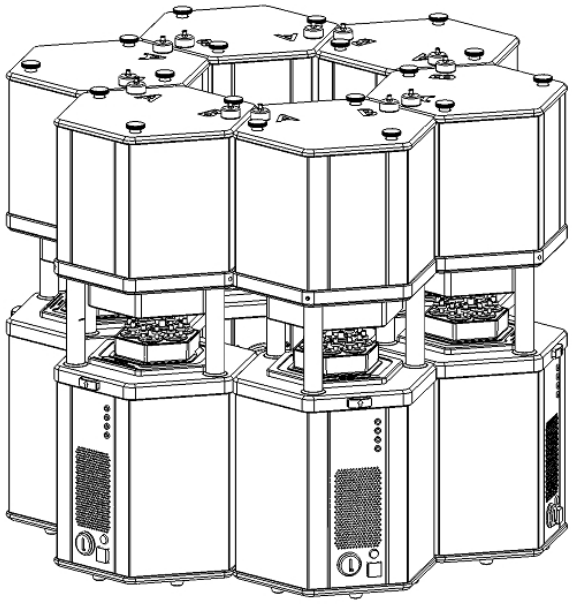

Figure 5
6-device array

Regarding the HexaScreen control & acquisition software, it basically acts as a wizard, designed to assist the user through the process. Experiments are executed in three stages, configuration, pre-culture calibration and data acquisition. Main features of the software are:

- Creation or edition of experiment recipes.
- Creation of customized graphs combining up to 6 variables.
- Creation of reports, including:
    - The results of the experiment.
    - Name of users involved on the experiment (design, execution, …)
    - Acquisition dates (Start time, End time and Time stamp)
    - Workstation ID number's (s/n, IP address, port, …)
    - Experiment set-up parameters.
    - Workstation's calibration parameters.
    - List of unexpected events (Errors happened)
- Exportation of reports to EXCEL and HTML files.
- 21CFR-11 administration
    - Data files encryption
    - Users administration (Supervisor, Operator, User)
    - System audit trail

4.1.2HexaScreen® architecture

The HexaScreen system is made of a significant number of parts of different kind: electronic circuits, fiber optic bundles, lenses, machined parts in a wide sort of materials, valves, TEC devices, etc… The cross-sectional view below shows a glimpse of the system's internal configuration: where the lower box contains most of the electronics and actuators as well as the opening mechanism, the upper box contains the gas circuit, fiber optic probes, the central stirrer, and heaters for thermoregulation, the walls are thermally insulated in order to keep the temperature some degrees over the culture's temperature to avoid condensation phenomena within any part of the gas circuit, and finally the insulation chamber provides visual inspection as well as thermoregulation, stirring, light excitation, and secures gas connections.

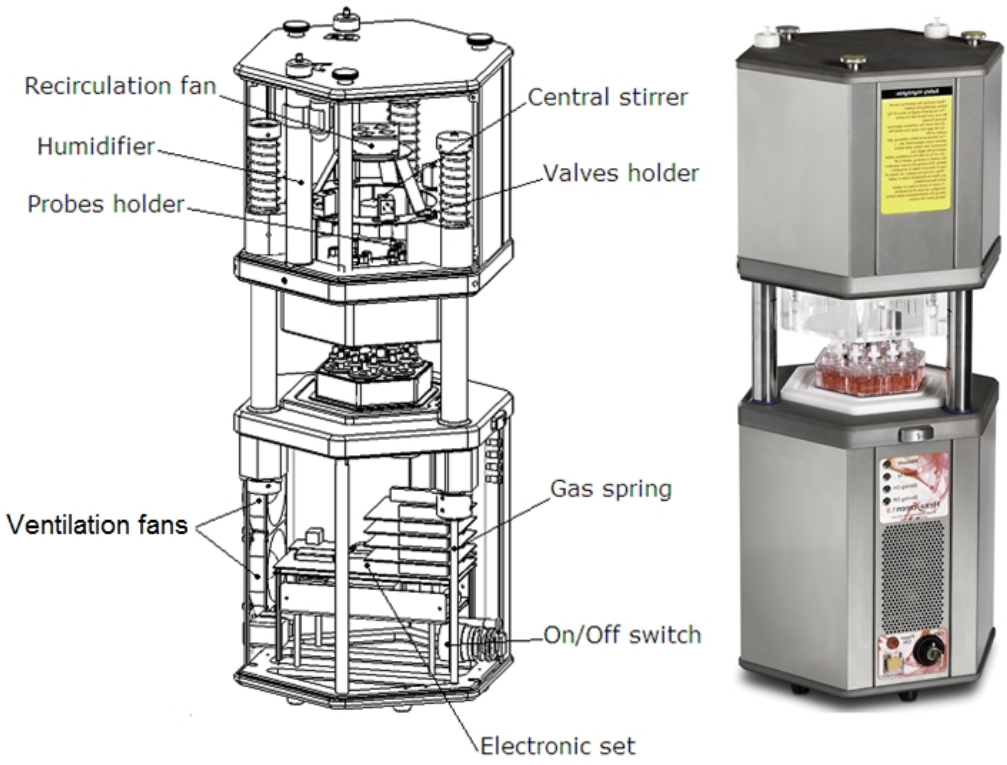

Figure 6
HexaScreen's workstation cross-sectional view and actual implementation

The control architecture is based on an RCM2200 Rabbit core; a C-programmable module with Ethernet connectivity especially suited for controlling embedded systems, two additional ADuC218 microcontrollers are also used to carry out especially critical functions. The ADuC812 MicroConverter® is also C-programmable and a fully integrated 12-bit data acquisition system-on-a-chip, featuring precision A/D & D/A converters. As shown in Figure 7 the system is made of four printed circuit boards: Control, Dissolved oxygen, Drivers and Temperature. The modules are connected each other in a PC104 like stackable way where all the logic and math functions are performed by the control board and the most of the signal conditioning and power driving functions are supported by specific circuits.

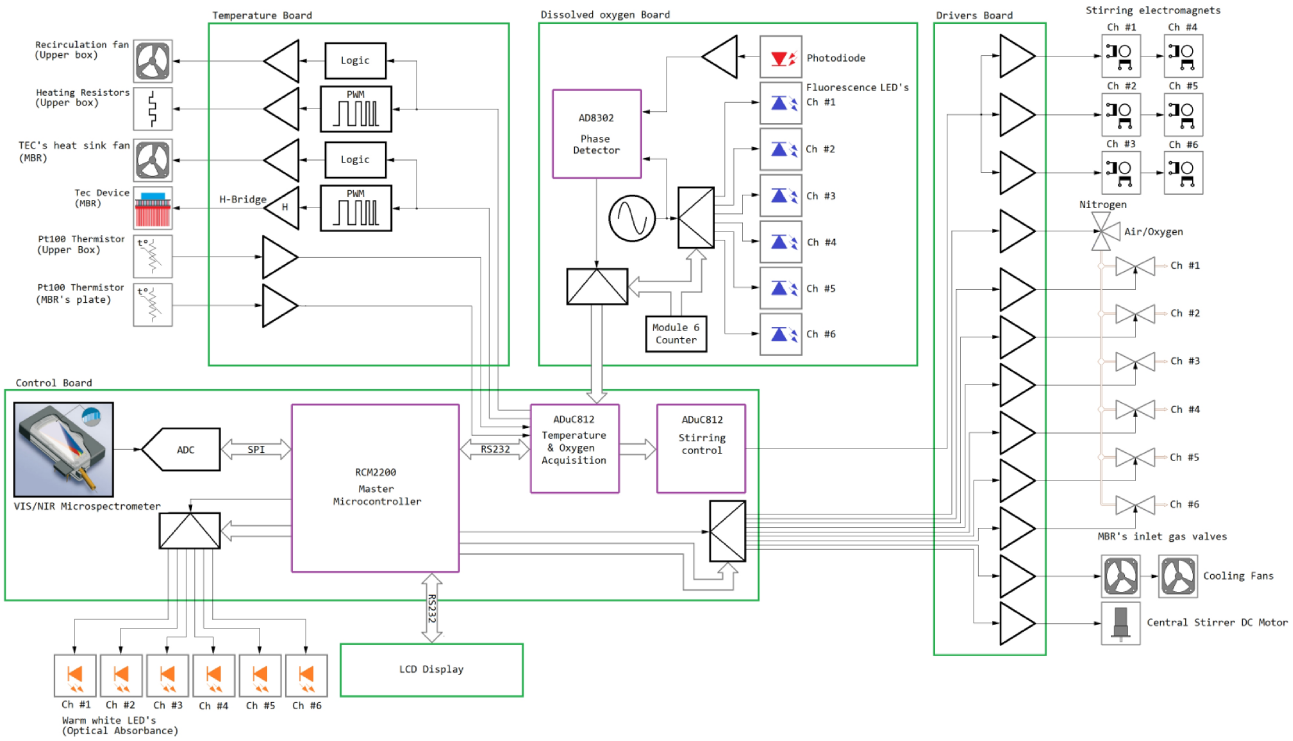

Figure 7
HexaScreen Block Diagram

A specific microcontroller (ADuC812) is used to synthesize the PWM stirring command signals where an 8 bit resolution sampled sinusoid is used for modulation, two pointers are constantly reading the signal profile keeping a constant π/4 phase delay, the returned values are used to load the microcontroller's internal timers that generate the command signals (further details will be explained in the 4.1.4 section, Minibioreactor aeration, stirring & mass transfer).

A second microcontroller (ADuC812) is also used for acquiring the multiplexed DO signals as well as the temperatures inside the lower and the upper boxes and in the Minibioreactor plate. The second ADuC812 is also in charge of solving the PID control signals for the upper box and Minibioreactors plate thermoregulation. Such control signals are provided to the Temperature board by means of two built-in digital to analog converters.

In order to allow optical absorbance spectroscopy measurements the control board holds an UV/VIS μspectrometer module (Steag Microparts). The μspectrometer is based on a hollow cavity waveguide design with no moving parts which is attached to a silicon-photodiode detector array (Hamamatsu S8378-256N24). Light is coupled into the spectrometer through a 300/330μm silica fibre and an entrance slit. A focusing flat field Echelette grating and a camera mirror lead the light inside the spectrometer cavity. These elements are arranged in the Rowland design, which guarantees mechanical, thermal and optical stability. Virtually, there is no thermal drift of the wavelength calibration due to the fixed geometrical position of the optical components. Hence, wavelength to pixel calibration function is stable over the device lifetime and no recalibration is required [2]. This is a very convenient feature for the monitorization of long term phenomena as cell growth.

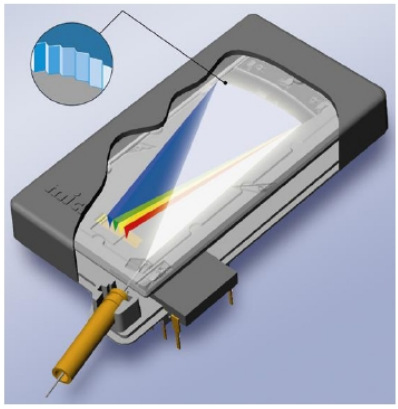

Detector array:		Hamamatsu S8378-256N24
Microspectrometer:	Entrance Fiber	300/330 µm; NA =0,22
	Entrance Slit	50 * 300 µm
	Spectral Range (specified)	350 – 850 nm
	Spectral Range in 1st diffr. order:	300 – 1050 nm
	Blaze Wavelength:	420 nm
	Dispersion	3,5 nm/pixel
	Spectral Resolution [$\Delta\lambda_{FWHM}$]	< 10 nm
	Operating Temperature	0°C to +40°C
	Storage Temperature	-40°C to +60°C
Peak Sensitivity at wavelength		540 nm
Sensitivity at 400 nm [with 16 bit ADC]:		typ. 250 *10E12 cts*nm/Ws
Signal to Noise Ratio		>= 5000:1
Linear Video Output [V]		0 to + 2,4 V

Figure 8
Steag Microparts µspectrometer features

The RCM2200 module is responsible for the remaining tasks of the control board: TCP/IP communications, Firmware downloading, LCD interface and control of the multiple peripheral devices (Reference LED's for optical absorbance spectroscopy, electrovalves for MBR's aeration, ventilation fans and DC motor for the water-bath central stirring). To perform such tasks the RCM2200 module executes a state machine observing the following ten conditions related to the system's different stages of operation:

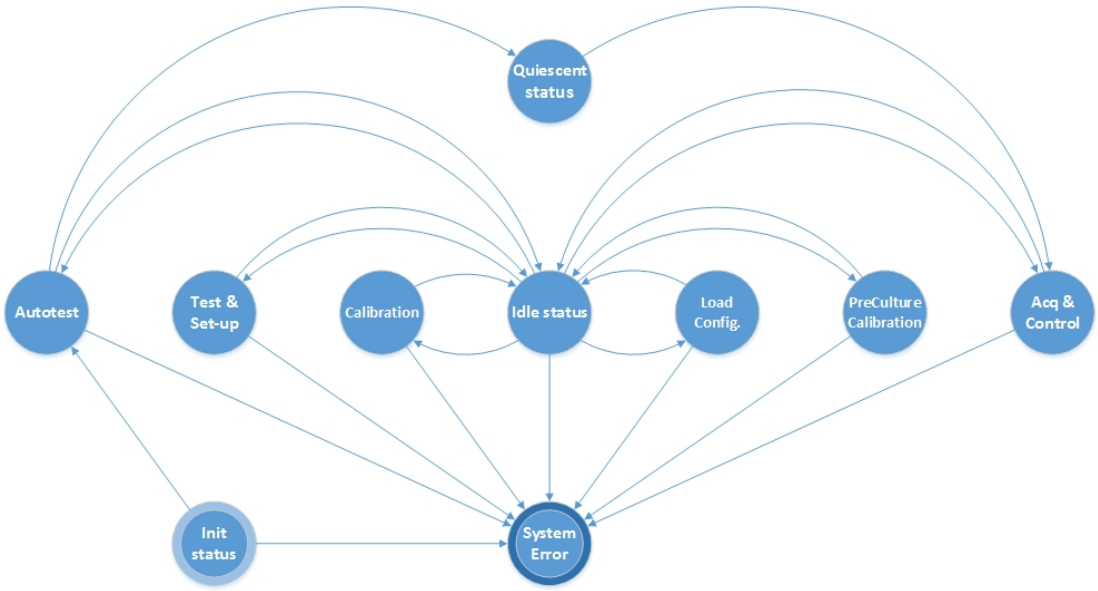

Figure 9
HexaScreen Bioreactor states diagram

- *Initialisation*: Default configuration is loaded from flash memory and all the working variables are initialised. If the loaded data is found to be corrupted or inexistent this circumstance is treated as a fatal error and the system moves to the "*Final Error*" state.

- *Autotest*: Automated check of the internal communications and sequenced actuation of the peripheral devices for fast inspection. If the internal communication check fails the system will move to the "*Final Error"* state.
  Next state depends on the value of the "*Last State"* parameter recorded on the flash memory, any value different than "*Idle"* points to an unexpected lack of power or analogue circumstance, if the recorded value was "*Acq & Control"* it means that something happened during the execution of the previous experiment so the last experiment configuration is restored and the system moves to the "*Quiescent Cell Culture"* state.
- *Idle*: Once the *"Autotest"* process has successfully been performed, the system starts "listening" the TCP port waiting for any service request coming from the host. This state can also be activated after any operation supported by the "*Test & Set-Up"* state, the *"Instrument Calibration"* state, the *"Load Configuration"* state, the "*Preculture calibration*" state, and the "*Acquisition & control*" state.
- *Test & Set-Up*: This state is intended for service tasks, on one hand provides access to the configuration data recorded on the flash memory, and on the other hand allows executing commands for testing single functions which are useful during the assembly procedure.
- *Instrument Calibration*: This state is analogue to the "*Test & Set-Up*" state but focused on the calibration procedure, it supports commands useful to obtain the thermometers calibration parameters, as well as to test the DO and the light spectra measurements.
- *Load Configuration*: It supports experiment configuration upload/download commands to/ from the host computer.
- *Preculture Calibration*: Automated procedure previous to the cell culture process itself. Supported commands are mostly related to thermoregulation, as well as to DO and OD calibrations.
- *Acquisition & Control*: Automated procedure that keeps the physical conditions constant all along the experiment (temperature, stirring, and aeration) and acquires real-time data on cell culture evolution (DO, pH & OD). If during the experiment the flux of data would be interrupted due to any reason, the system would try to re-establish the communication, if that would not be possible such circumstance would then be notified through the LCD and the system would move to the "*Quiescent Cell Culture"* state.
- *Quiescent Cell Culture*: The aim of this state is to preserve the contents of the Minibioreactors once a non-solved communication or unexpected power-up problem has been detected. In such circumstance the system restores the culture parameters according to the values established by the last valid experiment's configuration. Besides, the system stays "listening" the TCP port waiting for a service request from the host to re-establish the connection and move back to the normal "*Acquisition & Control" state.*
- *Final Error*: If some internal error happen a wait and retry procedure will take place in order to solve the problem, basically the internal errors that can be solved are the ones related to the communications between the RCM2200 module and the ADuC812

microcontrollers, if finally the wait and retry procedure times out the system moves to the "*Final Error*" state and notifies the corresponding error code through the LCD.

Since the treatment of other error types as the detection of aberrant and out of range data may require a certain interaction with the user. Then, high level error management is under control of the host computer software.

The Dissolved Oxygen board is in charge of measuring the fluorescence light emitted by the disposable oxygen sensors attached inside each MBR. The HexaScreen system uses the previously explained XOR phase detector (3.2.2 section) implemented by means of an AD8302 RF/IF gain and phase detector typically used for RF applications. However, it has been also documented for low frequency applications [3]. An oscillator block provides a 7…8 kHz sinusoid signal which is used to modulate the excitation LED's. Obviously the modulation signal is biased according to the LED's forward voltage. In order to reduce the cost of the DO measurement system a time multiplex technique was applied so it was possible to use only one photodetector to measure the fluorescence from every MBR. An optical long pass filter was directly mounted on the photodiode's window to reject the excitation wavelength light or other noise sources. Note that the hereby introduced module is a cost effective alternative to the proposed solution by the oxygen sensor manufacturer consisting of six multiplexed independent OEM modules [4].

Due to the relatively small magnitude of the light emitted by the oxygen sensor, about 3 % of the excitation peak (-15 dB), the long-pass filter must be carefully selected in order to maximize the detection sensitivity. Therefore, in order to consider that the excitation light compound reaching the photodetector is negligible in comparison with the emitted light, it is important to ensure a minimum crosstalk ratio between the of excitation and the detection channels in the order of -30 dB. Observe how for the selected filter (Deep orange - Wratten 22), the percentage of transmittance within the wavelength excitation region is < 0.01 % which is equivalent to a crosstalk ratio around -40 dB.

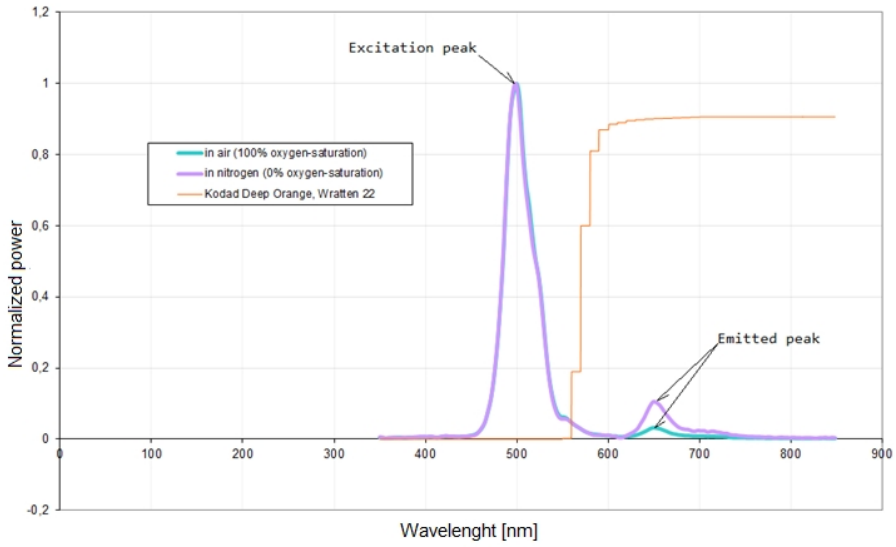

Figure 10
Backscattered light spectra emitted by a Presens SP-PSt3 oxygen sensor under two situations, 0 % and 100 % oxygen-saturation when irradiated at 505 nm.

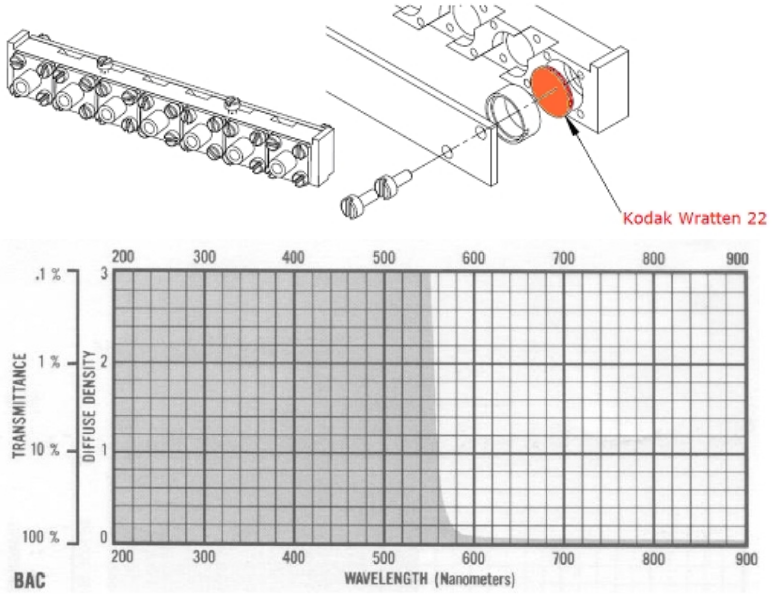

Figure 11
Deep Orange Wratten 22 assembly and Transmittance/Density curve [5]

Due to the significant number of actuators and the long required operation time per experiment the system was designed to avoid excessive power consumption. Therefore, in order to drive power consuming devices (TEC, heaters and electrovalves as well as any other actuator that could be necessary in the future), the Temperature and Drivers boards were based on PWM power management IC's like Texas Instrument's DRV593 and DRV103.

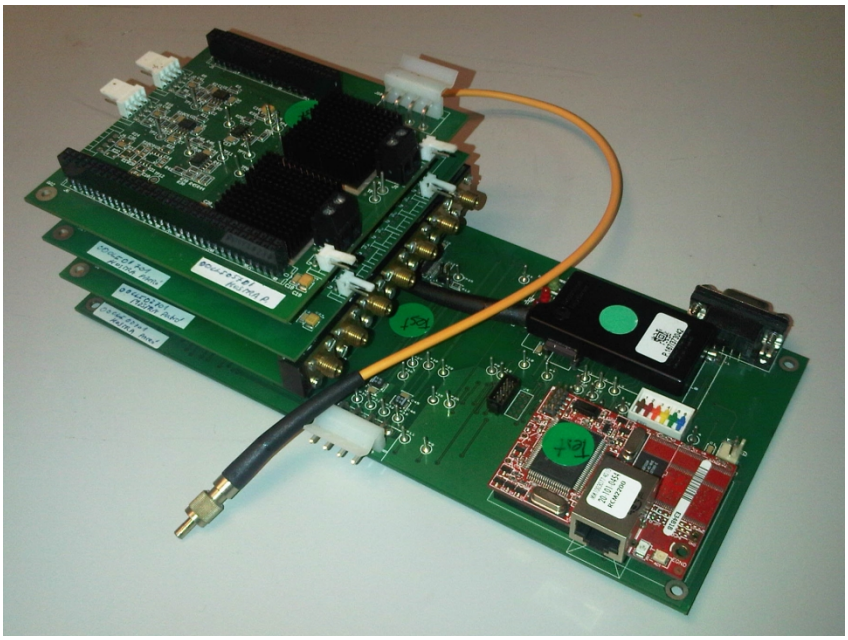

Figure 12
HexaScreen's Acquisition & Control hardware, inspired on the PC104 standard

4.1.3HexaScreen® optical layout.

In order to simplify manipulation and reducing the contamination chances, most of the measurements were designed to be performed using optical techniques where light beams are applied through the Minibioreactor's transparent walls and guided from the corresponding ports to the measurement electronics by means of a variety of optical parts. Two different optical set-ups were developed, one for absorbance spectroscopy measurements (used for pH and OD), and another for fluorescence measurements (used for DO). The following sections explain each set-up implementation as well as their theory of operation.

4.1.3.1 Optical absorbance spectroscopy measurement (pH & OD):

As mentioned above, absorbance spectroscopy was chosen to perform pH and OD measurements. One of the most common configurations used on optical density spectroscopy is based on the dual beam principle; on Figure 13 a possible optical layout for such configuration is shown. It is a complex instrument that allows solving spectral absorbance, compensating any change due to thermal drift or part's aging. It requires the use of some wide spectrum light source including optics to provide a parallel light beam, a beam splitter to produce a reference beam, two mirrors, one beam combiner, some diffraction system and one shutter or chopper device to alternatively select between the reference and the sample beam. Obviously, such approach implies a significant size and prize related to the mechanics used to hold the optics and to avoid unwanted movements.

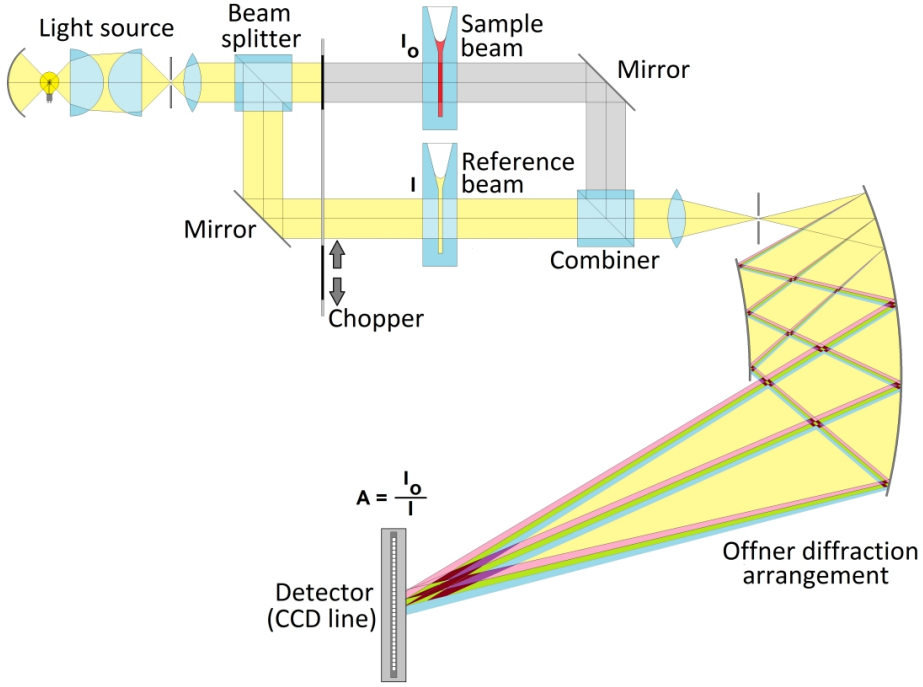

Figure 13
Double beam-Offner spectrometer.

The HexaScreen concept did not allow taking benefit of the dual beam configuration due to the reduced size of the Minibioreactor's plate; imposing the need of looking for some alternative realisation able to match the following requirements:

- Small size. It had to be integrated with the heating and the stirring subsystems.
- Multiplexing. It had to use a single detector device for the 6 Minibioreactors.
- Robustness and repeatability. The probes had to be connected and disconnected to the Minibioreactor's plate before and after every experiment.

The finally chosen optical layout it is shown on Figure 14 It is composed by a 6 legs fiber bundle (probes), one fiber optic taper, two inline SMA-SMA connectors, and 6 GRIN lenses working as collimators, the aim of all these parts is to collect the light that goes through the culture medium and to guide it to the sensing μspectrometer. The simulation in Figure 16 shows the light distribution into the medium and how is collected by the GRIN lens. GRIN lenses were primarily designed as components for fiber to fiber and laser to fiber connections [6]. However, they have been found to be useful for sensing purposes in multiple applications from analytical sensing to endoscopy [7] [8] [9] [10] [11] [12].

Due to the important trade-off between size and functionality the chosen light source was a wide spectrum white LED[1] which was embedded onto the heat pump's thermal plate in order to minimize any change of intensity produced by thermal drift. When the LED is switched on, the light travels through a 1 mm long and 0,5 mm diameter pinch hole which is filled with optical glue of known refractive index. The simulation (A) shows how the light beam is spread due to the pinch hole's numerical aperture and the refractive indexes of the different materials. It's important to mention that for such simulation seawater was used to mimic the culture broth. Nevertheless, seawater behaves as a homogeneous medium which is not true for actual cultures, where the presence of cells distorts the light beam producing a very well-known effect known as light scattering. So it was predictable that the final sensitivity shall be affected by this phenomenon. Simulation (B) shows the maximum numerical aperture of the GRIN probe able to focus the received light into a 300 μm fiber optic. It means that any ray out of the acceptance angle here represented will not reach the fiber entrance implying that only a small fraction of the emitted light is finally collected by the fiber. On the other side, it makes the probe more robust to the distorting effects of the scattered light and Fresnel reflections [13]. That is more obviously represented on simulation (C) where the excitation beam and the probe's numerical aperture were overlapped in order to show that only the transmitted and the scattered light within the intersected volume are contributing to the absorbance measurement. Experimental measurements proved that this is a good, and cheap, approach to a parallel beam compared to the ones produced by standard spectrophotometers.

During normal operation, each LED shall be switched on and off sequentially and the respective beams of light shall go through the culture medium with a relatively high numerical aperture. Hence, the light collected by each probe shall be affected not just by the Beer's law but the interaction of light through the interfaces (Fresnel reflections) and the suspended biomass.

[1] Luxeon Warm White Emitter LXHL-BW03

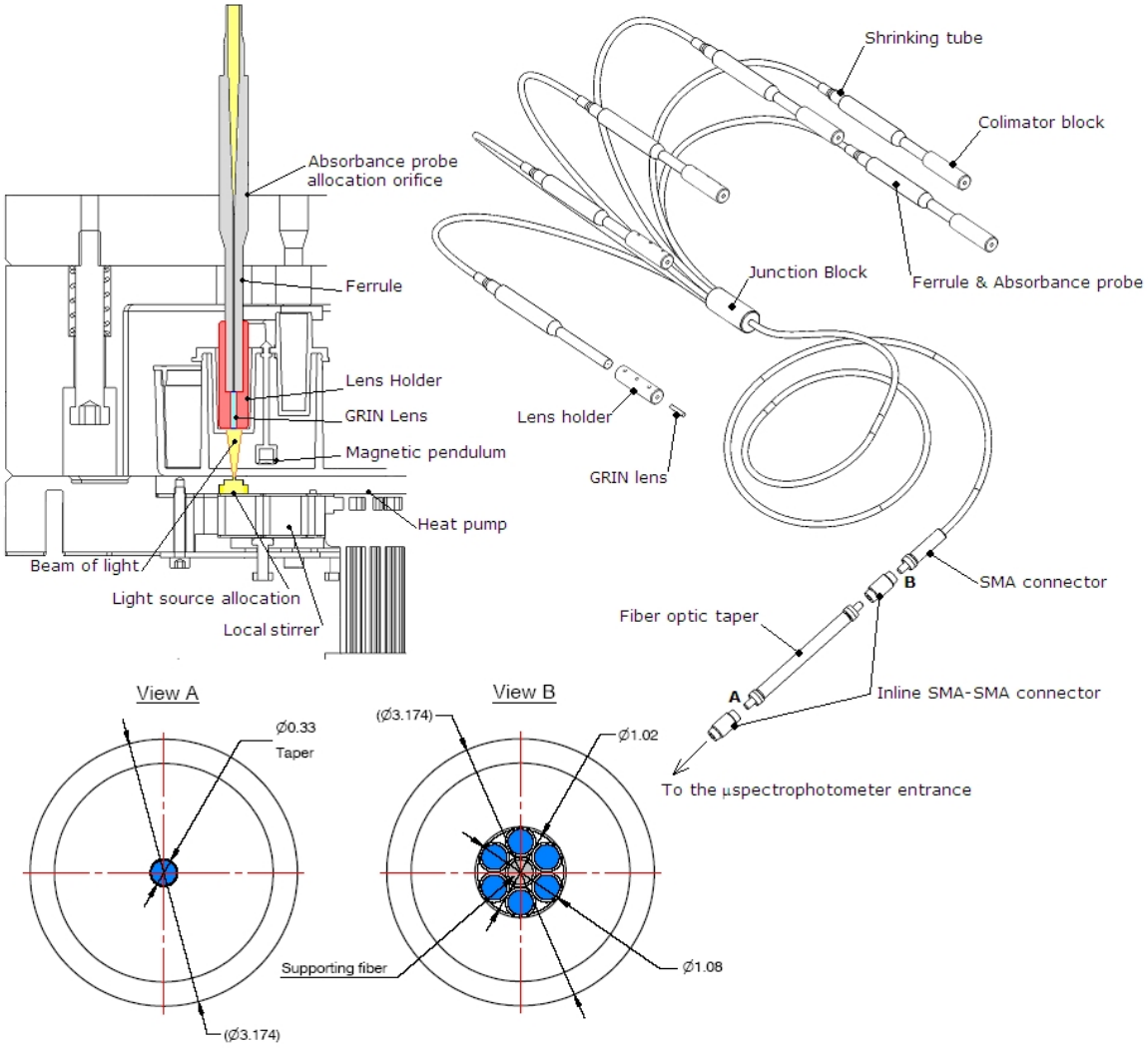

Figure 14
HexaScreen's Optical absorbance setup

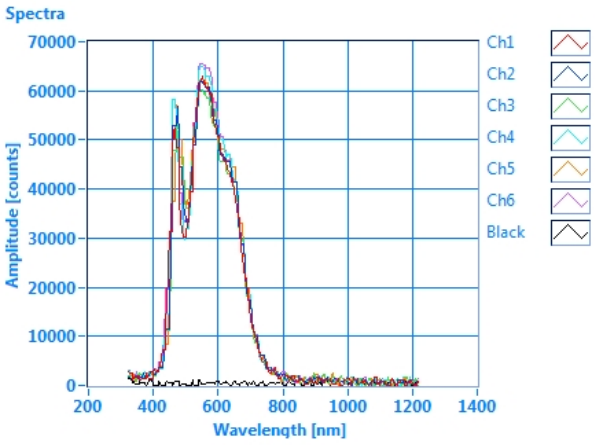

Figure 15
Post-equalization spectra profile per channel provided by the excitation LED's.

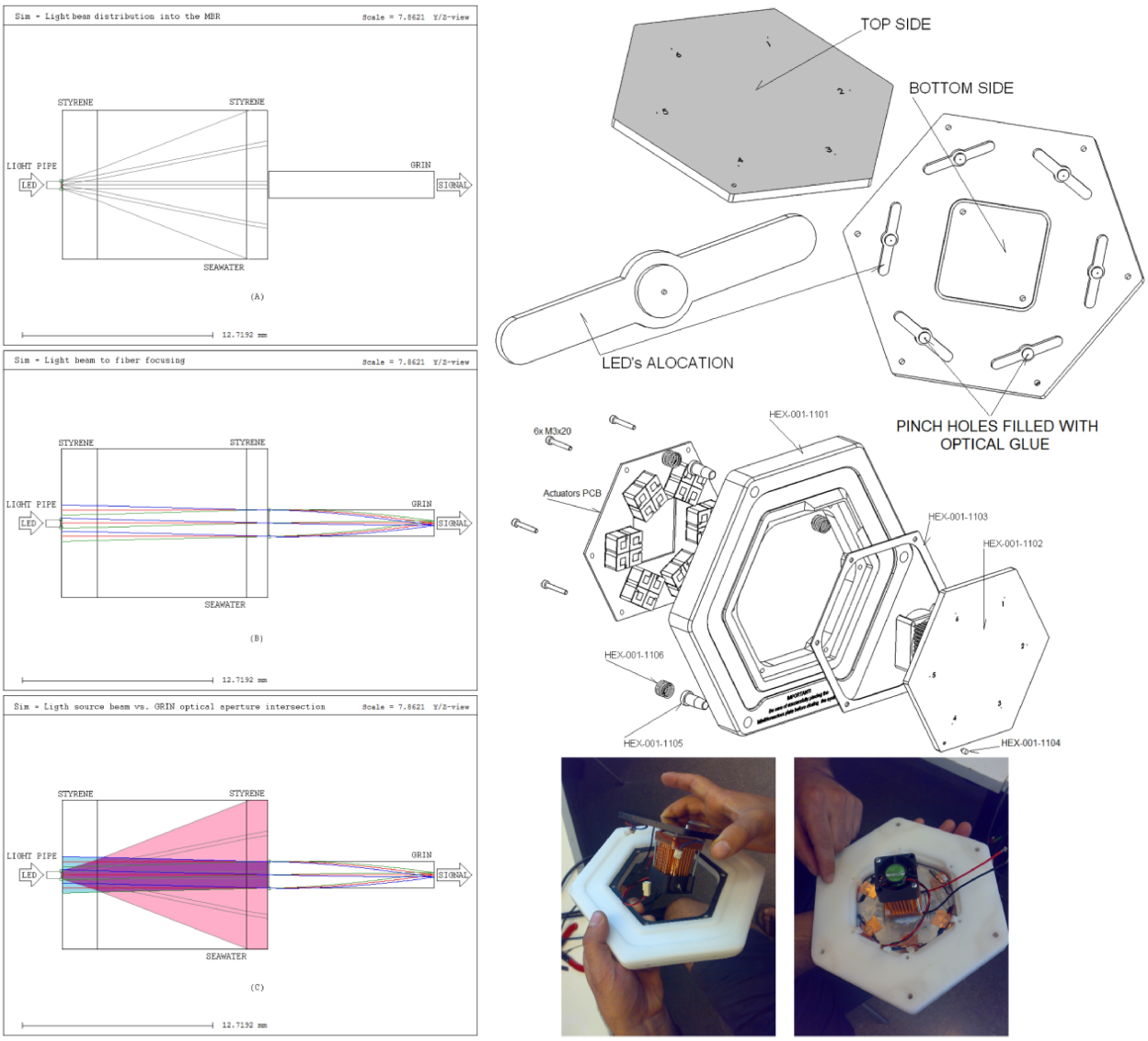

Figure 16
Left. - Geometrical simulation of the optical absorbance port.
Right. - LED's integration onto the thermal block.

Two important drawbacks of the presented arrangement are the lack of a reference beam and the need of quite complex mechanics to avoid positioning errors between the light source and the probe. Such lack of a reference beam may be overcome by controlling the power of light emitted per each LED or as the HexaScreen system does, by taking a reference measurement before starting the experiment. That requires keeping the same working conditions all over the experiment. On the other hand, probe's verticality and alignment vs. light sources was ensured by properly fixing each probe on a thermo-controlled aluminium plate which was guided by three stainless steel shafts with ball bearing and leading tips.

Once the light signal has been collected by each probe, the fibers are gathered in a junction block and connected to the μspectrometer by means of the fiber optic taper which consists of a diameter decreasing fiber enclosed inside of a stainless steel protecting tube; its

function is to adapt the different relative positions of the fibers in the bundle's side with respect the µspectrometer entrance.

The following paragraphs explain how the proper use of such device provides a cheap and robust method for fiber optic multiplexing, avoiding the need of expensive opto-mechanical systems, i.e.- Ocean Optic's MPM-2000 which is based on an encoded DC motor connected to an optical arrangement that switches sequentially from one channel to the next, the system provides accurate measurements over 16 channels with a repeatability of 99% and offers optical throughput of approximately 50%

Figure 17
Ocean Optic's MPM-2000 Optical Multiplexer

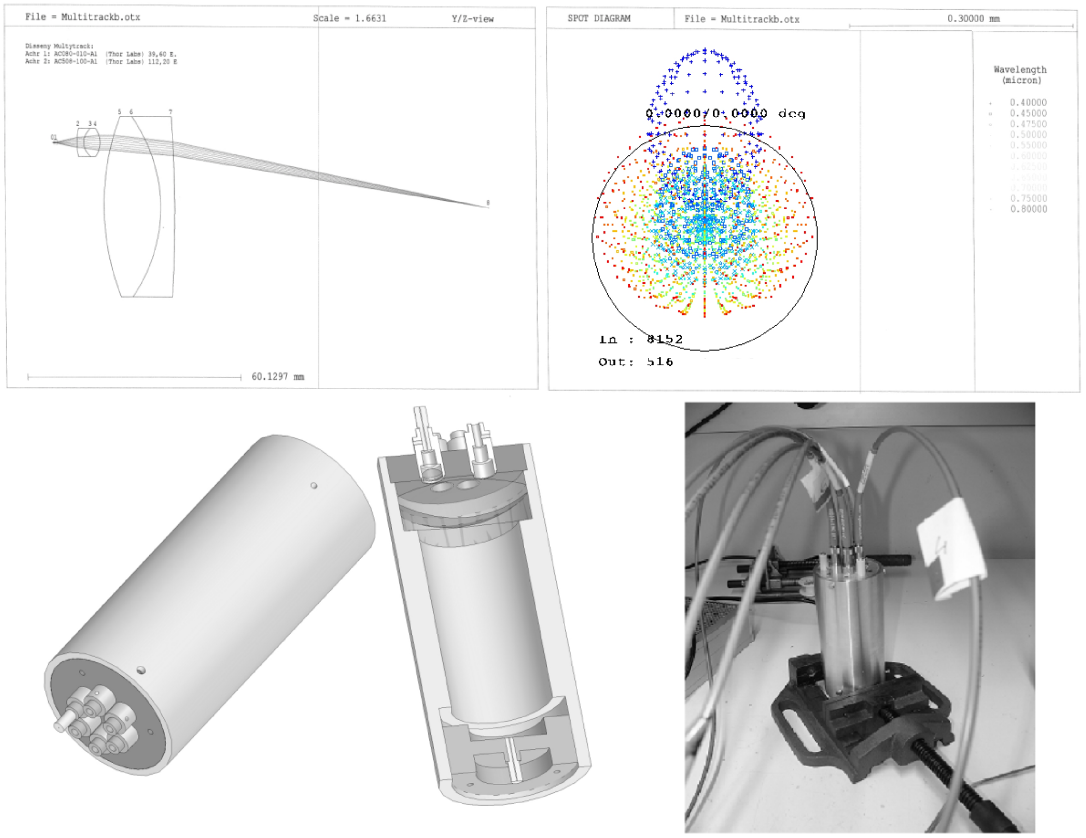

Figure 18
Custom fiber optic multi-track

The first solution investigated was an optic bench based on spherical lenses (Customised fiber optic multi-track), the system was made of 6 collimation units focusing the collected light from each fiber on the peripheral surface of a converging achromatic doublet, the resulting beam was then focused on the μspectrometer's fiber. This is illustrated by the simulations in Figure 18. In addition, the spot diagram shows how for the central wavelengths of the visible spectra (400 … 800 nm) most of the energy is distributed inside the area of the μspectrometer's fiber. Hence, the chromatic aberration may be considered negligible. Unfortunately, the experimental results were not successful enough to use such solution as an alternative to the fiber optic multiplexer, the custom fiber optic multi-track turned to be very sensitive to the assembling errors and mechanical imperfections, hard to adjust, and still quite expensive. Therefore, other options had to be considered.

An obvious solution could consist on using thinner fibers < 100 μm to allow the bundle's output match the 300 μm μspectrometer fiber entrance. However, such solution was discarded due to the direct reduction of light throughput, nine times or more depending on the diameter chosen and avoiding a non-uniform distribution of power on the μspectrometer's entrance fiber which is unacceptable for the μspectrometer proper operation.

Despite that the fiber optic taper is not better in terms of light attenuation due to the conservation of brightness law (Taper light throughput is inversely proportional to the square of the taper ratio) [14], it offers the possibility to collect light on its wide end and deliver a fraction of it through its narrow end, which provides a more uniformed distribution of power on the μspectrometer's fiber entrance. The figure below shows both the propagation modes along the fiber optic taper and the power distribution on its narrow end. It can be observed how for a decentred probe coupling the taper's narrow face shows a quasi-uniformed power distribution that will favour a proper use of the μspectrometer.

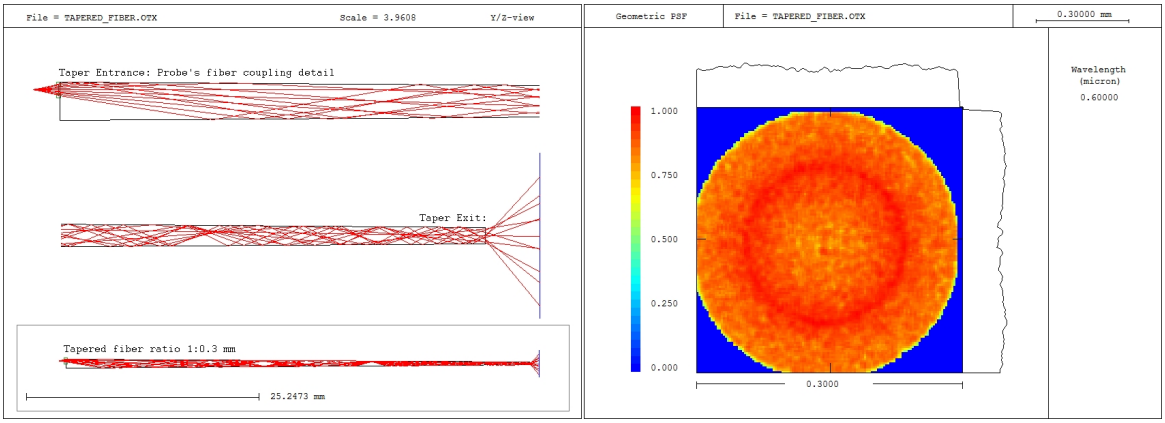

Figure 19
Fiber Optic Taper geometrical analysis and PSF. The diverging ring shown by the Airy disk is produced by the probe's fiber necessary misalignment. Such aberration will not produce significant μspectrometer misbehaviour.

The well-known Lambert-Beer Law states that the optical absorbance of a homogenous medium is affected by the chemical concentration (C) of the substances which it is made of [15]:

$$-log\left(\frac{I}{I_o}\right) = \varepsilon \cdot C \cdot \Delta x$$

Where ε is the extinction coefficient and Δx is the thickness of the medium. The optical density (OD) which is a commonly used parameter to estimate the cell concentration in microbial cell cultures [16] [17] [18] is in fact defined only for particles free medium where the light scattering phenomena is inexistent and the optical absorption is due to the absorbed energy by the vibrational and rotational movements of the chemical bonds in the molecules in the light path at specific wavelengths.

$$OD = \frac{1}{\Delta x} \cdot log\left(\frac{I_0}{I}\right)$$

The HexaScreen system applies optical absorption spectroscopy for both measuring pH and cell concentration. However, some restrictions must be taken into account:

- Due to the fact that a cell culture is not a homogenous medium the light scattering phenomena is present, so the OD to cell concentration ratio becomes easily non-linear and can only be applied for OD values below 0.4 AU depending on each specific calibration and cell specie.
- The use of some diluted pH dye in the culture medium is required.
- Due to the light attenuation produced by the cells, the pH estimator must be corrected by the OD. Hence, the pH measurement range is limited by the OD saturation threshold.
- The OD measurement refers to the total number of cells present in the medium, both viable and nonviable.

The following formula is applied to calculate the OD[2]:

$$OD = G_i \cdot \log_{10}\left(\frac{\int_{\lambda_{OD}-\Delta\lambda}^{\lambda_{OD}+\Delta\lambda}\left(S_{white}(\lambda) - S_{black}(\lambda)\right)d\lambda}{\int_{\lambda_{OD}-\Delta\lambda}^{\lambda_{OD}+\Delta\lambda}\left(S_{meas}(\lambda) - S_{black}(\lambda)\right)d\lambda}\right)$$

Where:

- λ_{OD} [nm]: Cell concentration measurement wavelength must be chosen depending on the cell specie and far enough from the region of the pH dye absorption spectra. For animal cells and phenol red indicator typical values ranges from 600 to 650 nm.
- $\Delta\lambda$ [nm]: Wavelength integration interval.
- S_{white}: Reference Spectral Power Density.
- S_{black}: Black Spectral Power Density. (Dark Current).
- S_{meas}: Measured Spectral Power Density.

[2] The above formula allows correcting any zero drift as well as to increase the signal to noise ratio thanks to Gaussian noise provided by the μspectrometer.

- G_i: Calibration Gain. Mostly due to mechanical imperfections each channel must be individually calibrated to provide an accurate OD value.

As far the previous restrictions are respected, a certain cell concentration can easily be correlated to OD[3] and solved by simply multiplying the measured OD by a previously calculated OD to cell concentration conversion factor.

$$X = \alpha_b \cdot OD$$

- α_b [cell/ml]: OD to Cell Concentration factor. Linear relationship between the optical density increase and cell density increase.
- OD []: Optical density (absorbance).

To monitor pH, an indicator dye absorbing within a certain wavelength range between 400 to 700 nm is to be used in the culture medium. In the case of mammalian cells, phenol red was selected since it is currently used in most culture mediums, and it shows a significant variation of the optical absorbance precisely around the optimal pH growth ranges (pH=6.5-8.5). The method it was previously reported and applied to monitor cell cultures by [19] however it has also been used for some other physiological measurement applications [20] [21]

Phenol red has two absorbance maximums at 430 and 560 nm, these correspond to the acid and alkaline forms respectively [22] [23]. Since the alkaline form is the one which shows maximum sensitivity to the pH variation, the optical absorbance to estimate the pH shall be calculated at such wavelength of 560 nm. However, the attenuation effect produced by cell growth must be taken into account and the formula needs to be modified as follows:

$$Abs_{pH} = G_i \cdot \log_{10}\left(\frac{\int_{\lambda_{pH}-\Delta\lambda}^{\lambda_{pH}+\Delta\lambda}\left(S_{white}(\lambda)-S_{black}(\lambda)\right)d\lambda}{\int_{\lambda_{pH}-\Delta\lambda}^{\lambda_{pH}+\Delta\lambda}\left(S_{meas}(\lambda)-S_{black}(\lambda)\right)d\lambda}\right)-OD$$

Where:

- λ_{pH} [nm]: pH measurement wavelength depends on the dye chosen.
- $\Delta\lambda$ [nm]: Wavelength integration interval.
- S_{white}: Reference Spectral Power Density.
- S_{black}: Black Spectral Power Density. (Dark Current).
- S_{meas}: Measured Spectral Power Density.
- G_i: Calibration Gain.

[3] OD can be representative of cell concentration for suspended cell cultures. However, it is not suitable for adherent animal cells growing on a monolayer.

- *OD*: The optical density can directly be used for the correction when the optical absorbance produced by the cell growth at both λ_{OD} and λ_{pH} wavelengths are approximately the same.

In order to monitor pH, the parameters of the sigmoidal ratio between pH and absorbance must be calibrated before the experiment. The sigmoid parameters depend on the phenol red concentration present in the culture medium. This implies that the technique's accuracy is highly dependent on the estimation of the sigmoid parameters. Experimental tests yield a ±0.03 accuracy within the 6.5 … 8.5 range.

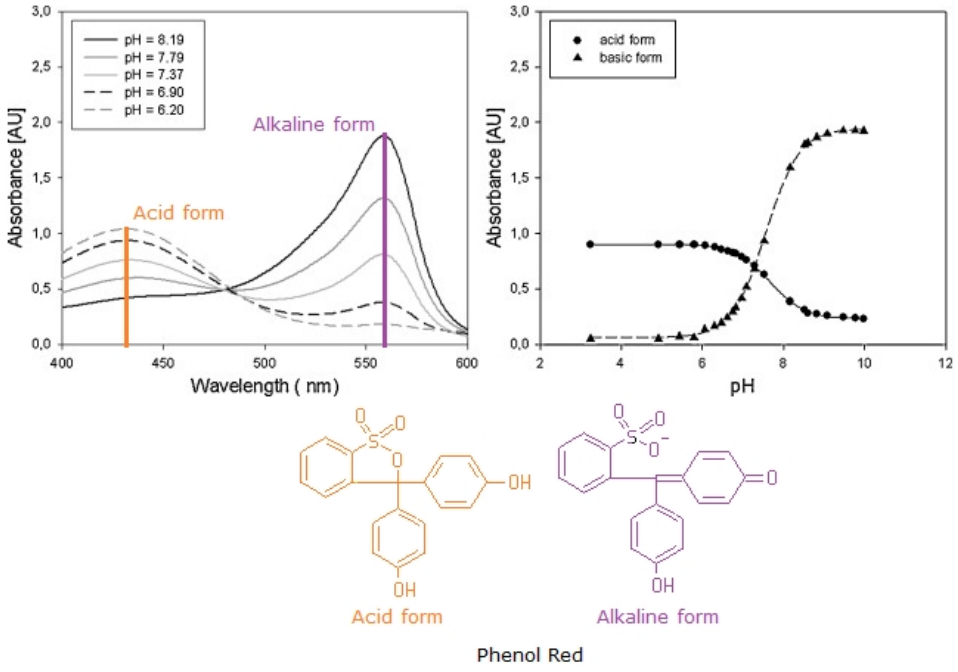

Figure 20
Left: Absorbance spectra of a phenol red solution at various pH values for determination. Right: Absorbance to pH sigmoid fitting curves for both acid and basic forms of phenol red. Adapted from [23]

Furthermore, due to the fact that the optical absorbance is a relative measurement, the initial medium's pH needs to be taken into account to provide and absolute estimation. Therefore, the actual medium's pH is required to be measured by some other means just before starting the experiment and after seeding the Minibioreactor to make sure that no significant pH drift can happen due to the CO_2 exchange between the liquid phase and the surrounding atmosphere.

The pH value shall be calculated by the following formula:

$$pH = C - B \cdot \ln\left(\frac{A}{Abs + Abs_0 - D} - 1\right)$$

Where:

- A: Sigmoid parameter.
- B: Sigmoid parameter.
- C: Sigmoid parameter, Residual pH value.
- D: Sigmoid parameter, Residual absorbance value for zero pH.
- λ_{pH} [nm]: pH measurement wavelength depends on the dye chosen.
- Abs []: Measured absorbance at the pH measurement wavelength (λ_{pH}).
- Abs_o []: Initial absorbance at the pH measurement wavelength (λ_{pH}) corresponding to the medium's pH initial value which it can be solved by:

$$Abs_o = D + \frac{A}{1 + e^{\left(\frac{C - pH_o}{B}\right)}}$$

4.1.3.2 Fluorescence measurement (DO):

The dissolved oxygen concentration is obtained by means of the light response produced by a fluorescence patch sensor attached inside each Minibioreactor using the Phase shift method. The fluorescence kit is composed by a unique part, a 6 to 6+1 leg fiber bundle which guides the excitation light from the excitation LED's to the fluorescence ports, and delivers the collected response to a sensing photodiode.

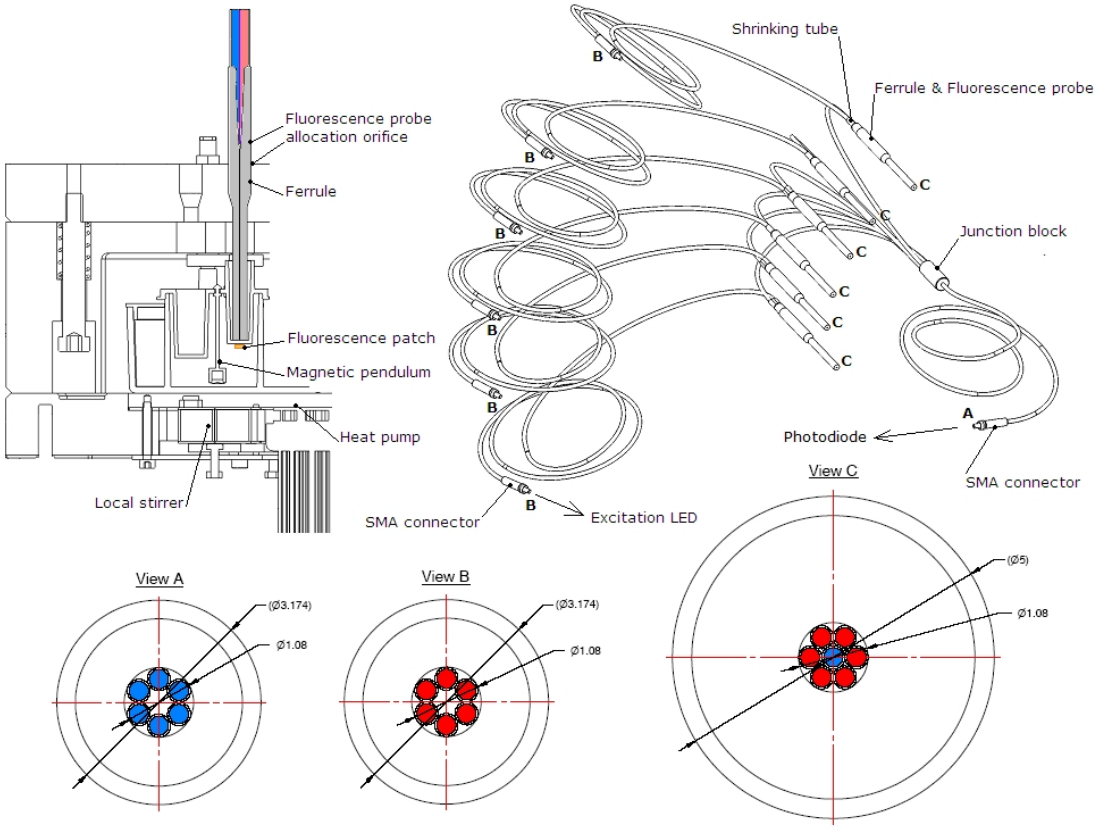

Figure 21
HexaScreen's DO fluorescence setup

The excitation fibers are hexagonally arranged around the collecting fiber in the probe's tip, such configuration was built based on the simulations performed by Papaioannou [24] to ensure a proper irradiation of the sensor spot. During operation, each individual excitation LED switches on and off sequentially, so the sensor spot's emitted light is synchronously read by the photodetector placed in the oxygen module. The principle of measurement was introduced in the 3.2.2 section of State of the art chapter.

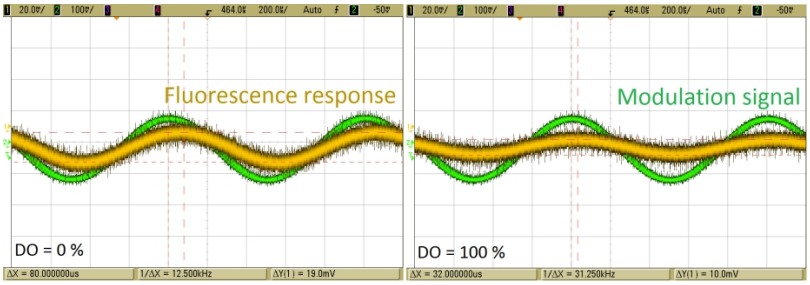

Figure 22
Phase shift acquired by means of the HexaScreen's DO measurement module and a Presens DO sensor.

4.1.4 Minibioreactor aeration, stirring & mass transfer.

System's aeration is performed by means of a set of seven electrovalves. Each Minibioreactor is connected to an On-Off electrovalve which opens periodically for a certain period of time in order to allow individual culture aeration. The system features two gas inlets that can be connected to air+CO_2 and N_2 gas supplies depending on the user's needs. An extra switching electrovalve allows selecting between both gas supplies which is useful to perform OUR estimation by removing the oxygen of the headspace volume and measuring the oxygen extinction profile into the liquid phase (Dynamic method). Additionally, both gas inlets include means for humidification in order to compensate the loss of volume in the Minibioreactors due to evaporation.

The following illustration shows the pneumatic model of the gas circuit, consisting of six solenoid valves one per each Minibioreactor connected to a common line served by the seventh solenoid valve which acts as the gas supply switcher.

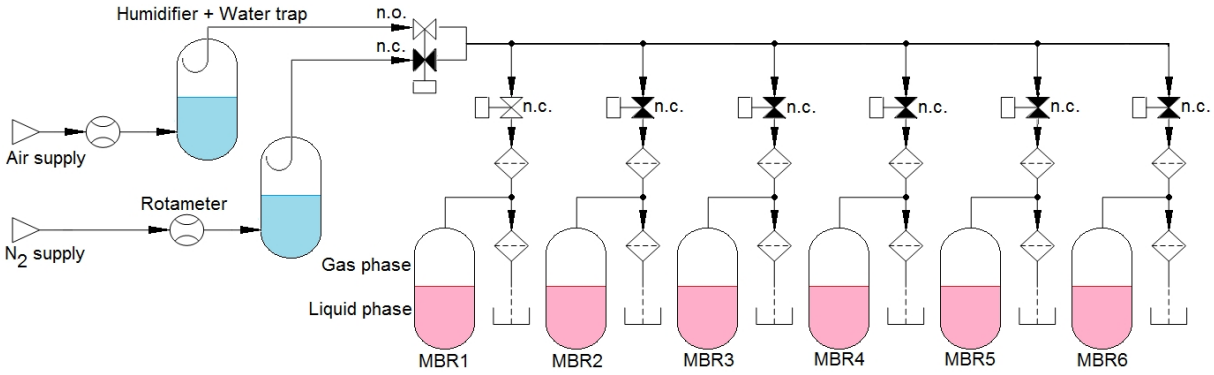

Figure 23
Aeration circuit model

Once the gas supplies are connected and both relevant pressures and flows are adjusted, air and nitrogen flow through the humidifier columns and water traps. However, given the fact that initially all valves are closed; gases will stop flowing once pressure equilibrium is reached.

Under normal operating conditions, electrovalves will operate sequentially, starting again at the first electrovalve once after the sixth Minibioreactor has been aereated. This ensures that the flow rate is approximately the same for each Minibioreactor during an individually programmed operating cycle which enables the user to apply different aeration regimes.

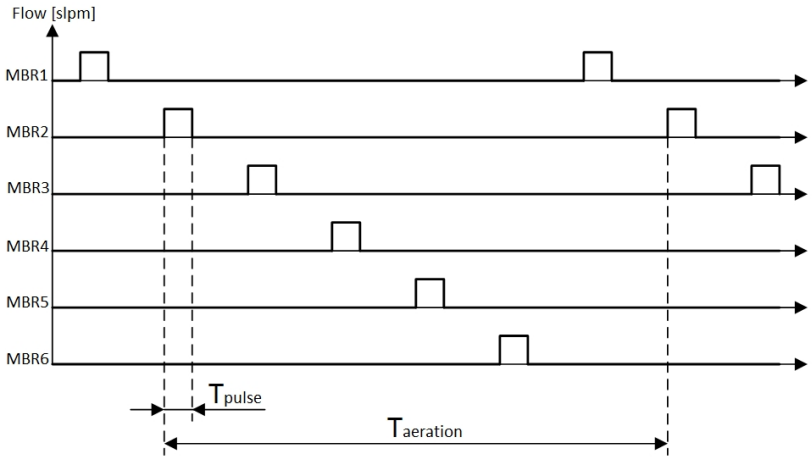

Figure 24
HexaScreen's Aeration electrovalves timing chart

The aeration method is a key point aspect in bioreactor design. However, is not the only parameter to take into account to ensure a sufficient mass transfer. Stirring shall also be considered if high cell concentration is wanted to be achieved.

In stirred tank bioreactors proper mixing is required to avoid gradients of oxygen, nutrients and cell density [25], for bench scale bioreactors and bigger volumes the most widely used types of impellers are Marine, Rushton and Pitch-Blade, the selection of a certain type of impeller or even a combination of them mostly depends on the productivity target for a specific bioreactor, as well as the cell specie that is going to be cultivated. For bioreactor's hydrodynamics characterization a number of parameters have been defined: Flow regime (turbulent, laminar), Mass transfer, Hold up time, Mixing time, Shear stress…

However, when the application involves single use miniaturized bioreactors some other constraints arise, on one hand the impeller must be cheap and small enough to be included on a disposable product and fit into a small volume, on the other hand it must be able to support the required culture conditions.

During the early stages of the development a simple stirrer was implemented by means of a stir barr located inside the Minibioreactor [1] driven externally by an electronically controlled electromagnet. However, it was found that the mechanical forces produced by the stir barr (friction and shear) were dangerous for growing mammalian cells. Hence, the finally

chosen stirrer for the construction of the HexaScreen's Minibioreactor plate consisted of a flexible pendulum made of biocompatible silicone[4] with an enclosed Neodymium magnet.

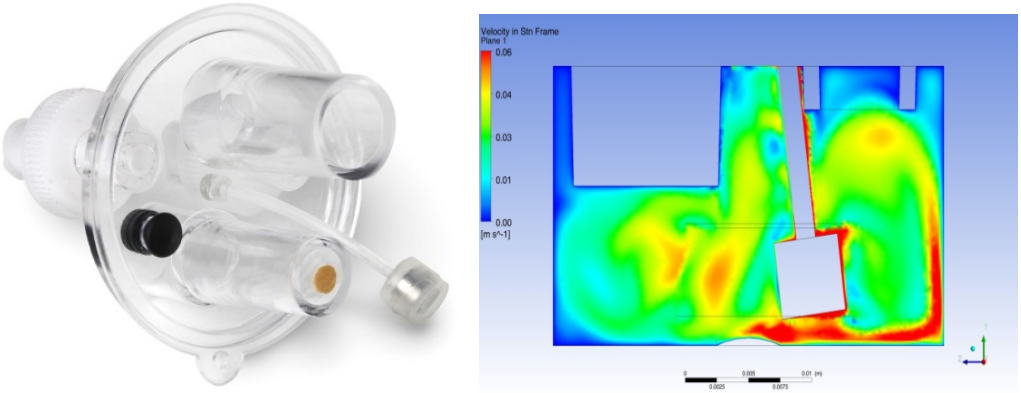

Figure 25
Flow topology simulation based on a flexible pendulum stirrer[5].

Experiments were carried out in order to test its functionality using Hybridoma as mammalian cell model; due to the vessel's geometry it was found the existence of dead volumes between the walls of the Minibioreactor and the optical ports, leading limitations in terms of power transfer and stirring smoothness. Nonetheless, the pendulum was finally selected since it shown to be useful for animal cells being able to keep a Hybridoma culture alive for several days avoiding sedimentation.

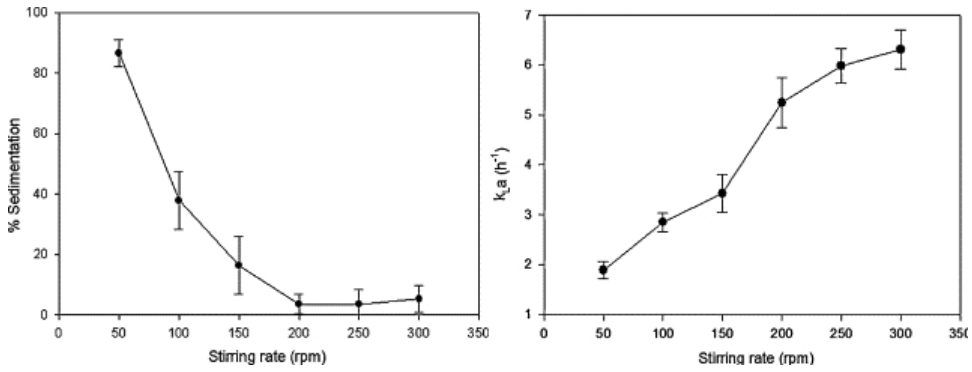

Figure 26
Left: Percentage of cell sedimentation. Right: k_La values
Both graphs are expressed as function of the stirring rate. [23]

Regarding the driver, the concept of the classical magnetic stirrer based on AC asynchronous motors was rejected due to the presence of perishable moving parts. A different approach with no moving parts was developed (Figure below):

[4] Rhodorsil® MF 970 USP (Bluestar Silicones)
[5] This simulation was performed in the frame of collaboration with the Dept. of Chemical Engineering - Federal University of Rio de Janeiro.

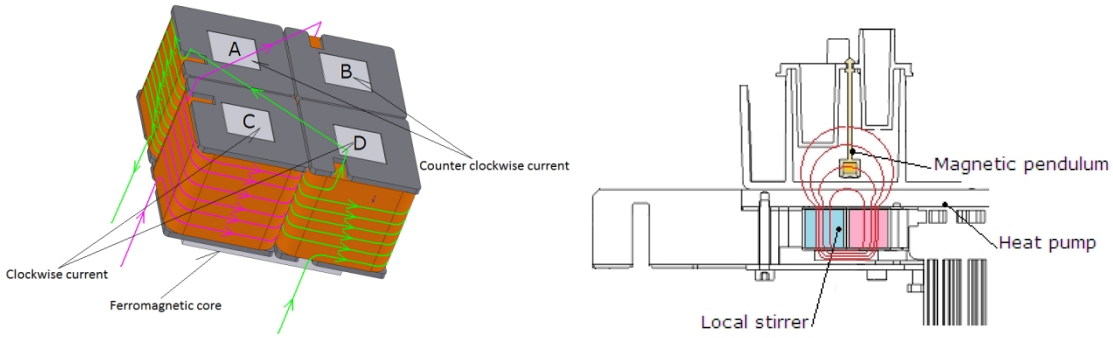

Figure 27
Left.- Electromagnet's connections and current senses. Right.- Magnetic field distribution.

A four pole electromagnet electronically controlled by means of PWM signals was implemented. Such electromagnet was made of four solenoids arranged orthogonally and a ferromagnetic core geometrically designed to maximize the magnetic field within the Minibioreactor's culture volume. In this way a driving magnetic field was obtained by the composition of the fields produced by the solenoids A, B, C, D which were connected in pairs A-D, B-C in such a manner that currents flow clockwise and counter clockwise producing complementary fields coming in and out on each pole.

With some slight differences such concept of electromagnet has been used by the German company VARIOMAG to develop a range of magnetic stirring products [26]. However, the fact that they are not able to produce low rotation speeds, which is required for some sensitive animal cells i.e. Stem Cells, suggests that the solenoids are activated sequentially. Therefore, if a too long sequence period would be applied the stir bar would rotate in a discontinuous and unexpected manner, producing unwanted shear forces over the cells. On the contrary, the solenoid's driving method used by the HexaScreen system allows a soft rotation from zero up to several hundred rpm's, which is the optimal range for most animal cell applications.

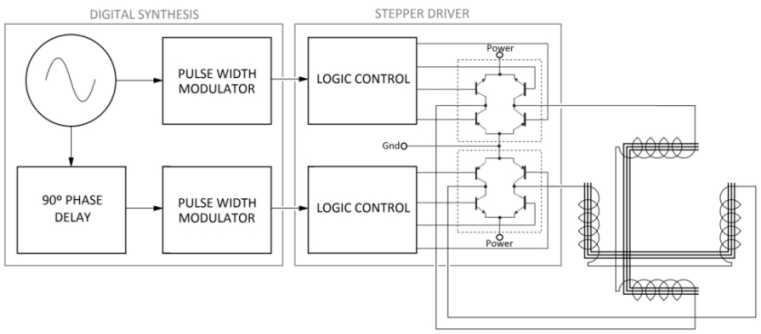

Figure 28
Electromagnet's driving signals generation

The block's diagram above shows the driving signals generation scheme, the front block consists of two H-bridges and logic control modules that convert the PWM signals into currents flowing through the solenoids, this part of the circuit may be implemented by any Stepper Motor IC. However, attention must be paid when choosing the right IC since the H-

Bridge must include fly-back diode protections in order to avoid voltage spikes due to the solenoids reactance. What it makes possible to obtain a soft stirring motion is the type of signal used for modulation, a sinusoidal oscillator was used to feed both modulators with a 90° phase difference, finally regardless of the stirrer's physical limitations like mass, geometry, or medium's viscosity, the obtained stirring rate was directly proportional to the oscillation frequency. This was proofed in the HexaScreen system for aqueous solutions between 0 to 400 rpm's.

Even though many different solutions were possible for the PWM signals synthesis. The fact that the required oscillation frequency to achieve a high stirring rate is still very low (167 Hz per 1.000 rpm's) made possible to use of an inexpensive microcontroller to generate the PWM signals by Direct Digital Synthesis.

4.1.5 Experimentation workflow & results.

In this section a brief explanation of the HexaScreen system experimentation workflow is developed, as well as the obtained results for some possible applications of the system using productive animal cell lines are explained. Further results including OUR estimation by means of the dynamic method will be discussed on section 5.3

Steps of the experimentation workflow:

- Experiment definition: It consists on the definition of the experiment's conditions and parameters for a certain application: Cell type, inoculum's concentration, stirring profile if needed (i.e. for adherent cells culture on micro-carriers), aeration rates per each MBR, temperature, composition of the culture medium, etcetera. Once all variables have been defined an experiment file is to be created and then being loaded by the acquisition software just before starting the cell culture.
- Workstation preparation: Some previous verification shall also be performed before starting the experiment. The pressure of the gasses supply and the humidification unit's water level shall be checked to ensure a proper mass transfer as well as to avoid medium evaporation along the culture time.
- Minibioreactor plate inoculation: It consists on the procedure of preparing the Minibioreactor plate to place it into the workstation. Filling the external water bath and each Minibioreactor with fresh medium and inoculate them with the selected cells. Before the inoculation step is advisable to preheat both water and culture medium in order to minimize the cell stress due to temperature changes. Moreover, due to the fact that most of the animal cell culture mediums are carbonated it becomes necessary to pre-set its pH to the cell's physiological value by placing it inside a CO_2 incubator for a certain period. Once the plate is ready for use and just before starting the experiment, the pH of the basal medium shall be measured using a bench-top pH-meter in order to provide the initial pH conditions required by the acquisition software.

Figure 29
Minibioreactors plate inoculation under sterile conditions

- PreCulture stage: Once the Minibioreactor plate is located inside the insulation chamber the experiment can be started. To do so, some previously defined experiment file may be loaded by the software and the initial pH values or other variables may be entered depending on the actual conditions. After that, the experiment configuration is uploaded to the workstation and the Preculture wizard is launched. This is a wizard like procedure to ensure the right temperature and aeration conditions before any reference measurement is acquired, once the temperature reaches the culture set-point both fluorescence and light spectra references are acquired per each channel and related to the 100% DO and the initial conditions of pH and OD respectively.

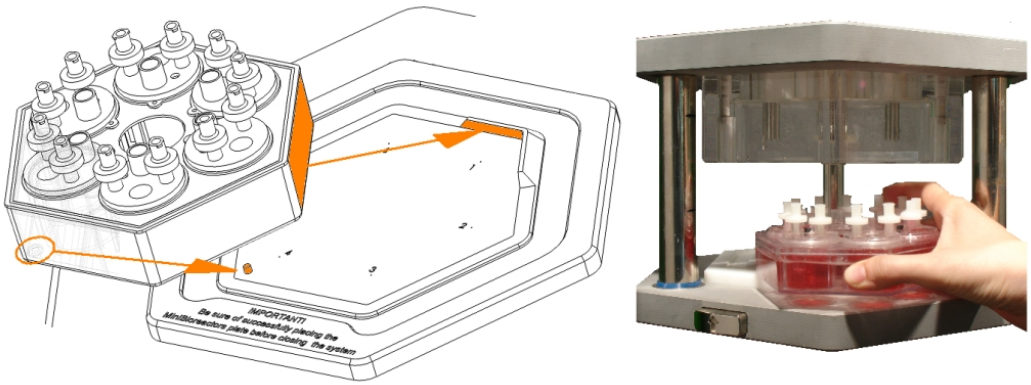

Figure 30
Placing the Minibioreactor's plate

- Acquisition and control stage (Results evaluation): Once the PreCulture stage finishes the system begins to display on-line data on Temperature, DO, pH, OD and Cell concentration. The following culture examples demonstrate the HexaScreen system as a useful tool for screening proposes in animal cell biotechnology.

Example I

Medium optimization – Fetal Calf Serum (FCS) efficiency evaluation

Experiment description

The aim of the experiment was to evaluate the efficiency of two different FCS supplements (batches A and B) in comparison to a commercially FCS (batch C) when culturing NS1 mouse myeloma cells. Prior to the experiment, cells were thaw out and cultured for a week in DMEM + 10% standard FCS (batch C). During inoculation, cells were rinsed twice to eliminate the FCS used during cell expansion, and every Minibioreactors was inoculated from this common inoculum at $2 \cdot 10^5$ cells/ml with a total volume of 12 ml per Minibioreactor. The three FCS batches were added as follows:

FCS batches and concentration used per each Minibioreactor

Minibireactor	FCS batch	FCS concentration
MBR1	A	10 %
MBR2	A	5 %
MBR3	B	10 %
MBR4	B	5 %
MBR5	C	10 %
MBR6	C	5 %

Culture Conditions

Medium: DMEM + 3 different FCS batches ("A", "B" and "C" as a control) at 5% and 10%
Cell line: NS1 mouse myeloma.
Volume: 12 ml
Initial cell concentration: $2 \cdot 10^5$ cells/ml
Stirring rate: 200 rpm
Bioreactor temperature: 37 °C
Aeration rate: 0.2 slpm (Duty cycle: 2%)

Results

The graphs below show the on-line profiles of optical absorbance, cell concentration, pH and dissolved oxygen obtained along 6 days of culture.

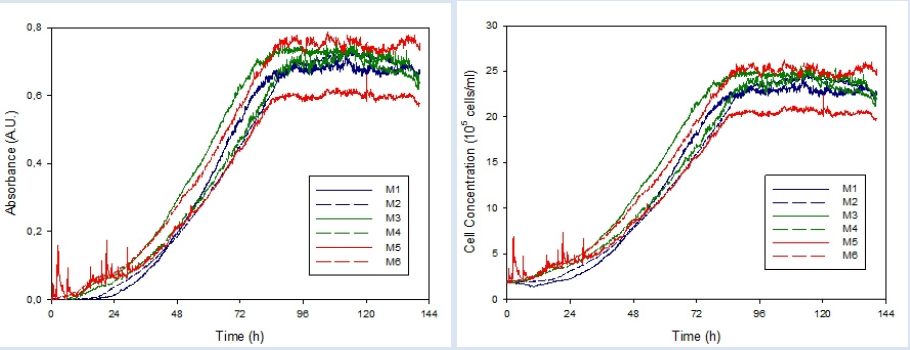

Optical absorbance and Cell concentration may be considered proportionally equivalent for OD values below 0.8

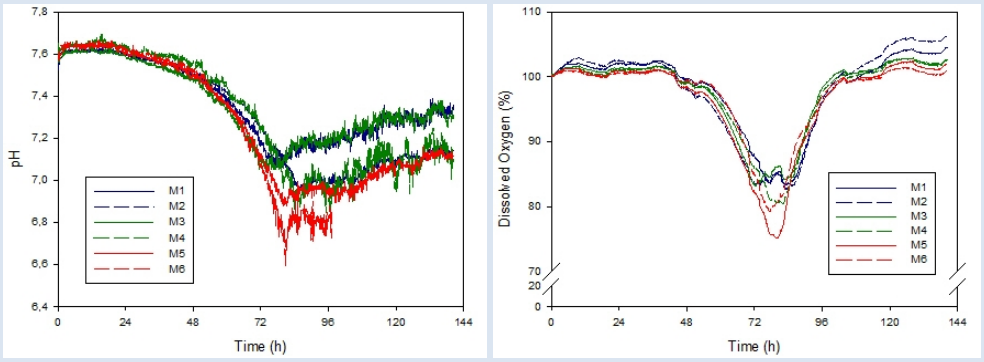

pH and DO evolution

Analyzing the different profiles it can be observed that the cell growth is quite similar for every one of the FCS batches tested, with almost the same profile during the tropophase and reaching the same cell concentration after stabilization $23{\cdot}10^5$ to $25{\cdot}10^5$ cells/ml. The slightly lower cell concentration reached by the MBR5 compared to the other MBR's it can be related to different error sources. For instance when the Neubauer chamber is used for the cell counting procedure previous to the inoculation typically yields an estimation error between 20 to 30 %. Another common source of error may be a drift of the optical absorbance measurements due to the existence of small bubbles interfering with the optical path during the PreCulture stage, such bubbles can easily appear if the water bath or the culture medium are not pre-heated or the Minibioreactor's plate preparation takes too long before placing it inside the workstation and starting the experiment.

The pH and dissolved oxygen graphs also shown similar profiles indicating almost the same acetic acid production and oxygen consumption rates independently of the FCS present in the medium. Only a slightly faster acidification of medium can be observed with controls, although it is barely significant. A deeper analysis yields the following data.

Cell growth parameters

Minibireactor /batch	Growth rate [h^{-1}]	Lag phase duration [h]
MBR1/A	26.4	11
MBR2/A	22.8	17
MBR3/B	20.4	2
MBR4/B	19.2	3
MBR5/C	16.8	5.5
MBR6/C	19.2	1.5

Conclusions

The reproducibility and time resolution of the measurements led not just to a proper determination of the culture yield and the tropophase duration, but also a good estimation of the cell growth parameters. In this case it was found that the efficiency of the two FCS batches tested was very similar compared to a commercial FCS batch, taking the same time to achieve the same maximum cell concentration. However, batch A lasted longer during the lag phase.

Example II

Clone selection – KB26.5 vs. BHRF1

Experiment description

Three parallel growths for each Hybridoma clone (KB 26.5 and BHRF1) for the same culture conditions. The aim is to establish which clone offers the best tradeoff between culture time and cell concentration reached.

Culture Conditions

Medium: DMEM + 10% (Fetal Calf Serum)
Cell line: Hybridoma KB26.5 and BHRF1
Volume: 12 ml
Initial cell concentration: $2 \cdot 10^5$ cells/ml
Stirring rate: 200 rpm
Bioreactor temperature: 37 °C
Aeration rate: 0.2 slpm (Duty cycle: 2%)

Results

Comparison of a Hybridoma culture growth (optical cell concentration) and its metabolic (pH and dissolved oxygen) curves obtained with HexaScreen® for the two different clones: KB 26.5 (black lines) and BHRF1 (green lines) after three days of culture.

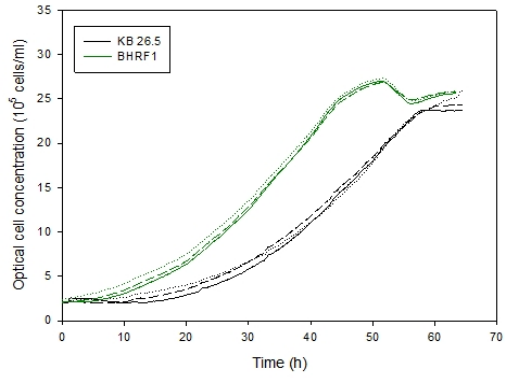

Cell concentration obtained from the OD measured at 650 nm.

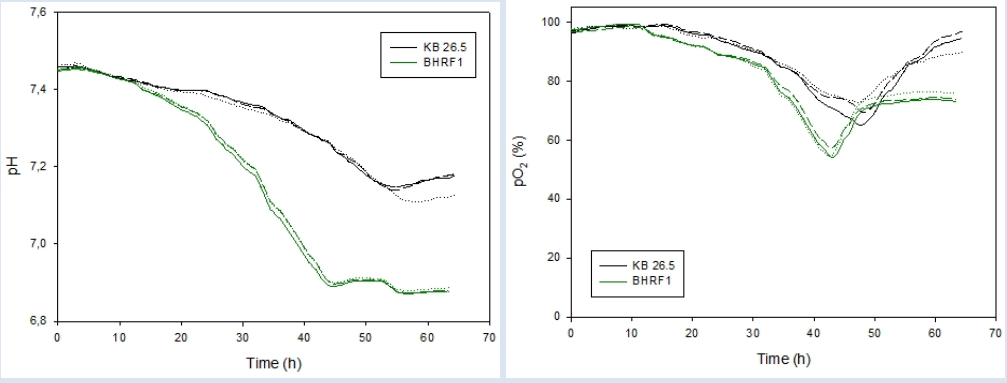

pH and DO evolution for both clones.

For a better comparison between both hybridoma clones, cell growth rate can also be

determined from their corresponding optical cell growth profiles, obtaining these results:

Cell growth parameters

Clone	μ Growth rate [h^{-1}]	T_d Duplication time [h]
KB 26.5	32.2	12.3
BHRF1	37.2	10.8

Conclusions

The monitoring of optical density at 650nm permits observation of differences between clones such as the time required to achieve the maximum cell density, being much higher for the KB 26.5 clone. These differences can also be observed with pH and DO profiles, where the exact moment of deprivation of the glutamine -and so culture limitation- can be determined (matching with pH and DO drifts)

Example III

Toxicity test – Neomycin

Experiment description

Comparison between different concentrations of a growth inhibitor component, such as neomycin, two parallel growths per each one of the neomycin concentrations were carried out (3 g/l, 1 g/l, 0 g/l).

Culture Conditions

Medium: DMEM + 10% (Fetal Calf Serum)
Cell line: Hybridoma KB26.5 and BHRF1
Volume: 12 ml
Initial cell concentration: $2 \cdot 10^5$ cells/ml
Stirring rate: 200 rpm
Bioreactor temperature: 37 °C
Aeration rate: 0.2 slpm (Duty cycle: 2%)

Results

Like in the previous examples in order to perform the comparison, cell growth parameters were calculated from the displayed graphs. Yielding the following results:

Cell growth parameters

Neomycin concentration	μ Growth rate [h^{-1}]	T_d Duplication time [h]
0 g/l	36.2	11.1
1 g/l	31.7	12.8
3 g/l	24.9	15.9

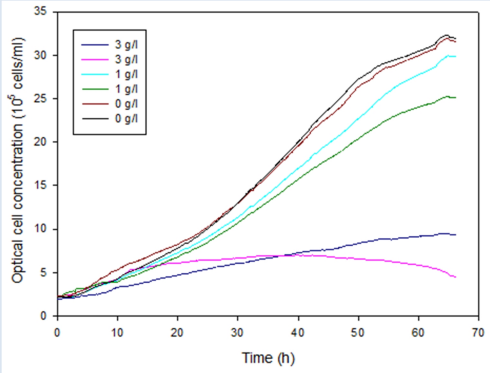

Cell concentration obtained from the OD measured at 650 nm.

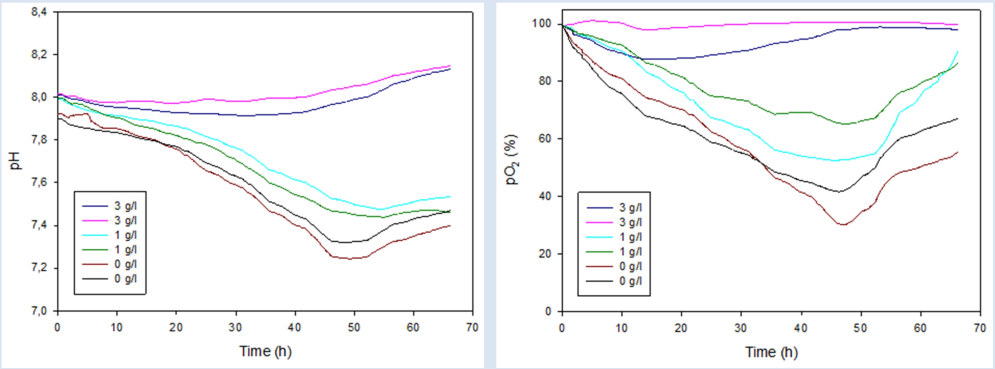

pH and DO evolution.

Conclusions

The OD showed a clear difference between the final cell concentrations after almost three days of culture. The more concentrated the neomycin was, the less cell concentration was reached, which is coherent with the expected antibiotic effect of neomycin. That also can be observed through the metabolic activity in terms of acidification and oxygen depletion since the cells cultured at 3 g/l of neomycin did not produce significant acidification or oxygen extinction as it was supposed to happen for cells cultivated without any growth inhibitor.

4.2 The MonoScreen® Fed-Batch Bioreactor.

MonoScreen Fed-Batch is the first prototype of a new series of Minibioreactor platforms that tries to overcome some limitations shown by the HexaScreen system regarding pH a DO control, Mass Transfer and Biomass monitoring in higher cell concentration conditions. Like its previous version MonoScreen Fed-Batch is also an expandable and automated Minibioreactor platform, based on the same idea of a workstation and a single use Minibireactor. The major difference is the fact that it features only one channel per workstation so screening studies implies the use of multiple workstations simultaneously. Further differences will be disclosed throughout the following sections. Due to its improved

capabilities, the use of MonoScreen Fed-Batch is not limited to a few applications or cell lines but to a huge range of applications with different types of cell species like yeast, bacteria, insect cells, mammalian…

Typical Culture volume:	20 … 30 ml
Stirring method:	Pitch blade / Rushton impellers , 60 ... 800 rpm ± 10 rpm
Aeration method:	Headspace / Sparger
Gas supplies:	3 channels (Air/O_2, N_2 and CO_2) Mixing humidifier volume (150 ... 420 ml)
Administration of pH control solutions & feed medium:	
-Type of addition pumps:	2 syringe pumps.
-Resolution of addition:	4… 6 µl[6]
-pH control reservoir volume:	up to 10 ml
-Feed reservoir volume:	up to 10 ml
Sterile sampling:	
-Sampling resolution:	100 … 1000 µl
MBR Temperature measurement method:	Pt100
Dissolved oxygen measurement method:	Non-coherent phase delay Fluorescence detection.
OUR estimation method:	Stationary liquid state global mass balance method. Based on the observation of the DO control loop variables.
pH measurement method:	Dual-lifetime Referenced Fluorescence (DLR)
Cell concentration estimation method:	NIR Laser Turbidimetry
Accuracy of measurements & control ranges:	
-Temperature control range:	+10 ... +40 °C
-Temperature Accuracy:	± 0,3 °C
-Dissolved oxygen control range:	10… 90 % (related to saturation)
-Dissolved oxygen Accuracy:	± 1 %
-pH control range:	4,5 …9[7]
-pH Accuracy:	± 0,1
-Cell concentration estimation range:	> 50 g CDW/l
Communications:	Ethernet (10Base-T) / RS232 for diagnostics
Power supply:	85 ... 250 V~, 50/60 Hz
Dimensions (approx.):	
-Height (closed/opened)	490 mm
-Width	330 mm
-Depth	510 mm
-Weight	15 kg

Table 2
MonoScreen® Fed-Batch Technical features

4.2.1System overview.

The MonoScreen® Fed-Batch Minibioreactor concept comes from the meeting of the single-use philosophy and the miniaturization of the classical Bench-Scale Bioreactor. On one side the disposable device includes: the vessel where the bioreaction is to be carried out, an sterile sampling circuit [27], optional gas sparger, ports for medium and pH control solution administration, an standardized stirring system based on Pitch-Blade or Rushton turbines suitable for a Range of cell species [28], embedded sensors for dissolved oxygen, pH and temperature, and optical windows arranged to carry out turbidity measurements.

[6] Drop's volume obtained for aqueous medium and 1/4"x30G dispensing needles.
[7] pH control range and measurement accuracy is highly dependent on the medium's ionic strength and the control method used (CO2 and base addition, base addition only, or acid addition only) [43] [44]

On the other side, the workstation is meant to perform the autonomous control of a single Minibioreactor, as well as to support the user whilst the executions of certain manual operations like sampling and installation of the Minibioreactor and syringe reservoirs. Major differences between the MonoScreen Fed-Batch and the HexaScreen workstations are:

- Only one Minibioreactor per workstation.
- Possibility to carry out both Batch and Fed-Batch cultures.
- High power number stirring method (Suitable for microbial applications).
- Dissolved Oxygen (DO) control.
- pH control and measurement by means of fluorescence without any pH sensitive diluted dye.
- Allows multiple dynamic set points.
- High Cell Concentration estimation method based on NIR Turbidimetry.
- Bioimpedance measurements

Data is collected, recorded and broadcasted by the workstation which features an embedded web and ftp server that provides an expanded GUI not just for real-time monitoring but for interacting with the cell culture and create/edit experiments. The possibility of performing screening studies will rely on the number of available workstations.

Like the HexaScreen disposable plate, the MonoScreen Fed-Batch Minibioreactor is also made of biocompatible Polystyrene and includes all the elements required for any stirred tank Bioreactor; it mimics the design of the bigger scale bioreactor by observing the canonic aspect rations between the size of the impeller, the vessel's dimensions and the height of the medium held inside the vessel [25].

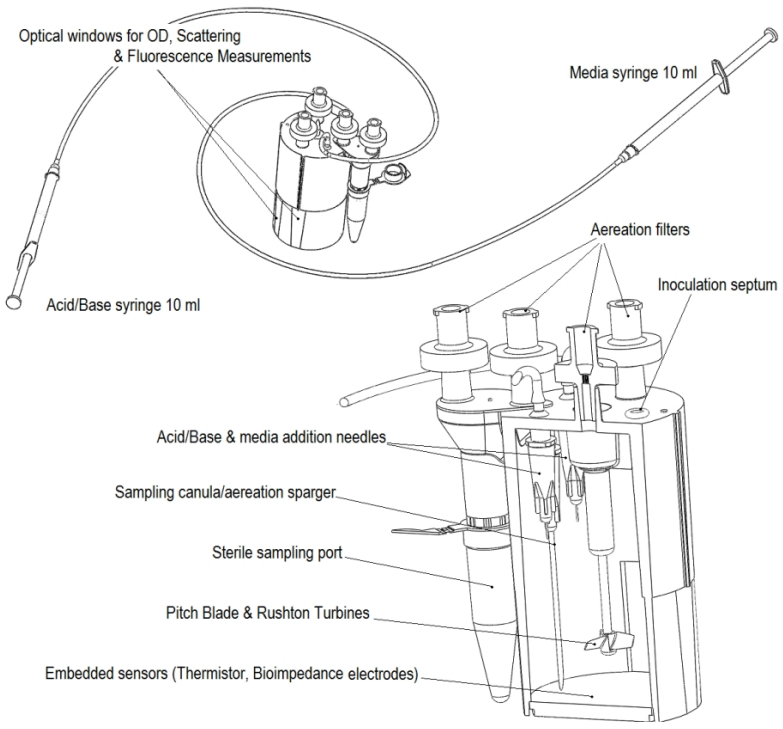

Figure 31
MonoScreen's Fed-Batch Minibioreactor & cross-sectional view.

The workstation has been designed for an easy interaction of the user with the cell culture. It's been conceived as a compact unit that removes the presence of cables, tubing and any external peripheral device like flow-meters, gas proportioners or pumps. To that end a touch panel and a set of servomechanisms have been built-in for supporting the user during the Minibioreactor installation and the sampling operation in a totally automated manner. The embedded sampling circuit is also a highlight since allows extracting an aliquot of the culture without assuming risks of contamination or disturbing the connections between the Minibioreactor and the workstation. On the other hand, a high interaction level like set points modification, introduction of off-line data and any operation regarding the experiment execution (recipes, export data, start, stop) shall be performed through the built in web server.

The workstation's front panel is divided into three sections with doors that may be opened during the system's normal operation or just for service purposes.

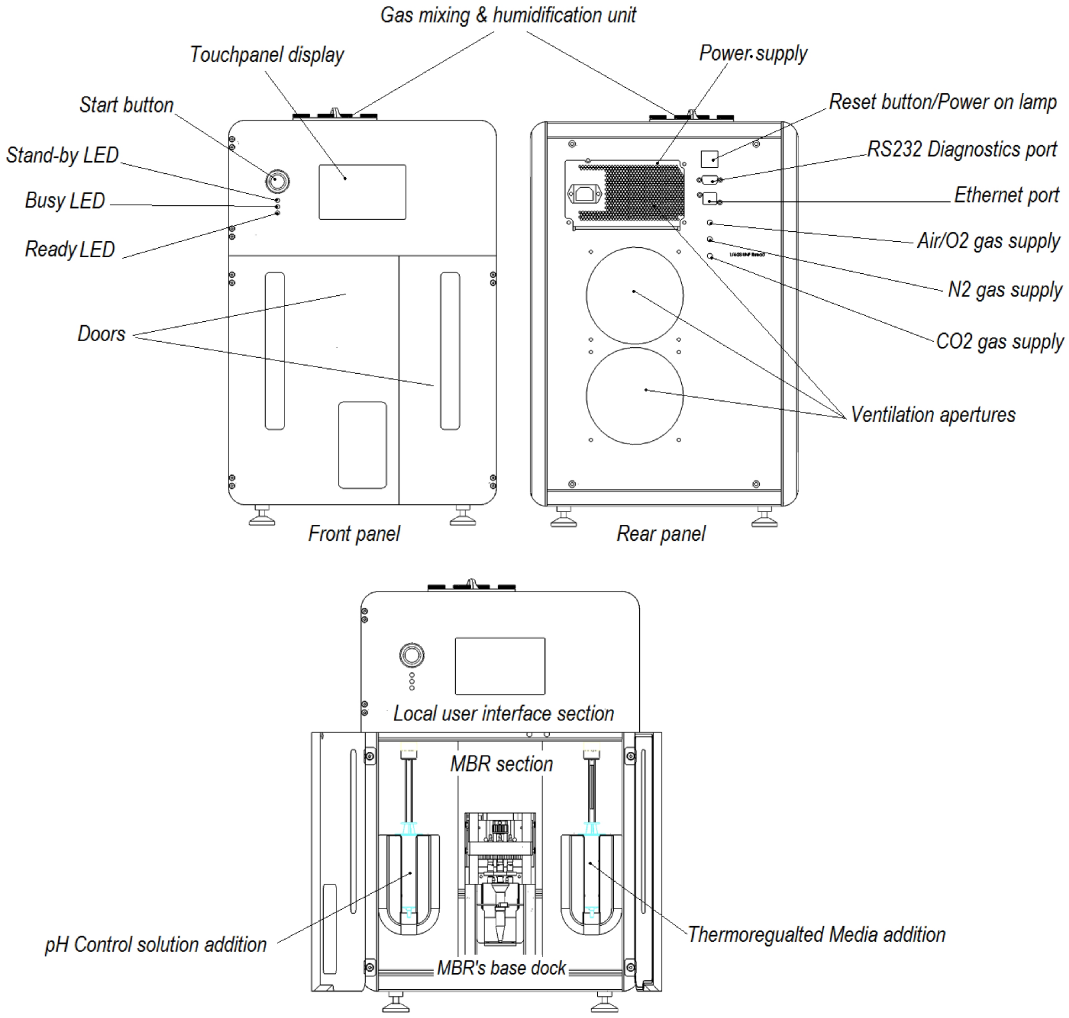

Figure 32
MonoScreen's Fed-Batch Front & Rear panel view.

- Local User Interface: It includes the Start button, three LED's (stand-by, busy and ready), and one touch panel display intended for launching messages and to allow

user interaction as well as displaying information about the workstation's and the experiment's current state.

- Medium feed addition section: Encloses the syringe pump in charge of delivering the feed to the Minibioreactor following a certain addition rate profile. Its main feature is that the reservoir holder may be cooled for feed preservation at temperatures between 2 to 4 °C.
- MBR's base dock and pH control pump section: It contents another syringe pump identical to the one used for the medium feed but without thermoregulation capability. The dock base is where the Minibioreactor remains attached to the workstation all along the culture accomplishing several functions:
    - Heat pumping for the thermoregulation.
    - Connecting the Minibioreactor's stirrer shaft to the workstation's mechanical drive.
    - Connecting the Minibioreactor's inlet gas filters to the workstation's gas circuit for aeration and actuation of the sample taking mechanism.
    - Holding the optical parts related to the DO, pH and Turbidity measurements.
    - Holding the Minibioreactor tight enough to avoid undesired movements that could be translated into measurement artifacts.

As mentioned, communications are based on www and ftp servers running on TCP/IP. Such communication scheme leads the possibility to monitor and control any workstation from any computer able to access the network. The figure below shows a possible implementation related to the concept of screening where the number of simultaneous experiments becomes the key point to obtain statistically significant results.

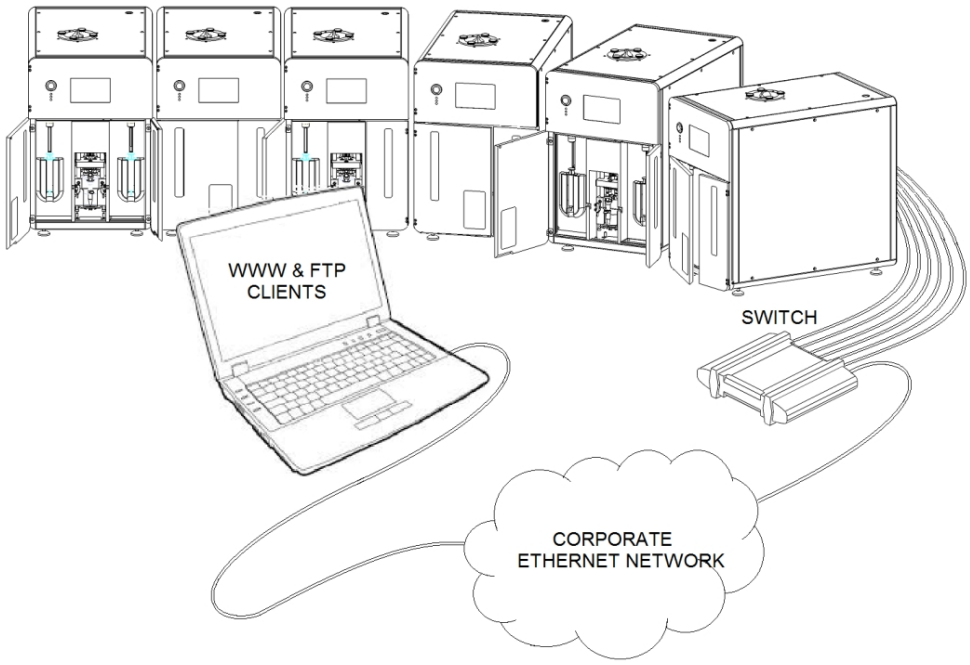

Figure 33
A 6-device array & client computer connected by means of a private LAN.

4.2.2 MonoScreen® Fed-Batch architecture

As its predecessor HexaScreen, the MonoScreen Fed-Batch system also includes customized electronics, mechanisms and some optical parts. The pictures below show a snapshot of its internal construction and front panel. The box is divided in two sections thermally insulated to ensure an almost constant working temperature of the gas circuit, to avoid the possibility of condensation within the gassing pipes or any unwanted thermal drift of the electronics. The non-insulated part holds the power supply unit and the liquid cooling circuit heat sink.

Figure 34
MonoScreen Fed-Batch.

The following diagram shows the main elements of the DO and pH control loops. Due to the fact that their operation is connected to each other and to the sampling mechanism, which is another important functionality of the system, such elements become especially sensitive parts of the workstation. That is why the design of the system's global architecture was not faced until the right control strategies were chosen for each variable and key parts selected.

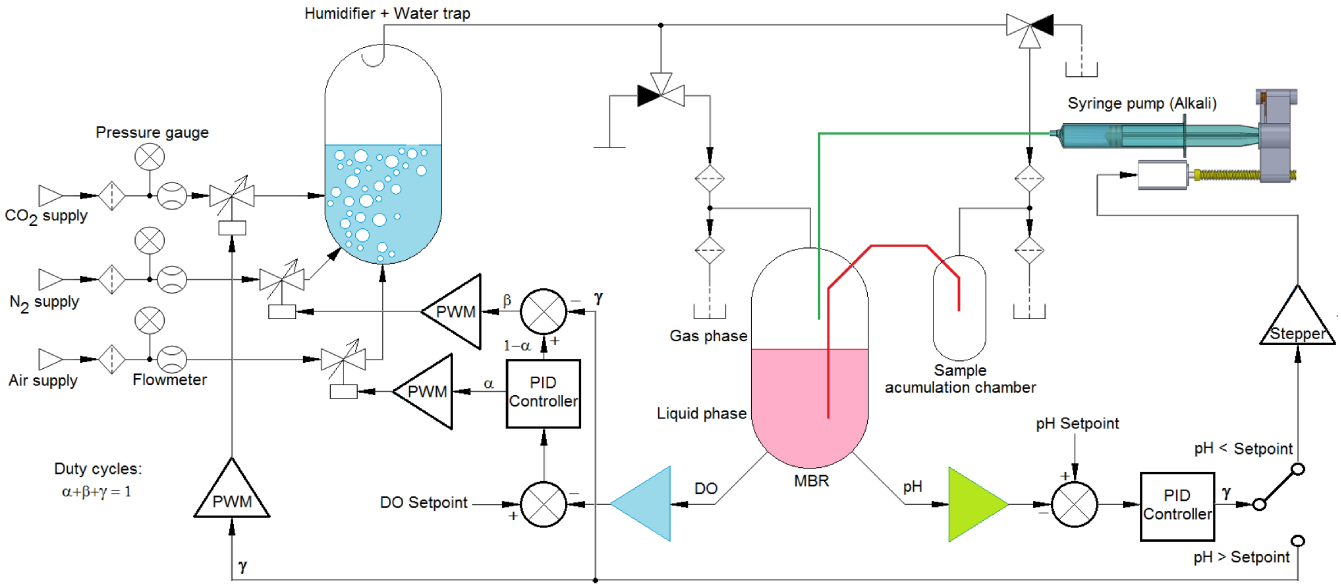

Figure 35
DO & pH control model.

Essentially, the DO & pH control loops are acting over the O_2 and CO_2 partial pressures within the gas phase of the Minibioreactor by properly regulating the Air, N_2 and CO_2 flows, which are mixed in the humidification unit. Each individual gas flow is regulated by means of a proportional electrovalve controlled by a Pulse Width Modulated (PWM) signal. In order to keep the total gas flow constant regardless of its composition, a condition must be observed. The addition of the duty cycles of every PWM signal must be constant. On one hand, the ratio between the Air flow and the other gases states the pO_2 and therefore DO, on the other hand increasing the ratio between CO_2 and N_2 increases medium's acidity. On the contrary, to reach a high pH value no CO_2 should flow through the Minibioreactor's gas phase and a certain volume of an alkali solution like NaOH should be delivered by means of the syringe pump.

The architecture was based on the RCM4300 Rabbit core; a more powerful C-programmable module than the one used for the HexaScreen system. It features a multichannel 12 bit A/D converter, Ethernet connectivity and mass storage capabilities by means of an on board 1 GB µSD card. Most of the communication with the different peripheral devices was based on an I_2C bus. The workstation is made of the following modules: Control, Power drivers, Syringe pump drivers and the Signal acquisition and conditioning module.

The Control module holds the system's intelligence and is in charge of the user interface functions (Touch panel, web & ftp server), data acquisition and logging and culture control and system's supervision. The control module counts with gas pressure and flow sensors as well as proportional valves for the gas mixing control, multiplexers for digital I/O and an on board thermometer for internal monitoring.

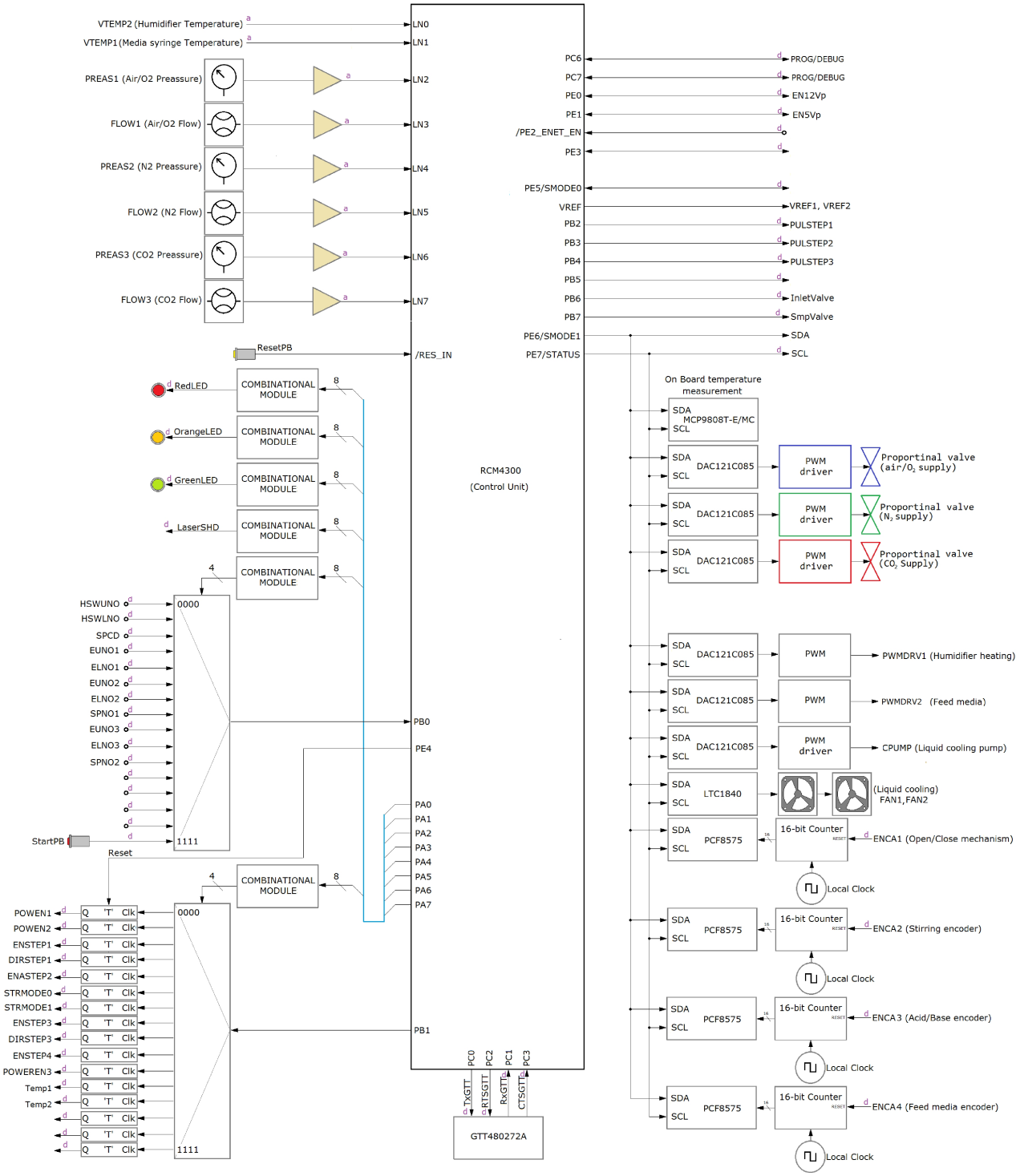

Figure 37
MonoScreen Fed-Batch Control Module block diagram

The Power driver's module holds the parts related to some of the main functions like the Minibioreactor's stirring and temperature control, and secondary functions like the Humidifier's temperature control, as well as the needed elements for the automated calibration of the Humidifier's thermometer. The Power driver's module is connected to the Control module by means of an I_2C bus which allows multiplexed access to different peripheral IC's. One additional feature is the possibility of dual operation; the module may be remotely controlled (by the RCM4300 microcomputer) or manually operated in order to simplify service tasks.

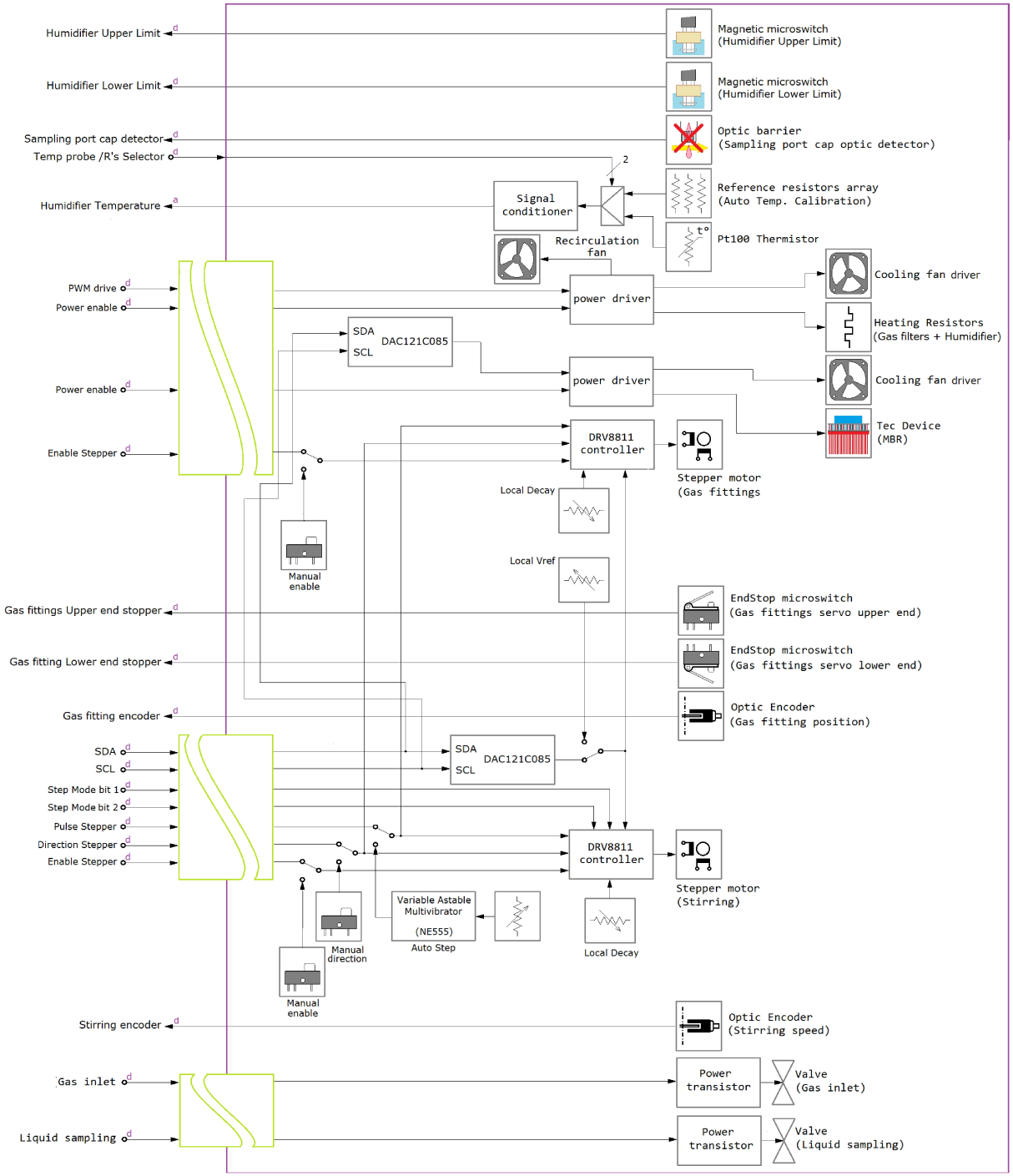

Figure 38
MonoScreen Fed-Batch Power driver's module block diagram

The MonoScreen Fed-Batch system features two identical Syringe pump driver modules consisting of a 10 ml syringe pump and its corresponding electronics, one module is meant for the administration of pH control solutions, the other is intended for feeding the Minibioreactor. The second features the additional capability to keep the syringe's temperature within a certain range. Therefore, the Feeding module's printed circuit board holds some extra elements not just for driving the mechanics but for temperature control and automated thermometer calibration. Syringe pump driver modules are directly controlled by the RCM4300 microcomputer by means of general purpose I/O bits in order to optimize control over the steppers motors and hence over the liquid addition resolution. Like the Power driver's module they also can be operated manually for service purposes.

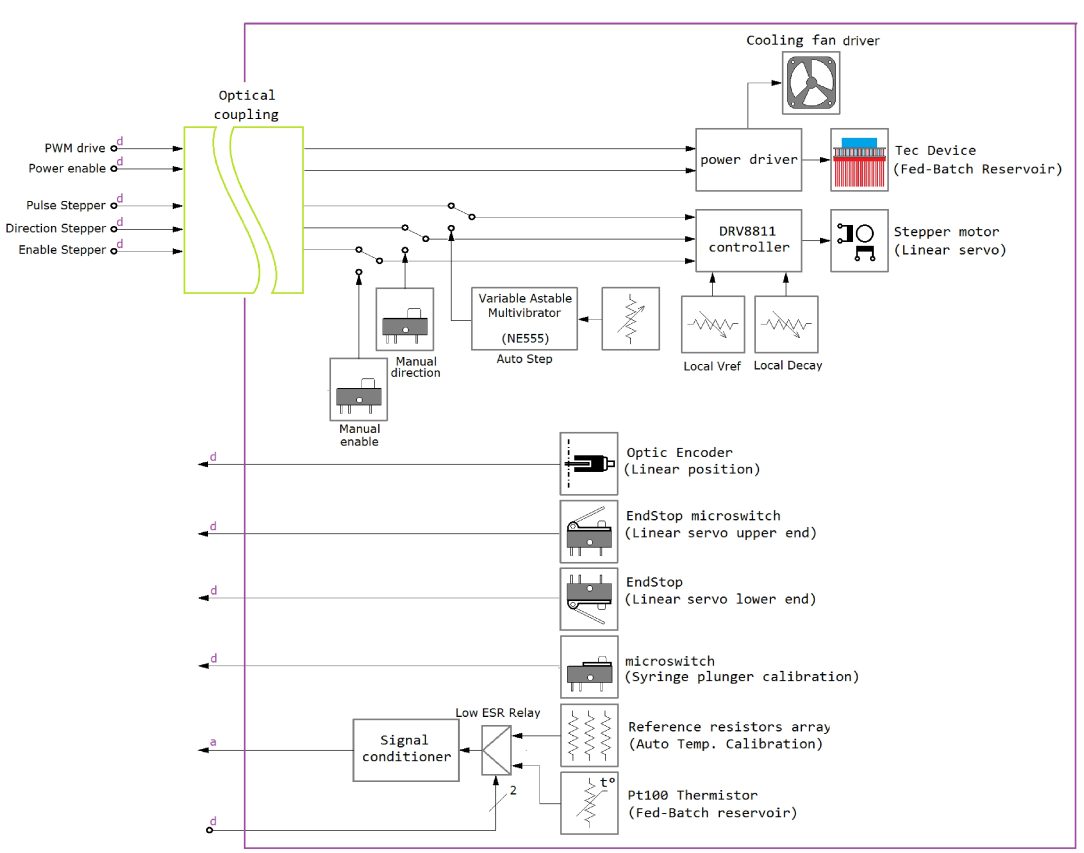

Figure 39
MonoScreen Fed-Batch Medium addition module block diagram.

The Signal acquisition and conditioning module is responsible for the conditioning and acquisition of the signals provided by the sensors directly applied to the Minibioreactor. The different analog signals are collected via a multichannel, 12-bit ADC, and transmitted to the control board via an I_2C bus. The module includes an auto-calibrated thermometer, two fluorescence detectors (DO – pH), and one NIR laser Turbidimeter made of a low power 850 nm laser and three logarithmic photodetectors, based on a LOG112 precision logarithmic amplifier to increase the Turbidimeter's measurement range. Turbidimeter's operation is represented by the figure below where the gain of the three photodetectors (Reference, Transmitted & Scattered) must be matched $k_{Ref} \approx k_{Fwr} \approx k_{Sctt}$.

$$v_0 = k_i \cdot \log \frac{I_{Pht\,i}}{I_i}$$

Where:

- v_0 [V]: Signal response.
- $I_{Pht\ i}$ [A]: Photocurrent proportional to the light intensity for every phodetector (Reference, Transmitted & Scattered)
- I_i [A]: Phodetector offset current control.
- k_i [ ]: Phodetector sensitivity.

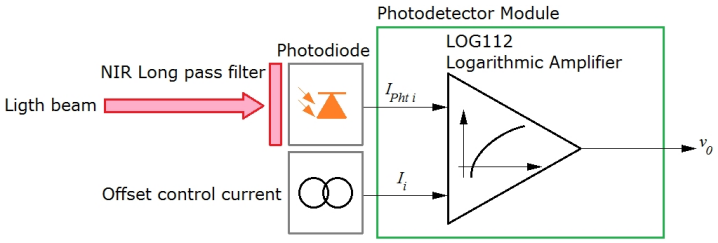

Figure 40
Turbidimeter's Photodetector module block diagram.

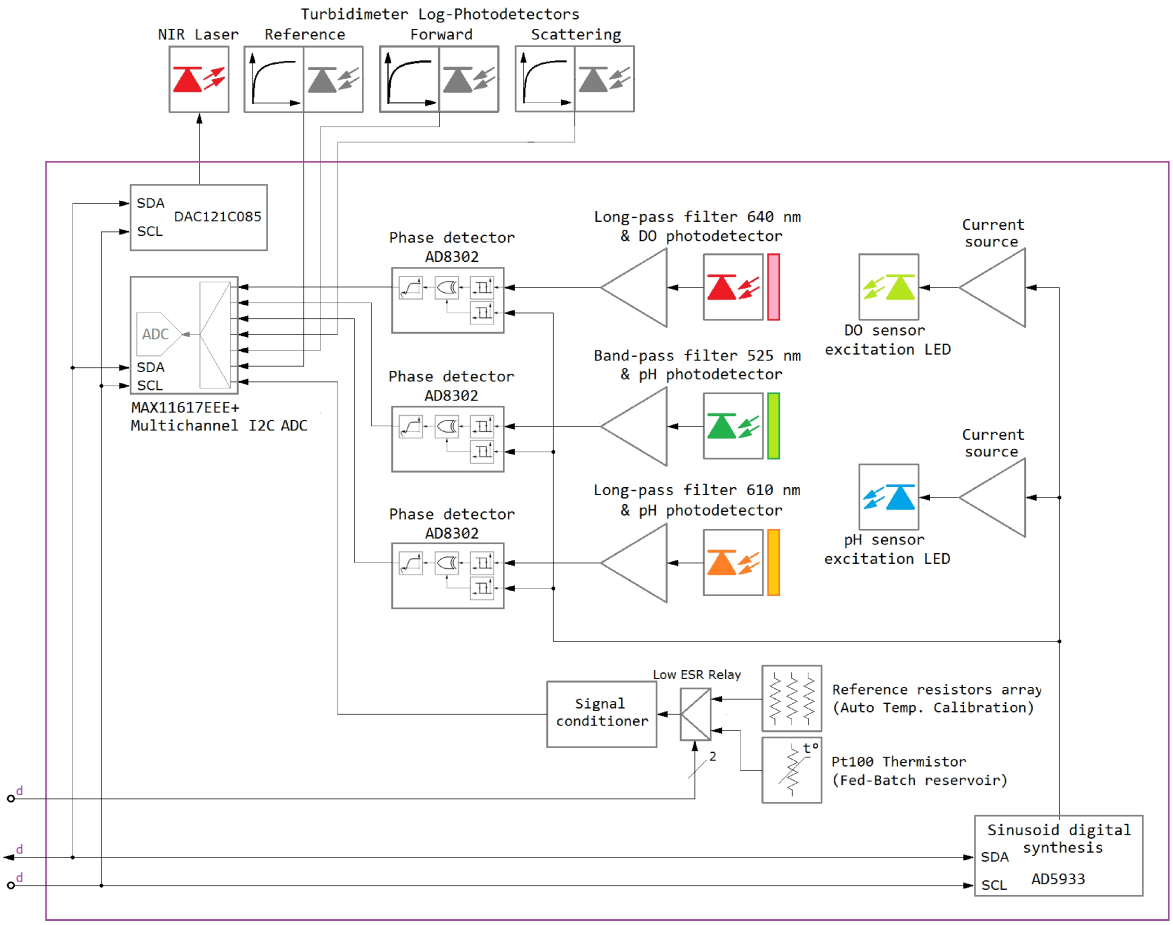

Figure 41
Signal acquisition and conditioning module block diagram.

The DO measurement is based exactly in the same instrumentation technique used by the HexaScreen system, XOR phase detection (3.2.2). Regarding the pH measurement, this is based on Dual Lifetime Referencing (DLR). Where pH is related to the fluorescent response of two independent fluorophores one of them used as the reference due to its lack of sensitivity to the pH and the other to record the pH evolution as its lifetime changes. The pH measurement circuit used is analogous to the DO measurement scheme but including a second phase detector for the reference signal. Figure 42 shows the pH sensor fluorescent response when irradiated at 470 nm. Two clearly differentiated emission peaks were detected at 525 nm (measurement wavelength) and 610 nm (reference wavelength) consequently two specific optic filters were chosen for rejection of the ambient light and the backscattered excitation. Figure 44(d) shows the optic filters attached to the photodiodes for both DO & pH measurement circuits.

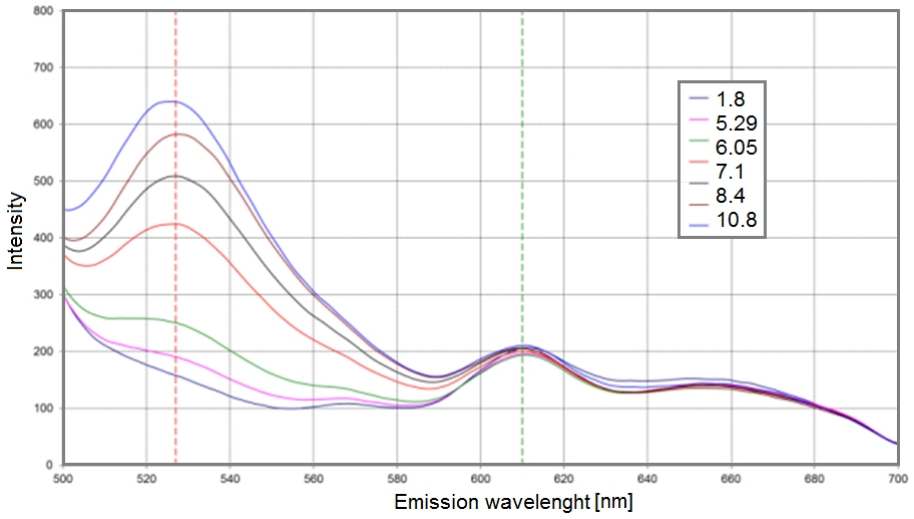

Figure 42
Fluorescent emitted spectra by a Presens sensor (PS-HP5-D5-US pH)
When irradiated at 470 nm, for different acidity conditions from 1.8 to 10.8 pH

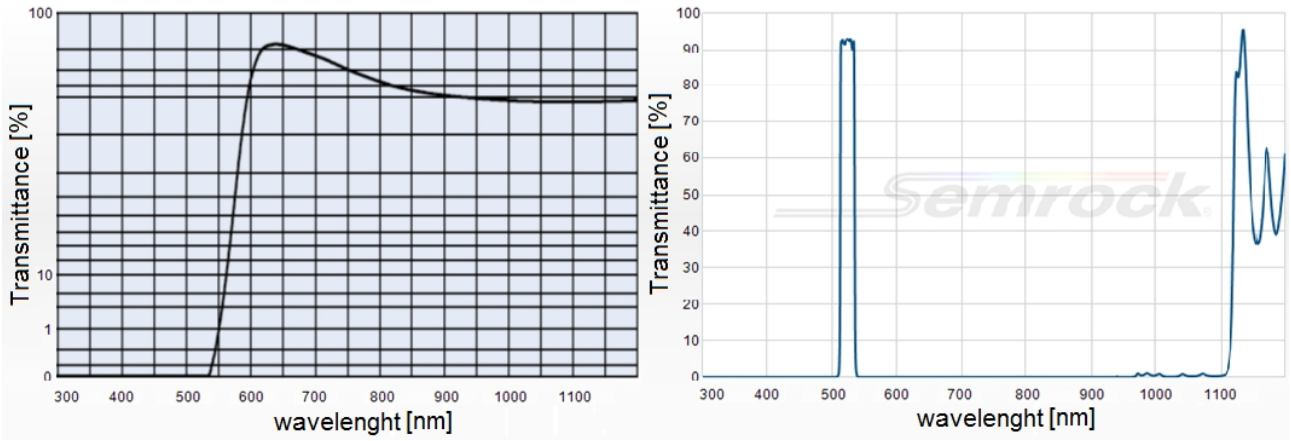

Figure 43
Schott OG570 & Semrock FF01-525/15-25 long-pass and band-pass filters Transmittance curves.
pH reference and measurement wavelengths. [29] [30]

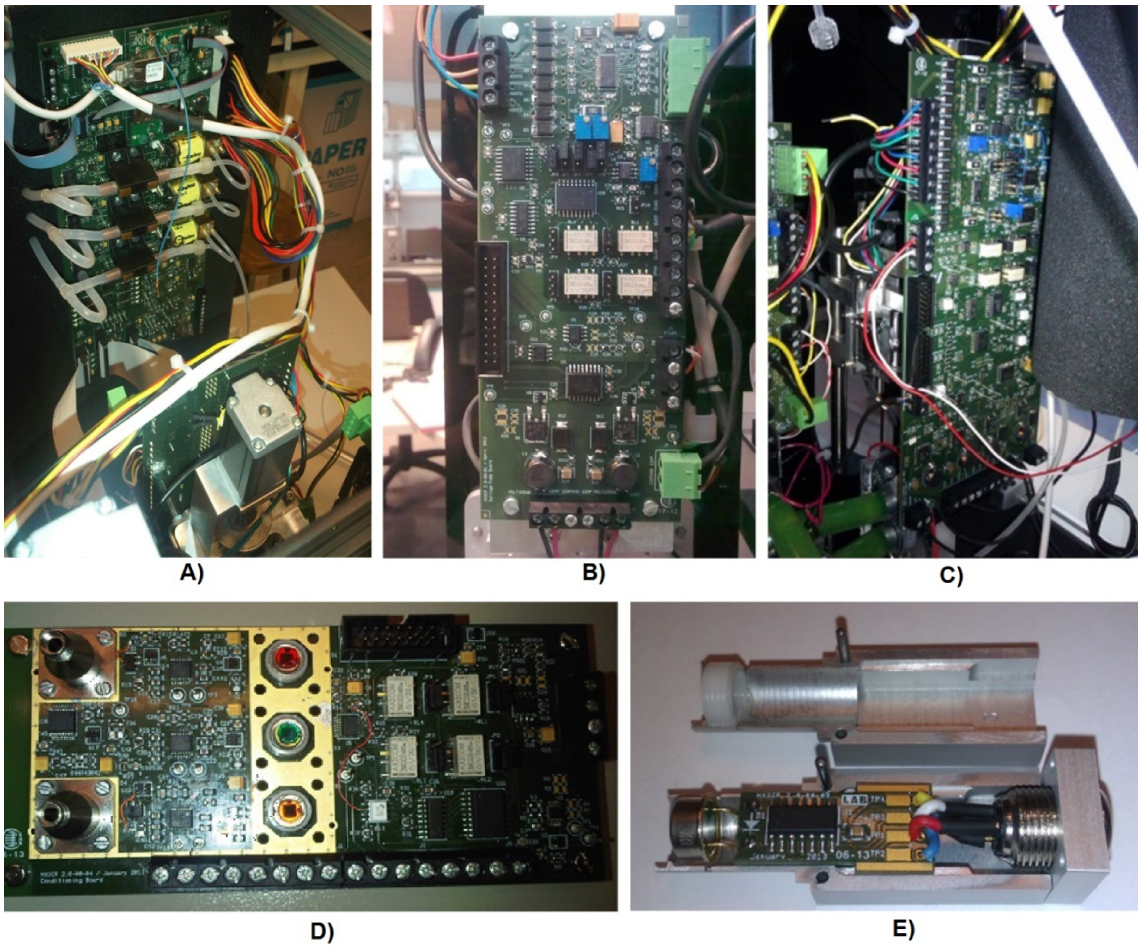

Figure 44
MonoScreen Fed-Batch Hardware: A)Control module, B) Medium addition module, C) Power driver's module, D) Measurement module, E) Logarithmic photodetector.

A big improvement on the MonoScreen's firmware was made in comparison with the HexaScreen system. The development of the built-in www and ftp servers made unnecessary the need for having a customized client software resident on the host computer. This way any computer or "smart" device running a standard browser or ftp client could easily gain access to each individual workstation as far they were connected to the same LAN. Additionally, a FAT file system was implemented for recording different type of data (setup parameters, calibration values, experiment results and culture recipes). Culture recipes are scripts describing all the conditions and events to be carried during the experiment i.e. Administration of a certain feed volume or the execution of a specific stirring profile.

The firmware code is mostly based on Digi's Dynamic C real time functions and consists of a number of concurrent processes to perform very specific tasks (acquisition and control, data logging, etc…) such processes are enabled and disabled depending on the conditions of a simple state machine.

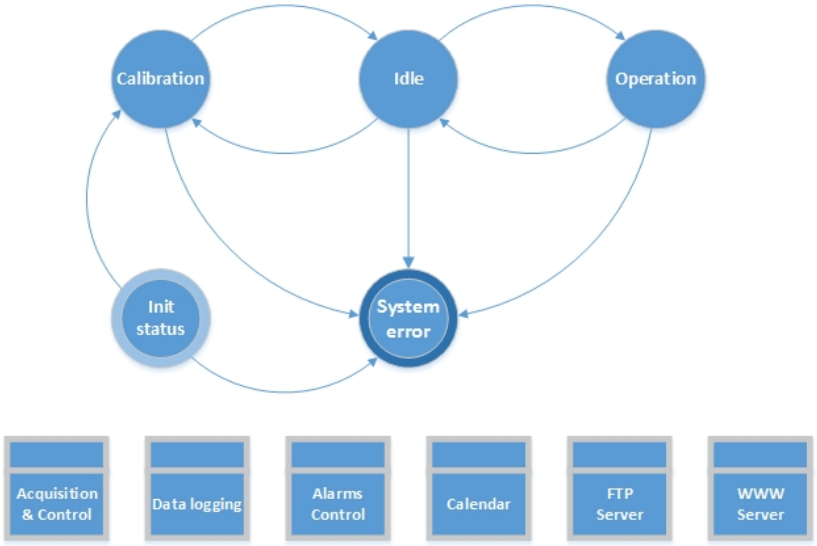

Figure 45
MonoScreen Fed-Batch states diagram and list of concurrent task

- *Initialisation*: All working variables are initialised with the configuration data recorded in the flash memory and different configuration files in the FAT file system. If the loaded data would be found to be corrupted or inexistent this circumstance would be treated as a fatal error and the system would move to the "*Final Error*" state. After successful initialization of the working variables an automated verification of the internal I^2C bus as well as on the proper operation of most actuators is performed. Failure of any peripheral device would be reported. However, the system would not immediately move to the "*Final Error*" state since the system could be still functional depending on the error importance.
  Next state shall be *"Instrument Calibration"*; However, depending on the value of the "*Last State*" parameter recorded on the flash memory, any value different than "*Idle*" points to an abnormal power up situation due to an unexpected lack of power or analogue circumstance and then the user is prompted to restart the system.
- *Instrument Calibration*: After initialisation, the user is prompted to calibrate the system at least once previously to any experiment. The calibration does not necessarily need to be executed immediately after the initialization. At this point the calibration step can be skipped and come back to it later from the "*Idle*" status. The Calibration process takes care of the following tasks:
  - *Determination of the syringe pumps resolution.*
  - *Determination of the off-set parameters for pressure gauges a flowmeters.*
  - *Automated calibration of the internal thermometers.*
  - *Testing the proper operation of the thermoregulation and stirring control loops.*
  - *Determination of the DO calibration parameters.*
  - *Determination of the NIR turbidimeter base-line value.*

  Whilst the *"Instrument Calibration"* stage the execution of any other concurrent tasks is interrupted.
- *Operation*: Once the Minibioreactor is placed and connected to the dock bay, the system enters the "Operation" status and the following concurrent tasks are activated:

"Data Logging", "Alarms Control" "Acquisition & Control". When the workstation enters this stage the active recipe is automatically executed. That means that the different control loops are started and set points are applied following the profile previously programmed by the user. Monitorization of the experiment must be done by means of a www client that retrieves the real time data from the instrument through the network. Nevertheless, critical data regarding the current culture conditions (Temperature, DO, pH, stirring, etc…) can also be locally checked via the touch panel. The operation status also allows the user to perform other tasks such as on-line modification of the active recipe, aliquot sampling and the introduction of off-line data that will later be included in the experiment's report file.

- *Idle*: After the *"Initialisation-Calibration"* process, the system enters the "*Idle*" state and the tasks "Calendar", "www Server" and "ftp Server" are started. They are the ones providing the user with access to the FAT file system to edit or upload recipes and download experiments results. The idle state can also be entered after finishing an experiment or a calibration process.
- *Final Error*: If some fatal error happens, the RCM4300 will try solving it by means of a wait and retry procedure. Errors that can be solved are the ones related to the I^2C communications bus, access to memory and the lack of some feedback signals i.e. The syringe pumps optical encoders or the power supply OK signal. If finally the wait and retry procedure would time out the system would move to the "*Final Error"* state and notify the corresponding error code through the touch panel.

4.2.3 MonoScreen® Fed-Batch Optical Layout.

Due to the more demanding requirements related to the maximum cell concentration for the MonoScreen Fed-Batch system and the fact that diluted pH indicators like Phenol red may interfere with some spectrophotometric and fluorescent essays, or even interact with some cell types [31] [32]. A different approach to the optical layout was planned for the MonoSreen Fed-Batch.

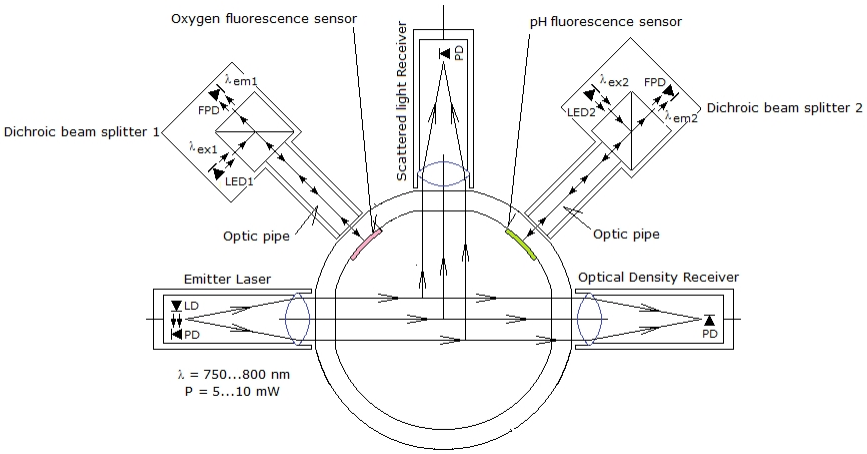

Figure 46
Preliminary optical layout initially considered.

This consisted on moulding five optical windows along with the vessel walls to implement not just optical DO measurements but pH and a NIR laser turbidimetry for being able to monitor the pH and Biomass evolution within die free culture mediums under high cell density conditions.

A preliminary approach to the fluorescence readers consisted of duplex modules able to isolate the emission and excitation wavelengths. Such readers shall be made of a dichroic beam splitter, a light source, a photodetector and optical filters to minimize the signal crosstalk. However, such configuration resulted to be extremely expensive and dual-wavelength detection would require additional complexity. Therefore, a cheaper alternative but still effective approach was carried out based on polymer optic fiber probes.

The MonoScreen's Fed-Batch predecessor, the HexaScreen system, was equipped with a 6-channel spectrophotometer to perform on-line OD measurements to obtain the cell concentration profiles per each vessel. However, as mentioned in section 4.1.3.1, although OD is considered as the golden standard for the estimation of biomass density, such technique is just suitable for very low cell concentrations, typically below 0.4 A.U. and always depending on the cell types. In consequence, in order to estimate a large cell concentration it is necessary to dilute the sample by a certain ratio before the measurement. This procedure gives an off-line OD "corrected" value that makes usual to see the biomass or cell concentration expressed in terms of tens or even hundreds of absorbance units, which is an accepted trick but a non-accurate use of the optical absorbance concept [16] [33] nor an appropriate method for on-line monitoring. In fact the IUPAC considers OD synonymous with absorbance and discourages its use due to such ambiguous common use. A more appropriate technique for on-line monitoring is Turbidimetry, which is based on the fact that when particles or cells in suspension are irradiated with a light beam a certain pattern of scattered light is produced depending on the particle's physical properties, especially when their size is bigger than the wavelength of the incident light. That's why Turbidimetry may be used not just for the determination of the cell concentration but for physical properties like size or shape [34] [35] [36] [37] [38].

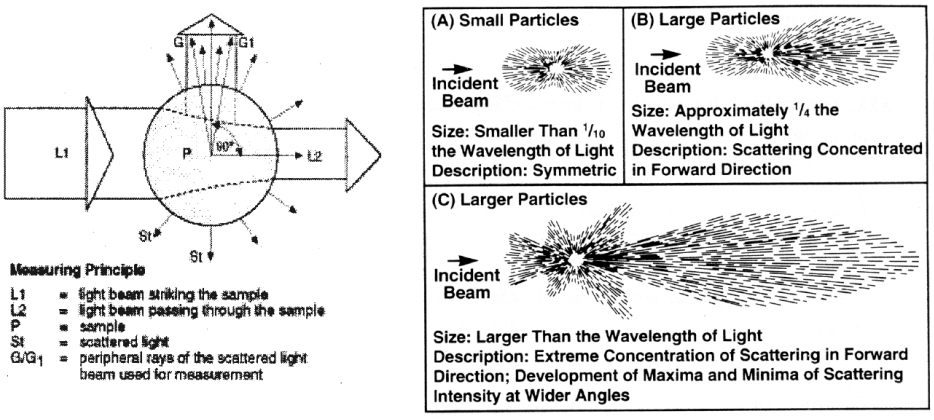

Figure 47
Left) Transmitted and 90º scattered light by a particle when stroke by a light beam.
Right) Light scattering patterns for different relative size particles versus the incident wavelength [36].

There are multiple possible implementations for turbidimeters being classified as Absorptioners and Nephelometers. On one hand, Absorptioners measure the intensity attenuation of a light beam passing through a sample. Despite that they work the same as spectrophotometers it is important to differentiate between the concepts of optical absorbance or OD and Turbidimetric Absorption (TA) due to light scattering since TA does not follow the Lamber-Beer's law. This is something to keep in mind when relating such parameters with the cell concentration. i.e. During the exponential phase of an ideal cell culture the use of TA as an estimator for the biomass density instead OD looks like offering a more realistic display of the cell culture evolution. This could lead to erroneous conclusions about the growth rate. Therefore, the on-line estimation of the cell concentration should not be directly related to the OD and less for very low densities.

Observe also that there is no zero-point on the TA and OD scales, growth can never start at TA = 1 or OD = 0 (which mean that there are no cells to grow), such lack of consistency shall be corrected previously through reference calibration, where I_t equals the transmitted intensity and I_o equals the intensity of the incident light or the transmitted intensity without cells.

$$\mathrm{TA} = \left(\frac{I_t}{I_0}\right); \quad \mathrm{OD} = \frac{1}{\Delta x} \cdot log\left(\frac{1}{\mathrm{TA}}\right)$$

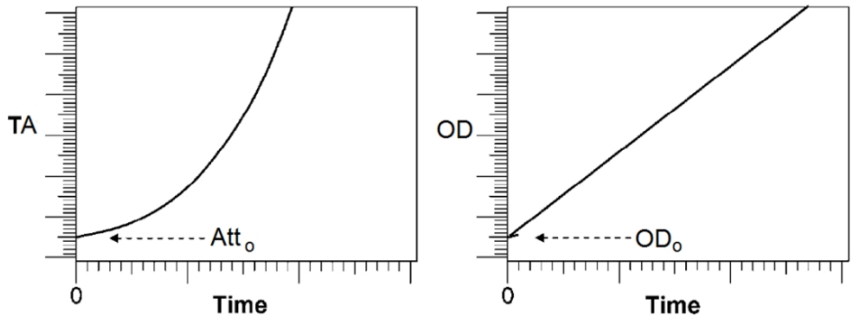

Figure 48
TA and OD graphs during the exponential phase of an ideal cell culture. Adapted from Widdel [16]

On the other hand, Nephelometers are based on the measurement of the scattered light at 90° angle from the incident beam, which is considered by the EPA (US Enviromental Protection Agency) as the most sensitive angle to measure scattered light and therefore presence of particles.

Despite these advantages, according the bibliography [36] [38], for very high turbidity values the existence of multiple scattering interferes with both phenomena direct absorption and 90° scattering, diminishing the instrument's sensitivity especially at short wavelengths. The election between the Absorptioner or Nephelometer implementations will rely on the particles size, its concentration, color of the medium and the lower measurement threshold.

The Nephelometer's most classical configuration is known as the Single Beam Design and is made of a light source and one photodetector located at 90° from the incident light. The

use of such instruments is very limited due to the need for frequent recalibrations because of the aging of the incandescent light and its wide spectra that may introduce additional errors related to the samples natural color, something which is common for the most cell culture mediums.

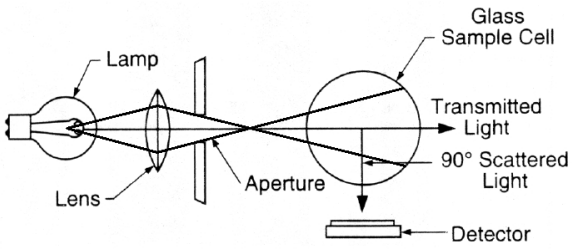

Figure 49
Basic Single Beam Nephelometer [36].

The Ratio turbidimeter expands the measurement range of the Single beam Nephelometer in addition to a better performance with colored samples thanks to the use of multiple phototedetectors and the ratio algorithm. This is because every wavelength is approximately equally affected for every direction and the color absorption effect is mathematically cancelled. Nevertheless, the ratio Turbidimeter still lacks of stability due to the use of the incandescent bulb and the number of photodetectors makes it a quite expensive option.

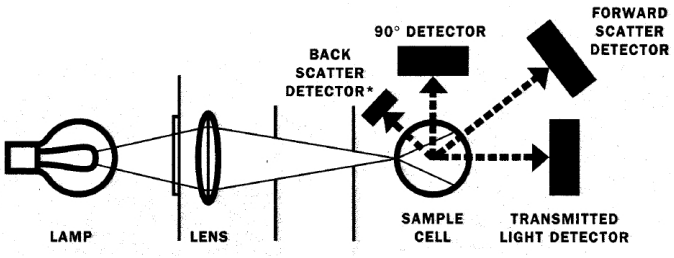

Figure 50
Ratio Turbidimeter [36].

$$T = \frac{I_{90}}{d_0 \cdot I_t + d_1 \cdot I_{fs} + d_2 \cdot I_{bs} + d_3 \cdot I_{90}}$$

Where:

- T [NTU]: Turbidity
- d_0, d_1, d_2, d_3 [ ]: Calibration coefficients.
- I_{90} [A, V, or counts]: 90º Scattered signal.
- I_{fs} [A, V, or counts]: Forward scattered Intensity.
- I_{bs} [A, V, or counts]: Back scattered Intensity.
- I_t [A, V, or counts]: Transmitted Intensity.

Therefore, taking into account the above mentioned limitations the proposed solution for the cell concentration monitorization system should withstand a compromise between stability, measurement range and price.

4.2.3.1 NIR Laser Turbidimeter (Cell density)

The requirement for the cell concentration measurement was to provide a reliable, cheap and wide-range instrument, suitable for most cell types (microbial, yeast and mammalian) as well as for most culture mediums. On one hand, regarding reliability and price, laser-based light sources have been reported as the most appropriate for the implementation of stable, sensitive and accurate turbidimeters [39], additionally they offer the possibility to avoid the need of collimation optics and the recurrent maintenance connected to incandescent bulbs. On the other hand, the size of the "particles" in fermentation and cell culture applications ranging from ≈ 1 μm (bacteria) to ≈ 100 μm (mammalian cells) is a wide range that will produce greatly different light scattering patterns, which means that the higher sensitivity direction will depend on the cell type, being the transmitted direction the most sensitive for the bigger cells (mammalian) and also the scattered directions for the smaller ones (bacteria and yeast). That is why the chosen implementation counts with a transmitted light photodetector basically related to the cell concentration, and 3 other optional positions at 45º, 90º and 135º angles from the incident beam to place one extra scattered light photodetector that could provide data about the presence of small particles related for instance to the rupture of the cell membrane. Finally, the laser was chosen within the NIR region at 850 nm, far away from the Phenol red absorbance region to avoid errors caused by the medium's color drift (Phenol red is the most commonly used pH indicator in culture mediums), maximum measurement range was expected thanks to the inexistence of other wavelengths causing multiple scattering. The study on how the scattered light is related to the biomass density and cell's morphology is a matter beyond the scope of this dissertation.

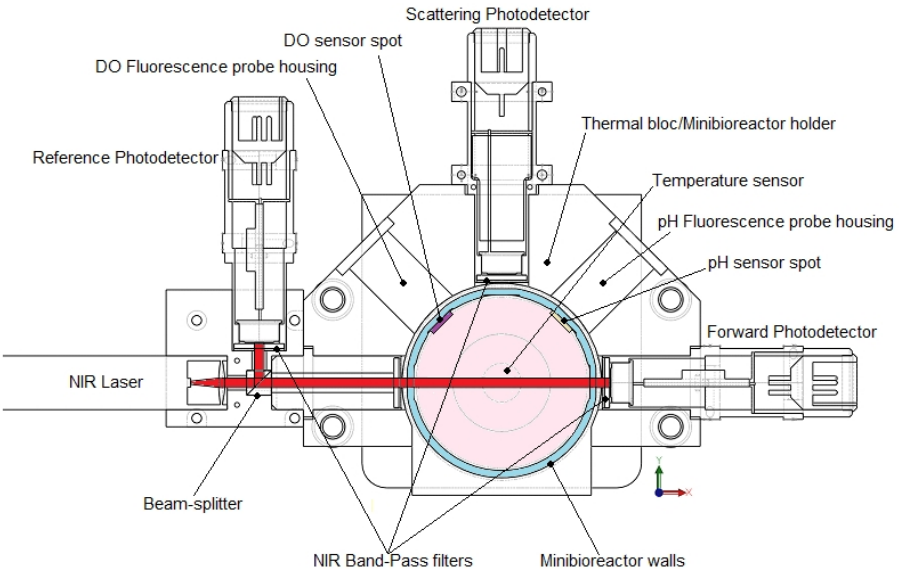

Figure 51
MonoScreen Fed-Batch NIR Laser Turbidimeter.

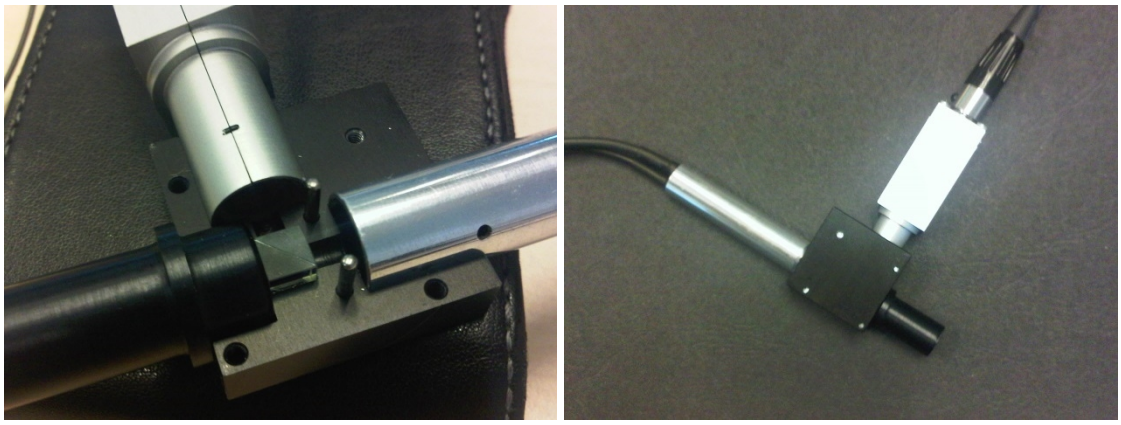

Figure 52
NIR Laser assembly with the beam-splitter and the logarithmic photodetector for the monitorization of the incident beam.

In order to obtain a wide range measurement it is important to note that in spite of the use of a NIR laser there is another important design aspect to take care of. Linear photodetectors are inadvisable since the ratios between the incident beam and the transmitted or scattered intensities may reach several orders of magnitude. That is why photodetectors must show a logarithmic response. Figure 51 shows the Turbidimeter implementation using three "identical" logarithmic photodetectors, where the laser beam is split fifty-fifty so half of the incident beam's intensity is monitored by the Reference photodetector and the other half is applied to the Minibioreactor. Therefore, according to the configuration of the logarithmic amplifiers (4.2.1) the TA and OD are related as follows:

$$\text{TA} = 10^{\left(\frac{v_{ref}-v_t}{k}\right)-c};\ \text{OD} = \frac{v_{ref}-v_t}{k} - c$$

Where:

- v_{ref} [V]: Reference photodetector response
- v_t [V]: Forward photodetector response.
- c [ ]: Offset term due to the actual mismatch between both photodetectors.
- k [V]: Photodetector's gain (must be approximately the same)

The configuration was tested with baker's yeast (Saccharomyces Cerevisiae) to check its viability for the determination of the biomass density. The results clearly showed how the Turbidimetric Absorption is a more appropriate way to represent the biomass density than OD, especially under high cell concentration conditions. This will be discussed in the results section (4.2.6).

4.2.3.2 Fluorescence measurement (DO & pH):

As previously mentioned, the DO & pH fluorescence readers were based on plastic optic fiber bundles, that's an evolution of the DO probes used by the HexaScreen system

where the fiber bundles where made of thinner fused silica. It was found that the use of wider plastic fibers with fluorescent sensor spots offers a more robust and increased sensitivity due to the obvious increment of luminous flux. However, to optimize the light collection it is important to choose the right focal length between the sensor spot and the tip of the fiber bundle. This was simulated for a 4 mm sensor spot, which was modeled as an isotropic light source and three NA = 0.5, 1 mm, plastic fibers arranged as a bundle. One of the fibers was used for irradiation and the other two for light collection. The simulation results shown a uniform and maximum collection around 1.6 % of the light emitted/reflected by the sensor spot for a 4 mm focal length. Some other configurations were also simulated using collimation optics. Nevertheless, an even lower light collection was obtained due to the isotropic nature of light emitted/reflected by the sensor spot.

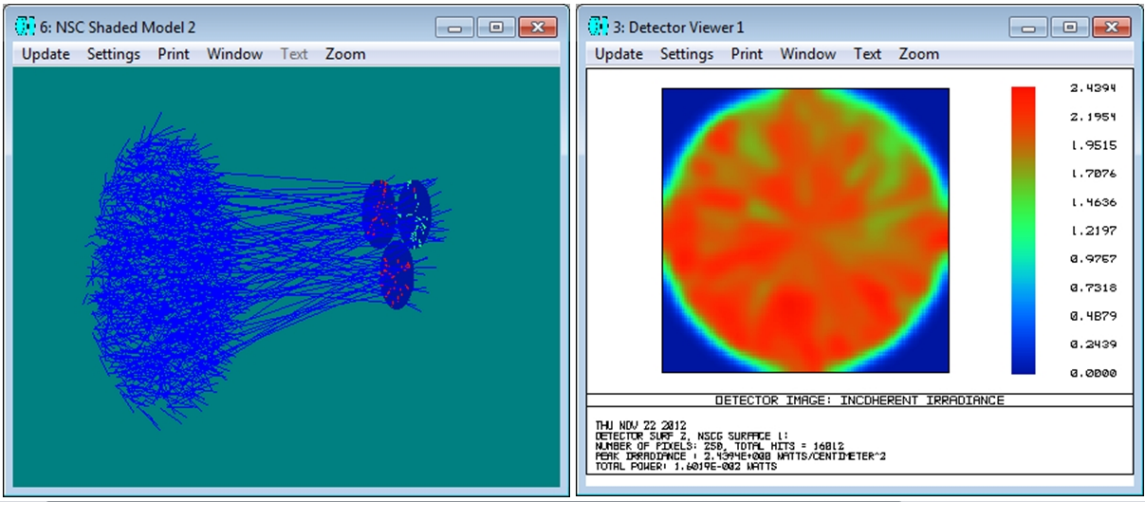

Figure 53
Fiber light collection geometrical analysis and PSF.[8]

The optical filters for wavelength discrimination are placed at the fiber's opposite end, just in front of the detecting photodiode. The filter's diameter is determined by the distance between the fiber's end and the filter itself in such a manner that all the light transmitted by the fiber's core will go through the filter. Otherwise, additional optical insulation could be necessary to protect the photodiode window from noise (ambient light or excitation crosstalk). Figure 54 illustrates the DO & pH optical lay-out, as well as the use of the different filters.

[8] This simulation was performed in cooperation with the company COSINGO S.L.

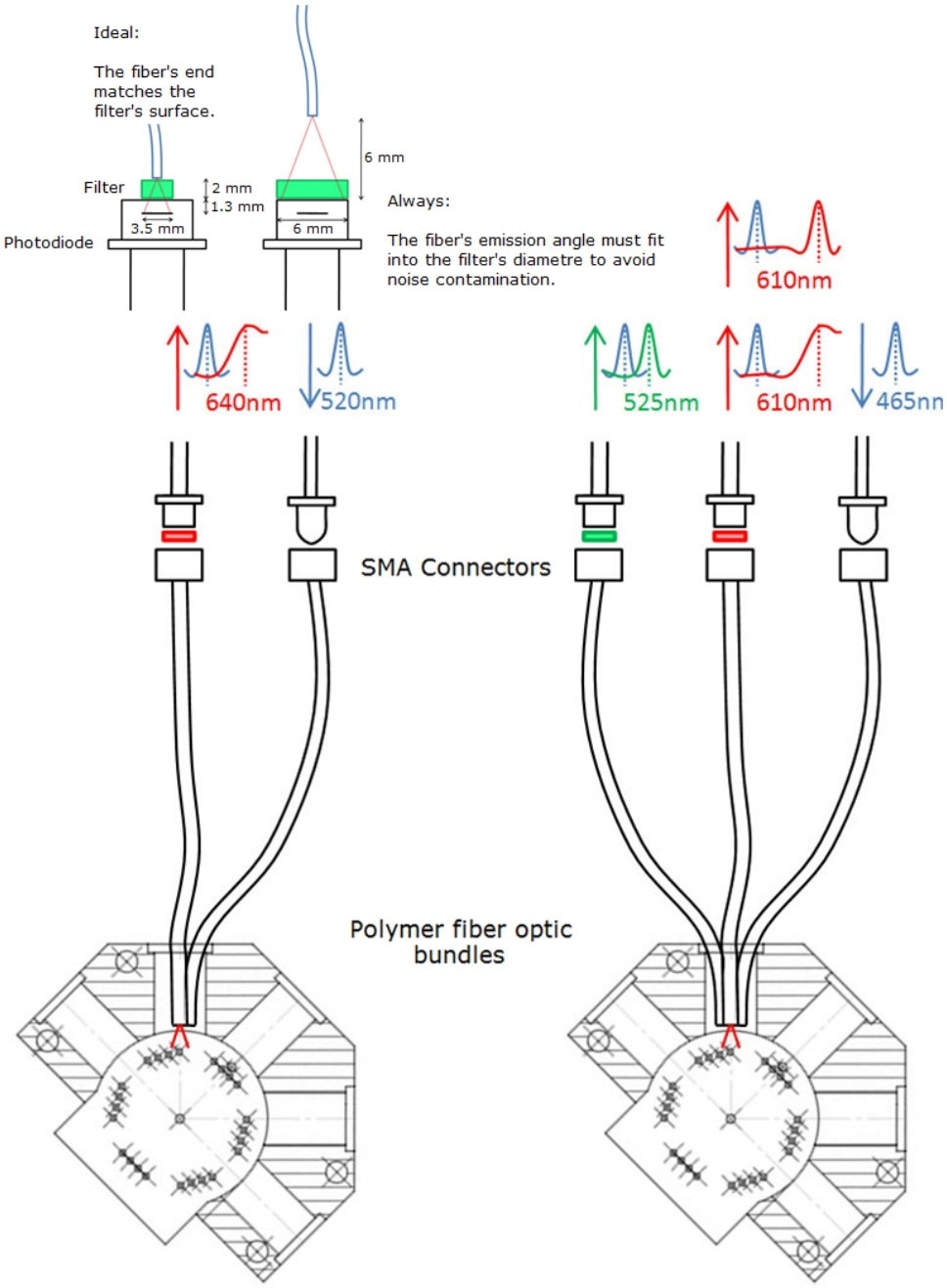

Figure 54
MonoScreen Fed-Batch DO an pH optical setup

4.2.4 Minibioreactor liquid handling (Medium addition & sampling)

The ability to take samples and adding mediums in an automated manner is a very important feature of any bioreactor; especially for fed-batch, perfusion or continuous operation. For the MonoScreen Fed-Batch system, the feeding mechanism was based on syringe pumps which are coherent with the single use product concept and provide an

unmatched addition resolution in comparison to the peristaltic pumps, something which is pretty important when coming to a bioreactor within the millilitres scale. Therefore, the reservoirs were made of two 10 ml syringes connected to the vessel by means of silicone tubbing and 30G x1/4" dispensing needles used to provide a typical addition resolution around 5 to 8 μl/drop. In some cases the feed medium may contain temperature sensitive components. That is why the second syringe pump was additionally equipped with a TEC device based cooling system capable for to keep the reservoir's temperature below 4 °C all along the experiment.

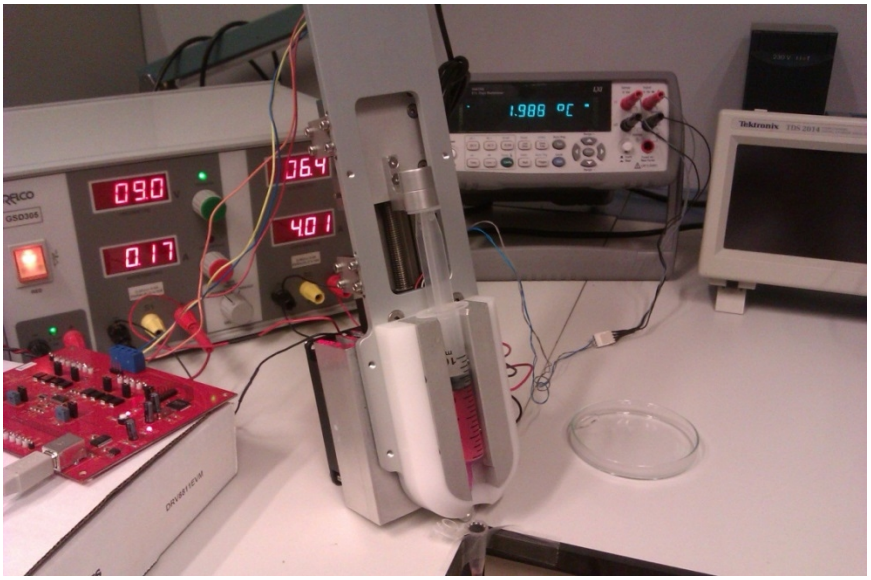

Figure 55
Syringe pump's testing setup. Observe the reading of the multimeter, 1.988 °C

An innovative sterile sampling device for single use bioreactors was also integrated within the system and constituted a patent request derived from the thesis evolution [27]. Its performance is based on the physical principles of fluid mechanics (Law of connected vessels, Tate's Law and Hydrostatic pressure) and the use of a non-sealed vessel pneumatically driven through gas filters. The cross-sectional view of the device is shown in the Figure 57.

The sampling procedure comprises three stages:

A) Normal regime. The pressure gradient through the suction cannula is null or too small to force the fluid flow towards the accumulation chamber.
B) Accumulation stage: The sampling port cap is replaced by an Eppendorf tube and the pressure gradient between the vessel's headspace and the accumulation chamber is increased to fill the accumulation chamber. Once filled, the sample volume remains there due to the fluid's surface tension experienced around the dispensing nozzle.
C) Sample dispensation: The pressure gradient is reversed and the sample volume is delivered in drops avoiding the presence of any sort of continuous stream between the accumulation chamber and the Eppendorf tube. Therefore, the possibility of external contamination is also minimized.

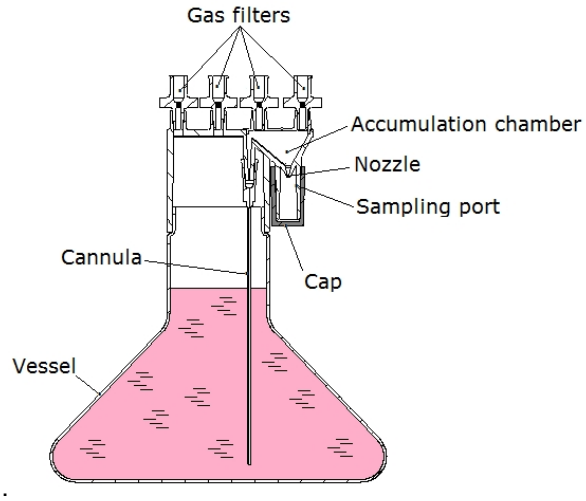

Figure 56
Parts of the sterile sampling device

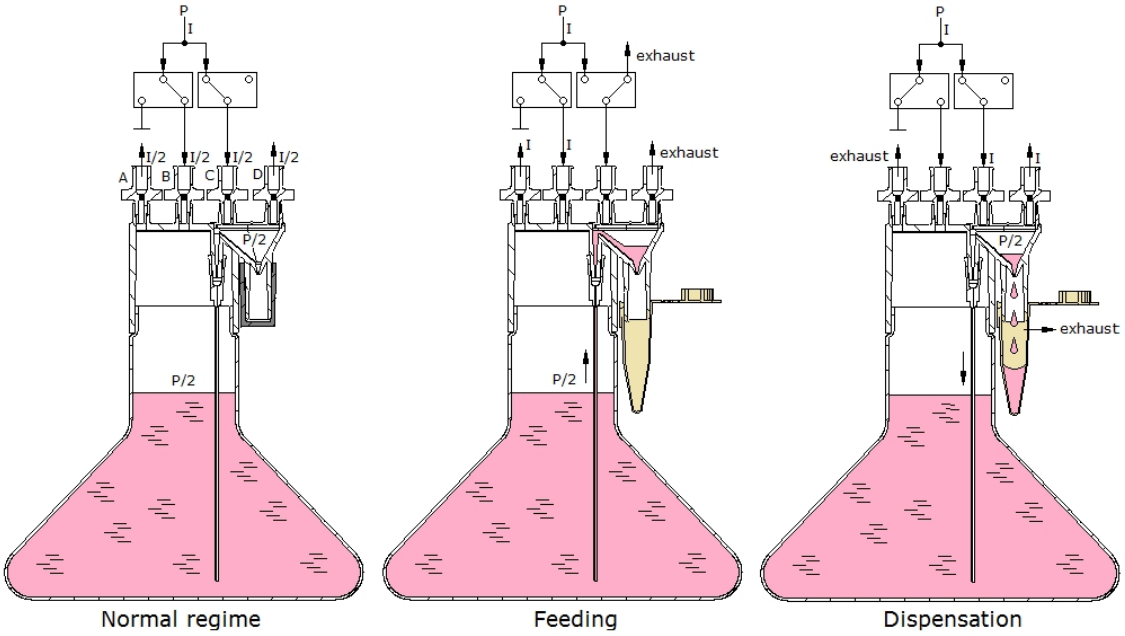

Figure 57
Stages of the sampling procedures

Still, there are certain dimensional aspects to keep in mind for a proper operation of the device. The first key point is the ratio between the nozzle's diameter and the height of the accumulation chamber. In order to avoid uncontrolled dripping of the sample volume, the weight of the mass accumulated over the nozzle's section must be smaller than the fluid's surface tension around the nozzle perimeter. This is an empiric ratio where the maximum height of the accumulated fluid is inversely proportional to the nozzle's radius and the drop's contraction and surface tension parameters may be determined through the Tate's Law, which states the minimum mass of a drop to break the surface tension around the nozzle where is hanging from and fall.

$$m_g \cdot g = k \cdot 2 \cdot \pi \cdot r_o \cdot \gamma$$

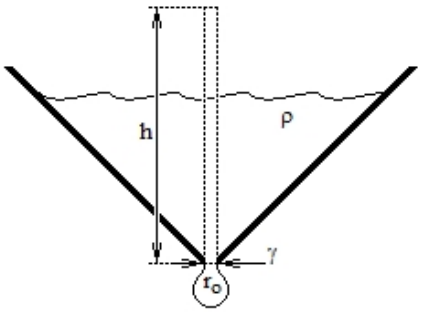

Figure 58
Representation of the Tate's Law.

$$\rho \cdot r_o \cdot h \cdot g > k \cdot 2 \cdot \gamma \rightarrow h \cdot r_o > \frac{k \cdot 2 \cdot \gamma}{\rho \cdot g}$$

Where:

- k [ ]: Experimentally found contraction factor for a given nozzle.
- γ [N/m^2]: Surface tension (72,75x10-3 N/m per water at 20 ºC).
- ρ [kg/m^3]: Fluids's density.
- h [m]: Fluid's column height.
- r_o [m]:Nozzle's radius.

i.e. For a nozzle's radius of 0.25 mm and water at 20 °C we get the following empiric data:

$$m_g = 11\text{mg}$$

$$k \cdot \gamma = 68{,}8 \times 10^{-3}\ {}^{N}/_{m}$$

Where:

- g [m/s^2]: Gravity's acceleration.
- m_g [kg]: The mass of a drop.

Then, it is possible to state the maximum height of the water column:

$$\frac{k \cdot 2 \cdot \gamma}{\rho \cdot g} = 1{,}4 \times 10^{-5}\ m^2 \rightarrow h > \frac{k \cdot 2 \cdot \gamma}{\rho \cdot g \cdot r_o}$$

$$h > 56\ \text{mm}$$

Obviously, these are very rough calculations, where other phenomena and fluid properties such as capillarity, viscosity or geometrical imperfections are not taken into account. Therefore, it is advisable to be conservative when designing the height of the accumulation chamber and to apply a correction factor no bigger than 0.5. This will make possible to extent its use to other application conditions different than the reference ones.

Additionally, the diameter of the sampling port must be wide enough to avoid drops touching its inner walls. Once the mass of a drop is known, if we approach its shape as a sphere, it will be possible to calculate its radius and therefore its ratio versus the nozzle's radius:

$$\rho \cdot V_g = m_g \rightarrow r_g = \left(\frac{3 \cdot m_g}{\rho \cdot 4 \cdot \pi}\right)^{1/3}$$

$$r_g = \left(\frac{3 \cdot k \cdot r_o \cdot \gamma}{\rho \cdot 2 \cdot g}\right)^{1/3}$$

This gives for the previous reference conditions a drop's radius of 1.38 mm. A sampling port with a minimum inner diameter bigger than twice the drop's radius should be enough to ensure a clean and dry wall which is the second key point to properly operate the sampling device. Of course, the fluid's characteristics, the geometrical design and other imperfections like verticality or the length of the sampling port could also modify the actual result and should obviously be taken into account to preserve the inner wall of the sampling port to get wet.

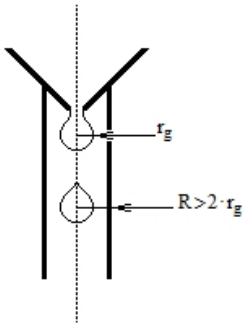

Figure 59
Simplified representation of the sampling port.

4.2.5 Minibioreactor aeration, stirring & mass transfer.

The MonoScreen's aeration strategy is completely different in comparison to the HexaScreen's system. Figure 35 shows the gas circuit with all the necessary valves and sensors for having an accurate control of the gas flow, as well as the humidification vessel used to compensate evaporation and for proper gas mixing. Due to the need for a constant ratio between the gas flow through the bioreactor with respect to the culture volume, the aeration circuit was conceived to provide a continuous gas flow even though continuous aeration uses to be an economical issue for bench-scale bioreactors. Fortunately, due to the reduced size of the MonoScreen Fed-Batch vessel the total gas consumption is not significant, typically from 15 to 30 smlpm for animal cell culture and from 30 to 60 smlpm for microbial. Additionally, the use of Rushton and Pitch-Blade turbines as well as the standardized dimensional design of the

vessel, leads to an optimized oxygen transfer that increases the Minibioreactor's capability to hold a higher cell concentration.

The flow topology and turbulence were investigated by means of Computational Fluid Dynamics (CFD) simulation. Such study gave three important results: a) Laminar flow happens approximately below 500 rpm and Turbulent flow starts over 750 rpm (Maximum $k_l{\cdot}a$ will be obtained over 750 rpm when using baffles. This is a very aggressive agitation condition typical of microbial fermentation). b) Dead volumes behind the baffle areas are almost negligible over 500 rpm (The whole culture volume will contribute to the cell growth). c) On one hand, mammalian cell culture will be possible even for a quite high stirring rate with Pitch Blade turbines. On the other hand, optimization of microbial growth could be achieved by the use of baffles and Ruston turbines over 750 rpm.

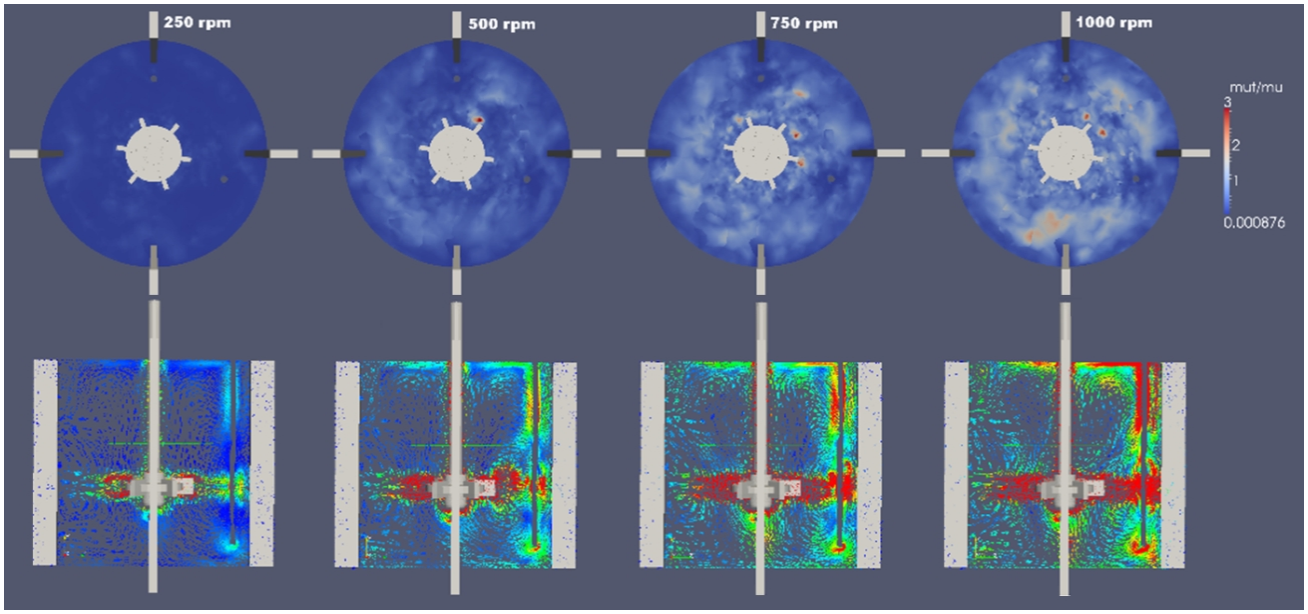

Figure 60
Up: Transition from laminar flow to turbulent regime. Down: Evolution of the Flow topology[9].

Some trials were carried out to evaluate the actual $k_l{\cdot}a$ values for different stirring and aeration rates. The results shown that for simple sparging (by means of a bent needle submerged into the medium with no baffles), the $k_l{\cdot}a$ values were high enough to ensure proper scalability with most Bench-Scale bioreactors. Despite that, if an even higher growth is wanted, it would be necessary to mimic the production conditions by using a microdifusor and/or baffles to reduce the bubble's size and increasing both, the gas to liquid interfacial area and the bubble's hold up time.

[9] This simulation was performed in the frame of collaboration with the Heat and Mass Transfer Technological centre – Polytechnic University of Catalonia

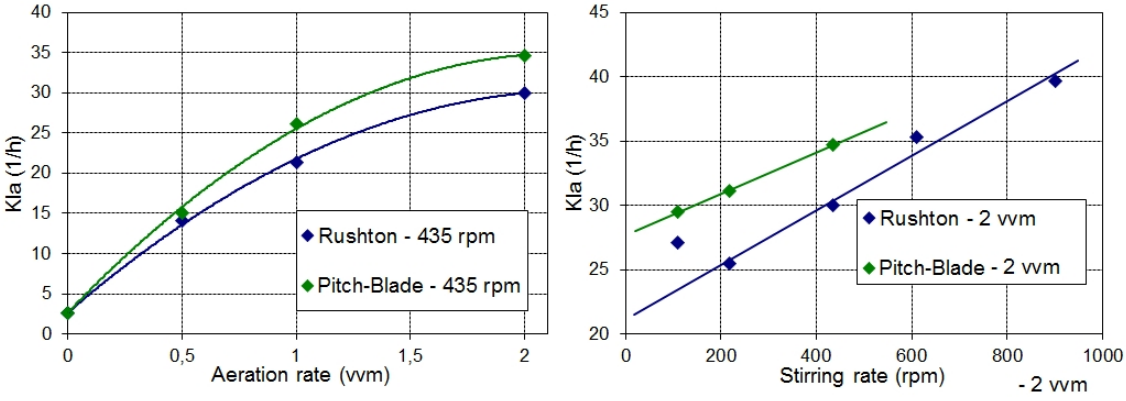

Figure 61
Left: k_La *values for Rushton & Pitch-Blade turbines for different aeration rates.*
Right: k_La *values for Rushton & Pitch-Blade turbines for different stirring rates.*

It was found that the effect on the $k_l{\cdot}a$ depending on the aeration rate shows a similar behavior for both turbines if no baffles were used, being slightly bigger for the Pitch-Blade. However, when coming to the effect of the stirring the Rushton turbine shown a bigger slope. These results were coherent with the previous simulations and reinforce the idea that the Pitch-Blade turbine is a good choice for cell species with moderate oxygen consumption [28]. On the contrary, the Rushton turbine is the one to be used, always with baffles, for very prolific cell lines. Nonetheless, the most important conclusion was that the achieved MonoScreen's mass transfer behavior is comparable to most common benchtop stirred tank bioreactors [40].

4.2.6 Experimentation workflow & results.

The MonoScreen Fed-Batch experimentation workflow is quite similar to the one for the HexaScreen system. However, MonoScreen is mostly intended for controlling the physical and chemical culture conditions which are connected to the algorithm for the OUR estimation and not that much for monitoring. A deeper discussion on the more relevant results will be conducted in section 5.3.4

Steps of the experimentation workflow:

- Workstation preparation: The system needs to be calibrated at least once before starting any experiment. It consists of several steps for obtaining the calibration parameters of the internal instrumentation (Temperature, pH, DO & OD) and to ensure a proper operation of the gas mixing system and servos (Temperature control loops, stirring and syringe pumps). Such process needs to be performed using the same Minibioreactor that will later be used to perform the experiment. Both, the Minibioreactor and the syringe reservoirs are required to be prefilled with the culture and feed mediums.

- Minibioreactor inoculation: After the calibration, the Minibioreactor and the workstation are ready to be used. However, it is advisable to pre-set the medium's pH to the cell's physiological value by placing the Minibioreactor together with a sample of the basal medium inside a CO_2 incubator for a certain period before being seeded. Then, the basal medium pH shall be measured using a bench-top pH-meter in order to introduce the initial pH conditions into the culture recipe.

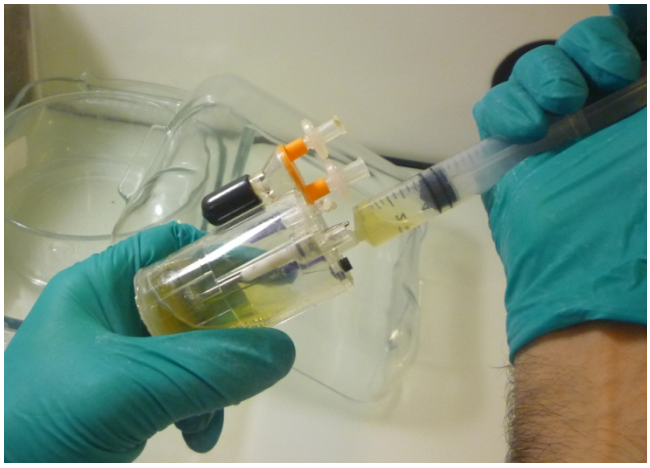

Figure 62
Minibioreactor inoculation under sterile conditions

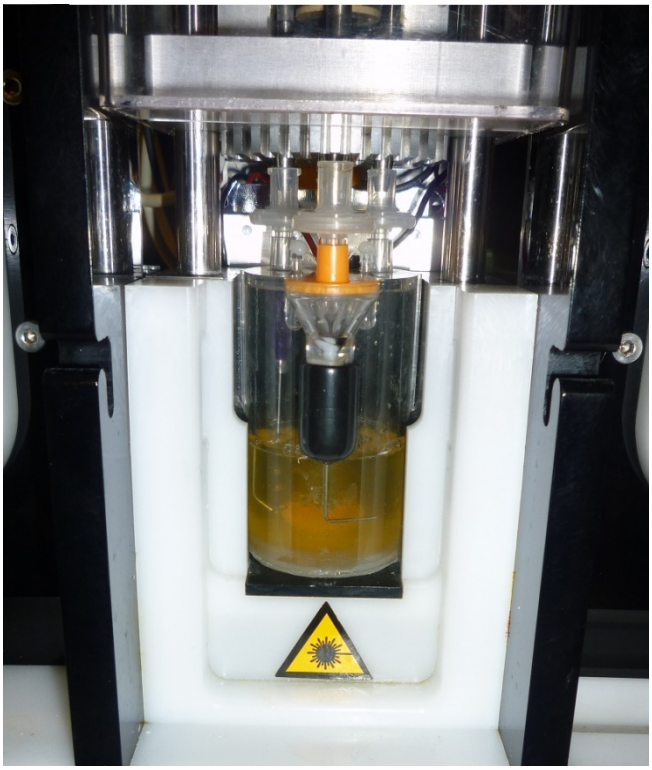

Figure 63
Minibioreactor attached to the workstation's dock bay

- Experiment definition: Before starting the experiment a culture recipe needs to be created; this can be done by editing a template recipe. Where besides of some information about the cell's type, the mediums used and the experiment's initial conditions, a set-points table for the operation of the different control loops needs to be defined as well as any user defined variable that could be wanted to be introduced during the experiment after some off-line analysis.
- Acquisition and control stage (Results evaluation): The experiment is started through the workstation's touch panel. Once the MBR is connected, the active recipe is executed automatically and data begin to be displayed and recorded. Interaction with the experiment in terms of modifying or adding new set-points as well as introducing Off-line data will need to be done remotely via the built-in web server.

Example I

Characterization of the NIR Turbidimetric response under high cell density conditions.

Experiment Description

A highly concentrated solution of fresh baker's yeast was used to study the accuracy of the NIR Turbidimeter. A Minibioreactor was filled with 20 ml of the mentioned solution and the absorption of light was measured. Afterwards, the solution was diluted 50 % and the absorption measured again. The operation was repeated until the detection limit was reached and a crystal clear solution was obtained. In order to ensure a homogeneous solution, stirring and temperature were kept constant. Finally the Turbidimetric Absorption (TA) characteristic was compared with its logarithmic form (OD).

Culture Conditions

Medium: Physiological saline (NaCl, 9.0 g per liter). Also used for the successive dilutions.
Cell line: Saccharomyces Cerevisiae
Volume: 20 ml
Initial cell concentration: 100 g per liter
Stirring rate: 500 rpm
Bioreactor temperature: 37 °C

Results

The comparison of both biomass representations can be observed in the figure below. On one hand, the OD shows the well-known saturation behaviour as the biomass density increases. On the other hand, it can be seen how up to an approximate concentration of 20 g/l TA displays a clearly linear trend, which is more than two orders of magnitude over the OD's "linear" range. Despite that TA becomes non-linear for the higher values of biomass density; it is obvious that offers a more appropriate expression to display the on-line evolution of the biomass. On the other side, the non-linear stretch of the TA characteristic can easily be calibrated by means of an error function of the form:

$$TA^{\square} = a \cdot TA^2 + (b+1) \cdot TA + c$$

Nevertheless, the calibration parameters a, b, c will not be valid for every cell type. Hence, in order to provide an accurate estimation a previous characterization of the NIR Turbidimeter will always be necessary.

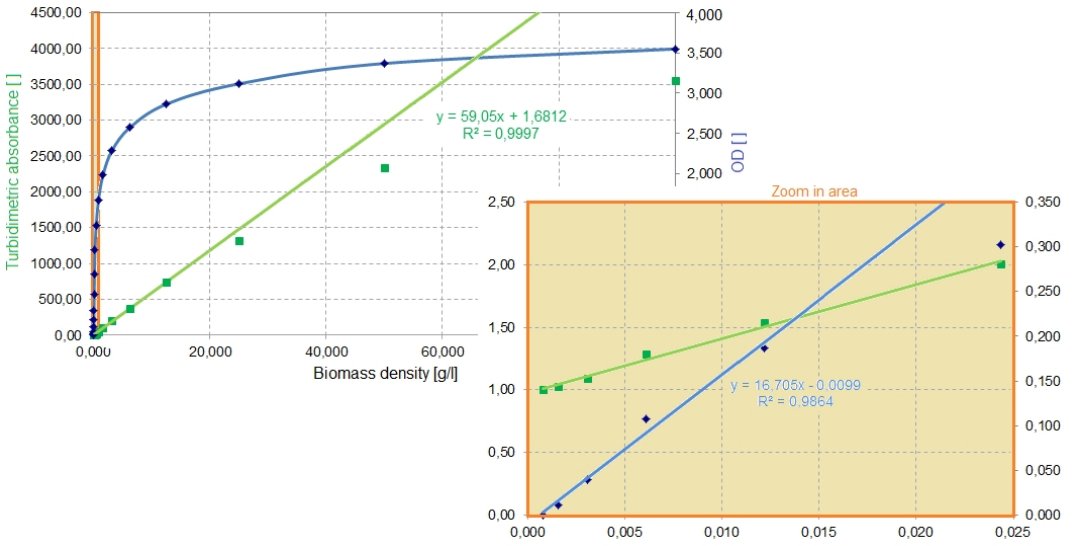

Comparison between the TA *and* OD *within a wide range of biomass density.*

This example can be considered as a worst case, and demonstrates the viability of NIR Turbidimetry for monitoring a wide range of cell species under high cell densities conditions.

Example II

Evaluation of the DO control capabilities.

Experiment Description

As widely explained throughout the introduction DO is one of the most important scale-up parameters in Bioprocess engineering. Accuracy of the OUR estimation is highly dependent on the stationary error of the DO control loop. Therefore, the optimization of the DO control Loop parameters, as well as the determination of the system's control accuracy within the specified control range is a must.

5 different DO set-points from 10 to 90 % were programmed every 2.5 hours at a constant temperature and stirring rate.

Culture Conditions

Medium: Distilled water
Volume: 25 ml
Stirring rate: 500 rpm
Bioreactor temperature: 37 ^{o}C
Aeration rate: An approximately constant gas mixture of 1.88 vvm was applied.

Results

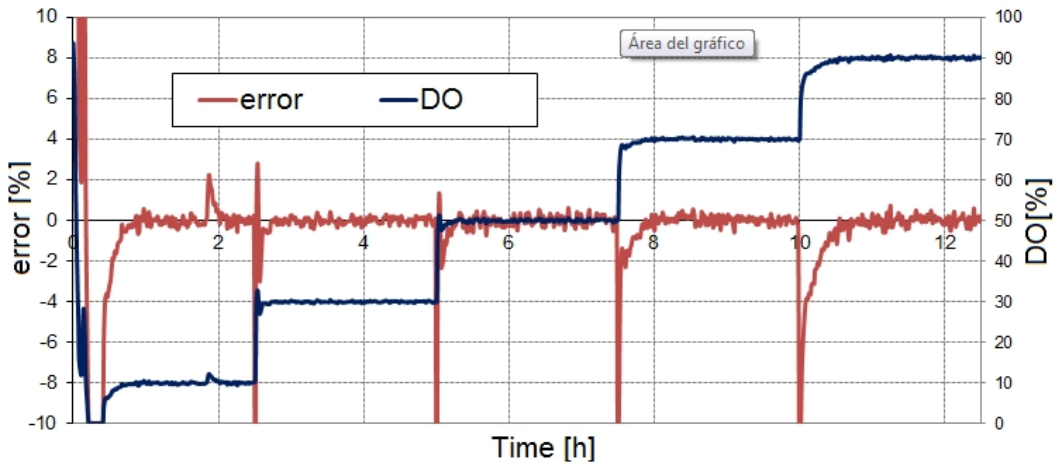

Performance of the DO control and error evolution.

The graphs above show the evolution of the dissolved oxygen concentration and the stationary error as the set-points values were changed. It can be seen how after the transient period, the mean value of the stationary error trends to be null and the accuracy always better than ±1%. This makes possible not just a realistic but a quantitative estimation of the OUR.

4.3 The BIOSTAT B-plus Bench-Scale Bioreactor & aeration Test Setup

As explained in the state-of-the-art chapter, the mass transfer capability of a given bioreactor is strongly linked to its size and topology. Therefore, it is important not to limit the study of the purposed OUR estimation method to its application with Minibioreactor systems only. That's why a test setup was built by customizing a 5 litre Biostat B-plus bench-scale bioreactor. The aim of the hereafter described setup was to evaluate the feasibility of the DO control method and hence the OUR estimation method under Bench-Scale and real conditions.

This part of the work was carried out in valuable cooperation with members of the Chemical Engineering Department of Universitat Autònoma de Barcelona.

4.3.1 Description of the Test Setup

The customization of the Biostat B-plus system consisted on bypassing its native DO control system based on ON-OFF valves, in order to use two PWM controlled proportional valves to regulate the inlet flow of the supply gasses (Air/O_2, N_2). The gas mixing was

performed by means of a humidification bottle and the valves were actuated by means of a custom driver connected to a computer by a RS-232 interface. The computer was in charge of reading the DO data acquired by the Biostat B-plus by means of an OPC client and running the DO control loop, as well as the OUR estimation algorithm.

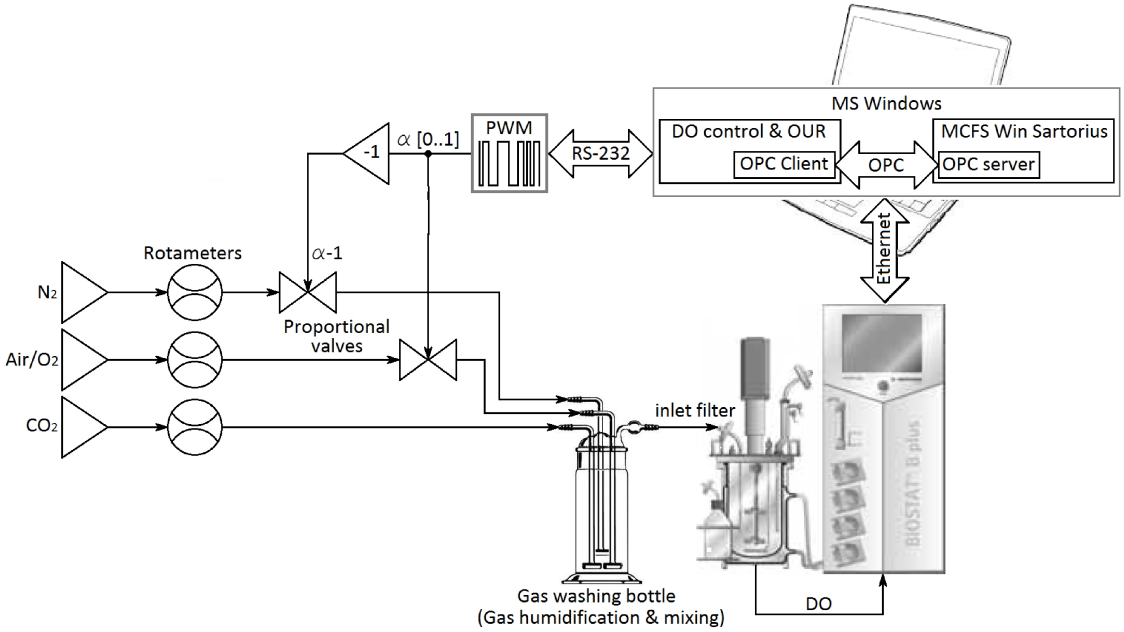

Figure 64
Block diagram for the bench-scale setup.

The Sartorius Biostat B-plus, also named as DCU (Digital Control Unit), is a polyvalent bioreactor system intended to be used with 5 litres UniVessel® stirred tanks. The unit is an embedded solution including all the basic probes and actuators to carry out most cultivation strategies (Batch, Fed-Batch, Perfusion, etc…). The DCU can be operated either manually from the local touch panel or by means of the control software (MFCS/win) through a remote computer connected to the DCU via Ethernet.

MFCS/Win is a proprietary SCADA like software intended for the simultaneous monitorization and control of several DCU's. The software lets the user to define recipes by stablishing events, operation conditions and control loop set points, not just as constant values but through mathematical expressions depending on any available variable. No matters if they are measured variables, calculated, provided by the user or any other instrument. Hence, on-line connectivity with other devices is a must. This is solved by means of the OPC Server, a software module intended for providing data exchange service between applications. The OPC protocol (OLE for Process Control) lets any OPC client read or write data from an OPC server. This way DO information is transferred to the custom controller (DO Control & OUR) which generates the control signal to command the Pulse Width Modulator to drive the proportional valves. The need for a constant gas flow through the bioreactor makes necessary that the addition of the duty cycles applied to both valves are constant too. The key for an adequate operation of the DO control loop as well as for the OUR estimate is the linearity of the valves used. In this case the valves selected (VSO-Low Flow from Parker) shown some hysteresis and

non-linearity errors that had to be compensated. This can be observed in the following picture where a sigmoid profile and the existence of a minimum current threshold are also appreciated.

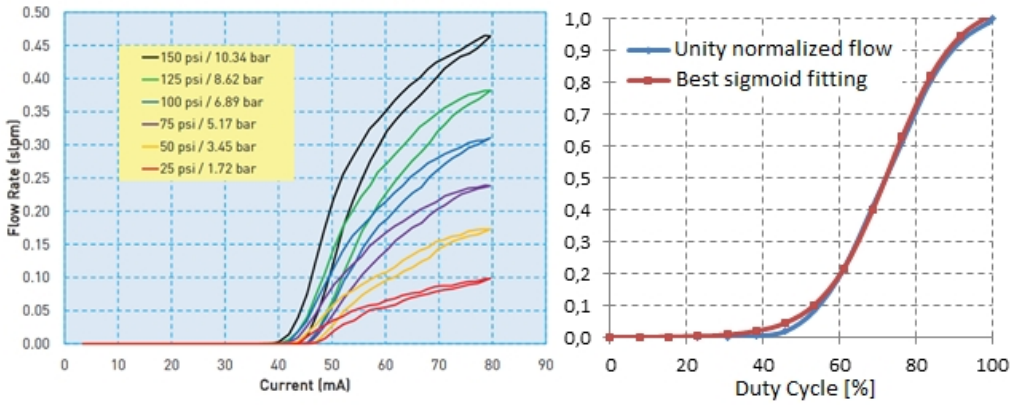

Figure 65
Left: Typical flow curves VSO-Low Flow miniature valves from Parker [41].
Right: Normalized flow and sigmoid fitting.

If such behaviour is unity normalized and the mean value of the upwards and downwards paths is represented in terms of the equivalent duty cycle instead of the mean current through the solenoid. Then, it can be seen how the valve's behaviour fits a sigmoid curve of the form:

$$f = \frac{A}{1 + e^{\frac{C+\alpha}{B}}}$$

Where:

- f [ ]: Gas flow through the valve (unity normalized)
- A [ ]: Magnitude of the sigmoid
- B [%]: Relaxation factor
- C [%]: Inflection point.
- α [%]: Duty cycle applied.

The compensation procedure consisted on the addition of a correction function related to the behaviour of each individual valve in order to obtain a linear characteristic. The scheme on how the correction function was applied and its expression is show below:

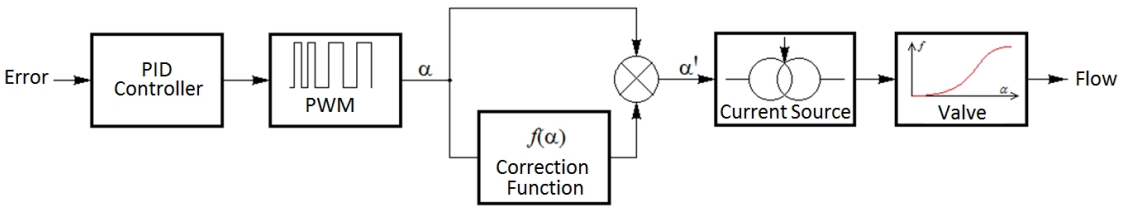

Figure 66
Duty Cycle correction scheme.

The correction function matches the following equation:

$$f(\alpha) = C - \alpha - B \cdot \ln\left(\frac{100 \cdot A}{\alpha} - 1\right)$$

Hence, the duty cycle is corrected as follows:

$$\alpha' = \alpha + f(\alpha)$$

The correction function was applied to several of the flow curves provided by the manufacturer. It can be observed how the compensation procedure comes out with a linear behaviour independent of the pressure (always within the operation range specified by the part's datasheet).

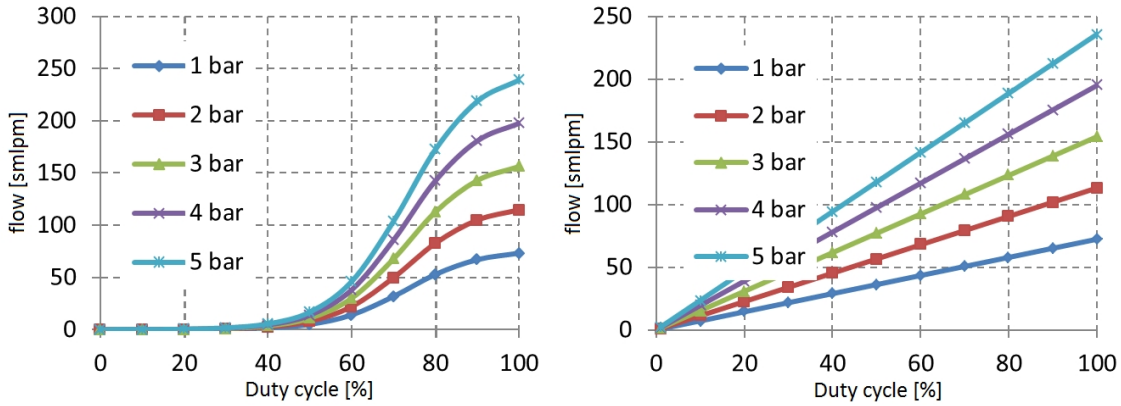

Figure 66
Flow profiles depending on the Duty cycle before and after applying the correction

4.3.2 Bioreactor aeration control & Mass transfer

Knowledge of the mass transfer capability is required for the later estimate of the OUR. The UniVessel® stirred tank features three possible aeration systems (Headspace, microdifussor, and a sparger). This test set-up was implemented for the experimentation of an animal cell line (HEK293). To that end, the aeration-mixing system was chosen to be based on gas sparging and on the use of a pitch blade turbine operated at a very low stirring rate. Moreover, in order to increase the cells robustness and to reduce the cell attachment, non-ionic surfactant, Pluronic F-68, was added to the culture medium. The $k_l{\cdot}a$ value was determined by means of the Van Riet's gassing out method and it was found to be 6.53 h^{-1} for PBS at 37 °C and 100 rpm.

It is important to emphasize the fact that the $k_l{\cdot}a$ value can be modified during the culture time due to several reasons. Hence, as for any estimation method but the Global Mass balance, the finally calculated OUR values must be considered as an approach dependent on the $k_l{\cdot}a$ stability. The following table shows some reported mass transfer coefficients for several benchtop stirred tank bioreactors for animal cell culture.

Reference	Volume [ml]	Aeration	Stirring rate [rmp]	$k_l \cdot a$ [h^{-1}]
Kyung et al., 1994	1000/500	Headspace + silicone membrane	50	4.29
Zhou et al., 1995	750/500	Headspace + silicone membrane	60	4.58
Kussow et al., 1995	1000/500	Headspace	60	0.93
Dorrestijn et al., 1996	6000/3000	Headspace	50	0.79
Zhou et al., 1994	1000/750	Headspace	10	1.13
Emery et al., 1995	1000	Silicone membrane	100	~2.7

Table 3
Aeration dynamics of several benchtop bioreactors for animal cell culture.
Adapted from Gàmez [42]

References:

[1] R. Bragós Bardia, X. Rosell Ferrer, P. J. Riu Costa, F. Gòdia Casablanca, J. Cairó Badillo, C. Paredes Muñoz and F. Rodríguez Omedes, "MODULAR SYSTEM COMPRISING MULTIPLE AUTOMATED MINI-BIOREACTORS FOR HIGH-THROUGHPUT SCREENING (HTS) IN BIOTECHNOLOGY". EU Patent 1580261, 10 February 2010.

[2] Boehringer Ingelheim - Microparts, *Product information: The UV/VIS Microspectrometer,* Dortmund, 2006.

[3] M. Pilotte, *AN-691 Operation of RF Detector Products at Low Frequency,* Norwood, MA: Analog Devices, 2005, rev.0.

[4] Presens, "Electro-Optical Module EOM-O2-mini," 30 April 2012. [Online]. Available: http://www.presens.de/products/brochures/category/transmitters/brochure/electro-optical-module-eom-o2-mini.html.

[5] Eastman Kodak Company staff, Kodak Photographic Filters Handbook, Kodak Publication, 1998.

[6] H. H. Kenjiro Hamanaka, "GRIN Lenses," in *Handbook of optical interconnects*, Taylor & Francisd, 2005, pp. 63-77.

[7] A. A. M. Anna Grazai Mignami, "Direct and Chemically-Mediumted Absortion Spectroscopy Using Optical Fiber Instrumentation," *IEEE Sensors Jounal,* vol. 2, no. 1, pp. 52-57, 2002.

[8] J. P. Golden, "Chemical Sensor Using Two Dimensional Lens Array". USA Patent 5.827.748, 27 October 1998.

[9] S. B. M. R. A. W. J. B. M. E. Alfredo E. Bruno, "All-Solid-State Miniaturized Fluorescence Sensor Array for the Determination of Critical Gases and Electrolytes in Blood," *Analytical Chemistry,* vol. 69, no. 3, pp. 507-513, 1997.

[10] P. J. M. a. T. P. Coursolle, “Fiber optic displacement sensor employing a graded index lens,” *Applied Optics,* vol. 24, no. 4, pp. 544-547, 1990.

[11] R. D. LaClaire, “Optical Point Level Sensor With Lens”. USA Patent 5.399.876, 21 March 1995.

[12] L. P. H. U. U. a. J. K. B. Alexandre R. Tumlinson, “Miniature Endoscope for Simultaneous Optical Coherence Tomography and Laser-Induced Fluorescence Measurement,” *Applied Optics,* vol. 43, no. 1, pp. 113-121, 2004.

[13] J. M. S. a. H. J. Dakin, “Chapter 7. Optical fibre chemical sensing using direct spectroscopy.,” in *Optical Fiber Sensors IV: Applications, Analysis, and Future Trends*, Artech House, 1996, pp. 2-43.

[14] R. J. T. J. H. S. James P.Clarkin, “Shaped Fiber for Medical and Industrial Applications,” in *SPIE - Optical Fibers and Sensors for Medical Applications IV*, Bellingham, WA, 2004.

[15] D. G.Buerk, «Absorption Spectroscopy,» de *Biosensors Theory and Applications*, Lancaster, Technomic Publishing Company, Inc-, 1993, pp. 126-127.

[16] F. Widdel, *Theory and Measurement of Bacterial Growth,* Bremen: Grundpraktikum Mikrobiologie, 4 (B.Sc.) Universität Bremen, 2010.

[17] H. L. &. Y. Kostov, “Optical Instrumentation for Bioprocess Monitoring,” in *Optical Sensor Systems in Biotechnology*, Heidelberg, Springer, 2009, pp. 7-10.

[18] B. SonnLeitner, “Measurement, monitoring, modelling and Control,” in *Basic Biotechnology*, Cambridge, Cambridge University Press, 2006, p. 254.

[19] S. V. T. D. M. M. A. Antony S. Jeevarajan, “Continous pH monitoring in a Perfused Bioreactor System Using an Optical pH Sensor,” *Biotechnology and Bioengineering, Vol. 78, No. 4, May 20,* pp. 467-472, 2002.

[20] P. J. F. R. Goldstein SR, “A miniature figer óptic pH sensor for physiological use,” *Journal Biomechanical Engineering 102(2),* pp. 141-146, 1987.

[21] W. D. M. F. Jordan DM, “Physiological pH fiber optic chemical sensor based on energy transfer,” *Anal Chem 59,* pp. 437-439, 1987.

[22] J. L. T. C. Zhihong Liu, “Phenol red immobilized PVA membrane for an optical pH sensor with two determination ranger anf long term stability,” *Sensor and Actuators B 107,* pp. 311-316, 2005.

[23] A. F. J. G. E. S. M. L. R. B. J. C. f. G. A. Soley, «Development of a simple disposable six Minibioreactor system for suspension mammalian cell culture,» *Process Biochemistry,* pp. 597-605, 2012.

[24] N. P. Q. F. H. K. M. C. R. R. A. B. G. C. L. J. L. M. Thanassis Papaioannou, "Performance evaluation of fiber optic probes for tissue lifetime fluorescence spectroscopy," in *SPIE - Advanced Biomedical and Clinical Diagnostic Systems*, San José, CA, 2003.

[25] P. M. Doran, "Fluid Flow and Mixing," in *Bioprocess Engineering Principles*, Sydney, Elsevier Science & Technology Books, 1995, pp. 141-153.

[26] 2-MagUSA, "2-MagUSA magnetic e-motion," [Online]. Available:

http://www.2magusa.com/. [Accessed 17 10 2012].

[27] A. Fontova and E. Sarró, "Sample Taking Device". ES-EU Patent P2144EP00, 9 March 2012.

[28] R. Mirro and K. Voll, "Which impeller is Right for your Cell Line? A guide to Impeller Selection for Stirred-Tank Bioreactors," *BioProcess International,* pp. 52-57, 2009.

[29] UQG Optics, [Online]. Available: http://www.uqgoptics.com/materials_filters_schott_orange_OG570.aspx. [Accessed 26 5 2014].

[30] Semrock, [Online]. Available: http://www.semrock.com/FilterDetails.aspx?id=FF01-525/15-25. [Último acceso: 26 May 2014].

[31] Y. Berthois, J. A. Katzenellenbogen y B. S. Katzenellenbogen, «Phenol red in tissue culture medium is a weak estrogen: Implications concerning the study of estrogen-responsive cells in culture,» *Proceedings of the National Academy of Sciences of the United States of America,* vol. 83, nº 8, pp. 2496-2500, 1985.

[32] A. Bukovsky, M. Svetlikova y M. R. Caudle, «Oogenesis in Cultures Derived from Adult Human Ovaries,» *Reproductive Biology and Endocrinology,* vol. 3, nº 5, p. 17, 2005.

[33] M. P. D. &. E. T. Davies, *Non-Invasive Biomass Monitor with Wide Linear Range,* BugLab LLC (www.bugbab.com), 2012.

[34] J. McFarland, «The Nephelometer:An instrument for estimating the number of bacteria in suspension used for calculating the opsonic index and for vaccines.,» *Journal of American Medical Association,* vol. 49, nº 14, pp. 1176-1178, 1907.

[35] T. R. L. K. K. N. T. A. M. Paw Dalgaard, "Estimation of bacterial growth rates from turbidimetric and viable count data," *Food Microbiology 23 (1994),* vol. 23, pp. 391-404, 1994.

[36] EPA, «EPA Guidance Manual, Turbidity Provisions,» nº 11, pp. 1-13, April 1999.

[37] P. W. K. B. H. Asa Kolmert, "A fast and simple turbidimetric method for the determination of sulfate in sulfate-reducing bacterial cultures," *Journal of Microbiological Methods,* vol.

41, p. 179–184, 2000.

[38] M. Z. B. M. Ahmad Fairuz Bin Omar, «Turbidimeter Design and analysis: A review on Optical fiber Sensors for Measurement of Water Turbidity,» *Sensors,* vol. 9, pp. 8311-8335, 2009.

[39] M. Sadar, *Turbidity Measurement: A simple Effective Indicator of Water Quality Change.*

[40] V. Glaser, «Bioreactor and Fermentor Market trends,» *Genetic Engineering & Biotechnology News,* vol. 29, nº 19, 2009.

[41] Parker, "VSO-Low Flow Miniature Proportional Valve," August 2013. [Online]. Available: http://ph.parker.com/us/en/vso-low-flow-miniature-proportional-valve. [Accessed January 2015].

[42] X. G. Montoya, "Estudi d'estratègies de cultiu per cèl·lules animals basades en eines de instrumentació i control," Memòria per optar al grau de doctor per la UAB, Progama de doctorat en Biotecnologia, Bellaterra, Novembre 2000.

[43] B. M. Weidgans, New Fluorescent Optical pH sensors with Minimal Effects of ionic stregth - Dissertation zur Erlangung des Doktorgrades der Naturwissenschaften, Regensburg: Naturwissenschaftlichen Fakultät IV – Chemie und Pharmazie der Universität Regensburg, 2004.

[44] Presens, *pH-10 Mini Instruction Manual,* Regenburg: Precision Sensing GmbH, 2010.

Simplified implementation of the OUR stationary liquid mass balance method.

The OUR stationary liquid mass balance estimation method offers advantages in terms of estimation accuracy and cells stress due to the constant DO concentration. However, the need for sophisticated instrumentation like mass flow controllers and sometimes gas analyzers, has historically limited its use. In this chapter, a new simplified implementation for the continuous estimate of the OUR based on inexpensive electrovalves is introduced. It will be demonstrated to be not just a cheap but a reliable alternative to monitor the metabolic activity in many biotechnological processes where the lack of knowledge on the culture conditions could become a limiting factor.

5.1 Method description and modelization.

The proposed method consists on controlling the gas phase oxygen molar fraction by means of regulating the flow provided by two independent gas supplies (Oxygen and Nitrogen). Such regulation will be performed by two PWM driven electrovalves leading to the accurate control of the DO concentration. Additionally, the control loop internal signals will be used for solving the OUR without generating a glimpse of cellular distress.

For a better understanding of the control mechanism, it will be useful to look at the model of the simplest bioreactor and consider some physical analogy. An electrical circuit in this case. The model below shows a gas supply P_s, connected to a bioreactor through an ideal pipe (no resistance against the flow or accumulation will happen) and an inlet filter represented by pneumatic resistance R_{inlet}, a certain volume of gas flows from the supply to the Bioreactor G_{in} and finally goes out through the outlet filter R_{outlet}. Then, as stated by the Henry's Law diffusion will happen between the gas phase and the liquid phase until the equilibrium situation is reached. Notice that this is no more than a simple serial circuit where if we consider the filters to be identical, a voltage divider analogy can easily be applied and the oxygen's partial pressure in the gas phase calculated as follows:

$$pO_2 = \left(\frac{P_s - P_{atm}}{2} + P_{atm} \right) \cdot {y_{O_2}}/{100} = \left(G \cdot R_{filtre} + P_{atm} \right) \cdot {y_{O_2}}/{100}$$

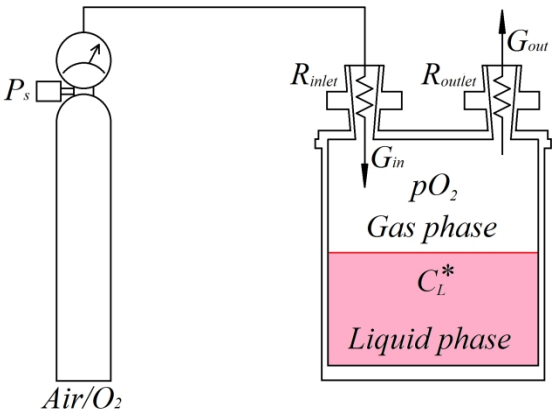

Figure 1
Simplest aeration bioreactor model

Hence, for a continuous air flow the DO concentration in equilibrium with the gas phase is:

$$C_L^* = \frac{pO_2}{H} = \frac{\left(\frac{P_s - P_{atm}}{2} + P_{atm} \right) \cdot {y_{O_2}}/{100}}{H}$$

Where:

- P_{atm} [atm]: Atmospheric pressure.
- y_{O2} [%]: Oxygen's molar fraction in the gas phase.
- H [l·atm·mol^{-1}]: Henry's constant.

Let's now take into account the same model adding a switching valve that follows a certain duty cycle and periodically interrupts the inlet flow. In this case, the mean value of the oxygen partial pressure can be suspected to be modulated by such duty cycle:

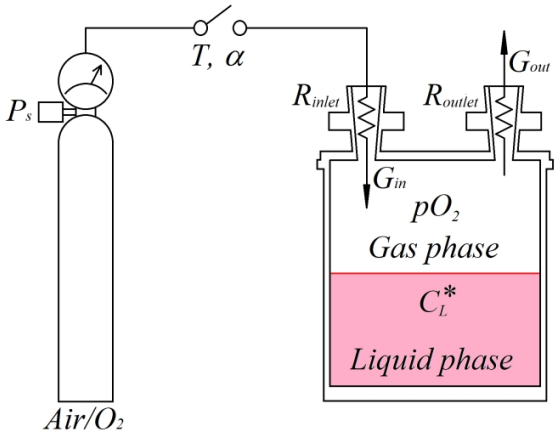

Figure 2
Simplest aeration bioreactor model

Where:

- T [s]: Switching period.
- α [%/100]: Duty cycle (0…1)

This would be true for an ideal model free of any "dead" volume conferring memory properties to the pneumatic circuit, i.e., to assert that there is a direct relationship between the oxygen's partial pressure and the duty cycle operating the valve some element must be incorporated in order to get rid of the inherent "capacity" introduced by the gas phase. The strategy will consist on the rapid replacement of the air volume existent in the gas phase by means of another gas containing no oxygen (typically nitrogen).This implies the following two approaches:

1) The replacement speed must be virtually instantaneous so the global flux can be considered continuous.
2) No existence of dead volumes. Therefore, the pneumatic circuit admits a linear model without memory elements.

In order to keep ahead with the development the following agreement is also taken:

All the pressure expressions are related to the atmospheric pressure.

The direct relationship between the mean value of the oxygen partial pressure and the duty cycle can be demonstrated through the Mean value theorem for integrals, which is visually represented by the following figure:

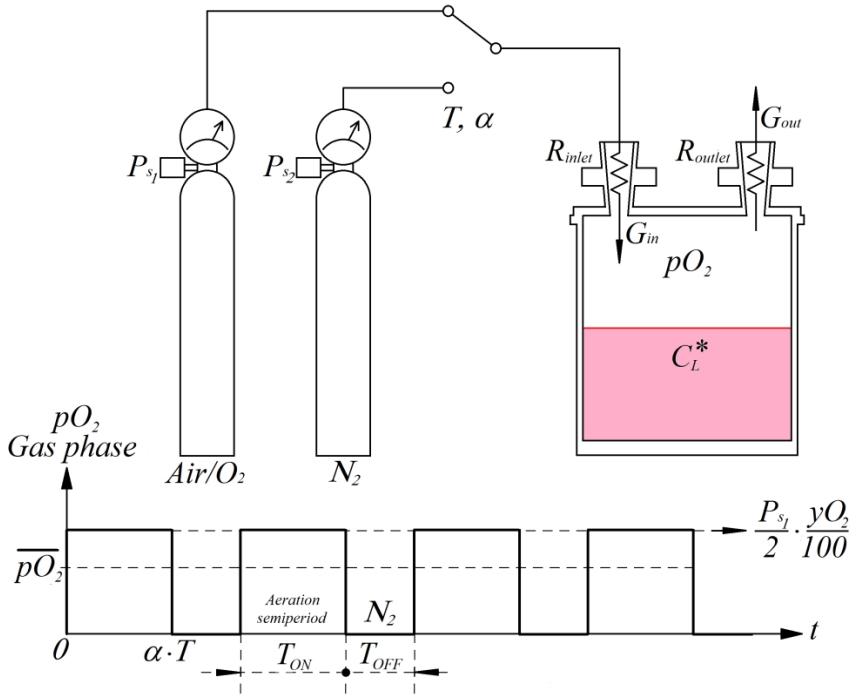

Figure 3
Gas switching makes the DO concentration proportional to the mean value of the oxygen partial pressure in the gas phase.

$$\overline{pO_2} = \left(\alpha \cdot G \cdot R_{filter} + P_{atm}\right) \cdot {}^{y_{O_2}}\!/_{100} = \left(\alpha \cdot \frac{P_s - P_{atm}}{2} + P_{atm}\right) \cdot {}^{y_{O_2}}\!/_{100}$$

Once the linear relationship between the mean value of the oxygen partial pressure and the duty cycle is proofed, is equally possible to calculate the DO concentration in equilibrium with the gas phase for a discontinuous air supply C_L^*:

$$\overline{C_L^*} = \frac{pO_2}{H} = \frac{\left(\alpha \cdot \frac{P_s - P_{atm}}{2} + P_{atm}\right) \cdot {}^{y_{O_2}}\!/_{100}}{H}$$

Obviously, for a discontinuous but periodic air flow the value of C_l^* will tend to be α times the value obtained for a constant flow. This suggests the possibility to implement a DO control loop by means of the iterated switching between both gas supplies. Figure 4 shows the basic diagram of such control loop. Nevertheless, two key conditions regarding the switching and measurement periods need to be taken into account in order to keep the DO concentration constant:

$$T \leq \frac{0.1}{K_L \cdot a};\ T_m < \frac{T}{10}$$

i.e., Imagine a bioreactor intended for low concentration microbial fermentation, which features a mean mass transfer coefficient of $k_L{\cdot}a$ = 20 h^{-1}. That implies a switching

period smaller than 18 s and a maximum measurement period of 1.8 s. This is technically feasible. However, the use of the switching valve topology could become problematic for bioreactors with higher $k_L{\cdot}a$ values.

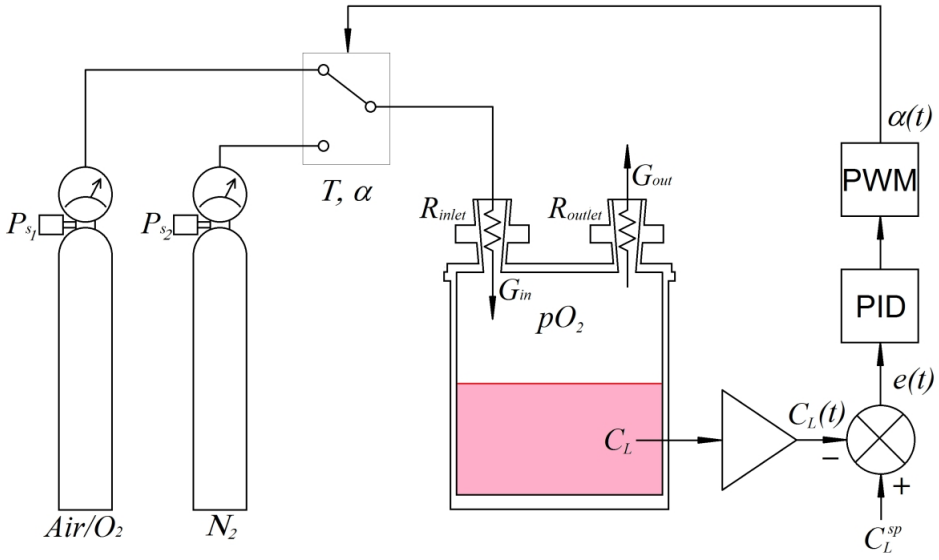

Figure 4
Gas phase replacement control loop topology.

Hence, the mass balance equation may be written as a function of the duty cycle applied to the switching valve:

$$\frac{dC_L(t)}{dt} = k_L{\cdot}a{\cdot}\left(\alpha \cdot C_L^* - C_L(t)\right) - \mathrm{OUR}$$

Now, considering how the signals around the error detector are related and their differential form for a given constant set point. It is obvious to find an expression of the OUR in function of the control loop parameters $\alpha(t)$ and $e(t)$:

$$\frac{de}{dt} = \frac{dC_L^{sp}}{dt} - \left.\frac{dC_L}{dt}\right|_{C_L^{sp}=ctn} \Rightarrow \frac{de}{dt} = -\frac{dC_L}{dt}$$

$$\mathrm{OUR} = k_L{\cdot}a{\cdot}\left(\alpha \cdot C_L^* - C_L(t)\right) + \frac{de}{dt}$$

Notice that for the PI and PID controllers the stationary error will tend to disappear. Hence, as far the previously mentioned conditions are respected, a time domain defined expression for the OUR estimation is proposed, proportional to the duty cycle and the mass transfer coefficient. In order to overcome the limitation related to the ratio between the measurement period and the mass transfer coefficient a new approach based on proportional valves is considered. The new scheme considers a continuous proper gas mixing before

reaching the bioreactor's gas phase by means of said proportional valves which are equally operated through PWM signals. In this case the duty cycle of the control signal α is not related to the replacement of the gas phase. Hence, its period is independent of the control loop operation. Section 4.3.1 provides an additional description on the operation of the proportional valves.

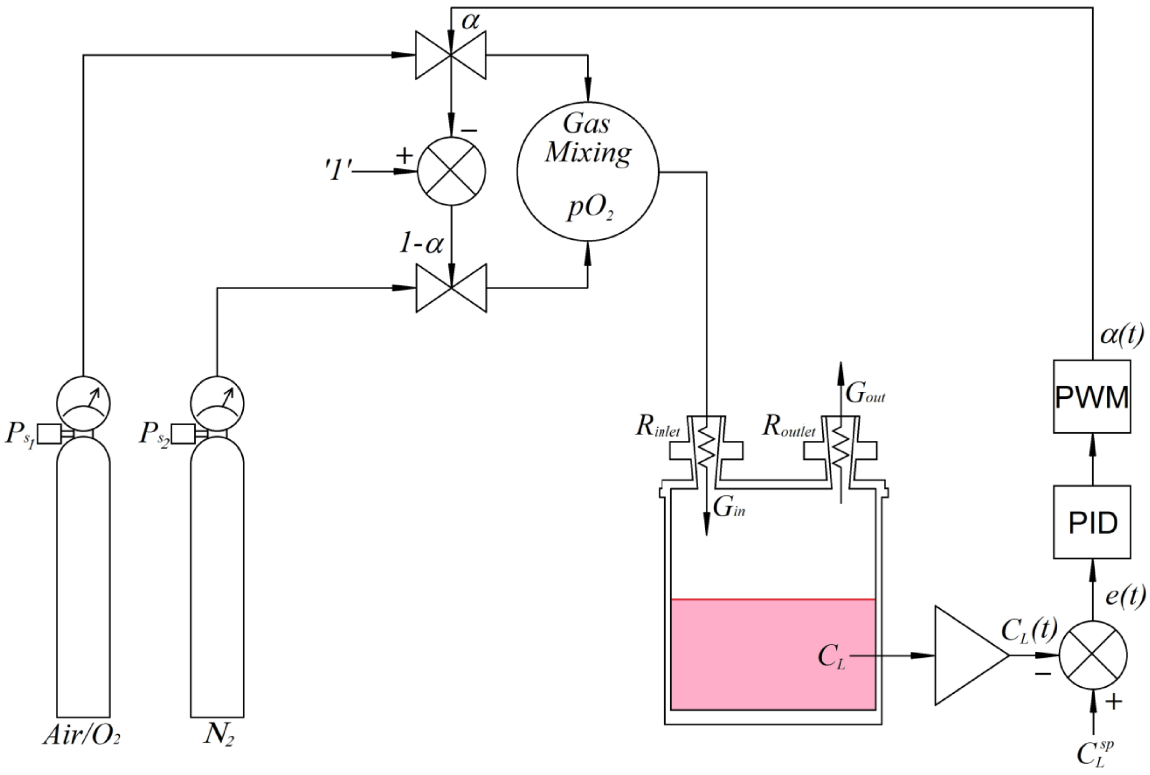

Figure 5
Continuous flow control loop topology.

In order to obtain the oxygen partial pressure in the bioreactor's gas phase, it is possible to do it by redrawing the gas circuit of the diagram above using an electrical analogy and applying basic electrical circuit theory:

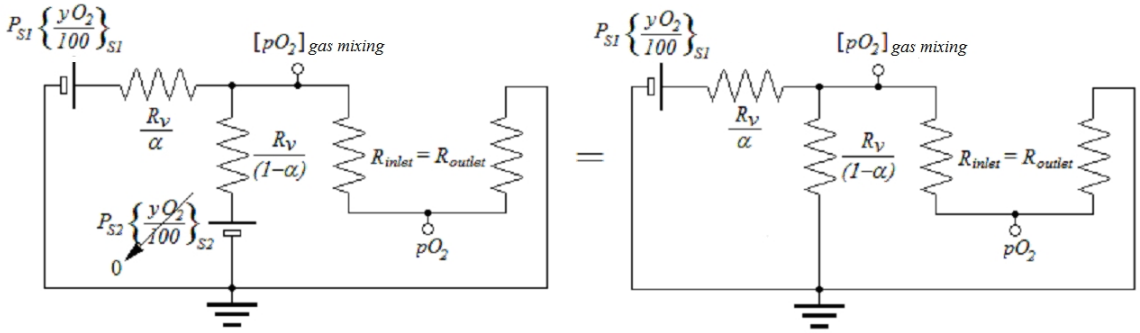

Figure 6
Gas circuit electrical analogy.

Where R_v represents the pneumatic resistance featured by the proportional valves when they are completely open and some gas is flowing through. So then, if the condition R_v >>> 2·R_{inlet} is met, it possible to state that:

$$[pO_2]_{gas\ mixing} \approx \alpha \cdot P_{S1} \cdot \left\{\frac{yO_2}{100}\right\}_{S1} \rightarrow [pO_2]_{Bioreactor} \approx \frac{\alpha \cdot P_{S1} \cdot \left\{\frac{yO_2}{100}\right\}_{S1}}{2}$$

This is equivalent to the mean partial pressure obtained for the discontinuous model. Therefore, it has been considered that both control topologies under the appropriate conditions of switching period and mass transfer behave as a causal linear and time invariant system, which can be modelled by a transfer function in the Laplace domain. This can be useful for a better understanding of the system dynamics as well for the optimization of the control loop parameters.

As previously stated, the mass balance equation considering the control signal α is:

$$\frac{dC_L(t)}{dt} = k_L{\cdot}a{\cdot}\left(\alpha \cdot C_L^* - C_L(t)\right) - \mathrm{OUR}$$

This matches the form of a first order differential equation that can be solved and expressed by means of the Laplace transformation:

$$\frac{dC_L(t)}{dt} + k_L{\cdot}a \cdot C_L(t) = k_L a \cdot \alpha \cdot C_L^* - \mathrm{OUR}$$

$$C_L(t) = \alpha \cdot C_L^*\left(1 - e^{-k_l{\cdot}a{\cdot}t}\right) + C_o \cdot e^{-k_l a{\cdot}t} + \frac{qO_2 \cdot x_o}{\frac{\ln 2}{t_d} + k_l{\cdot}a}\left(e^{-k_l{\cdot}a{\cdot}t} - e^{\frac{\ln 2}{t_d}t}\right)$$

$$C_L(s) = \mathcal{L}\{C_L(t)\} = \frac{\alpha \cdot C_L^*}{s\left(s + k_l{\cdot}a\right)} + \frac{C_o}{s + k_l{\cdot}a} - \frac{qO_2 \cdot x_o}{\left(s + k_l{\cdot}a\right)\cdot\left(s - \frac{\ln 2}{t_d}\right)}$$

Where:

- C_o [mol/l]: Initial value of the DO concentration
- qO_2 [mol/l·h]: Oxygen specific consumption.
- x_o [cell/ml]: Initial cell concetration.
- t_d [h]: Duplication period

The expression of the mass balance frequency behaviour can now be used for drawing the control loop block diagram, next figure. Where it can be seen how, despite that the open loop transfer function is only dependent on the bioreactor's mass transfer capability, the dynamics is also clearly affected by the biological evolution. Since the aim of the current approach is to use control loop internal variables to estimate the oxygen consumption, it will be necessary an adequate design of the controller to have a good compromise between the control loop performance and the sensitivity of the control signal $\alpha(t)$ respect to the biological

"disturbance". As well as keeping in mind that any artifact or stationary drift on the control loop variables will be propagated to the OUR estimate.

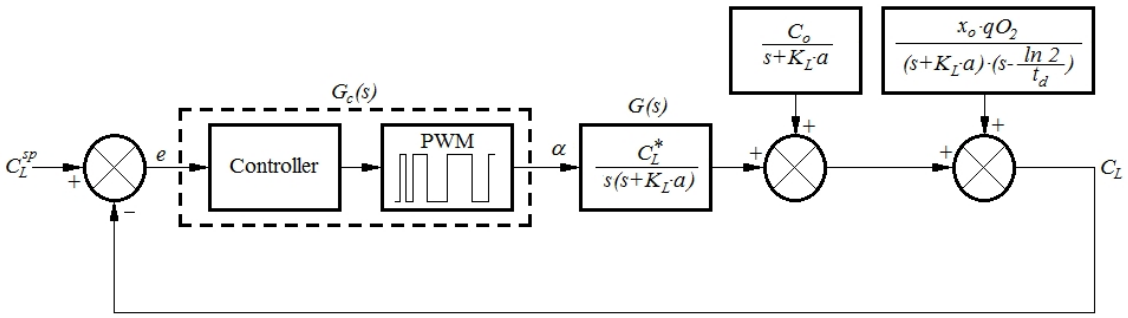

Figure 7
Control loop block diagram in the frequency domain.

5.2 Simulations.

As part of the feasibility assessment, several numerical simulations were performed in order to guess the operational ranges as well as identifying possible design compromises (All the simulations were carried out assuming an exponential growth model with no existence of other limiting factors than the lack of oxygen). The goal of the first simulation was to investigate the convergence conditions between both control topologies: Continuous flow by means of proportional valves or through gas phase replacement by means of a switching valve. This is shown below:

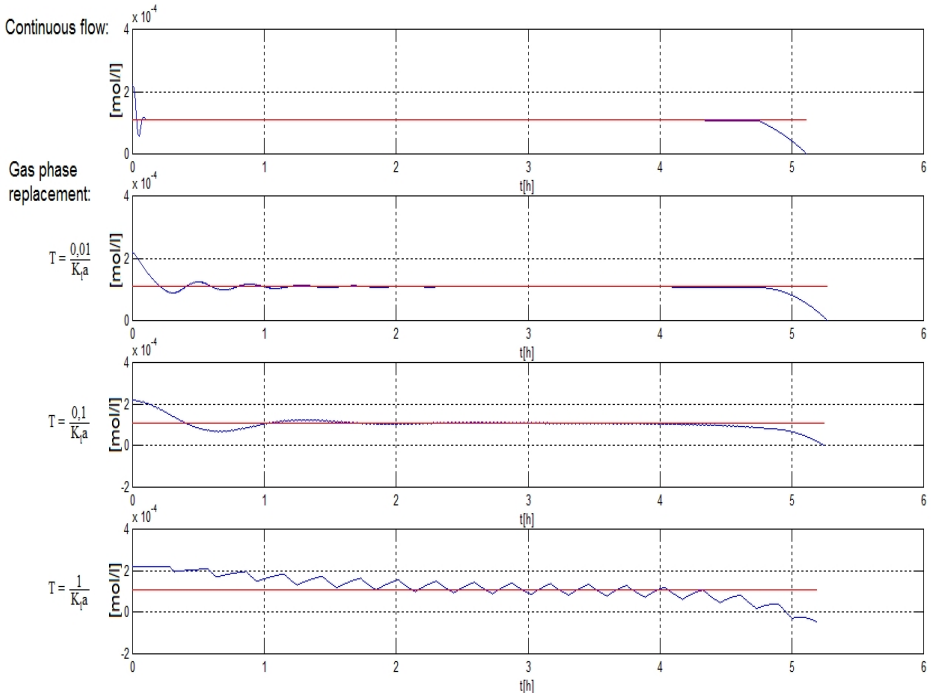

Figure 8
DO control profiles for both topologies: Continuous flow & Gas phase replacement.

The graphs display the DO concentration profile for both control topologies and different ratios of the gas switching period versus the mass transfer coefficient. It can be observed how for every case the DO concentration reaches the set point and stays around until the disturbance caused by the microorganism's consumption of oxygen is excessive and the bioreactor's mass transfer capability is brought to limit. Then, oxygen is depleted. The second observation displayed demonstrates that the switching period must be significantly faster than the mass transfer rate. The shorter the switching time, the more continuous the DO concentration profile becomes. The third important observation is the increase of the transient response with the switching period. This becomes especially obvious for the lower switching rate, which implies that the tuning of the controller should be done not just depending on the bioreactor's physical and biological characteristics but on the switching period too and this is something that needs to be done empirically. Hence, despite that the gas replacement topology promises to be a cheap and feasible option for the control of the DO concentration, the possibility of the system's measurement rate becoming a limitation for high mass transfer applications as well as the dependence of the controller performance on the switching period makes the continuous flow topology the preferred option.

The second simulation consisted on comparing the control loop performance for the three basic linear control strategies (P, PI, PID) in terms of the dynamic response, stationary error and OUR estimate when applied to the continuous flow topology and the disturbing condition of an arbitrary cell line.

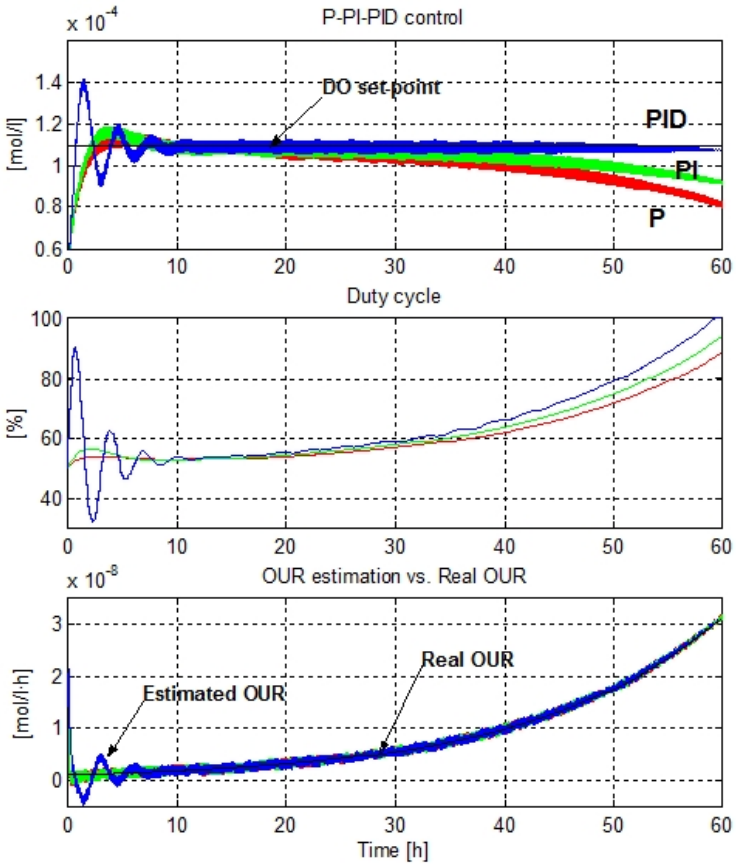

Figure 9

P-PI-PID performance under the disturbing condition of an arbitrary cell line

The control parameters were chosen in order to emphasize the effect of the oxygen consumption on the performance of each control strategy. The results showed the need for a trade-off between the transient response and the long term stability of the stationary error. On one hand, it is interesting to notice that in the long term, the three control strategies provided a good estimate of the OUR regardless of the stationary error drift. On the other hand, the control performances obtained were pretty different. The P controller featured the smoothest transient response but the highest drift of the stationary error. The PID controller instead, worked the opposite being able to provide a minimum long term drift but with the consequence of a longer transient response that interfered with the oxygen consumption estimate. Despite that a different transient response would be possible using the adequate tuning criteria; there are several reasons to reject the PID controller for this application. Real systems may show unpredictable phenomena such as inertia or dead times that could easily produce unexpected behaviours due the action of the differential term. Something which is highly undesirable due to the obvious sensitivity of cells to the changes of the DO concentration.

Therefore, it was the PI controller the one offering the best trade-off. Other considerations concerning the closed loop stability and the characteristics of the transient response can be analyzed by means of the root locus diagram, which is obtained through the open loop transfer function:

$$G_c(s) \cdot G(S) = \frac{K_p \cdot C_L^*}{T_i} \cdot \frac{T_i \cdot s + 1}{s^2 \cdot (s + k_L \cdot a)}$$

Where:

- K_p [ ]: Proportional gain.
- T_i [h]: Integration period.

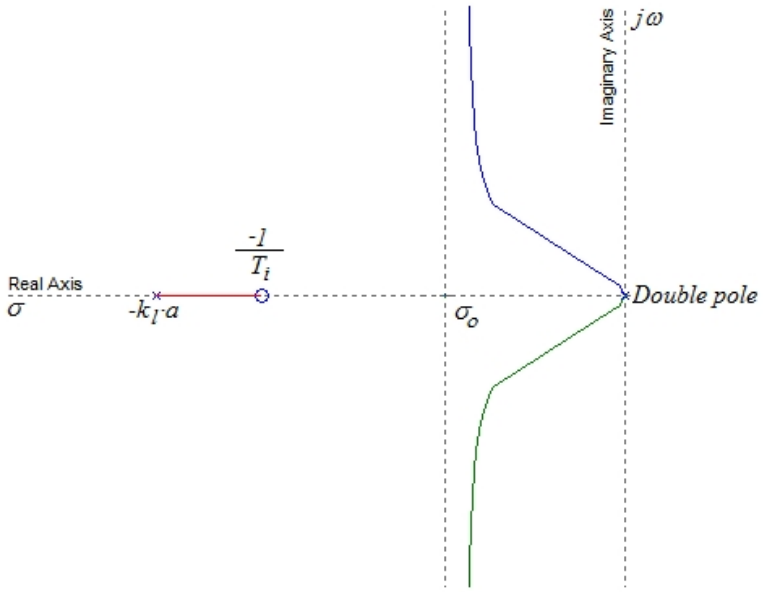

Figure 9
Root locus of the open loop transfer function when using a PI controller

The relative stability of the control loop depends on the zero's position with respect to the pole in - $k_L{\cdot}a$. If the integration period would be such that the zero was located at left or even at the same pole's position then the control loop would become unstable. On the other hand, if the zero would be too close to the origin, then the control loop would trend to behave as a P controller. Hence, in order to ensure the stability but at same time optimizing the transient response two conditions will must be observed. To that end the closed loop transfer function needs to be considered:

$$T(s) = \frac{G_c(s) \cdot G(S)}{1 + G_c(s) \cdot G(S)} = \frac{K_p \cdot C_L^* \cdot (T_i \cdot s + 1)}{s^3 + k_L \cdot a \cdot s^2 + K_p \cdot C_L^* \cdot s + {K_p \cdot C_L^*}/{T_i}}$$

The first condition consists in moving the branches of the closed loop imaginary roots away from the imaginary axis by placing the zero ten times below the pole:

$$T_i \geq \frac{10}{k_L \cdot a}$$

After applying the condition the closed loop transfer function looks as follows:

$$T(s) = \frac{K_p \cdot C_L^* \cdot \left(\frac{10}{k_L \cdot a} \cdot s + 1\right)}{s^3 + k_L \cdot a \cdot s^2 + K_p \cdot C_L^* \cdot s + \frac{K_p \cdot k_L \cdot a \cdot C_L^*}{10}}$$

The second condition consists on choosing the K_p value that makes the real part of the imaginary poles to be ten times smaller than the zero. This way the duration of the transient response, which is inversely proportional to the real part of the imaginary poles will be minimized, but still the dominant pole approach can be applied. So that the transient response will only be dependent on the position of closed loop imaginary roots:

$$s_1 = \frac{\chi_1^{1/3}}{30} - 30 \cdot \frac{\frac{K_p \cdot C_L^*}{3} - \frac{(k_L \cdot a)^2}{9}}{\chi_1^{1/3}} - \frac{k_L \cdot a}{3}$$

$$s_{2,3} = -\frac{\chi_1^{1/3}}{60} - 15 \cdot \frac{\frac{K_p \cdot C_L^*}{3} - \frac{(k_L \cdot a)^2}{9}}{\chi_1^{1/3}} - \frac{k_L \cdot a}{3} \pm j \cdot \frac{\sqrt{3}}{2} \cdot \left(\frac{\chi^{1/3}}{30} - 30 \cdot \frac{\frac{K_p \cdot C_L^*}{3} - \frac{(k_L \cdot a)^2}{9}}{\chi_1^{1/3}}\right)$$

$$\chi_1 = 3150 \cdot K_p \cdot C_L^* \cdot k_L \cdot a - 1000 \cdot (k_L \cdot a)^3 + 150 \cdot \sqrt{\chi_2}$$

$$\chi_2 = 1200 \cdot K_p^3 \cdot C_L^{*3} - 759 \cdot K_p^2 \cdot C_L^{*2} \cdot (k_L \cdot a)^2 + 120 \cdot K_p \cdot C_L^* \cdot (k_L \cdot a)^4$$

Second condition: $K_p \left| \mathbb{R}\{s_{2,3}\} \right| \leq \frac{1}{10 \cdot T_i}$

Now, the characteristics of the over-damped response can be solved:

Overshooting: $M_p = e^{-\frac{\mathbb{R}\{s_{2,3}\} \cdot \pi}{\mathbb{I}\{s_{2,3}\}}}$

Time to peak: $t_p = \frac{\pi}{\mathbb{I}\{s_{2,3}\}}$

Length of the transient response (2% error): $t_s = \frac{4}{\mathbb{R}\{s_{2,3}\}}$

Finally, the DO control performance and the transient and the long term OUR estimate were also simulated for the previously explained growth model using realistic culture parameters and the continuous flow topology with a PI controller. Such simulations were carried out for two extremely different cell species E. Coli and Hybridoma (NB1).

The simulation parameters included the culture temperature (37 °C), the air supply's oxygen molar fraction (21 %), the supply pressure (1 atm), the mass transfer coefficients $k_L{\cdot}a$, k_{des}, the initial cell concentration X_0, the specific oxygen consumption rate qO_2 and the duplication period T_d. The mass transfer coefficients used are typical bench-scale bioreactor values that can easily be obtained by means of the gasing-out method (Dynamic method) at moderate stirring rates ($k_L{\cdot}a$ = 30 h^{-1} ,k_{des} = 25 h^{-1} Despite that the interfacial area remains constant, the lower diffusivity of the nitrogen molecules leads to a significant difference of the absorption and desorption coefficients).

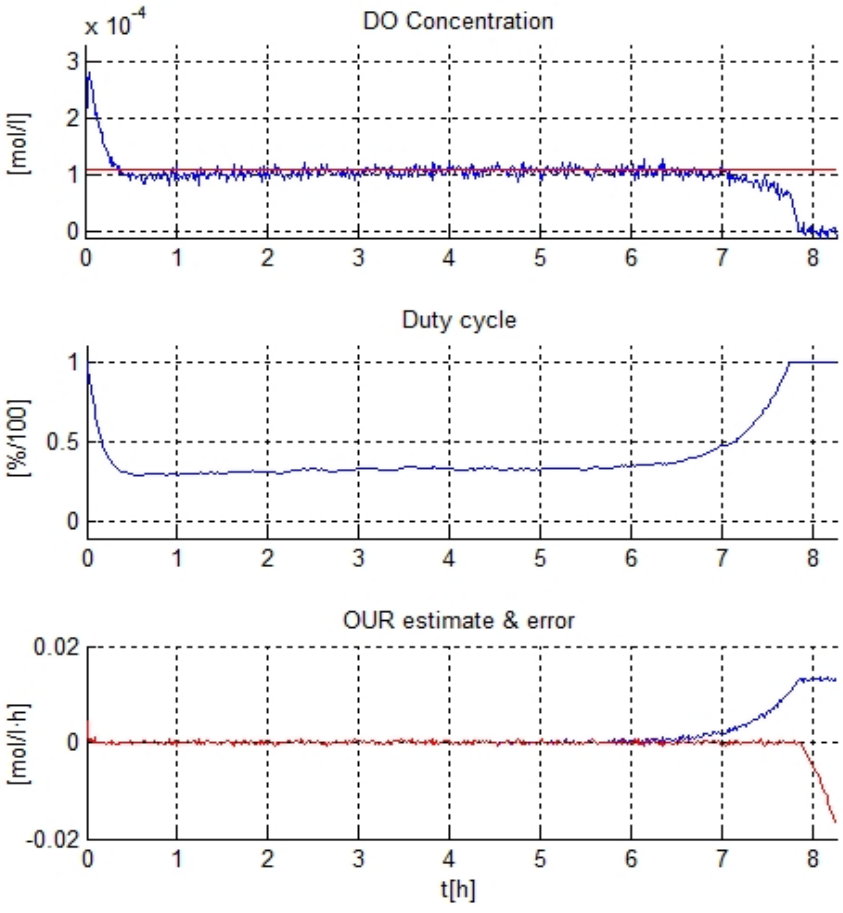

Figure 10
Simulation of an E. Coli culture in a stirred tank bench scale bioreactor

The E. Coli simulation was featured by the following values (X_0 = 0.1 gdw·l^{-1}, qO_2 = 9.05·10^{-3} mol·gdw^{-1}·h^{-1}, T_d = 1 h). The corresponding results are displayed by the graphs in the previous figure. It can be observed how after a short transitional period of approximately 30 minutes, the control loop was able to keep the DO concentration constant for about seven hours. Then, due to the exponential increase of the oxygen consumption some drift correlated with the evolution of the duty cycle was produced. The saturation of the duty cycle indicates the moment when the mass transfer capability is reached and the sudden extinction of oxygen happens. Regarding the OUR estimation, the simulation offered a good accuracy throughout all the culture period until the very moment of the oxygen transfer limitation.

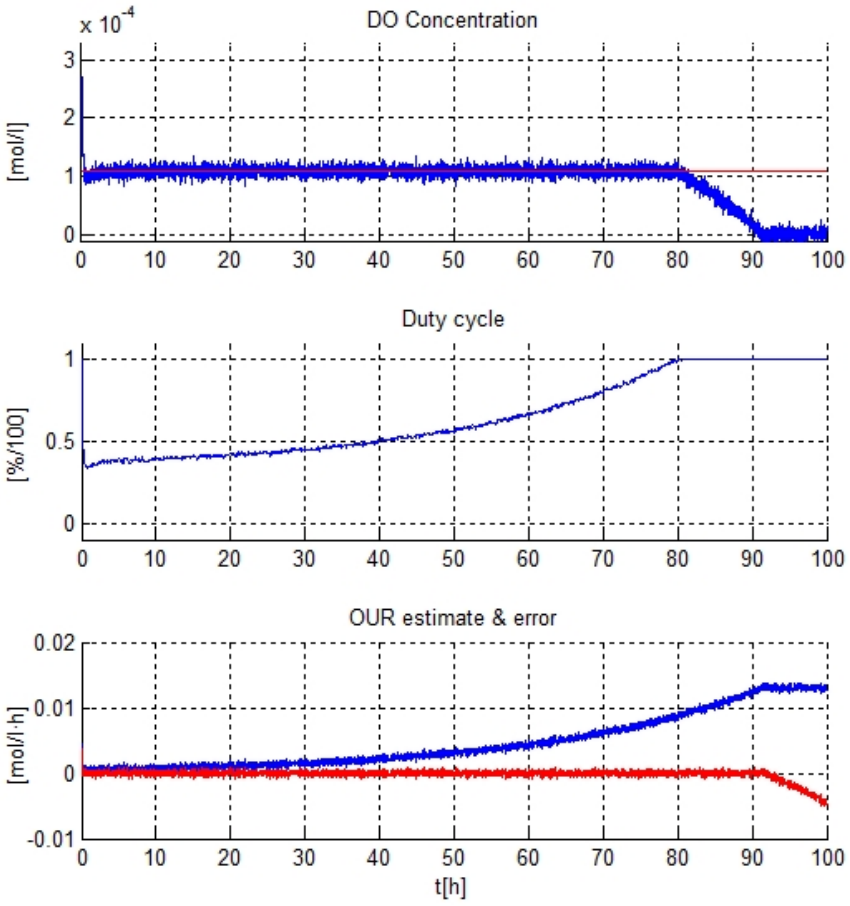

Figure 11

Simulation of a Hybridoma (NB1) culture in a stirred tank bench scale bioreactor

The Hybridoma (NB1) simulation was featured by the following values (X_0 = 2·10^6 cell·ml^{-1}, qO_2 = 23·10^{-14} mol·cell^{-1}·h^{-1}, T_d = 20 h). The graphs in figure 11 displayed a similar behaviour like for the E. Coli simulation. Nevertheless, the fact that animal cells are less prolific than bacteria produced a softer evolution of the oxygen demands. Hence, no drift of the DO concentration was observed before the oxygen transfer limitation.

These simulations illustrated the potentiality of the purposed method to be applied for both microbial and animal cell culture. Where the accuracy of the OUR estimate will depend only on the DO probe's accuracy and the stability of the mass transfer coefficient.

5.3 Experimental results.

The current section explains the experiments carried out and the results obtained by means of the different systems previously explained in chapter 4. The HexaScreen system was used to test the OUR Dynamic estimation method. On the other side, the Simplified OUR stationary liquid mass balance estimation method was implemented on the MonoScreen Fed-Batch system and the customized BIOSTAT B-plus. The number of experiments and variety of cell species used was quite restricted due to the fact that not always was possible to count with the optimum laboratory conditions and cells availability.

Experiment I
Reproducibility test

Experiment description

Due to the fact that the HexaScreen system was specifically designed to work with animal cells. An experiment was designed to show the reproducibility between its different channels. The six wells of the plate were filled and seeded with the same medium and cell concentration. The Minibioreactors were sequentially aereated through their headspaces to ensure a constant concentration of oxygen in the gas phase but during the performance of the Dynamic protocol. Every 10 h, the oxygen was replaced with Nitrogen for a short period to produce the partial extinction of oxygen (>30 %) and the OUR was calculated.

Culture Conditions

Medium: DMEM + 10% (Fetal Calf Serum)
Cell line: Hybridoma BHRF1
Volume: 12 ml
Initial cell concentration: $2 \cdot 10^5$ cells/ml
Stirring rate: 200 rpm
Bioreactor temperature: 37 °C
Aeration rate: 0.2 slpm (Duty cycle: 2%)

Results

The results obtained in each bioreactor were similar, reaching optical densities about 0.35 AU (equivalent to 30×10^5 cells/ml), pH decreased about 1.2 pH units, and the maximal Oxygen Uptake Rates was 0.25 mmol/l·h (considering the existing cell concentration in the time lapse, the specific consumption rate can be calculated, qO_2 = 150 nmol/10^6 cell ·h)

The online monitoring of the OD at 650nm permitted a proper monitorization of the cell culture until the growth limitation was reached, this occurred approximately 48 hours after the starting the experiment. As it is seen in the next figures, a change on the trend of the OD was observed due to the increase of dead cells and debris. At this point, there's a deprivation of some nutrient (Glutamine in this case). This was also properly detected by the change on the pH trend but especially by the decrease on the Oxygen Uptake Rate. This indicates the lack of consumption due to some change of the metabolism or cell death.

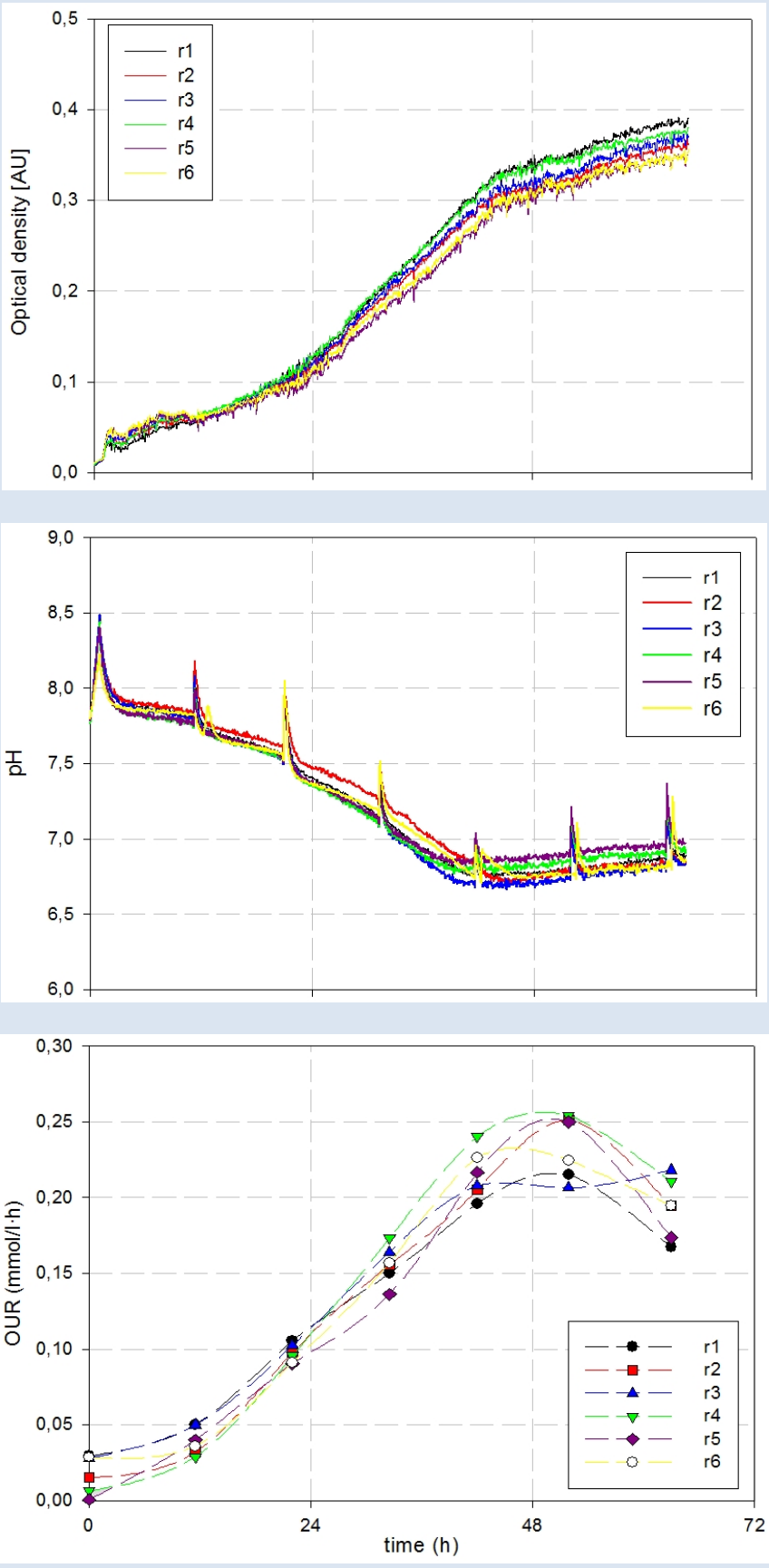

DO, pH and OUR evolution.

Conclusions

The HexaScreen system was successfully able to provide the culture conditions and monitor the metabolical activity of a Hybridoma culture. The span of the OD measurement was small enough to provide a good estimation of the cell concentration.

Another evidence of the success of the experiment is the obvious correlation of the graphs that matches the expected behavior of the cells.

Regarding the performance of the Dynamic method for the OUR estimate, despite it demonstrated to be a robust technique, it clearly shown two important drawbacks: The lack of temporal resolution, only 7 measurements along the whole culture is not enough to take some decisions, i.e.: An accurate reading of the limitation time, and the periodic disturbance on the pH and the DO concentration produced by the sudden replacement of the gas phase. This implies a serious danger for many cell species. That's why the Dynamic method could only be addressed as an appropriate method for research applications and experimental essays were non GLP or GMP rules need to be applied.

Experiment II

Validation of the DO controller and the OUR estimation method for microbial applications

Experiment description

The extremely fast duplication time of bacteria in comparison with animal cells makes microbial applications more demanding in terms of oxygen transfer and robustness of the DO control loop. In this experiment the MonoScreen Fed-Batch system was evaluated under such worst case condition. After calibrating the system using the same disposable Minibioreactor and culture medium to be used for the experiment, the Minibioreactor was inoculated and a Batch culture was carried out along 17 hours. Regarding the OUR estimate, since the aeration system of the MonoScreen Fed-Batch is based on the continuous mixing of several gas flows (Air, N_2, CO_2), the Simplified stationary liquid mass balance method was applied.

Culture Conditions

Medium: LB
Cell line: Escherichia Coli
Volume: 25 ml
Initial cell concentration: 0.2 gdw/l
Stirring rate: 500 rpm
Bioreactor temperature: 37 °C
Aeration rate: 53 smlpm (≈2 VVM)

Results

The overall behaviour of the DO controller worked as expected. After a transient response of approximately 30 minutes, the DO concentration reached the set-point of 20 %. Besides of some artifacts due to an excessive gain of the integral term, the DO concentration was kept constant around the set-point during the following 2.5 hours. Then, the sudden

extinction of the dissolved oxygen happened just as predicted in the previous section. This event is correlated with the increase of the biomass density and the evolution of the oxygen demand. When the signal that controls the gas flow mixing reached the maximum, it became impossible for the system to keep on transferring the required oxygen to maintain the primary metabolism of the cells. Hence, during the following hours the bacteria adapted to the new environment and kept on growing at a slowing down rate.

After 14 hours of culture the cell death happened. This was clearly pointed by two signs: A slight decrease of the Turbidimetric absorbance and the sudden increase of the DO concentration due to the lack of oxygen consumption and also by the OUR estimator.

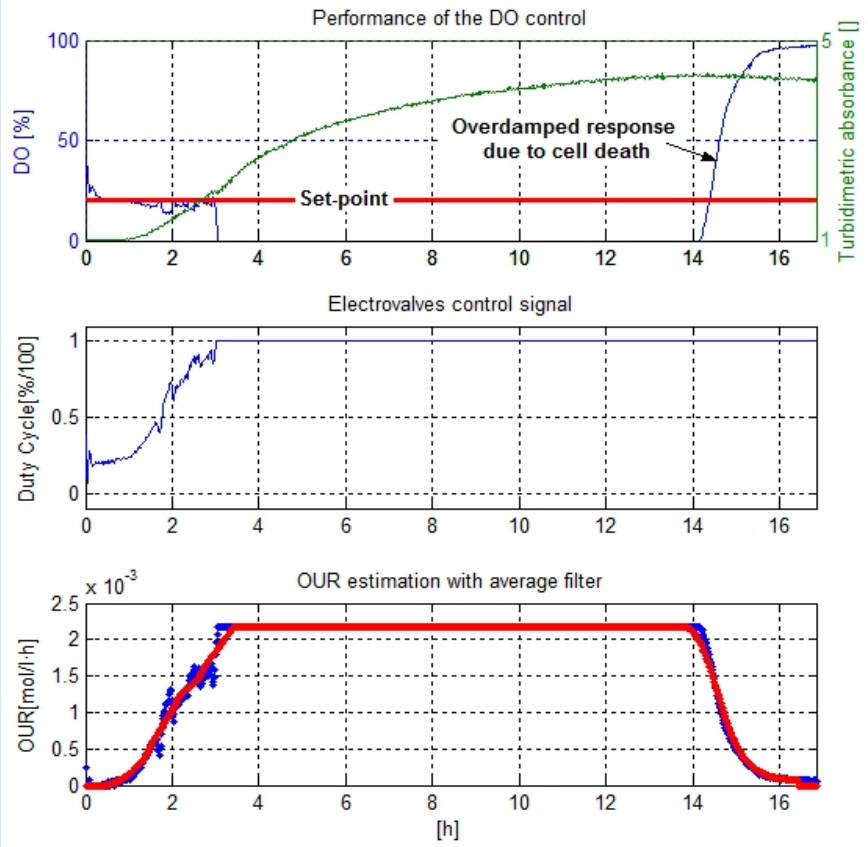

DO, TA, Duty cycle and OUR evolution.

Conclusions

The MonoScreen Fed-Batch system was also successful on providing the culture conditions and monitoring the metabolical activity of a typical microbial application. The NIR turbidimeter demonstrated to be a feasible tool for monitoring the biomass concentration in microbial applications. And the Simplified OUR stationary liquid mass balance estimation method provided realistic data on the evolution of the oxygen demand.

Nevertheless, the mass transfer coefficient was found still too low to support high biomass densities. This will require in the future some additional effort to improve the system's mass transfer capability, by means of including a miniaturized sparger or microdiffusor.

Experiment III
Effect of the culture temperature on the growth dynamics of the E. Coli

Experiment description

In order to evaluate the DO controller of the MonoScreen Fed-Batch system for a longer period, a new experiment was designed to compare the evolution of the same E. Coli strain at three different culture temperatures, based on the fact that a reduction of the temperature will produce and increment of the duplication time. Therefore, after a slight correction of the PI gains, three consecutive batch cultures were carried following the same procedure explained for the previous experiment.

Culture Conditions

Medium: LB
Cell line: Escherichia Coli
Volume: 25 ml
Initial cell concentration: 0.2 gdw/l
Stirring rate: 500 rpm
Bioreactor temperature: 37, 30, 23 °C
Aeration rate: 53 smlpm (≈2 VVM)

Results

After the initial transient response, the DO concentration was kept constant around the set-point (20 %) until the saturation of the control signal. This occurred in increasing times, consistent with the temperature increase. Obviously, the Turbidimetric absorbance and the OUR estimate also displayed great differences in the biomass evolution of every batch.

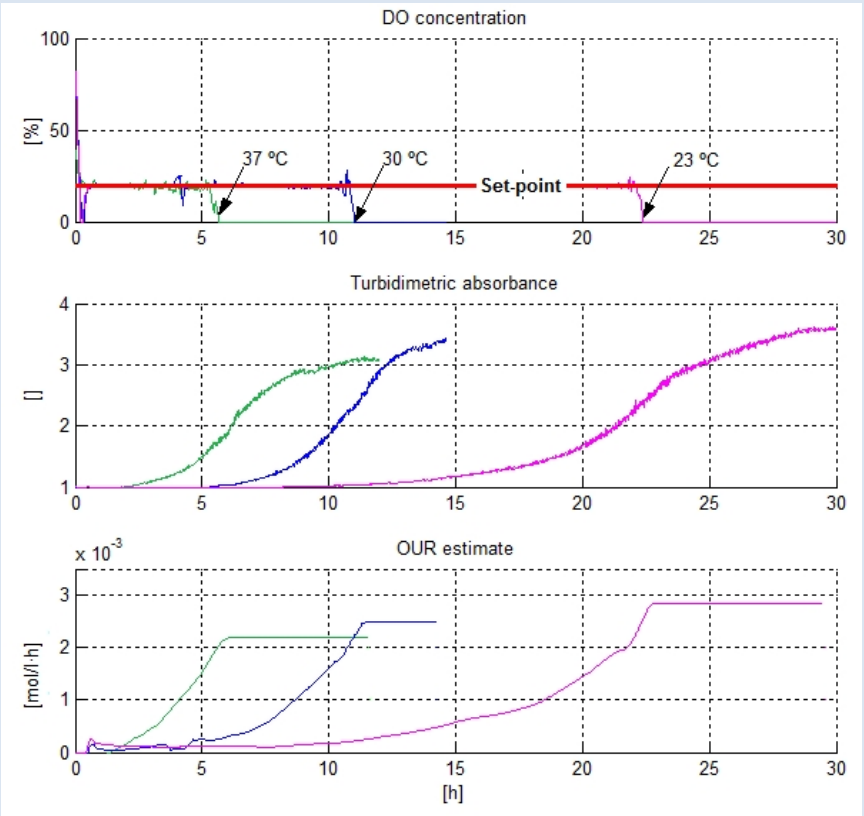

DO, TA and OUR evolution.

Conclusions

After some fine tuning of the DO controller, the stability of the DO concentration around the set-point was increased for the three cases without showing any drift before the saturation of the gas mixing system. Additionally, a reduction of the noise on the OUR estimations was also observed.

The three graphs above clearly demonstrated the effect of culture temperature on the growth dynamics. It was possible to notice a curious effect. The decrease of the temperature produced not just a slower growth rate but a bigger biomass concentration. This is especially visible in the comparison of the OUR graphs.

Experiment IV

Validation of the DO controller and the OUR estimation method for animal cell applications

Experiment description

The use of the simplified stationary liquid mass balance OUR estimation method has already been demonstrated for Microbial cultures by means of the MonoScreen Fed-Batch system. In this new experiment the method is applied for animal cell culture using the customized BIOSTAT B-plus bench scale bioreactor. The bioreactor's vessel was inoculated and a Batch culture was carried out for 10 days at a fixed DO concentration 30 %. The gas supply consisted initially of a mixture of Air, N_2 plus a minimum constant flow of CO_2 for adjusting the physiological pH. After four days the Air supply was replaced by pure O_2 in order to avoid the saturation of the gas mixing system. Additionally, a number of parameters were also analyzed through different techniques after daily manual sampling (Lactate, Glucose, Cell concentration and Viability).

Culture Conditions

Medium: SFM4TransFx + 5 % FBS + 10 % CB5 + 4 mM GlutaMAX + 0.2 % Pluronic F69
+ 50 ppm Antifoam C
Cell line: HEK293
Volume: 1500 ml
Initial cell concentration: $0.25 \cdot 10^6$ cells/ml
Stirring rate: 100 rpm
Bioreactor temperature: 37 °C
Aeration rate: 0.35 slpm

Results

The DO set-point was reached after an initial transient period of 6 hours and the concentration was kept constant along the culture time. A short transient occurred after the substitution of the air supply by pure O_2. Then, the control signal was biased and compressed due to the increment of the oxygen partial pressure in the gas phase. Such increment had to be taken into account in order to correct the signal before the calculation of the OUR estimate.

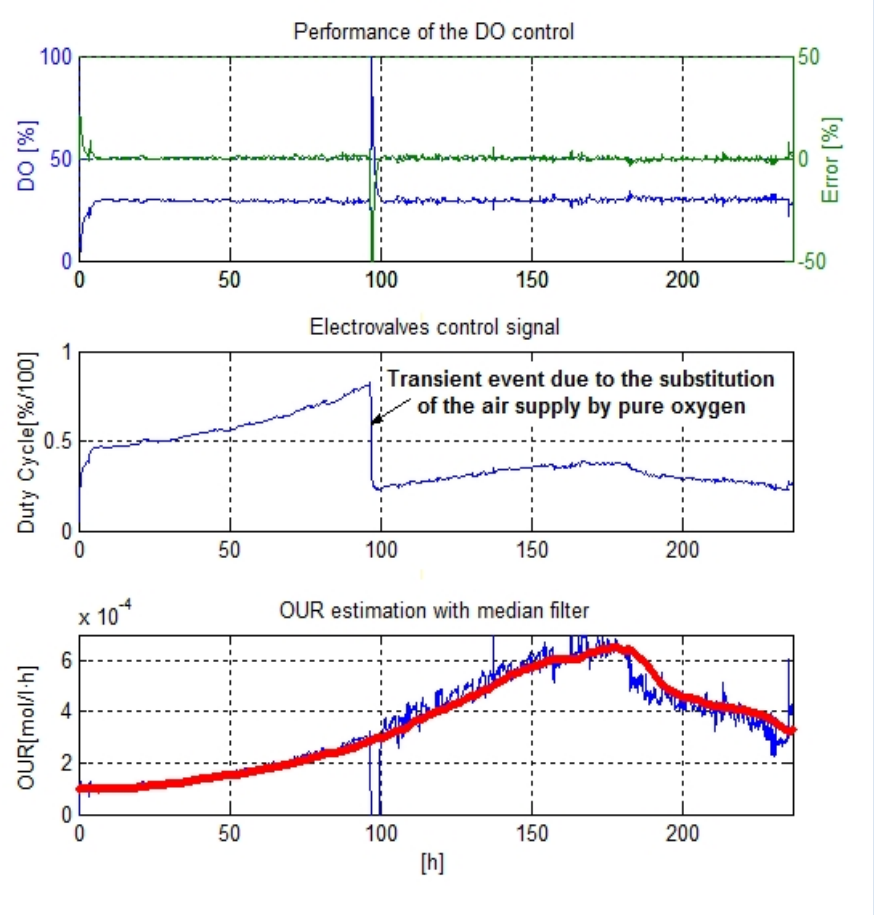

DO, Duty cycle and OUR evolution.

The evolution of the OUR shown the typical behavior of any cell culture. During the first 6 days the cell concentration grown exponentially consuming glucose and producing lactate. When the remaining glucose was not enough to feed the current cell concentration a secondary metabolic path was activated and the lactate previously produced started being consumed by the cells. Once that both analytes became too low the oxygen consumption started to fall down dramatically and the number of viable cells decreased. This is shown in the following graph.

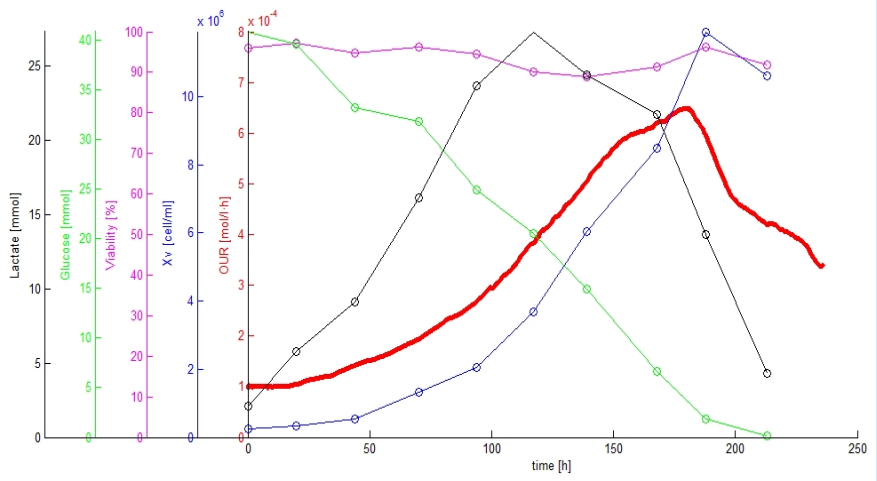

DO, pH and OUR evolution.

Conclusions

Additionally to the obvious demonstration of the method's viability for cell culture processes and bigger volumes (Bench Scale). The off-line data available in this experiment permitted a crucial observation: the fact that the turning point in the OUR graph allowed anticipating the time of maximum viable cell concentration (75 hours before). This is a very important advantage that leads to multiple possibilities regarding the culture strategy. i.e.: When the administration of a bolus may be required to avoid cell death, to maximize the cell concentration or to define some feeding profile. This fact has been confirmed in several (not shown) experiments.

Conclusions & work in progress.

As for the explanation of the state-of-the-art, the conclusions will regard not just to the simplified implementation of the OUR stationary liquid mass balance estimation method but also to other aspects like the development of the several Minibioreactor systems and their complementary instrumentation techniques.

6.1 Conclusions

The fact that the all the work in this thesis was strongly imbricated with the business project of the start-up company HEXASCREEN CULTURE TECHCNOLOGIES made that any aspect had to be faced from a product development point of view in order to match the market's requirements. Four different Minibioreactor systems were developed for testing and evaluating the most appropriate control architectures, instrumentation and operational ranges. It was found that tiny microcomputers such as the ones selected from Rabbit Semiconductor were a cost effective option for developing even complex and technologically demanding instruments. However, the development time required for such devices used to be much higher than for other platforms specifically designed for the rapid prototyping of

embedded systems. On the other hand, the initial Master-Slave communication scheme where a host computer was in charge of the monitorization and control of the different instruments was finally replaced by a web server based user interface. This offered a more robust solution since only one piece of software had to be developed and the need for a custom Master-Slave communication protocol became unnecessary. Hence, despite that the last version of the system is still a prototype; it must be seen as a preindustrial Minibioreactor system including all the state-of-the-art features.

Figure 1
Evolution of the different Minibioreactor systems developed

One of the most important parameters to measure in any cell culture is obviously the cell concentration. To that end, several non-invasive optical probes and configurations were investigated and finally the differences between Optical density and NIR Turbidimetric absorbance were pointed. It was confirmed that Optical Density, which is a well stablished method for off-line measurement in microbial applications, was only useful for on-line monitoring when low cell concentration values were achieved. This happened due to the effect of the light scattering phenomena within the whole visible spectra. On the other side, NIR Turbidimetric absorbance demonstrated a wider linear range of measurement feasible for almost any application with animal cells. This achievement was possible thanks to the use of a NIR laser source which offered a highly collimated light beam that combined with its narrow spectral pattern minimized the effect of the light scattering.

The second key parameter was pH. Optical absorbance spectroscopy was initially chosen as the appropriate technique. Nevertheless, the need for some diluted dye as well as the fact that the optical absorbance at the dye's characteristics wavelengths is interfered by the Optical Density makes this option not useful for many cases, even with mammalian cells where in spite of the relatively small drift of the pH, sometimes the use of indicator dyes can be unacceptable. Therefore, the development has evolved towards the use of disposable pH fluorescence sensors and the DLR (Dual Lifetime Referencing) detection method, whose response is independent of the cell concentration and the presence of any diluted pH indicator. Unfortunately, the DLR method has not been yet tested enough. It is in fact the last development milestone to provide the MonoScreen Fed-Batch system with complete functionality.

The third basic parameter from the metabolical point of view is DO (Dissolved Oxygen). During the development and testing of the first prototypes, several approaches were carried out for the implementation of a non-invasive polarographic probe (Clark's electrode). However, the difficulty to avoid mechanical defects or positioning mismatches of the electrode with respect to the permeable membrane led to the generation of quite noisy signals. This problem was finally overcome by means of the use of disposable DO fluorescence sensors. Despite that OEM readers for such sensors were commercially available; a custom low cost coherent XOR detector was designed and validated for the application.

Such complementary instrumentation permitted to successfully face the challenge of proofing the feasibility of the previously mentioned Minibioreactor systems. The high degree of innovation associated to the development of these products becomes obvious when observing that the development rate of the commercial business ran in parallel with the evolution of the different systems developed by HEXASCREEN CULTURE TECHNOLOGIES.

With respect to the major original contribution of this thesis, the simplified implementation of the OUR stationary liquid mass balance estimation method, the feasibility of the procedure was demonstrated for both animal and microbial cells; it also was demonstrated for two different culture scales. In comparison with the Dynamic method the proposed method shows obvious advantages in terms of time resolution and DO stability (lack of cell stress). Regarding the method's accuracy, unfortunately any standard method to set a known value of oxygen consumption has been reported yet. Hence, it is not possible to provide a measured value on the estimation error. Nevertheless, the accuracy is expected to be comparable to the non-simplified stationary liquid mass balance method due to the fact that both procedures are dependent on the previous knowledge of the mass transfer coefficient and the DO control's stationary error. That is, a precision of 1% on the DO control allows measurement of the consumption of 10^4 cells·ml^{-1} assuming a typical consumption rate of $0.2x10^{-12}$ mol·cell·h^{-1} (Ruffieux et al. 1998)

6.2 Work in progress

In order to promote the use of the method, another experiment is currently being conducted out in cooperation with members of the Chemical Engineering Department of the Universitat Autònoma de Barcelona. The goal is to compare the performance of the simplified method versus the global de mass balance through the use of an in-line Bluesens O_2 and CO_2 analyzer. The following figure shows the diagram of the experiment set-up. The four valves around the Bluesens analyzer are periodically switched on an off in order to sequentially measure the oxygen molar fraction in the bioreactor's inlet and outlet. This lets to solve the global mass balance.

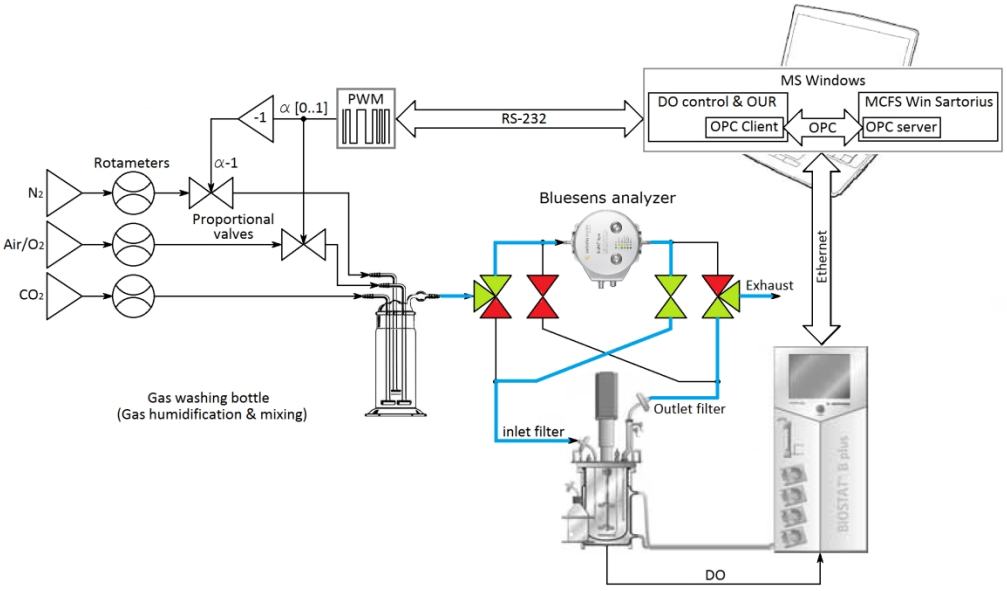

Figure 2
Experiment set-up of the current experiment in progress

Another line of work in progress is the integration of embedded solid state DO and pH sensors as an alternative to the fluorescent patches that should let to a reduction of the overall prize of the disposable Minibioreactors. Some non-enough successful tests were carried out by means of thick film electrochemical sensors attached to conventional printed circuit boards. More successful results have already been obtained around the integration of electrodes to measure the Bioimpedance of the cell culture for both suspended and adherent cell lines. Bioimpedance offers a cheaper alternative to the optical methods to measure the cell concentration and has two important advantages: Higher dynamic range, it would be possible to measure higher biomass densities than with any optical procedure. However, the sensitivity in the low range would not be able to accurately record small changes. The second advantage is that offers the possibility to distinguish between dead and living cells (viability). This is due to the fact that Bioimpedance is basically a macroscopic measurement highly connected to the integrity of the cell wall. The following figures show one the electrode topologies tested and the results obtained for a simulated culture consisting on a baker's yeast sedimentation process along several hours.

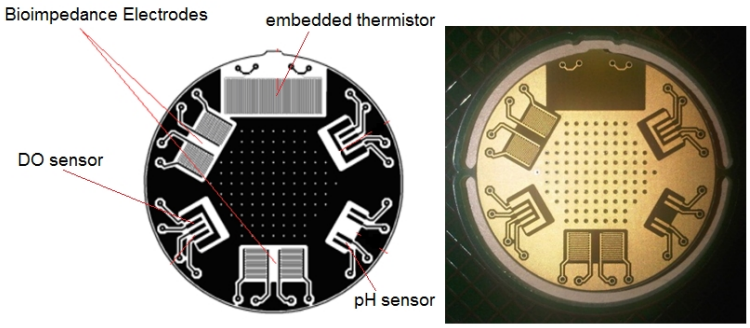

Figure 3
Layout of the different solid state sensors tested include Bioimpedance

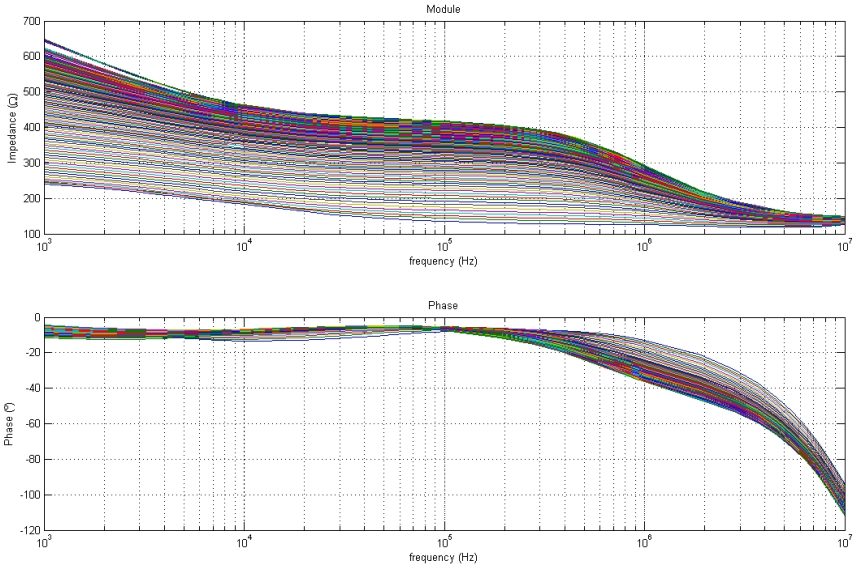

Figure 4

Evolution of the Bioimpedance spectra during a baker's yeast sedimentation process when measured by means of a set of interdigitated electrodes.

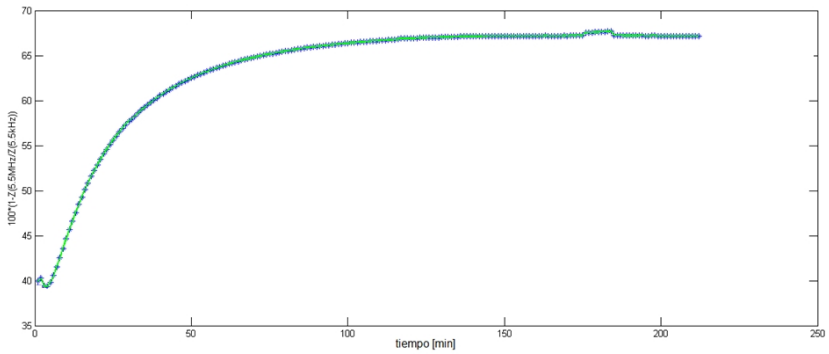

Figure 5

Relative variation of the impedance during a baker's yeast sedimentation process when measured at 5.5 kHz and 5.5 MHz by means of a set of interdigitated electrodes.

On one hand, It can clearly be seen how there's a progressive increment of the magnitude that in a real experiment could be related to the cell concentration in suspension. On the other hand the phase evolution in the relaxation area happened due to the deposition of yeast between the interdigitated electrodes. This effect could be used in the future for the monitorization of monolayers growing in adherence.

Therefore, Bioimpedance is a powerful tool for the monitorization of cell culture, where the simultaneous measurement of other parameters like the OUR and Turbidimetric absorbance could provide a multiparametric estimator of the biomass density and viability.

Unforeseen results were also obtained through the cooperation between HEXASCREEN CULTURE TECHNOLOGIES and scientists from the Biochemistry & Molecular Biology department from the University of Calgary. The application of the HexaScreen system to its use with extremely shear stress sensitive cell lines such as human Embryonic Stem Cells (hESC's) and Induced Pluripotent Stem Cells (IPSC's) was investigated. To that end, a set of Minibioreactors tailored to fit the requirements of Embryonic Stem Cells were developed and are currently being used. Yielding key conclusions on the stirring requirements and bioreactor's morphology and materials in order to promote cell proliferation in low volume miniaturized stirred tanks to produce highly uniform non-differentiated embryonic bodies. Professor D. Rancourt research team reported the following conclusions:

- The impeller morphology was found to be a key point on the cell proliferation since an extremely soft stirring leads to a poor and irregular growth of the embryonic bodies.
- A proper hydrodynamic profile of the Minibioreactor allows optimum cell growth in suspension at low stirring rates.
- The distance between the tip of the stirring shaft and the summit of the dome on the vessel's bottom, was identified as a crucial parameter. Such distance acts as a modulating variable on the embryonic bodies' size and the cell differentiation. It was observed that an excessively reduced distance produces too small spheroids and their cells the trend to differentiate prematurely. On the other hand, if the distance is too big the spheroids grow in very different sizes where some of them can die due to nutrient diffusion problems. This way it was pointed the need for a certain level of shear stress to obtain a homogeneous population of embryonic bodies without inducing cell differentiation.

Figure 6
Modified version of the HexaScreen Minibioreacto's plate to hold hESC's and IPSC's

The developments and results presented in this dissertation are a cross-cutting modest contribution to very different aspects deeply related to the field of Bioreactor design and to a wide range of engineering disciplines applied to Biotechnology. Hopefully, in the near future, after the adequate hardware refinement, it will be possible to use such new tools and knowledge to improve the outcomes of the nowadays most straightforward screening and culture strategies based on Design of Experiments (DoE) and Perfusion Biomanufacturing methodologies.

Papers, patents, and conference contributions.

A SIMPLIFIED IMPLEMENTATION OF THE O.U.R. STATIONARY LIQUID MASS BALANCE ESTIMATION METHOD FOR ON-LINE MONITORING IN ANIMAL CELL PRODUCTION PROCESSES.

A. Fontova, J. López, L. Liste, M. Lecina, R. Bragós & J.J. Cairó.

ESACT 2015 - *24th European Society for Animal Cell Technology Meeting*. Barcelona, SPAIN

(Poster accepted)

APPROACH FOR A CONTINUOUS OXYGEN CONSUMPTION ESTIMATION METHOD, BASED ON THE ACCURATE CONTROL OF THE CULTURE MEDIUM'S DISSOLVED OXYGEN CONCENTRATION, INTENDED FOR ANIMAL CELLS.

A. Fontova, A. Soley, J. Gálvez, E. Sarró, M. Lecina, J. Rosell, P. Riu, J. Cairó, F. Gòdia & R. Bragós

IFMBE Proceedings - *4th European Conference of the International federeation for Medical and Biological Engineering.* Atwerp, BELGIUM

(23.11.2008 – 27.11.2008)

Vol: 22, pp. 2190–2194

MULTIPLE AUTOMATED MINIBIOREACTOR SYSTEM FOR MULTIFUNCTIONAL SCREENING IN BIOTECHNOLOGY.

A. Fontova, A. Soley, J. Gálvez, E. Sarró, M. Lecina, J. Rosell, P. Riu, J. Cairó, F. Gòdia & R. Bragós

EMBS '06. Proceedings. -*28th Annual Internacional Conference of the IEEE.* New York, USA

(30.8.2006-2.9.2006)

pp. 632-635

SISTEMA DE MÚLTIPLES BIOREACTORES AUTOMATIZADOS PARA SCREENING MULTIFUNCIONAL EN BIOTECNOLOGIA.

A. Fontova, A. Soley, J. Gálvez, E. Sarró, M. Lecina, J. Rosell, P. Riu, J. Cairó, R. Bragós & F. Gòdia

CASEIB 2005 - *XXIII Congreso anual de la Sociedad Española de Ingeniería Biomédica.* Madrid (10.11.2005 - 12.11.2005).

pp. 237-240

EQUIPOS PARA CULTIVOS DE CÉLULAS ANIMALES

F. Gòdia., J.J. Cairó, A. Soley, R. Bragós & A. Fontova.

Biotech Magazine, Ed. MKM

November 23rd, 2009.

DEVELOPMENT OF A SIMPLE DISPOSABLE SIX MINIBIOREACTOR SYSTEM FOR SUSPENSION MAMMALIAN CELL CULTURE.

A. Soley, A. Fontova, J. Gàlvez, E. Sarró, M. Lecina, R. Bragós, J.J. Cairó & F. Gòdia.

Process Biochemistry 2012.

Volume 47, Issue 4, April 2012, pp. 597-605

MINIBIOREACTORS FOR ANIMAL CELL CULTURE: MONITORING OF CELL CONCENTRATION AND CELLULAR ACTIVITY.

A. Soley, J. Gàlvez, E. Sarró, M. Lecina, A. Fontova, R. Bragós, J.J. Cairó & F. Gòdia.

ESACT 2005 - *19th European Society for Animal Cell Technology Meeting*. Harrogate, UNITED KINGDOM

(5.06.2005 – 8.06.2005).

Vol: 3, pp. 803-806

ELECTRICAL IMPEDANCE SPECTROSCOPY MEASUREMENTS USING A FOUR ELECTRODE CONFIGURATION IMPROVE ON-LINE MONITORING OF CELL CONCENTRATION IN ADHERENT ANIMAL CELL CULTURES.

E. Sarró, M. Lecina, A. Fontova, C. Solà, J. Cairó, F. Gòdia, J.J. Cairó & R. Bragós

Biosensors & Bioelectronics 2012

Vol: 31, pp. 257-263

FOUR ELECTRODE EIS MEASUREMENT ON INTERDIGITATED MICROELECTRODES FOR ADHERENT CELL GROWING AND DIFFERENTIATION MONITORING.

E. Sarró, A. Fontova, A. Soley, J. Cairó, A. Bayés-Genís, J. Rosell & R. Bragós

IFMBE Proceedings. - *13th Internacional Conference on Electrical Bioimpedance and 8th Conference on Electrical Impedance Tomography*. Graz, AUSTRIA

(29.8.2007 - 2.9.2007)

Vol: 17, pp. 77-80

FOUR VERSUS TWO-ELECTRODE MEASUREMENT STRATEGIES FOR CELL GROWING AND DIFFERENTIATION MONITORING.

R. Bragós, E. Sarró, A. Fontova, A. Soley, J. Cairó, A. Bayés-Genís & J. Rosell

EMBS ’06 Proceedings. -*28th Annual Internacional Conference of the IEEE.* New York, USA

(30.8.2006-2.9.2006)

pp. 2106-2109

Other publications not related with the thesis main topic:

MULTIPARAMETRIC MEASUREMENT SYSTEM FOR DETECTION OF CARDIAC GRAFT REJECTION.
J. Ramos, R. Bragós, M. A. García, Y. Salazar, A. Fontova, A. Bayés, J. Cinca & J. Rosell.
IMTC 04 - *21th IEEE Instrumentation and Measurement Technology Conference.* Como, ITÀLIA
(18.05.2004 - 20.05.2004).
pp. 1701-1705

SISTEMA DE MEDIDA MULTIPARAMÉTRICO PARA LA DETECCIÓN DE RECHAZO EN TRANSPLANTE CARDÍACO.
J. Ramos, R. Bragós, M. A. García, Y. Salazar, A. Fontova, A. Bayés, J. Rosell & J. Cinca.

CASEIB 2003 - *XXI Congreso Anual de la Sociedad Española de Ingeniería Biomédica*. Mérida

(13.11.2003 – 15.11.2003)

pp. 45-48

ENDOCARDIAL IMPEDANCE SPECTROSCOPY SYSTEM USING A TRANSCATHETER METHOD.
R. Bragós, J. Ramos, Y. Salazar, A. Fontova, M. Fernández, P. Riu, M. A. García, A. Bayés, J. Cinca & J. Rosell.
ICEBI 2004 - *XII International Conference on Electrical Bioimpedance & V Electrical Impedance Tomography*. Gdansk, POLÒNIA (20.06.2004 - 24.06.2004).
pp. 465-468

Patents:

A DEVICE AND A METHOD FOR MANIPULATING BIOLOGICAL MATERIALS IN A PROCESS OF CRYOPRESERVATION.

R. Morato, A. Fontova & T. Mogas.

Patent application number: EP20100380072 20100521

A STERILE SAMPLE TAKING DEVICE FOR BIOPROCESS DEVELOPMENT.

A. Fontova & E. Sarró.

Patent application number: EP2012/12382086.2